



<https://theses.gla.ac.uk/>

Theses Digitisation:

<https://www.gla.ac.uk/myglasgow/research/enlighten/theses/digitisation/>

This is a digitised version of the original print thesis.

Copyright and moral rights for this work are retained by the author

A copy can be downloaded for personal non-commercial research or study, without prior permission or charge

This work cannot be reproduced or quoted extensively from without first obtaining permission in writing from the author

The content must not be changed in any way or sold commercially in any format or medium without the formal permission of the author

When referring to this work, full bibliographic details including the author, title, awarding institution and date of the thesis must be given

Enlighten: Theses

<https://theses.gla.ac.uk/>
research-enlighten@glasgow.ac.uk

**Phosphodiesterase 4 isoforms in macrophage
development and function**

Malcolm Cameron Shepherd

B.Sc. Hons Experimental Pathology

M.B. Ch.B

Submitted in partial fulfilment of the requirements for the Degree of

Doctor of Philosophy

University of Glasgow
Department of Medicine and Therapeutics
Institute of Biomedical and Life Sciences

October 2002

ProQuest Number: 10390863

All rights reserved

INFORMATION TO ALL USERS

The quality of this reproduction is dependent upon the quality of the copy submitted.

In the unlikely event that the author did not send a complete manuscript and there are missing pages, these will be noted. Also, if material had to be removed, a note will indicate the deletion.



ProQuest 10390863

Published by ProQuest LLC (2017). Copyright of the Dissertation is held by the Author.

All rights reserved.

This work is protected against unauthorized copying under Title 17, United States Code
Microform Edition © ProQuest LLC.

ProQuest LLC.
789 East Eisenhower Parkway
P.O. Box 1346
Ann Arbor, MI 48106 – 1346

GLASGOW
UNIVERSITY
LIBRARY:

13127

copy 2.

Summary

Phosphodiesterase 4 (PDE4) is a family of around 20 cyclic AMP (cAMP) hydrolysing enzymes. Expression of each isoform is regulated in a tissue and developmental specific manner. Such regulation suggests as yet undefined functions for each isoform. Understanding these functions will highlight likely therapeutic targets. I have employed various methods to identify possible functional roles for various PDE4 isoforms.

PDE4B4 is a novel enzyme cloned from a rat brain cDNA library. By characterising the biochemical properties of this isoform in comparison to known, previously characterised members of the PDE4B family, I highlighted similarities and differences within this sub-family. Recombinant PDE4B4 was characterised in a COS-1 cell, temporary expression system. I demonstrated that PDE4B4 has a molecular weight lying between PDE4B1 and PDE4B2, is largely cytosolic, has a relatively low K_m cAMP and is highly sensitive to inhibition by rolipram. As it has a UCR1 region it conforms to long form structure and is activated by PKA. It has an extreme N-terminal region homologous to PDE4D3 and behaves in a similar way in response to PKA phosphorylation.

Development of macrophages from monocytes involves differential expression of various biochemical mediators. I developed a cell line model using the U937 pro-monocytic cell line and compared it against ex-vivo monocytes cultured in plastic. Using this model I identifies developmental changes in PDE4 isoform expression. PDE4A activity increased dramatically which was due in part to novel expression of PDE4A10. PDE4D isoform expression was entirely lost with no immunologically detectable enzyme present in macrophage like cells. PDE4B2 expression more than doubled in the mature cell. Loss of PDE4D and gain of PDE4B2 represents a shift from long to short form PDE4 dominance. I demonstrated a resultant switch in PDE4 response to extracellular signal related kinase (ERK) activation. Thus in monocytic cells EGF resulted in a decrease in total PDE4 activity, while in macrophage like cells PDE4 activity increased.

To demonstrate a role for PDE4 in regulating macrophage function I stimulated the RAW 264.7-macrophage cell line with LPS in the presence of rolipram. I demonstrated a PGE2 dependent increase in iNOS expression and a PGE2 independent increase in COX2 expression. Such differential effects, suggests a compartmentalisation of rolipram's action. Inhibition of TNF α production was not dependent on PGE2 production. I then found that LPS activates PDE4 in an ERK dependent manner, but inhibits PDE3, highlighting further

compartmentalisation of cAMP regulation. PDE4 activation was in part due to ERK dependent activation of the short form PDE4B2, downstream of LPS stimulation of RAW cells. Such activation may be associated with physical interaction between members of the ERK signalling cascade and PDE4B2.

Next I demonstrated that crosstalk between ERK signalling and cAMP occurs in the opposite direction as rolipram leads to an early and elevated activation of ERK 1/2 in LPS stimulated RAW 264.7 macrophages. In an attempt to explain this effect I used rap1 activation and PKA phosphorylation mutants, transfected into RAW cells to interfere with normal inflammatory signalling. No significant changes were observed in these studies.

Finally I attempted to develop HIV-tat, PDE4 N-terminal, fusion proteins to inhibit individual PDE4 isoforms. I used primers encoding the HIV-tat peptide and PDE4 sequence to produce a cDNA fusion. This was cloned into a GST-expression vector and transformed into E-coli. Recombinant protein was expressed and purified using sepharose beads. Various problems were encountered in the course of this project, including the development of appropriate cloning primers and the production of proteins in inclusion bodies. The strategies employed to resolve these difficulties are discussed.

Two further experiments are discussed. Firstly rolipram was found not to affect tritiated thymidine incorporation into proliferating IIEK cells. This work argues against a role for PDE4 in regulating cell cycle in these cells. I also attempted to characterise PDE4 activity from the induced sputum of normal subjects. While PDE4 activity was found to survive the isolation process the intra-subject variability meant that useful interpretation of fluctuations based on therapeutic intervention would be impossible.

In conclusion I have characterised a new member of the PDE4B family. It shares many characteristics with other members of the sub-family and long form PDE4 enzymes in general. I have shown upregulation of PDE4A10 and PDE4B2 in the maturation of macrophages and the loss of long form PDE4D3 and PDE4D5. This was found to have biochemical significance. PDE4B2 was shown to be important in the regulation of LPS activation of RAW cells and ERK/PDE4 crosstalk was found to occur in both directions. Rolipram was demonstrated to influence the behaviour of stimulated macrophages in a compartmentalised fashion, while LPS was found to activate PDE4 and inhibit PDE3. Finally I was unsuccessful in the development of a novel strategy for inhibiting individual PDE4 isoforms, by developing an HIV-tat fusion protein.

Contents

Chapter 1	Introduction.....	1
1.1	Biological diversity	1
1.2	Cyclic amp signaling.....	2
1.3	Phosphodiesterase 4 a study in biological diversity.....	13
1.4	PDE4 in inflammation.....	25
1.5	Alveolar Macrophages	31
1.6	Cyclic AMP in the macrophage.....	39
1.7	Phosphodiesterase isoforms in macrophages and monocytes	46
1.8	Conclusions and hypotheses	52
Chapter 2	Materials and Methods.....	54
2.1	Materials	54
2.2	Buffers and Solutions	60
2.3	Mammalian cell culture.....	67
2.4	Biochemical Techniques.....	71
2.5	Molecular biology techniques.....	82
2.6	Statistical analysis	88
Chapter 3	Characterisation of PDE4B4	89
	Introduction	89
	Results	90
	Discussion	111
	Conclusion.....	114
Chapter 4	PDE4 isoform expression during U937 differentiation	116
	Introduction	116
	Results.....	118
	Discussion	147
	Conclusions	148
Chapter 5	Lipopolysaccharide regulation of PDE4 isoforms and PDE4 inhibition in activated RAW 264.7 cells	150
	Introduction	150
	Results.....	153
	Discussion	182
	Conclusion.....	190
Chapter 6	The synthesis of HIV-Tat fusion protein PDE4D3 and PDE4B2	193
	Introduction	193
	Results	195
	Discussion	211
	Conclusion.....	216
Chapter 7	Discussion	217
7.1	The new PDE4B isoform PDE4B4.....	218
7.2	PDE4 inhibition in macrophages	221
7.3	U937 differentiation.....	227
7.4	Effect of LPS on macrophage PDE4 isoforms	235
7.5	Raf-MEK-ERK1/2 / cyclic AMP crosstalk	239
7.6	Rap1 mutants in RAW macrophages	241
7.7	HIV-tat fusion proteins.....	243
	Future directions	245
Appendix 1	Standard curves and quantification.....	247
Appendix 2	Lactate Dehydrogenase (LDH) analysis of cellular fractionation.....	255
Appendix 3	Phosphodiesterase 4 activity in induced sputum from normal subjects	257
References	260

List of figures

Chapter 1 Introduction

1.1 Cyclic AMP regulatory molecules: multi-member families.....	3
1.2 PDE domain structure	12
1.3 PDE4 isoforms heterogeneity	16

Chapter 3 Characterisation of PDE4B4

3.1.1 Schematic representation of PDE4B4	91
3.1.2 PDE4B4 plasmid integrity	92
3.1.3 Specific activity of transfected PDE4B4.....	94
3.2.1 Molecular weight of PDE4B4.....	96
3.2.2 Subcellular distribution of PDE4B4 (activity).....	97
3.2.3 Subcellular distribution of PDE4B4 (western blot)	98
3.3.1 Km PDE4B4	101
3.3.2 PDE4 transfection efficiency	102
3.3.3 PDE4B4: IC50 for rolipram.....	104
3.4.1 Cyclic AMP alters PDE4B4 electrophoretic mobility	107
3.4.2 Ser14-Ala mutation PDE4B4 activity	109
3.4.3 Ser-Asp mutations on PDE4B4 activity.....	110

Chapter 4 U937 differentiation with PMA

4.1.2 β 2 Integrin expression in U937PMA	121
4.1.3 PKC β / COX-2 expression in U937PMA.....	122
4.1.4 Effect of PMA on PDE U937 expression	124
4.1.5 Cellular PDE activity with macrophage differentiation	125
4.2.1 PDE4A activity changes in U937PMA.....	130
4.2.2 PDE4A protein increases in U937PMA.....	131
4.2.3 PDE4A10 expression increases with differentiation.....	132
4.2.4 PDE4A activity in ex-vivo monocytes	134
4.2.5 PDE4D expression changes	135
4.2.6.0 PDE4D activity in U937PMA	136
4.2.6.1 PDE4D expression in ex-vivo monocytes	137
4.2.7 PDE4B expression in U937PMA	139
4.2.8 PDE4B activity in U937PMA	140
4.2.9 Densitometry of PDE4 isoform expression in U937PMA.....	142
4.3.1 Changes in PDE4 response to EGF in U937PMA development.....	145
4.3.2 Changes in PDE4 response to salbutamol in U937PMA development	146
4.3.3 Changes in molecular crosstalk in macrophage development.....	149

Chapter 5 Raw 264.7 cell regulation by PDE4

5.1.1 LPS increases PDE4 activity and reduces PDE3 activity	154
5.1.2 Inhibitors of signal transduction mediators	155
5.1.3 Raw cells express 4 PDE4 isoforms.....	157
5.1.4 PDE4B2 is activated by LPS treatment.....	158
5.1.5 Increase in PDE4B2 activity is inhibited by UO126.....	159
5.2.1 Coimmunoprecipitation of PDE4 isoforms and ERK1/2.....	163
5.2.2 Back phosphorylation of PDE4B2.....	165
5.2.3 PDE4D5 co-distributes with RACK-1.....	166
5.2.4 LPS does not alter PDE4D5 distribution.....	167
5.3.1 Rolipram enhances LPS induced iNOS expression.....	171
5.3.2 Indomethacin abolishes increased iNOS expression.....	172

5.3.3 Rolipram increases cyclo-oxygenase 2 expression	173
5.3.4 Indomethacin does not inhibit increased cyclo-oxygenase 2 expression	174
5.3.5 Rolipram increases PGE2 production	174
5.3.6 Indomethacin does not prevent rolipram inhibition of TNF α production	176
5.4.1 Differential activation of ERK1/2 in RAW cells	179
5.4.2 Rolipram alters ERK1/2 activation	180
5.4.3 LPS and Rolipram phosphorylate CREB	181
5.5.1 RAW cells successfully transfected with Rap1 mutants	184
5.5.2 Rap1 activation mutants: TNF α production	185
5.5.3 Rap1 activation mutants: PGE2 production	187
5.5.4 Rap1 PKA phosphorylation mutants: TNF α production	188
 <i>Chapter 6 PDE4 IIIIV-tat fusion protein synthesis</i>	
6.1.1 Strategy for fusion protein synthesis	196
6.1.2 Sequence of PDE4-IIIIV-tat fusion	198
6.2.1 Optimisation of PCR	200
6.2.2 RFLP analysis of fusion construct	201
6.2.3 Optimisation of fusion protein expression	203
6.2.4 Optimisation of bacterial lysis	205
6.2.5.1 Sarkosyl lysis: GST pull down	207
6.2.5.2 Sarkosyl lysis: ranging experiment	208
6.2.5.3 Sarkosyl lysis: triton X100	209
6.2.6 Urea denaturation of inclusion bodies	210
 <i>Appendix</i>	
App 1.1 PDE4B4 quantification	248
App 1.2 TNF α ELISA	250
App 1.3 PGE2 ELISA	252
App 2.1 LDH assay of fractionated cells	254
App 3.1 PDE4 activity in induced sputum cells	257

List of tables

1.1 Characteristics of mammalian PDE families	9
1.2 Biochemical properties of PDE4 isoforms	14
1.3 Anti-inflammatory effects of PDE inhibitors	28
2.1 Antibodies used in thesis	55
2.2 Oligonucleotides used in thesis	56
2.3 Plasmids used in thesis	57
3.4 Kinetic characteristics of PDE4B isoforms	105
3.4.1 PKA activates PDE4B4	107
4.1 PMA increases U937 cell surface adhesion	120

This thesis is dedicated to my wife Marie Anne

I am indebted to the following people for their help in producing this thesis.

I acknowledge with thanks the support and advice I have received from both of my supervisors Professor Miles Houslay and Professor Neil Thomson.

All the members of the Houslay Lab throughout my sojourn here helped in the work described herein. I would however like to acknowledge the help offered by Dr Ian McPhee with the molecular biology techniques painfully taught and painfully learned.

The completion of this work was dependent on funding from the Medical Research Council UK. I was funded by a MRC Clinical Training Fellowship and Professor Houslay receives a programme grant from the MRC, UK.

The work described in this thesis has not been presented for submission of any other qualification or doctorate.

This thesis was composed by myself and the work described herein was performed by myself, unless noted otherwise.

Abbreviations used in the text:

AC	Adenylyl Cyclase
AM	Alveolar Macrophage
cAMP	Cyclic Adenosine Mono-Phosphate
CaM	Calmodulin
cGMP	Cyclic Guanine Mono-Phosphate
COPD	Chronic Obstructive Pulmonary Disease
COX	Cyclo-oxygenase
CRE	cAMP Response Element
ERK	Extracellular signal Regulated Kinase
GAF	cGMP binding proteins, <i>anabaena</i> adenylyl cyclase and <i>E. Coli</i> fh1A
GEF	G-protein Effector Factor
KIM	Kinase Interaction Motif
LPS	Lipopolysaccharide
5-LO	5-Lipo-oxygenase
PBM	Peripheral Blood Monocytes
PI 3-Kinase	Phosphatidyl Inositol 3-Kinase
PKA	Protein Kinase A
PKC	Protein Kinase C
RT-PCR	Reverse Transcriptase Polymerase Chain Reaction
SDS-PAGE	Sodium Dodecyl Sulphate Polyacrylamide Gel Electrophoresis
STR	Serine Target Residue
UCR	Upstream Conserved Region

..... to reflect that these elaborately constructed forms, so different from each other, and dependent on each other in so complex a manner, have all been produced by laws acting around us.

..... There is grandeur in this view of life, with its several powers, having been originally breathed into a few forms or into one; and that, whilst this planet has gone cycling on according to the fixed law of gravity, from so simple a beginning endless forms most beautiful and most wonderful have been, and are being, evolved.

Charles Darwin
(from *The Origin of Species*)

Chapter 1 Introduction

1.1 Biological diversity

Darwin identified species diversity as the stimulus to scientific investigation that eventually led to our modern understanding of evolution. Careful cataloguing inspired observation, thoughtful interpretation and the willful incorporation of ideas from different scientific disciplines all led to the theory. Appreciating the similarities and differences between species has led to greater understanding of animal behavior and interaction in nature. Recently similar methods have been applied across biological science disciplines. Understanding molecular diversity offers the modern investigator the keys to unlocking the complexity of the cell, as species diversity did for nature 150 years ago. That it takes just 30,000 genes to produce a fully mature human suggests there is little redundancy in the expressed genome and that each transcribed gene serves a specific or multiple defined purposes. Understanding the purpose of each gene or protein product will eventually lead to a fuller understanding of biological life. One means of achieving these insights is to compare proteins with a high level of sequence homology and to identify how they differ. Just as Darwin observed with Galapagos finches such differences might reveal structural adaptations designed to fulfill specific purposes.

Families of molecules generated by gene duplication exist abundantly within the genome. The phosphodiesterase (PDE) family of cyclic nucleotide hydrolysis enzymes is such a family. This thesis represents work performed to observe the characteristics of one sub-family of this group, the PDE4 family, within the context of inflammation and specifically with reference to macrophage function. By observing differential behavior of PDE4 isoforms I hope to gain insights into the overall role of these molecules in regulating inflammation.

This introduction will begin by describing the molecular diversity of cAMP signaling apparatus before focussing on the PDE4 family itself. I will describe previous insights into PDE4 in inflammation generally and then discuss macrophages in detail. Finally I will describe work that has looked at PDE4 and cAMP regulation of some key macrophage mediators that I will later expand on in the experimental sections.

1.2 Cyclic amp signaling

Cyclic AMP (cAMP), signalling can be considered in three phases, synthesis, detection and hydrolysis. Enzymes involved at each step of this process exist as multiple isoforms. Figure 1.1 illustrates the different levels of diversity.

1.2.1 An Overview

Cells receive information from extracellular signals that must be transformed into intracellular information to produce behavioural change. The discovery in the late 1950's of cyclic AMP by Sutherland et al, introduced the era of the second messenger [1]. These are a diverse family of molecules allowing signal amplification and refinement. Cyclic AMP and its relative cyclic GMP are cyclic purine nucleotides synthesised from their respective triphosphate precursors by cyclase enzymes. In response to various ligands, Gs α coupled receptors activate adenylyl cyclase which produces cAMP. Due to the high availability of its substrate ATP, adenylyl cyclase (AC) operates at V_{max} when active. Therefore the levels of cAMP generated by a signal depend partially on adenylyl cyclase, but also on the rate of degradation.

The sole means of degrading cyclic nucleotides and thus signal limitation are hydrolysing enzymes called phosphodiesterases [2]. These enzymes form a family of cAMP specific, cGMP specific or dual specificity 3',5'cyclic nucleotide hydrolysing enzymes [3]. Normally they function at less than V_{max} and can be up or down regulated in activity to

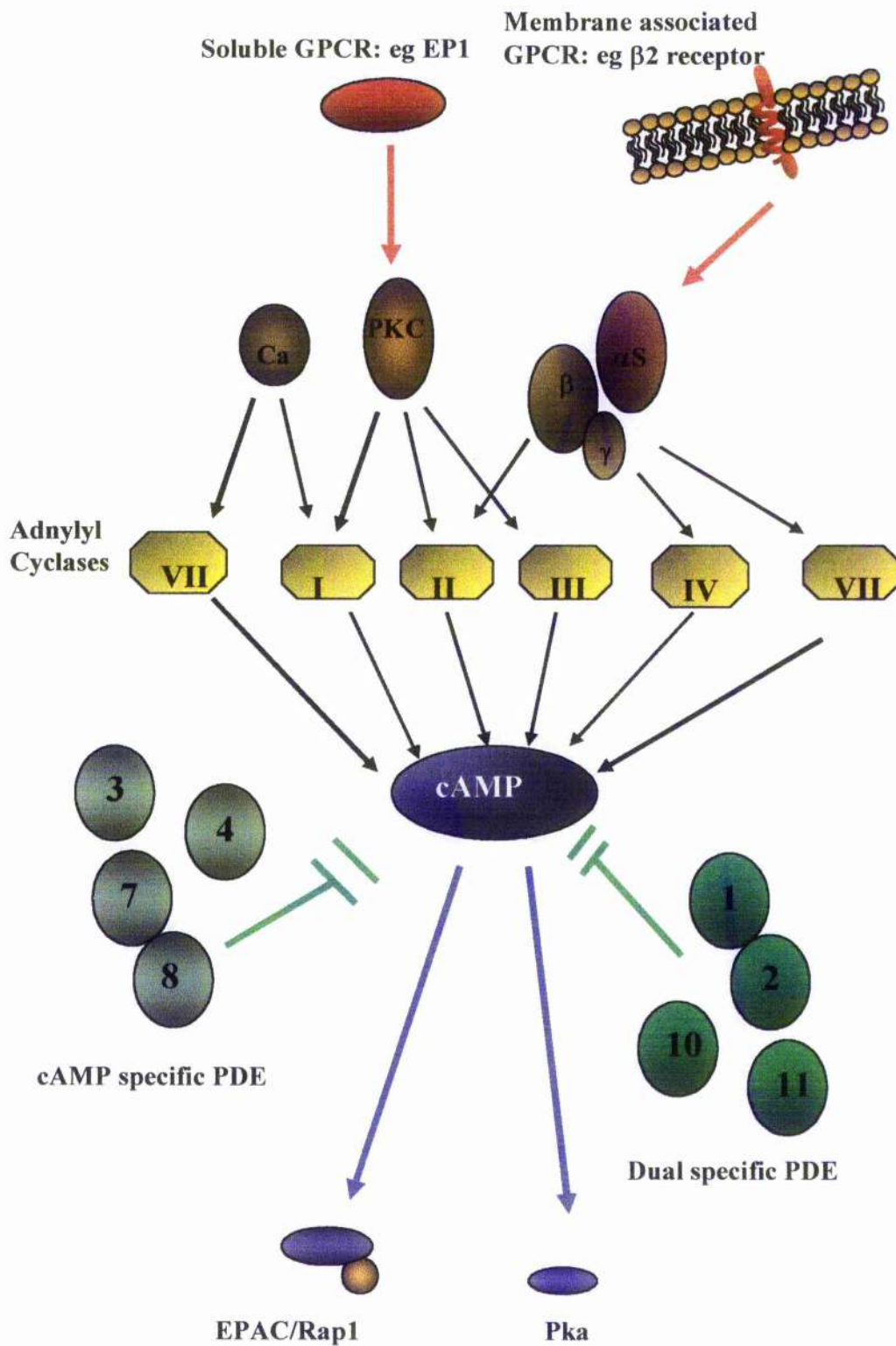


Fig 1.1 Multiple signalling proteins involved in regulating cAMP signal transduction

Many proteins that influence cAMP signals exist as multi-member families. Illustrated above are the PDE and Adenylyl cyclase families and some of the factors that influence their activity.

limit or enhance a cyclic nucleotide signal and can therefore influence both the magnitude and the duration of a signal [4].

I will describe the molecular diversity of each level of cAMP regulation and attempt to demonstrate functional significance for this molecular variation.

1.2.2 Adenylyl Cyclase

At least 9 adenylyl cyclase (AC) genes exist encoding AC types 1-9 [5] with differential splicing of the mRNA products of AC5, AC6 and AC8, increasing molecular diversity [6]. Each AC contains 2 membrane-spanning units called M_1 and M_2 and 2 catalytic units C_1 and C_2 . Each M unit consists of 6 transmembrane domains with an ion channel like structure [5]. Further complexity exists due to splice variation of the C sub-units resulting in C_1A and C_1B isoforms and C_2A and C_2B isoforms [7] with C_1B containing many regulatory domains[8]. Significant degrees of molecular diversity therefore exist at the point of cAMP synthesis.

Molecular diversity underlies differential AC activation and regulation [8]. Thus while most AC enzymes are activated by the GTP bound form of G-protein $S\alpha$ (GTP- $Gs\alpha$) and Forskolin, AC 9 is not, [9, 10]. AC isoforms are under specific regulatory control. For example, inhibition of AC by Mn^{2+} occurs to different degrees in different AC isoforms [11]. Inert purine rings can inactivate AC by P site inactivation. AC isoforms are differentially regulated by such P site inhibitors, [12]. The G protein $Gi\alpha$ selectively inhibits AC5 and AC6, while PKC can specifically activate AC2 [8] [13]. Finally, while the G protein complex $G\beta\gamma$ inhibits the function of AC 1 it synergises with $Gs\alpha$, in the activation of AC2 and AC4 [14]. Molecular diversity therefore translates into isoform specific biochemical regulation.

Granneman et al demonstrated the physiological significance of molecular differences in brown adipose tissue where a variety of AC isoforms are expressed. Cyclic AMP production was increased by β 2 agonists, but only AC3 activity was increased [15]. Diversity of the molecular structure of AC isoforms has therefore been shown to have biochemical and functional significance.

1.2.3 Cyclic AMP detection

Until recently it was believed that the sole means of propagating a cAMP signal was to activate protein kinase A (PKA). This remains an important downstream target, but has been joined by a small G-protein Effector Factor (GEF) molecule called EPAC.

1.2.3.1 Protein Kinase A

Protein kinase A (PKA) is a heterotetramer composed of two regulatory and two catalytic subunits termed R and C, forming a holoenzyme termed R_2C_2 [16, 17] for which the crystal structure has been solved [18, 19]. PKA is activated by cAMP binding to the R subunit leading to a conformational change and release of the active C [18, 20]. PKA C subunit is a serine threonine kinase and targets domains containing X-Arg-Arg-X-Ser/Thre-X motifs [21]. Targets for C subunit kinase range from ion channels to transcription factors, [22-24]. Elevated cAMP can increase or decrease gene transcription by virtue of PKA dependent phosphorylation of cAMP response element binding protein (CREB) [6, 25, 26]. Therefore functional diversity exists at a cellular level by virtue of the range of substrates expressed by a cell.

The molecular diversity of PKA was initially identified by DEAE elution of 2 isoforms [27] corresponding to 2 isoforms of the R subunit RI and RII. Genetic analysis has revealed further complexity by demonstrating four isoforms RI α , RI β , RII α and RII β [16, 28]. Three C subunit isoforms have been identified C α , C β and C γ . C subunits express

tissue specificity with C β being enriched in brain [29] and C γ being exclusively expressed in testis [30]. Tissue specific expression of R subunit isoforms suggests important functional differences. For instance RI β is highly expressed in brain, while responses of certain regions of the brain to cAMP correlates with the expression of RII β subunit [31, 32]. Differences between the classes of R subunit also exist in terms of intracellular distribution, with RI being predominantly cytosolic and RII occurring mainly in the particulate fraction[33]. Kondrashin et al took this analysis further and found RII α enriched in the golgi and mitochondria of cells fractionated in sucrose gradients [34]. The R subunit thus serves to target the holoenzyme to specific subcellular locations.

The nature of this targeting has recently been illuminated by the discovery of a new family of proteins known as A Kinase Anchoring Proteins (AKAP) [35]. These structurally diverse proteins are targeted within the cell by protein-protein and protein-lipid interactions. Tissue specific AKAP expression may refine the response of a particular tissue to an adenylyl cyclase activating hormone [36]. AKAP proteins bind PKA R subunits at their N-terminal and target the PKA holoenzyme within the cell.

Finally the sensitivity of different R subunits to cAMP is known to vary. Thus RI β is relatively insensitive to cAMP, and the regions of rat brain rich in RII β are those areas known to be less responsive to cAMP [32].

Variations in intracellular targeting, tissue specific expression and sensitivity to cAMP concentration all regulate the PKA mediated response, allowing the cell to precisely control its response to cAMP by differential protein expression.

1.2.3.2 Rap-1 a novel cAMP signal transducer

The discovery of the cAMP sensitive, Rap-1 activating GEF, EPAC added to the complexity of cAMP signaling [37, 38]. Rap-1 is a GTPase sharing 50% sequence

homology with Ras, particularly at the Ras protein interaction domain [39]. Rap-1 has significant homology to a drosophila gene which when knocked out led to a lethal mutation [40], suggesting that its function is non-redundant despite significant homology to other proteins. Cyclic AMP, calcium (Ca^{2+}) and diacyl glycerol (DAG), can all activate Rap-1 [41, 42]. Cyclic AMP was shown to phosphorylate Rap-1 in a PKA dependent manner in prostacyclin treated neutrophils [43] and it was believed that cAMP activation of Rap-1 was due to this effect. The only Rap-1 PKA target sequence is at the C-terminal some distance from the sites of GTP binding, however and it may be that PKA phosphorylation affects targeting rather than activity [44]. Kawasaki et al demonstrated that a PKA deficient CHO cell could activate Rap-1 in response to cAMP [45]. Finally EPAC was discovered to directly activate Rap-1 in a cAMP dependent manner and PKA was shown to reduce Rap-1, raf binding activity [38, 46].

Evidence for two separate mechanisms of cAMP detection and downstream signaling have therefore been found. Cyclic AMP signaling thus displays molecular diversity at synthesis, sensing and substrate levels, leading to variable functional outcomes as I have described. It is essential that the cell can limit the “dose” of cAMP to which it is exposed. This limitation is provided by the cyclic nucleotide phosphodiesterases. I will next outline some of the salient features of this family, and deal with PDE4 in detail in the next section.

1.2.4 Phosphodiesterases

1.2.4.1 Homogeneity and heterogeneity

Sutherland described cyclic nucleotide hydrolysing activity from heart extract in 1970 [47]. It soon became apparent by anion exchange chromatography that this activity existed in different forms, suggesting the existence of a family of enzymes with similar biochemical properties [48, 49]. The development of advanced molecular biological techniques has

confirmed this assumption and shed light on the enormous degree of complexity within this family [50]. Nineteen genes encode members of the eleven PDE families suggesting some degree of differential function. Differential tissue and developmental expression, different kinetic properties and specific affinities for substrate and inhibitors supports the notion that individual PDEs exist to serve specific functions [4].

Two major classes of PDE have been described. Class I enzymes share homology over a region of approximately 300 amino acids, of which 56 amino acids are identical between the *Drosophila dunce* gene product, the slime mould *Dictyostelium reg-A* gene product, the putative *C. elegans* PDE and human PDE4s [51]. This highly conserved region correlates to the catalytic domain and points to a single ancestral gene. Class II PDEs are a group of enzymes conserved in yeast, bacteria and slime moulds. They lack the catalytic domain as in class I and are secreted proteins. To date no mammalian homologue of class II PDEs has been identified [51].

The PDE4 family will form the focus of this thesis, but some important aspects of PDE biology are learned from studying the shared or divergent characteristics of the other members of this superfamily. The agreed convention on nomenclature grouped PDE families by functional characteristics, based on substrate specificity and inhibitor sensitivity. PDE characteristics are summarised in table 1.1. Important functional aspects are outlined below.

PDE	Defining Characteristic	Substrate specificity	Number of genes	Chromosomal locations	Number of isoforms
PDE1	Ca ²⁺ /CaM activated	CAMP	PDE1A	A-?	A-2
		CGMP	PDE1B	B-12q13	B-1
			PDE1C	C-7	C-5
PDE 2	cGMP activated	CAMP CGMP		?	
PDE 3	cGMP inhibited	CAMP	PDE3A PDE3B	11p15.1 11p15	A-3 B-1
PDE 4	Rolipram inhibited	CAMP	PDE4A	19p13.2	A-6
			PDE4B	1p31	B-3
			PDE4C	19p13.1	C-3
			PDE4D	5q12	D-5
PDE 5		CGMP	PDE5A PDE5B		
PDE 6	Photoreceptor	CGMP	PDE6A PDE6B PDE6C		
			PDE7A		A-2
			PDE7B		B-1
PDE 8	IBMX resistant	CAMP	PDE8A PDE8B		
PDE 9	IBMX resistant	CGMP			
PDE10		CGMP			
PDE11		CAMP CGMP	PDE11A		A-3

Table 1.1 Characteristics of mammalian PDE families

Cyclic nucleotide phosphodiesterase activity exists as a multi-member family of enzymes each with specific characteristics. Three groups of enzymes are recognised: Dual specific PDE; cAMP specific PDE and cGMP specific PDE. Each family is further subdivided into gene products and mRNA splice variants, resulting in multiple isoforms.

1.2.4.2 Structural organisation

Phosphodiesterase enzymes share a common modular structure with different domains encoding different biochemical properties [50]. Figure 1.2 details the important domains.

I. Catalytic domain

The highly conserved region described above encodes the catalytic region located towards the C-terminal of PDE proteins. Analysis of the conserved regions within the catalytic domain demonstrates further modular organisation with 10 putative functional regions [51]. These regions regulate the activity of the enzyme and have been studied in a variety of PDE families. For example domains II and IV encode regions homologous to zinc binding domains in other zinc binding hydrolases. Mutations of charged amino acids in these domains reduce or abolish PDE activity in PDE3, PDE4 and PDE5 [52]. Zinc has been shown to support PDE3 and PDE5 activity [53]. Other catalytic domains of interest are I and III which regulate rolipram binding to PDE4, whereas mutation of regions VIII and IX abolish rolipram inhibition of PDE4, but do not affect binding [51, 54]. The modular organisation of the entire molecule is therefore mirrored in the conserved catalytic domain. Less structural homology exists between PDE isoforms over the non-catalytic regions.

II. Carboxyl Terminus

The extreme C terminus contains an hydrophilic region in which conserved regions of acidic amino acids exist [50]. The role of these amino acids is not known. With the exception of PDE1, PDE C-terminal regions are shared by PDE gene products. This allows the immunological identification of PDE4 gene families by raising antiserum against the C-terminal regions. Thus PDE4A, PDE4B, PDE4C and PDE4D can be differentiated on immunological grounds.

III. NH₃ terminus

The PDE N-terminal region lies up stream of the catalytic core and is known as the regulatory domain (Figure 1.2). It is in this region that molecular modifications regulate PDE activity. For example it is in this region that the calmodulin (CaM) binding site on PDE1 is found [55]. Ca²⁺/CaM binding to this domain increases PDE1 activity and individual PDE1 isoforms are structurally distinct at this domain suggesting differential regulation by Ca²⁺/CaM [56]. A protein module known as GAF (cGMP binding proteins, *anabaena* adenylyl cyclase and *E. Coli* fh1A) has been found on PDE 2, PDE5, PDE6, PDE10 and PDE11 [57, 58]. Each family expresses two GAF domains in close proximity that bind cGMP increasing the enzyme activity (Fig 1.2).

Further regulatory domains are to be found in the N termini of other PDE families. These include PDE4 enzyme regulated kinase (ERK) substrate domains at which phosphorylation influences activity described in more detail in a later section. Thus molecular diversity of the N-terminals results in enzymes with the same catalytic function with specific regulatory properties.

1.2.4.3 Genetic Organisation

Early studies carried out on the drosophila dunce gene complex were the first to give insight into the complexity of PDE gene organisation [50]. Dunce gene deletion gave rise to learning difficulties and sterility in fruit flies [59]. Each problem could be produced alone or together by differential mutation of the various promoters in the notch complex upstream of the dunce gene itself. Thus it was clear that different tissue expression of the dunce gene product was under the control of different promoters regulating specific

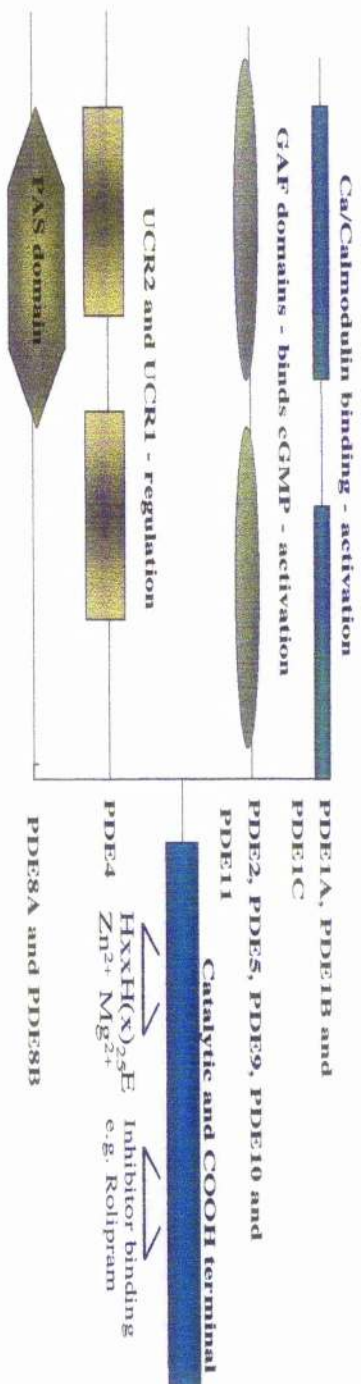


Fig1.2 PDE N terminal regulatory units unique and shared domains between families

The N terminal regions of PDE family members contain modules that regulate enzyme activity and subcellular targeting. Some of these, such as UCR domains are unique to one family (PDE4), while others e.g. GAF domains have been incorporated into the structure of multiple members of the family. Such diversity at the N terminal region is in contrast to the high level of homology at the C-terminal, and catalytic domain.

transcriptional units [50]. Further studies on slime moulds demonstrated that different promoters regulated PDE genes at different stages of maturation.

Similar differential regulation of PDE expression between tissues and at different stages of maturation is seen in mammalian tissues. Rat brain provides a rich source of PDE isoforms, which are not found elsewhere in the body e.g. PDE4A1, and various models of cellular differentiation have demonstrated stage specific expression of PDE in a manner reminiscent of the *drosophila dunce* gene [60, 61].

1.3 Phosphodiesterase 4 a study in biological diversity

It is outwith the scope of this review to detail all the structure-function relationships that define specific PDE4 isoforms. In summarising these relationships I will select specific domains within the molecules and attempt to show how these produce functional diversity based on molecular difference. Table 1.2 details specific characteristics of each PDE4 isoform. PDE4 is a family of cAMP specific, rolipram sensitive cyclic nucleotide hydrolysing enzymes. The family is encoded by 4 genes A, B, C and D and splice variation provides additional complexity [50]. As described for PDE enzymes in general significant homology exists at the catalytic domain between all PDE4 isoforms. Gene families are defined at the molecular level by sharing an extreme C-terminal, while N-terminal regions have varying degrees of homology between specific PDE4 isoforms. Finally isoform specificity is defined at the extreme N-terminal.

1.3.1 PDE4 structure

PDE4 genes each code for multiple forms of their enzyme product. This occurs by mRNA splicing at specific splice domains.

Gene	Isoform (clone)	Rat homologue	Molecular Wt (kDa)	Km(μ M) Cytosol	Vmax		IC ₅₀	Distribution %			Regulation	
					P	C		P	C	P1	P2	S2
PDE4A	1(huRD1)	RD1	85	3	N.A	0.3	-	All				
	4(pde46)	Rnpde4A.5	99 / 125	2	0.5	1	0.2	1.6	12		88	
	10	Rnpde4A10	XX / 120	2.9	0.3	1	0.52	0.56	4	13	83	+
PDE4B	1(TM72)	rpde4B1	84 / 104	2	1	0.05/0.08	17	11	71			+
	2(pde32)	rpde4B2	64 / 80	3	4	0.21/0.02	26	12	61			+
	3	rpde4B3	82 / 103	1.5	2	0.1 / 0.05	23	17	58			-
PDE4C	1 (pde21)	Rpde4C1										
	2		68 / 80	0.6	0.6		0.08					
PDE4D	1(dun 411)	Rpde4D1	66 / 68	1.2	1.0	N.A./0.05						
	2(pde82)	Rpde4D2	58 / 67	1.3	1.1	N.A./0.05						
	3(pde43)	Rpde4D3	77 / 95	1.0	1.2	0.32/0.14	50		50			+
	4(pde39)	Rpde4D4	91 / 119	1.0	2.9	0.05/0.06						+
	5(pde79)	Rpde4D5	84 / 105	1.0	1.5	0.59 / 0.08						+

Table 1.2 Biochemical properties of the major PDE4 isoforms expressed in mammalian tissues

Physical data as reported in the literature is presented. Where little or no information is available on the human isoforms no information is given. Thus only three of the multiple variants of the PDE4A gene are reported. (Pred, predicted molecular weight based on amino acid sequence; Obs, observed molecular weight based on electrophoretic mobility; P, particulate bound PDE4; C, soluble PDE4).

1.3.1.1 Splice Junctions – "Long form" and "Short form" distinction

All PDE4 genes encode two splice junctions [62], the first lies immediately upstream of the sequence of the conserved region upstream conserved region 2, (UCR2). Splicing of mRNA at this site produces "short-forms" with N-terminal sequence immediately following UCR2 and "long forms" with common sequence including UCR1. Long forms have N-terminal sequence after UCR1 [63]. Every PDE4 gene except PDE4C encodes both long and short form enzymes. In addition to this distinction the PDE4A gene encodes two 'super-short' enzymes known as PDE4A1 and PDE4A8 [64]. The former has N-terminal sequence extending from approximately half the UCR2 region while the latter, recently shown to exist in vivo, lacks any UCR domains and encodes the 'core' catalytic domain[64].

1.3.1.2 UCR1 and UCR2

By aligning different long form PDE4 sequences Bolger et al identified two regions of sequence homology [63], conserved within PDE4 isoforms but not found in other PDE families. The 33 residue linker region 1 (LR1) separates UCR1 and UCR2. The net polarity of UCR1 is +1 making it an attractive site for conformational regulation by phosphorylation. This has been demonstrated by Mackenzie et al [65] who demonstrated ERK2 phosphorylation of PDE4D3 led to inhibition by the UCR1/UCR2 module. This confirmed the work of Hoffman et al [66]], who demonstrated that EGF treatment of cells overexpressing PDE4D3 reduced PDE4 activity. Further confirmation was provided by Baillic et al [67] who showed that short form PDE4 isoforms, lacking UCR1, were activated by ERK2 phosphorylation of the catalytic region.

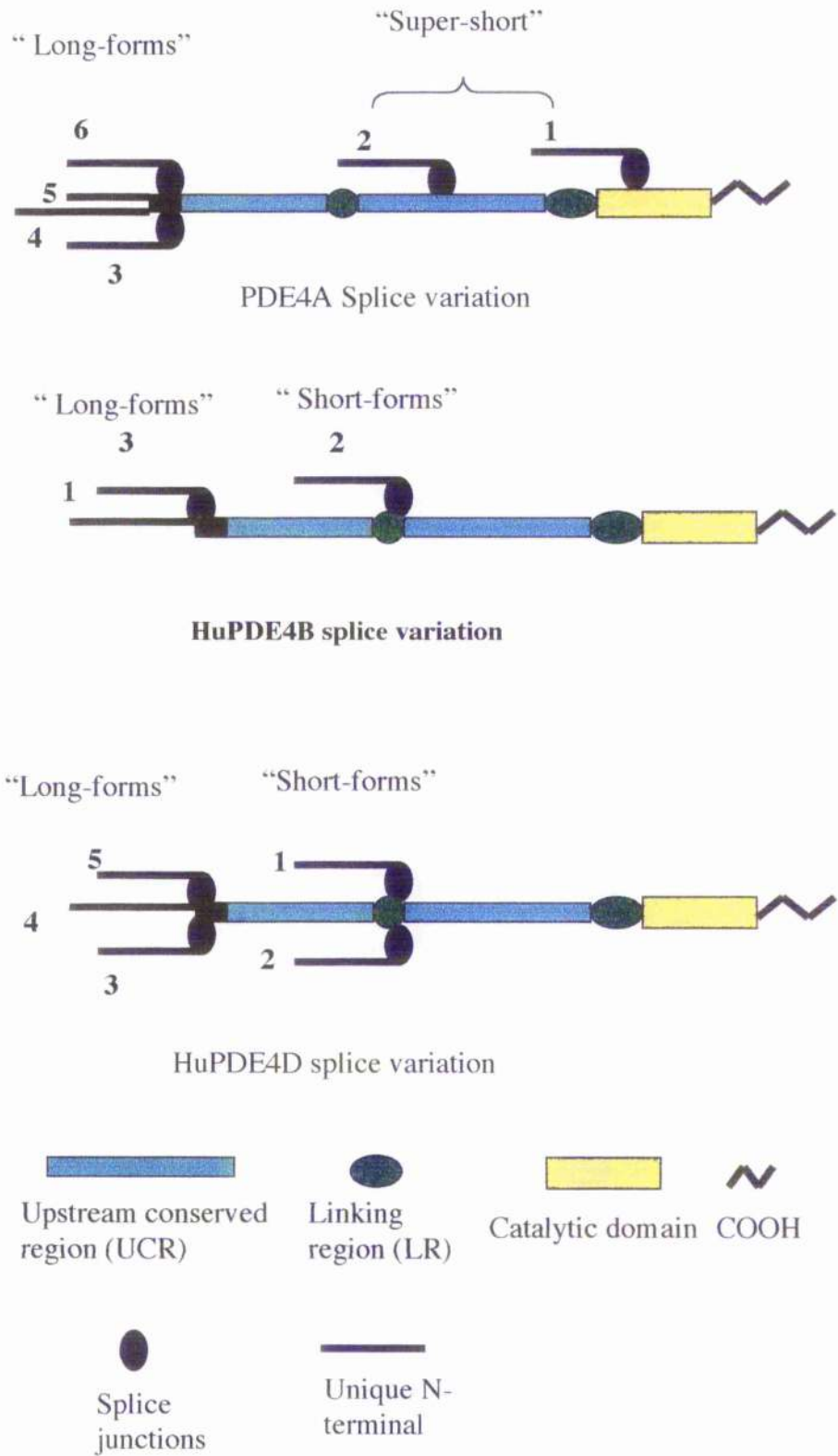


Fig 1.3 The variability between *PDE4* isoforms is governed by mRNA splice variation. Each *PDE4* gene codes for a variety of isoforms in which size (long or short form), number of regulatory regions (UCR) and site of unique N terminal region, is governed by differential use of splice junctions. *PDE4A*, *PDE4B* and *PDE4D* are schematically represented. Conserved regions are colour coded, unique regions are black.

UCR1 contains a substrate site for phosphorylation by PKA (serine target residue, STR), [68]. In PDE4D3 this is Ser54, although this isoform also contains a PKA STR at Ser13. Sette et al demonstrated that it was Ser54 that was responsible for the rapid activation of PDE4D3 in FRTL-5 TSH sensitive cells [68]. PKA phosphorylation of PDE4D3, also prevents the inhibitory effect of ERK2 phosphorylation [65]. This is likely to be due to uncoupling of the protein-protein interaction between UCR1 and UCR2 demonstrated by Beard et al [69].

N-terminal regions of PDE4 isoforms therefore limit the activity of the enzymes. This is probably due to interaction of UCR1/UCR2 modules altering substrate access to the catalytic domain. It follows that enzymes lacking these regions should have enhanced activity. A synthetic enzyme containing the core of the PDE4A enzyme, (the catalytic region and the extreme C-terminal) known as met²⁶-RD1 was shown to have significantly higher activity than its progenitor PDE4A1 or other PDE4A enzymes [70, 71]. Indeed h6.1 an N-terminal truncation of PDE4A4, had a Vmax relative to its progenitor enzyme 11.5 times greater.

The region of most variability between PDE4 isoforms therefore dictates functional regulation of each isoform.

1.3.1.3 Targeting

I. Sub-cellular distribution

Analysis of the characteristics of met²⁶-RD1 described above found it to be entirely soluble [70, 71] suggesting that the N-terminal region was involved in targeting PDE4 isoforms to subcellular locations [72]. The addition of the PDE4A1 23 N-terminal residues absent from met²⁶-RD1 to make a chimera with the normally soluble chloramphenicol acetyl

transferase (CAT) resulted membrane binding [73, 74]. This is due to N-terminal tryptophan residues in PDE4A1 that allow the Ca^{2+} dependent association with phosphatidic acid enriched domains in the cell membrane. This region of PDE4A1 has been termed TAPAS-1 [75]. In comparison to PDE4A1 the long form PDE4A4 co-distributes between particulate and soluble compartments [76]. The long form PDE4D isoforms (PDE4D3, PDE4D4 and PDE4D5) which are co-distributed between particulate and cytosolic compartments of disrupted cells, differ from their short form counterparts (PDE4D1 and PDE4D2) which are exclusively cytosolic [77, 78].

The N-terminal variable region therefore also regulates subcellular targeting of PDE4 isoforms.

II. Protein – protein interaction

Protein-protein interaction domains on signalling proteins allow incorporation into macro-molecular signalling complexes and association with scaffold proteins. SH3 domains bind to proline rich regions of other proteins [79, 80]. Analysis of PDE4A5 reveals two class 1 SH3 binding domains in the N-terminal region [81]. These were shown to confer association with the SH3 domains of the src family kinases lyn, fyn and src [81, 82]. This interaction reduced PDE4A5 activity suggesting that association with Lyn kinase leads to an increase in the local cAMP concentration. Analysis of PDE4D4 revealed SH3 binding domains, and src family association is therefore not exclusive to PDE4A5 within the PDE4 family [83].

PDE4D5 has been shown to bind the protein RACK1 [84]. RACK1 was originally described as a protein able to bind and translocate activated PKC- β [85, 86]. It has since been shown to be a scaffold protein binding other signal transduction proteins including Integrins, c-src and the common β chain of the interleukin receptor [87-89]. PDE4D5

interacts with RACK1 via an N-terminal domain and the last 3 WD repeats of RACK1's 7 WD repeat structure [90].

The N-terminal regions of PDE4 isoforms have therefore been shown to be important in both localisation and regulation of activity.

1.3.1.4 Catalytic domain

The sequence of the PDE4 catalytic domain has excited considerable interest, as it corresponds to the site of rolipram binding and governs the therapeutic potential for PDE4 inhibitors. Two conformations of this site have been described, high affinity for rolipram binding site (HARBS) and a low affinity site (LARBS) [91]. HARBS binding by rolipram appears to occur with an affinity that relates closely to rolipram's ability to induce emesis. LARBS binding affinity conforms to anti-inflammatory and bronchodilator properties [92, 93]. Torphy et al demonstrated that histidines 506 and possibly 505 were required for cAMP binding to the catalytic core of PDE4A but were not required for rolipram binding [94]. Mutational analysis of other histidine sites at amino acids 433, 437, 473 and 477 demonstrated decreased rolipram association. The same group later demonstrated that two conserved histidine containing domains HNXXH (motif I), and HDXXH (motif II), were essential for cAMP hydrolysing activity [52]. Motif I inactivity mutants lost all activity while motif II mutants lost 50% activity. Each domain proves to be a ligand for divalent cations such as Zn^{2+} or Mg^{2+} suggesting that full activity and rolipram binding activity depends on structural conformation dependent on metal ion binding. Thus structural analysis demonstrates that different PDE4 isoforms may interact with both substrate and inhibitors differentially depending on the ability of regions of the catalytic domain to form particular conformations. The importance of overall molecular structure influenced by N-terminal domain binding becomes apparent.

A second level of regulation based on molecular structure lies in two sequences found in the catalytic core of PDE4D3. These ERK2 docking domains provide the necessary sites for ERK2/PDE4D3 interaction to allow phosphorylation of the Ser residue at 579. Phosphorylation results in inhibition of long form PDE4 isoforms. Figure 1.2 highlights these important regions of the catalytic core [66].

1.3.1.5 COOH-domain

The biological purpose of the extreme C-terminal remains obscure. This region is shared between all members of a gene family and thus allows immunological identification. Separation of immunologically related PDE4 isoforms by migration on SDS-PAGE allows discrimination between family members. The purpose of this domain is not understood.

1.3.2 Biological diversity - consequences

The existence of a large family of enzymes with the same or closely related biochemical properties begs the question why do we need so many? The differences in regulation and expression outlined above suggest that each PDE and PDE4 in particular may serve specific functions. This in turn would suggest that cAMP though pluripotent is strictly regulated to perform specific tasks under certain conditions.

1.3.2.1 Compartmentalisation of cAMP signalling

The hypothesis of compartmentalisation suggests that functional pools of signalling chemicals and proteins exist in discrete "compartments" within the cell [95, 96]. By regulating the mix of proteins within these compartments cells can regulate the specific response to any given signal. By varying the enzymes, substrates and chemical messengers in different compartments at the same time a cell could generate multiple responses to a

given signal. This hypothesis waits rigorous testing, but offers a neat explanation for the diversity of PDE4 isoforms.

1.3.2.1.1 Evidence for compartmentalisation

Keely et al, demonstrated that epinephrine and PGE2 elevated myocardiocyte cAMP causing the PKA phosphorylation of a range of proteins, but isoproterenol caused the phosphorylation of approximately 16 more PKA targets [97]. Further examples of functional compartmentalization exist. Of interest in the context of this thesis is the work of Dousa et al, who demonstrated in renal mesangial cells, a distinction between PDE3 and PDE4 regulation of cellular behaviour despite equivalent increases in intracellular cAMP, [98].

Compartmentalisation would require physical localisation of the elements of cAMP signaling within the cell and such targeting was shown by Jurevics and Fischmeister when they treated frog ventricular myocytes with isoproterenol [99]. They found that although L-type Ca channels were widely disseminated in cells only those close to β_2 receptors were phosphorylated by PKA. Initial attempts to localise cAMP within cells were hampered by the tendency for cAMP to diffuse or leach out of areas. Using microwave fixing technology Barsony and Marx demonstrated discrete pools of cAMP forming after stimulation with different ligands [100]. More recently fluorescent RII subunits of PKA has allowed FRET analysis to be used by Tsien et al [101]. They demonstrated 5-HT induced pools of cAMP within neuronal dendrites. Thus evidence has accumulated that non-random distribution of cAMP occurs within cells.

Finally evidence supporting the functional compartmentalization of cAMP signaling in inflammation was provided by Ahmad et al [102]. This group observed a distinction between the PDE isoforms activated by different pro-inflammatory agents. Thus while IL-3 activated both PDE4 and PDE3, IL-4 selectively activated PDE4.

Thus considerable evidence exists, from diverse experimental fields supporting the concept of compartmentalization.

1.3.2.1.2 The molecular basis of compartmentalisation

For compartmentalization of a second messenger to occur certain prerequisites must be met [4]. First both a synthetic and a sensing device must exist that can be targeted within the cell. In the case of cAMP these criteria are met. I have described multiple forms of Adenylyl cyclase targeted by 6 transmembrane helices. The strongest evidence for targeting however exists for the cAMP sensing system PKA and its binding partner AKAP described above. Neurone post-synaptic densities are enriched in AKAP79 [103], AKAP15 is associated with skeletal muscle Ca^{2+} channels [104] and S-AKAP84 expression is developmentally regulated in male germ cells [105]. Therefore PKA targeting can be regulated in a subcellular and developmental fashion. If discrete pools of cAMP can be synthesised, targeting PKA to these pools regulates which of the various R_2C_2 enzyme modules is activated.

The second requirement for Compartmentalisation of signaling molecules, is a means to prevent 'spillage' that could result in random activation of sensing molecules. This requires cAMP hydrolysing activity targeted within the cell. PDE is the only means of hydrolysing cAMP and I have already described the accumulating evidence for PDE4 targeting.

PDE targeting may explain why such a diversity of molecules exists. An elegant study by Juilfs et al, looked at PDE distribution in olfactory neurones, by immunofluorescence [106]. They demonstrated that PDE1C2 co-localised with AC3 in the cilia that protrude into the nasal mucosa and respond to odorants. It is believed that this complex regulates the early phase of odorant receptor signaling. While PDE1C is absent from the axon and cell body, PDE4A can be found. These studies suggest that within the complex structure of a neurone

PDE isoform distribution is not random. Like the studies described above for individual PDE4 isoforms, the PDE3 family has been intensively investigated with regards to intracellular targeting. PDE3A1 and PDE3B have each been isolated from membrane structures including ER and SR of mycardiocytes and adipocytes [107]. The N-terminal region of these isoforms contains a hydrophobic rich region believed to form 6 transmembrane helices. Deletion analysis shows loss of membrane association when these regions are removed. A third PDE3 species, PDE3A2 has been identified recently. Sequence analysis demonstrates alternative splicing to provide a short N-terminal highly polar region [108]. As expected, recombinant expression of this molecule yields a mainly cytosolic distribution.

1.3.2.1.3 Compartmentalisation - summary

All the requirements for compartmentalisation can be met by the molecules involved in cAMP signal transduction. This theory may therefore partially explain the requirement for such a large degree of molecular diversity within the PDE4 family. Alternative explanations for the evolutionary persistence of such a large family, however include the concept of inter-molecular crosstalk.

1.3.2.2 Molecular Crosstalk

Integration of multiple signalling pathways allows refinement of these pathways to take account of additional intracellular messages. This concept is known as crosstalk. [96].

1.3.2.2.1 Evidence for crosstalk

Evidence for crosstalk between the cAMP signalling cascade and other pathways is accumulating. Lin et al demonstrated in RAW murine macrophages, that activation of PKC potentiated the prostaglandin E2 activation of AC [109] and Dowd et al found cAMP

potentiation of Ca^{2+} induced gene transcription en route to apoptosis [110]. Another group examined the integration of PKA and ERK1 and ERK2 activation [111] and demonstrated PKA phosphorylation at the Kinase Interaction Motif (KIM) of ERK isoforms prevented the dephosphorylation by phosphatase. Therefore multiple examples of other signalling pathways feeding into cAMP signal transduction have been described.

1.3.2.2.2 PDE4 and molecular crosstalk

Both the cAMP cascade and the ERK1/2 MAPKinase signalling pathways regulate PDE4. PDE4B, PDE4C and PDE4D families have an ERK1/2 KIM domain in the catalytic region [65, 66]. This allows phosphorylation of Ser579 (named as for PDE4D3) and the inhibition of long form PDE4 activity, the short form PDE4B2, however is activated by ERK1/2 [67]. PDE4A isoforms appear to be insensitive to ERK1/2 phosphorylation. PDE4A4 however, is sensitive to PI-3 kinase and may integrate a different series of signalling pathways [112]. Varying PDE4 isoform expression will alter the overall PDE4 response to a specific signalling environment.

1.3.2.2.3 Summary molecular crosstalk

PDE4 isoforms may thus play an important role in the integration of signalling cascades. By altering their activity in response to different environments the level of cAMP can be tightly regulated.

1.3.3 PDE4 Diversity – Conclusions

PDE4 isoforms are a diverse group of enzymes, each of which has the same catalytic activity. Such a multitude of isoforms in spite of evolutionary pressure to economise the expressed genome implies specific functions for each. I have demonstrated that molecular diversity exists at every level of cAMP signalling from synthesis by adenylyl cyclase,

sensing by PKA and Rap-1 and most impressively degradation by PDE. Clues to the specific function can be made from analysis of the molecular sequence for each PDE4 isoform. Thus KIM domains in the catalytic region allows crosstalk between ERK1/2 and cAMP. PKA phosphorylation complicates molecular crosstalk by abolishing the effects of ERK1/2 inhibition. Finally targeting of PDE4 isoforms could allow compartmentalisation of cAMP signal and provide a mechanism for large macromolecular complexes to be formed.

Differential expression of PDE4 isoforms at different stages of development and in response to specific signalling environments would allow refinement of the response to a cAMP signal. Thus understanding the molecular diversity of PDE4 has offered insights into the complex organisation of cell signalling.

1.4 PDE4 in inflammation

1.4.1 Introduction

Since the description of coffee as a useful treatment for bronchospasm in the mid-nineteenth century [113] non specific PDE inhibitors have been used to treat airway disease. The appreciation that methyl xanthines such as caffeine and theophylline had immunomodulatory activity came from the work of Lichtenstein in the early 70's [114, 115]. Significant volumes of work have been produced looking at the role of PDE inhibitors in inflammatory cells and these have been collected in a Series of review articles [50, 116-118]. I will summarise the main concepts to be gleaned from this work and concentrate in a later section on the work pertaining to macrophages, which is the cell of particular interest in this thesis.

1.4.2 PDE content of immune cells

An understanding of the PDE expression profile of inflammatory cells offers insights into specific roles for these molecules. In summary PDE3 and PDE4 appear to be the main cAMP PDE species expressed in inflammatory cells. Some interesting work suggests that in monocytes at least compartmentalisation of PDE species occurs with PDE4 being the main soluble species and PDE3 being particulate associated [119].

1.4.2.1 Mast cells and Basophils

Basophils isolated from human blood contain PDE3, PDE4 and PDE5 [120, 121]. PDE3 and PDE4 account for the majority of cAMP PDE activity in these cells. Mast cells are significantly more difficult to harvest and as such the studies of these cells are more circumspect [117]. Notwithstanding this however PDE3 and PDE4 have been identified in mast cells isolated from guinea pig and human lung [121].

1.4.2.2 Eosinophils

Significantly more work has looked into eosinophil PDE expression profile [122-124]. By far the largest cAMP PDE activity expressed is PDE4. In eosinophils this activity co-distributes in both the particulate and the soluble fractions. PDE3 and PDE1 are present in small amounts, but no independent functional activity has been found for these.

1.4.2.3 B lymphocytes

Suzuki et al have demonstrated PDE4 in B lymphocytes, but little more work in this important cell type was reported until Gantner et al compared cells from atopic and non-atopic donors [125]. They demonstrated that the greatest cAMP PDE activity represented was cytosolic PDE4 followed by cytosolic PDE7. Small amounts of PDE3 were also

present. RT-PCR was used to further define the PDE4 isoform expression profile, and they demonstrated PDE4A, PDE4B2 and PDE4D were represented.

1.4.2.4 Monocytes and Macrophages

I will review the work relating to macrophages in more detail later, however a significant body of work has investigated the expression of PDE isoforms in monocytes and macrophages [119, 126, 127]. In monocytes significantly more PDE4 activity is expressed. With the differentiation to macrophages however this balance is rectified [127]. In both cell types PDE4 is mainly soluble while PDE3 associates with the particulate fraction.

1.4.2.5 Summary

PDE4 is widely expressed in cells of the immune system. As inhibiting PDE4 leads to elevated intracellular cAMP it would be expected that PDE inhibitors would have anti-inflammatory properties. I will discuss the evidence for this next.

1.4.3 Immunomodulation by PDE4 inhibitors

Many studies have confirmed that cAMP derived from PDE4 inhibition has anti-inflammatory activity. Again I will summarise the main focus of this research for each cell type and deal with macrophages in more detail in a later section. Table 1.3 details the major effects of PDE4 inhibitors in inflammatory processes.

1.4.3.1 Mast cells and Basophils

Inhibition of PDE4 prevents IgE stimulated histamine release and platelet activating factor (PAF) stimulated Leukotriene (LTC₄) production from human basophils

Cyclic AMP: Source	Eosinophil recruitment (R) chemotaxis (Ch)	Eosinophil degranulation	Bronchospasm	AHR
Non-selective PDE inhibitors	1 Ch: Theophylline	5: Theophylline	6:	4: Isobutylamine
	3 R: Theophylline			
	4 R: Isobutylamine			
Phosphodiesterase 3 inhibition	7 R: No effect		9: CL 930	
	3 R: No effect		7: Siguzadan (no effect)	
	8 R: No effect			
Phosphodiesterase ₄ inhibition	11 Ch: Rolipram	16: RP 73401	20: Rolipram	23: Rolipram
	12 Ch: Rolipram	17: Rolipram	21: RP 73401	21: RP 73401
	13 R: Rolipram	18:	22: Cilomilast	22: Rolipram
	14 R: RP 73401	Cilomilast/NVP-		
	15 R: Cilomilast	ABE 171		
		19: Rolflumilast		

Table 1.2 Inhibitory effects of the major inflammatory PDE isoforms on features of bronchial asthma

[120, 121, 128, 129]. Although these effects were dose dependent on intracellular cAMP concentration, some functional compartmentalisation was seen by the absence of an inhibitory effect of PDE3 or PDE5 inhibition [120]. Although PDE4 inhibition was capable of elevating cAMP in mast cells conflicting evidence exists for its role in mast cell regulation. Weston et al have found no effect on mast cell mediator release with IgE challenge in the presence of PDE4 inhibitors, while Anderson et al suggest inhibition is achieved [121].

1.4.3.2 Eosinophils

PDE4 accounts for almost all eosinophil cAMP PDE activity, thus it is not surprising that PDE4 inhibition has profound effects on eosinophil function. Table 1.3.2 details these effects. Mediator release, surface molecule expression, oxygen radical release and chemotaxis have all been shown to be reduced by PDE4 inhibitors in a concentration dependent fashion. Again compartmentalisation of function is suggested by the lack of effect of PDE3 and PDE1 inhibitors. It must be noted however, that the effect on cAMP of either one of these inhibitors is small given their relative low expression.[122-124, 130-134]

1.4.3.3 B Lymphocytes

Inhibition of PDE4 in B lymphocytes appears to have conflicting effects depending on the context. [135] This group demonstrated that PDE4 inhibition increased IgE production in the presence of low IL-4, however if IL-4 concentration is higher IgE was inhibited. Another group demonstrated that LPS stimulated proliferation of B lymphocytes was increased in the presence of rolipram [125] This effect was mimicked by a lipid soluble analogue of cAMP (db cAMP) and inhibited by H89, an inhibitor of PKA.

1.4.3.4 *T Lymphocytes*

PDE4 inhibitors prevented the antigen, mitogen and MHC class I stimulated proliferation of T lymphocytes, while PDE3 inhibition did not [136, 137]. This distinction lends more weight to the theory of compartmentalisation as PDE3 and PDE4 are fairly evenly represented in T cells. PDE4 inhibitors also reduced the stimulated production of cytokines from T cells [138]. The combined effect of PDE3 and PDE4 inhibitors failed to mimic completely the effect of non-specific PDE inhibitors such as [139] Theophylline. Thus it may be that PDE7 may play a significant role in the regulation of T cell cAMP. PDE7 has since been shown to be important in the activation of T cells [140]. Another explanation for the differences in activity between both groups of drugs could be non-PDE effects of theophylline such as adenosine agonism.

1.4.3.5 *Monocytes and Macrophages*

Due to the relative abundance of monocytes a wealth of information demonstrates a role for PDE4 in regulating pro-inflammatory activity. Most significantly TNF α production by LPS stimulated macrophages is profoundly inhibited in the presence of PDE4 inhibitors. [141, 142]. Other pro-inflammatory effects are inhibited by PDE4 inhibition such as fMLP induced arachadonic acid release and calcium ionophore stimulated leukotriene production [143].

1.4.3.6 *Summary*

Thus non-specific and specific PDE4 inhibitors have anti-inflammatory properties across most of the cells involved in inflammation and immunity. This makes PDE4 isoforms attractive therapeutic targets. A large volume of pharmaceutical research is dedicated to developing new agents with PDE4 inhibitory properties.

1.4.4 Development of new PDE4 inhibitors

Unfortunately just as non-specific PDE inhibitors such as theophylline are limited by toxicity, PDE4 inhibitors are also limited by their side effect profile. The main side effects experienced are nausea and headache, both of which are believed to be due to an effect on the CNS due to the high affinity binding site (HARBS) [91]. As PDE4 itself is a complex family with different isoforms possibly regulating different cellular processes it is not surprising that side effects are seen with relatively non-specific agents.

Many new PDE4 inhibitors are in development, some of which may offer relative isoform specificity [118]. To further understand the role of each PDE4 isoform in cell function it will be necessary to investigate a cell type in more detail. I have selected the macrophage/monocyte cell to address phenotype specific roles for PDE4 isoforms. I will discuss the macrophage in terms of development, pathogenesis in inflammation, its role in asthma and cAMP signalling. Asthma is discussed as increasing interest in PDE4 inhibition in this disease is leading to considerable research into cAMP molecular mechanisms. It should be noted however that to date PDE4 selective inhibition has proven therapeutically disappointing in asthma as opposed to in COPD where it has been found to be therapeutically efficacious[144].

1.5 Alveolar Macrophages

Macrophages are a useful model to study PDE4 regulation of inflammation. They represent a highly differentiated mature cell with a defined progenitor, the monocyte. Comparison of these cells can offer insights into the important biochemical changes involved in maturation. Macrophages also have well defined and measurable pro-inflammatory behaviour which is useful for studying biochemical modulation. Finally alveolar

macrophages (AM) are important in the development of lung disease and offer a potential therapeutic target.

1.5.1 Lung Macrophage - a heterogeneous population with specific developmental phenotypes

Macrophages are tissue specific accessory cells derived from circulating peripheral blood monocytes (PBM) both constitutively and in response to inflammation [145]. Alveolar macrophages (AM) are mobile phagocytic cells that reside on the surface of the alveoli and small bronchi of normal lung and represent approximately 3-5% of all lung cells [146]. Given that the lung is the largest interface of internal and external environment AM have a fundamental role in host defence by surveying airborne particles along this surface. AM are more adherent, less phagocytic, morphologically distinct and have increased capacity to produce cytokines than either peritoneal macrophages or PBM. [147]. Thus AM represent a phenotypically defined stage of differentiation. This differentiation is a biochemically regulated process.

1.5.1.1 Maturation and migration

Migration from blood to the alveolus is a process of adherence to and passage through vascular endothelium, extracellular matrix and the alveolar epithelium. This requires the sequential interaction of monocyte surface receptors with selectins expressed on neighbouring cells. Transendothelial migration involves $\beta 2$ integrins (CD11/CD18) VLA₄ and 5, P-ECSEL, PECAM and I cam 1 and Vcam 1 [148]. Rosseau et al demonstrated the importance of $\beta 2$ integrins CD11a, b, c and d, VLA 4, 5 and 6 and CD47 in transalveolar migration [149]. Cell recruitment and adhesion molecule expression is biochemically controlled by the monocyte chemokines MCP-1 and RANTES [150, 151]. Both of which are produced by resident cells in the lung including alveolar type II cells in response to

TNF α , IL-1, IL-2 and TGF β [149]. Galactin 3 is a recently described lectin involved in monocyte migration and macrophage development and has been shown to be specifically expressed in lung tissue [152].

1.5.1.2 Intermediate macrophages may represent stage specific development

A second population of macrophages have also been described accounting for ~2% of lung cells or 40% of lung macrophages [146]. These cells are found in the interstitium of lung tissue and are known as interstitial macrophages (IM). Whether these represent maturing macrophages or a separate population of active macrophages is not clear.

Thus distinct developmental regulation of alveolar macrophages takes place in lung tissue. Understanding the biochemical changes governing this process may increase our understanding of the cells involved.

1.5.1.3 Cell line models as surrogates for macrophage development

While AM are relatively abundant their isolation remains difficult and yields are often insufficient for biochemical analyses. Investigators have thus developed models of macrophage differentiation based on leukaemic cell lines. Huberman and Callahan demonstrated that a granulocytic cell line HL-60, could be made to develop macrophage-like features by treating with the phorbol ester PMA [153]. Subsequently other related cell lines including the premonocytic cell U937 have also been similarly shown to respond [154]. Such cells when treated become adherent to plastic, develop phagocytic capability and change their surface markers to a more mature display including the expression of β 2 integrins (CD11 β) and MIF [155, 156]. Monocytes isolated from the circulation and cultured on plastic develop in a similar fashion a model known as the “ex-vivo” model.

1.5.1.4 Biochemical regulation of development

Two studies have shown the importance of biochemical regulation in the control of macrophage development using the cell line U937. Firstly Kim et al found that the inhibition of ERK1/2 prevented the full expression of the macrophage phenotype [157]. Secondly, Prudovsky used CD11b antisense to reduce the expression of this $\beta 2$ integrin, previously discussed as important in monocyte migration, and prevented the expression of the macrophage phenotype [156]. Therefore biochemical systems control the development of mature cellular phenotypes. What can be learned by comparing mature cells with progenitor cells?

1.5.1.5 Biochemical changes with macrophage development

PKC is a large family of Ca dependent and independent kinases. Monick et al, mapped the changes in isoform expression between immature PBMs and AM [147]. They demonstrated that monocytes have a relatively high level of PKC activity with the Ca dependent isoforms PKC β 1 and PKC β 2 being dominant. In AM however Ca independent isoforms PKC ϵ and PKC ζ were relatively over expressed. PKC subcellular location was also different in AM with a greater proportion of PKC being membrane associated than in monocytic cells a distribution which is associated with activation of the kinase [158]. To determine if functional changes matched the PKC profile Monick et al, demonstrated reduced PMA stimulated ERK activation in AM compared to PBMs and suggested that this could impact significantly on a number of macrophage specific functions. It is interesting that many groups have shown that LPS activate two different PKC isoforms ie PKC ϵ and PKC β [159, 160#].

1.5.1.6 Summary

Thus macrophage development is accompanied by biochemical changes with potentially important functional outcomes. Equivalent changes in PDE isoform expression will be discussed in a later section. What relevance to disease do AM have?

1.5.2 Function of Alveolar macrophages

Alveolar macrophages are capable of secreting a large variety of inflammatory mediators and cytokines that are implicated in the pathogenesis of lung disease. The overall role of the AM in resting lung is believed to be immunosuppressive [161] [145] partly related to inhibition of T lymphocytes [145] in which they are able to induce apoptosis. Although poor antigen presenting cells, IL-10 a cytokine active in asthmatic lungs, promotes this activity [162]. IL-10 is an important product of cAMP treated macrophages and has been shown to be increased by PDE4 inhibition [163].

1.5.2.1 Alveolar macrophage in disease

The important role played by AM in resolving inflammation through recognition and phagocytosis of apoptotic neutrophils is becoming clear [164]. The role of pulmonary based macrophages in ARDS, shock lung and pulmonary fibrosis has long been accepted. Their role in obstructive lung disease and especially asthma is more contentious. Evidence is accumulating, however that activated macrophages at least participate and may initiate the chronic inflammation that underlies both allergic and smoking induced obstructive airways disease [165]. Asthma is of particular interest to this thesis given the weight of research aimed at producing asthmatic therapies based on PDE4 inhibition. It should be noted that AM are heavily implicated in the pathogenesis of COPD and that novel PDE4 inhibitors have proven more effective in this disease than in asthma.

1.5.2.2 Mediator release

Many of the chemical mediators and chemokines implicated in asthma pathogenesis are produced by AM. These include $\text{TNF}\alpha$ [166], $\text{IL-1}\beta$ [167, 168], leukotrienes, and nitric oxide and their production is limited by inhaled corticosteroid use in asthma [169-171]. Conversely AM are known to express receptors for pro-asthmatic mediators eg LTD4 [172]. In this study pre-treatment of AM with LTD4 was shown to enhance stimulated cytokine production. Therefore AM can produce and respond to inflammatory mediators important in asthma.

1.5.2.3 Functional differences in atopic macrophages

Some functional differences exist between AM isolated from healthy and asthmatic subjects. AM from patients with pulmonary fibrosis were capable of producing IL-4 and IL-5 which are known to be important cytokines in the Th2 response [173]. Furthermore AM isolated from atopic asthmatics were capable of causing enhanced IL-5 production compared to non-asthmatic atopics. AM isolated from asthmatic lungs have an “activated” phenotype defined by the expression of ICAM-1 and LFA-1 suggesting that they were actively participating in the inflammation [168]. Viksman et al found that activation marker expression on AM from asthmatic lungs was greater than normal donors [174] and when stimulated with LPS, AM from asthmatic subjects produced more GM-CSF, $\text{TNF}\alpha$, IL-8 and LTB₄. Finally Lensmar et al, compared AM from atopic asthmatics before during and after chronic low dose exposure to pollen [175]. They demonstrated increased macrophage content of broncho-alveolar lavage from exposed patients and found a shift in surface marker expression from a CD16 and CD11a bias to a CD14 and CD11b dominance. CD14 expression in particular correlated closely with the drop in FEV₁. CD14 is more classically considered to be a monocyte marker and overall it appears that AM cells were developing a more immature phenotype [176, 177].

1.5.2.4 Mechanisms by which macrophages may support airway inflammation

It may be that in the background of an active inflammatory process such as asthma where a Th2 dominance has already been asserted then cells of the innate immune response can, by producing general lymphocyte growth factors such as IL-2, promote and maintain inflammation [178]. Indeed IL-10 produced by macrophages is known to support a TH2 profile preferentially. There are other possible mechanisms.

Firstly, AM are capable of suppressing immune activity partly by the production of NO which inhibits T lymphocyte proliferation, AM are twice as good at this inhibition than PM [161]. It has been noted that Th1 cells are more sensitive to such inhibition than Th2 cells, and thus selective expansion of Th2 cells may result from activated AM producing NO [179]. Secondly it has been suggested that IM, by virtue of their close proximity to DC may influence accessory cell function and thus regulate the adaptive immune response. Thirdly AM and DC are the only lung cells capable of phagocytosis and thus functioning as antigen presenting cells to T and B lymphocytes. In a recent study of pollen starch granule (PSG) phagocytosis, it was found that AM bound and internalised PSG in a lectin and β 2-integrin dependent fashion, [165]. Uptake of PSG in this study was associated with the expression of iNOS and nitric oxide production from the AM cells studied. Thus the AM in the lung and bronchus may serve to screen inspired air for allergens and by internalising them become activated and promote the inflammatory response.

A final mechanism by which AM may promote airways inflammation is by responding to airborne bacterial wall products such as LPS. LPS and other bacterial proteins are recognised by microbial recognition receptors on AM such as CD14. By stimulating the production of cytokines and mediators these molecules can influence the behaviour of the adaptive immune response. Endotoxin (LPS) has been found associated with aeroallergens such as pollen and house dust mite and asthma symptoms have been reported to correlate

with the level of household endotoxin. Macrophages from asthmatics express increased levels of CD14 when compared with non-asthmatics [168]. Direct inhalation of endotoxin in both mouse and human subjects causes acute inflammation, bronchoconstriction and airways hyper-responsiveness [180]. In other studies intravenous LPS resulted in bronchoconstriction mediated by COX-2 expression [181] and CD14 +ve cells exposed to inhaled LPS cells have been shown to prolong eosinophil survival [182]. GM-CSF treatment of isolated lungs significantly increased the sensitivity to the LPS induced bronchoconstriction [183]. This was believed to be due to priming of lung cells and probably AM to produce COX-2. Finally Schwartz et al demonstrated that topical application of synthetic inhibitors of LPS into the airway could block inflammation and subsequent AHR [180]. Thus by virtue of their sensitivity to airborne LPS, AM can activate and perpetuate an inflammatory response in the airway that has many of the hallmarks of asthma. This model not only supports the use of AM as a model for therapeutic manipulation but suggests that understanding the complex biochemistry associated with LPS stimulation could also aid our understanding.

1.5.2.5 Alveolar macrophages may induce bronchoconstriction by eicosanoid production

Accumulating evidence suggests that AM influence airway inflammation resulting in AHR, but it is also possible they are involved in producing bronchoconstriction. The molecular mechanisms promoting bronchoconstriction lie in the chemical mediators released from activated macrophages. Martin et al [184] demonstrated in precision cut lung sections that COX-2 inhibition reduced the constrictive response to asthmatic airway milieu. COX-2 and the bioactive lipids that it produces including PGE2 and TXA2 are pathogenic for both asthma and COPD [185]. Studies comparing lung cells found that IM expressed most COX-2 mRNA in non-inflammatory lung closely followed by epithelial

cells. It is interesting to speculate that in the asthmatic airway where AM may undergo a monocytic “de-differentiation” that COX-2 may be more active in the AM.

Finally as has already been discussed the capacity for AM to produce leukotrienes is enhanced by maturation. The enhanced activity is related to the nuclear localisation of 5-lipoxygenase the synthetic enzyme of LTA₄. This molecule is the precursor of LTB₄, which acts as a neutrophil chemoattractant and the cysteinyl leukotrienes (LTC₄, LTD₄ and LTE₄). These chemicals promote bronchial smooth muscle contraction and vascular permeability. Interestingly Fuller et al found that while agents which indirectly elevate cAMP in AM, such as PDE inhibitors could prevent the release of TXB₂, the β_2 agonist isoprenaline was ineffective[186]. This was thought to be due to a lack of responsive β_2 -adrenoceptor.

1.5.3 Conclusions

The alveolar macrophage is an attractive model to study the role of PDE4 isoforms in the regulation of inflammation. Defined developmental stages and a clear progenitor cell allow analysis of isoform expression as seen for PKC isoforms. Biochemical regulation is important in the development and it is likely therefore that distinct PDE4 isoforms will be expressed at specific stages. Finally macrophages are important cells in airway disease and PDE4 inhibition is likely to result in significant therapeutic interventions.

1.6 Cyclic AMP in the macrophage

Cyclic AMP regulation of macrophage function and macrophage control of cAMP signal transduction will provide the final topic for this discussion. Cyclic AMP is largely inhibitory to macrophage function thus PDE4 promotes inflammation. The effect of cAMP on pro-inflammatory functions is cell specific and I will limit the discussion to monocytes and macrophages as these form the subject of investigation in this thesis.

1.6.1 Cyclic AMP Signalling in Macrophages

It is clear that cyclic AMP signalling can regulate important inflammatory functions of macrophages. The outcome of a cAMP signal depends on the range of proteins involved in signal transduction expressed at a cellular level. What is known of these molecules in macrophages?

1.6.1.1 Adenylyl cyclase and receptors

Cyclic AMP is generated by adenylyl cyclase in response to ligand binding to various receptors. Multiple AC coupled receptors are expressed by macrophages with endogenous ligands ranging from bioactive lipids such as prostanoids to amino acid hormones such as adrenaline.

1.6.1.1.1 Adrenergic Receptors

Of particular significance to respiratory disease is the expression of a range of adrenergic receptors. These are receptors for the endogenous catecholamine hormones adrenaline and nor-adrenaline. β_1 , β_2 and α adrenergic receptors are expressed on alveolar and peritoneal macrophages [187]. Regulation of macrophages during sepsis is mainly mediated through the β_2 receptor [188]. The β_2 receptor is a classical G-protein coupled receptor that activates AC upon ligand binding. Therapeutic manipulation of this receptor using agents such as isoproterenol have proven effective in reducing LPS stimulated cytokine production from macrophages, including TNF α [189] and IL-12 [190]. This does not represent a general suppression of macrophage function however as IL-6 production is not inhibited [189] and the production of IL-10 can be increased [191]. Hasko et al however reported a widespread suppression of multiple cytokines from isoproterenol treated RAW 264.7 macrophages [192].

1.6.1.1.2 Prostaglandin receptors

Prostaglandin receptors are also coupled to AC. Prostaglandins are important macrophage derived mediators of inflammation and have autocrine effects on their cells of origin. Hubbard et al demonstrated regulation of expression of prostaglandin receptors with isoforms EP2, EP3 and EP4 being expressed in resting RAW 264.7 macrophages with a preponderance of EP4 [193]. LPS treatment caused increased EP2 production while interferon γ resulted in a reduction in EP2 and EP4 expression. PGE2 a macrophage derived ligand for both EP2 and EP4 exerts significant inhibitory effects over macrophage activity. For example exogenous PGE2 reduces TNF α and IL-12 production in response to LPS [194]. Prostaglandins have also been shown to inhibit phagocytosis of apoptotic cells by macrophages [195].

1.6.1.1.3 Cytokine receptors

Cytokines represent intercellular messengers signalling between inflammatory cells. GM-CSF is an important macrophage growth factor and cytokine controlling proliferation and activation. Coleman et al found that treatment of macrophages with GM-CSF led to increased AC activity in membrane preparations of isolated macrophages with a resultant increase in cAMP [196].

Therefore a range of chemical mediators of inflammation are ligands for AC coupled receptors. While the majority result in suppression of activity, others such as GM-CSF are important in the full expression of macrophage dependent inflammation.

1.6.1.2 Signal transduction

Cyclic AMP dependent signals can be communicated by both PKA and the cAMP dependent GEF, EPAC, via Rap-1 activation. Both of these cascades have been found to regulate important macrophages processes.

1.6.1.2.1 PKA

The role of PKA in regulating macrophage activation is generally thought to be inhibitory. Cyclic AMP prevents macrophage apoptosis [197] and probably explains AC activation by GM-CSF. Interestingly in the context of this thesis agents that elevate cAMP by PDE inhibition show diverse effects. Thus while theophylline at therapeutic concentrations causes apoptosis and reduces IL-5 or GM-CSF inhibition of apoptosis, PDE4 selective agents do the opposite [198]. Rolipram was found to prevent apoptosis induced by Fas ligand in eosinophils and increase the anti-apoptotic effects of IL-5 and GM-CSF. Otherwise PKA activation by IL-13 activates arginase reducing nitric oxide production [199], inhibits TNF α production [200] and is involved in cyclic AMP prevention of phagocytosis [195]. Among the PKA targets expressed by macrophages is the cyclin B protein, cdc2 kinase. PKA phosphorylation of this protein leads to delayed progression through cell cycle during proliferation and a G2 phase delay [201]. This might partially explain the inhibition of macrophage proliferation by PGE2 described by Banner et al [202]. Finally Delgado et al found that vasoactive intestinal peptide (VIP) and pituitary adenylyl cyclase activating peptide (PACAP), both enhanced the expression of B7.1 co-stimulatory molecule in a PKA dependent manner [203]. This had the effect of enhancing macrophage stimulated T cell proliferation and may reflect accessory cell function in vivo.

1.6.1.2.2 EPAC – Rap1

The discovery of the small cAMP activated GEF, EPAC, has recently offered an alternative pathway for cAMP dependent signalling [38]. No studies have yet been published demonstrating EPAC in macrophages, but its partner Rap-1 has been found to regulate macrophage behaviour. Caron et al have found constitutively active Rap-1 mimics the effects of $\beta 1$ integrin activation [204]. Rap-1 and Ras express competitive behaviour and constitutively activated Ras did not have the same effect. It appears that Rap-1 may regulate macrophage binding and therefore chemotaxis and phagocytosis.

Signal transduction of a cAMP signal can therefore be accomplished in macrophages in a complex fashion. Understanding the roles of cAMP signal transduction has therefore expanded our understanding of cAMP regulation of macrophage function.

1.6.1.3 Transcription factors

Ultimately cellular regulation is achieved by gene transcription and cAMP response elements (CRE) are present in the promoters of various macrophage expressed proteins. Cyclic AMP response element binding protein (CREB), is activated by PKA by phosphorylation at Ser133 [22]. CREB can promote or repress gene transcription. For example Parry et al demonstrated activated CREB competed with NF κ B for a binding protein (CBP) thus reducing its potential for gene transcription [26] whereas Proffitt et al found CREB dependent expression of MIP-1 β in murine macrophages [205]. Of particular interest to macrophage function, Delgado et al found that VIP and PCAP decreased LPS induced TNF α production by CREB activation and NF κ B repression [206].

Cyclo-oxygenase and i-NOS represent two important macrophage derived proteins regulated by cAMP. I will now discuss these enzymes in some detail as they form important subjects in the work to be described.

1.6.1.4 Cyclooxygenase 2

Cyclooxygenase (COX) is the prostaglandin synthase, which converts arachadonic acid to PGH, the substrate for the more specific prostaglandin synthase enzymes [207]. Two COX isoforms are recognised, COX1 and COX2 the latter being an inducible form found at sites of inflammation [207]. COX2 is capable of producing a variety of lipid mediators of inflammation including prostaglandin E2 (PGE2), PGD2 and thromboxane A2 (TXA2). While macrophage expressed PGE2 is believed to promote a healing phenotype by the production of the fibroblast growth factor IGF-1 [208], PGD2 is thought to support a more tumourocidal pattern of behaviour[209]. TXA2 on the other hand is capable of inducing bronchospasm in asthmatic airways [210]. COX-2 products exist therefore in a complex balance in the pathogenesis of asthma [211].

Fournier et al demonstrated that at sites of high TNF α production such as asthmatic airways COX-2 was most likely to produce PGE2 supporting the hypothesis that COX-2 expression is protective in airways disease [209]. PGE2 is important in macrophage biology by virtue of its capacity to maintain a specific phenotype. PGE2 promotes the expression of the LPS receptor CD14, which I have described as being increased in macrophages in asthmatic airways. This would be expected to enhance LPS sensitivity of these cells, which itself increases COX-2 and therefore PGE2 production [212]. Finally in the presence of LPS, PGE2 enhances its own production ensuring that in a state of LPS induced inflammation positive regulation of receptor and COX-2 enzyme promotes phenotypic stability [213].

Studies using exogenous cAMP and AC activators have shown cAMP to cause and enhance LPS induced COX-2 expression [214, 215]. The role of PKA is more controversial. While zymosan stimulation, a model of phagocytosis caused H89 resistant COX-2 production, TNF α induced COX-2 was reduced by H89 co-stimulation. Caivano et al warned that H89 was capable of inhibiting MSK1 and MSK2, as well as PKA and that this may interfere with post LPS signalling [216]. Examination of COX-2 promoter regions

suggest that cAMP can upregulate expression. Miller et al found co-stimulation of AP-1 and the CRE sites in the COX-2 promoter to explain the synergism between LPS and cAMP stimuli [217]. Gorgani et al found that mice deficient in C/EBP, an important transcription factor binding protein involved in cAMP response elements (CRE) in promoter regions, were unable to produce COX-2 in response to multiple stimuli [218]. Finally Wadleigh et al made multiple deletions of the COX-2 promoter and found that while both cAMP response elements and NF κ B response elements are present, only the CRE box was essential for LPS induced activation of COX-2[212].

COX-2 therefore represents an important macrophage enzyme, promoting an asthmatic airway and lies under the control of cAMP.

1.6.1.5 Inducible nitric oxide synthase

Inducible nitric oxide synthase (iNOS), represents another macrophage product under cAMP control. Three NOS enzymes exist of which iNOS is inducible at sites of inflammation including the asthmatic airway [219]. The role of macrophage derived NO is not clear but some evidence points to an anti-inflammatory bronchodilatory activity [179].

Cyclic AMP can increase or decrease the expression of iNOS in activated macrophages and the precise outcome appears to depend on the cell type examined and the stimulus applied. Nusing et al found that both db-cAMP and PGE₂ applied to mesangial cells caused enhanced LPS stimulated iNOS production [220], while Delgado found that vasoactive intestinal peptide prevented LPS and interferon γ (IFN γ), stimulated iNOS production from RAW 264.7 macrophages. Thus another important promoter of inflammation and macrophage regulation is regulated by cAMP signalling pathways.

1.6.1.6 Summary

It appears therefore that the molecular apparatus for activating and transducing a cAMP dependent signal are available in macrophages. These molecules regulate macrophage function and the degree of complexity and the molecular variety suggests a high degree of control can be exerted by manipulating cAMP signals. The limiting factor to any cAMP signal is cAMP phosphodiesterase.

1.7 Phosphodiesterase isoforms in macrophages and monocytes

1.7.1 PDE Profile

In 1976 Thomson et al found that the greatest cAMP phosphodiesterase activity in human inflammatory and immune cells correlated with PDE4 [221]. Many subsequent studies looking at lymphocytes and monocytes have confirmed this analysis. Interest in the field was generated by studies demonstrating that PDE4 inhibitors prevent proinflammatory behaviour in these cells. Mapping the PDE profiles and changes in response to stimuli in inflammatory cells has developed into a major research interest.

1.7.1.1 Ex-vivo monocytes

Many groups have shown a PDE4 dominance in the cAMP PDE profile of monocytes isolated from human blood and found PDE4 to represent between 60-75% of the total activity [119, 126, 222, 223]. While Thompson in the original work on monocytes found very little PDE3 represented, subsequent studies have recorded between 9 and 40% of the total cAMP PDE activity to be inhibited by cGMP. While the majority of PDE3 is found in the particulate fraction of disrupted monocytes, all studies that have looked have shown

90-100% of PDE4 to be cytosolic [223, 224]. This suggests specific isoform targeting in these cells.

1.7.1.2 Alveolar macrophages

Investigating the PDE profile of AM is much harder due to the lower abundance of these cells and the complexity in acquiring them. Tenor et al looked the PDE isoforms expressed in isolated alveolar macrophages and found PDE3 and PDE1 to represent 45% each of total PDE activity while PDE4 was significantly less [127]. Again PDE4 was entirely soluble, while PDE3 was membrane associated. Due to the difficulties in acquiring macrophages Gantner et al investigated the PDE activity of peripheral blood monocytes cultured on plastic and found a profile very similar to AM. PDE1 activity rose from approximately 0 to 55% of total PDE activity and PDE3 increased to 55%. PDE4, however fell to between 15-20% [119]. In contrast to this Kelly et al have found AM isolated from guinea pig lungs express significant amounts of PDE4 [225].

It appears therefore that the maturation of macrophages from the monocyte progenitor cell is accompanied by a change in the mechanisms of cAMP control. This suggests that each PDE family is important for regulating functions specific for each type of cell.

1.7.1.3 PDE4 isoforms

Although changes in the contribution of PDE4 to the total cAMP activity have been described less work has been reported on the changes in PDE4 isoform expression. Attempts have been made to profile PDE4 isoforms in monocytes and macrophages using RT-PCR and western blot analysis. Manning et al demonstrated mRNA transcripts for PDE4 A, B and D in resting ex-vivo monocytes, but little detectable protein [222]. After treatment with the β_2 adrenergic receptor agonist salbutamol, for 4 hrs increases in total PDE4 activity, increased levels of PDE4A and B mRNA and detectable PDE4 protein were recorded. Souness et al found PDE4A and PDE4B mRNA in monocytes, but also identified a faint band corresponding to PDE4D [223]. Studies using the U937 cell line

have confirmed the presence of three PDE4 isoforms and demonstrated an increase in enzyme expression with salbutamol [226]. McKenzie and Houslay have shown that PDE4 A, B and D are present in resting U937 cells and by immunoprecipitation have demonstrated that these contribute approximately 1%, 20% and 80% respectively. No work specifically reporting the PDE4 isoform profile of macrophages has been reported to date. This may represent a combination of the difficulty in acquiring sufficient cells to identify members of a low abundance enzyme family.

1.7.2 Functional importance of PDE4

Regulation of PDE4 during cell specific maturation suggests important functional roles in cellular control. Evidence for such important roles is hard to provide. If dysregulation of PDE4 function was shown to cause a disease state then the significance of PDE4 could be implied.

1.7.2.1 PDE4 in disease

Early studies of PDE activity in disease found that peripheral blood monocytes from patients with atopic dermatitis had greater PDE4 activity than the same cells from normal donors [227]. Other groups have not found a similar difference however [126] Gantner et al went further and mapped the PDE4 isoforms and found no significant differences in expression between normal donors and patients with atopic dermatitis. No significant differences have been found in any cell type from atopic donors including B lymphocytes [125] and eosinophils [228]. Studies on cells purified from asthmatic subjects have been similarly unrewarding [229].

Inhibitors of PDE4 on the other hand suggest that this family might have a role to play. While in vivo studies make it difficult to tease out the cells responsible for a therapeutic response. Studies of isolated cells or cell line models allow careful cell identification.

1.7.2.2 PDE4 inhibitors in monocyte and macrophage regulation

PDE4 inhibition potently reduces TNF α production from LPS stimulated monocytes [223], and to a lesser extent macrophages [163]. Gantner et al looking at *ex-vivo* monocytes demonstrated that rolipram was capable of preventing TNF α release at levels where cAMP increases were undetectable [119]. Souness et al also found that while low levels of rolipram were capable of inhibiting TNF α release, to measure a significant increase in cellular cAMP PGE₂ had to be added to activate AC [223]. That this combination increased cAMP over PGE₂ alone demonstrates the functional importance of PDE4 in monocytes as the main cAMP hydrolysing enzyme. Seldon et al found β 2 adrenergic receptor agonists had the same effect as PGE₂ with rolipram by generating an excess of cAMP over the presence of inhibitor alone [142]. Thus PDE4 is capable of altering pro-inflammatory behaviour at concentrations below that which result in measurable cAMP. This suggests that while dysregulation may not cause disease the normal functioning of PDE4 is permissive for inflammation to progress. What of other PDE isoforms?

Inhibitors of PDE3 do not have the same effects on TNF α production as PDE4 inhibitors [141]. This may simply reflect the smaller contribution of PDE3 to total cAMP PDE activity seen in many inflammatory cells. The capacity for rolipram to inhibit TNF α without substantial changes to cellular cAMP argues against a dose effect as do equivalent studies in macrophages where PDE3 is found in greater quantities than PDE4. Gantner et al found rolipram to have a weak inhibitory effect on TNF α production in monocyte derived macrophages while PDE3, now representing a greater proportion of the total PDE activity had no effect whatsoever [119]. If cAMP production was augmented by the addition of PGE₂ then the effect of rolipram was significantly enhanced, as was, to a lesser extent that of PDE3.

Thus the functional importance of PDE4 in macrophages and monocytes is seen when inhibition of pro-inflammatory behaviour is investigated. PDE4 inhibition can prevent

TNF α production at very low inhibitor concentrations. This effect can be enhanced by exogenous stimulators of AC and an equivalent effect is not found with PDE3 inhibitors even though PDE3 represents an major cAMP PDE in macrophages.

1.7.3 Compartmentalisation / crosstalk

The apparent ability of rolipram to inhibit cellular function at concentrations less than are required to generate cAMP requires explanation. The principle behaviour of rolipram is PDE4 inhibition and it is this behaviour that has been shown to cause immunomodulation. Rolipram may alter intracellular cAMP concentration to levels below the sensitivity of experimental testing. Could such small changes in cAMP have demonstrable effects on cellular behaviour however?

One other explanation may lie in the principle of compartmentalisation described in section 1.1.3 [96]. The generation of localised pools of cAMP contained by targeted PDE4 isoforms implies that very low levels of cellular cAMP could mask high local concentrations. In this case inhibitors causing a relatively small total increase in cellular cAMP could have significant influence over a signalling cascade in the same cellular compartment by the principle of crosstalk. The principle of compartmentalisation remains to be rigorously tested in inflammatory cells, however several lines of evidence support the concept.

1.7.3.1 Functional specificity of PDE isoforms

Firstly studies mentioned above describe a functional distinction between PDE3 and PDE4 inhibitors in terms of TNF α inhibition from LPS stimulated macrophages. Chini et al describe a similar distinction between proliferation and superoxide release by PDE3 and PDE4 inhibitors in renal mesangial cells [98]. They found cAMP suppressed both proliferation and superoxide radical release but while PDE3 inhibitors prevented cell division, PDE4 inhibitors prevented superoxide radical production. Monocyte ROM

generation has also been shown to be reduced by PDE4 inhibitors. Further evidence for functional compartmentalisation comes from work carried out in a myeloid cell line FDCP2 cells [102]. This cell line was reported to have roughly equal amounts of PDE3 and PDE4 but they were shown to be under different control. Total cAMP PDE activity was increased by treatment with IL-3, IL-4 and GM-CSF and the PKC activator PMA each PDE isoform responded differently. While all 4 stimulants activated PDE4 activity only IL-4 activated PDE3. IL-4 was shown to activate total PDE activity by PI-3 kinase dependent system, but while PDE4 was activated by ERK1/2 activation of PDE3 was ERK1/2 independent. ERK signals were also shown to be responsible for the activation of PDE4 by IL-3 and PMA. Thus different PDE isoforms are under different control mechanisms which are functionally relevant as they represent the signalling moieties of different pro-inflammatory cytokines. It is interesting from the pathological perspective that IL-4 a classical Th2 cytokine activates PDE3 while other cytokines do not.

1.7.3.2 Targeting of PDE4

While this work supports functional compartmentalisation of PDE3 and PDE4 it does not suggest that PDE4 isoforms are similarly distinct. Some circumstantial evidence does support PDE4 isoforms compartmentalisation. It has been suggested that compartmentalisation implies certain prerequisites must exist [4]. A regulated source of signal, a detector for that signal and a destroying activity are required. Adenylyl cyclase, PKA and PDE4 are all present in macrophages as described above. Another requirement is that these molecules are all targeted in the cell. Evidence for targeting of PKA and AC is accumulating from other tissues, although little work has been done in inflammatory cells. Circumstantial evidence from non-inflammatory studies supports the targeting of PDE4 isoforms in general and suggests possible means of targeting in inflammatory cells specifically.

The PDE4D5 binding partner RACK1 is important in macrophage function [84]. For example, impaired TNF α production due to ageing was overcome by replacing RACK

1[230], RACK 1 has also been shown to associate with the intracellular portions of cytokine receptors [89] and β integrins [88]. Lyn kinase, a binding partner of PDE4A4, is only expressed by haemopoietic cells and has been implicated in LPS activation of macrophages [82] [231]. Huston et al showed that PDE4A was a substrate for caspase3 a regulator of apoptosis and was cleaved to produce a more active enzyme [232]. The region found to be removed was the SH3 interaction domain implying a possible role for protein protein interactions as controlling cAMP in normal cells.

Thus Targeting of PDE4 isoforms within inflammatory cells has a theoretical basis, but the concept of compartmentalisation dependent on differential targeting of PDE4 isoforms requires further testing.

1.7.4 Conclusions section 1.7

I have described the molecular basis for cAMP signalling in macrophages. The variety of molecules involved in the regulation of this single compound suggest that its control is important to the cell and that it may play a number of roles in cell function. PDE4 inhibitors, by virtue of their capacity to elevate cAMP, influence pro-inflammatory behaviour. This behaviour has been taken advantage of by the pharmaceutical industries who require to address a number of outstanding questions before rational therapeutic manipulation of PDE4 can be achieved. These questions and possible means of answering them will form the conclusion to this introduction.

1.8 Conclusions and hypotheses

Cyclic AMP signalling depends on a cascade of events and at every level of this cascade nature has provided a selection of molecules from which effectors can be chosen. The pressure on nature for efficiency suggests that these choices are not random and that redundancy in these families of signalling molecules is unlikely. Individual PDE4 isoforms are therefore likely to provide specific control over cAMP governing specific outcomes

and in specific circumstances. Considerable circumstantial evidence suggests that subcellular compartmentalisation and inter molecular crosstalk explains the roles of each molecule in a given setting.

Macrophages are important cells in the inflammatory response producing important mediators and responding to foreign agents and toxins. They are also regulated to a high degree by intra cellular cAMP. Cell line models offer a useful tool for examining the control of macrophages in vitro.

I hypothesised that individual PDE4 isoforms would regulate specific macrophage functions. I tested these hypotheses by isolating individual PDE4 isoforms from LPS treated macrophages and measuring their activity. I further hypothesised that macrophage development from monocyte progenitors would be accompanied by a change in the PDE4 isoforms expressed. These changes would suggest which isoforms are important in regulating macrophage functions. Due to the difficulty in acquiring sufficient tissue macrophages to measure these low abundance proteins I aimed to develop a cell model of macrophage development. I selected the U937 model previously described due the high level of characterisation already reported.

Alongside these aims I wished to measure macrophage responses to inhibition of PDE4. I used LPS as a stimulus for activation and rolipram as a specific inhibitor of PDE4. I also hypothesised that PDE4 engaged in molecular crosstalk with signalling cascades downstream of LPS receptors. In particular I aimed to identify a crosstalk model between ERK1/2 and PDE4 via Rap-1. I tested this hypotheses by measuring ERK2 activation in the presence and absence of rolipram.

Chapter 2 Materials and Methods

2.1 Materials

Unless otherwise stated all chemicals were from Sigma-Aldrich (Gillingham UK, SP8 4XT) or Fischer Scientific (Loughborough, UK) and were of analytical grade. All solutions were prepared in de-ionised and filtered water and sterilised where appropriate by autoclave or filter.

2.1.1 Bioactive Reagents

The following cell signalling reagents were used. From Sigma Aldrich UK. (Gillingham UK SP84XT): Phorbol 12 Myristate 13-Acetate (PMA, Cat No 79346); Salmonella Minnesota Lipopolysaccharide (LPS γ irradiated and phenoli extracted for cell culture, Cat No L4641); Human recombinant Epidermal Growth Factor (EGF, Cat No E9644); Salbutamol (Cat No S8260); Wortmannin Penicillium Funiculosum (Wortmannin, Cat No W1628); Cilostamide (Cat No C7971); Tumour Necrosis Factor Alpha (TNF α , Cat No T7539); Actinomycin D (Cat No A4262) and Protein Kinase A Inhibitor Fragment Myristilated (PKA Inhib Myr, Cat No P9115). From Promega UK (Southampton UK, SO16 7NS): UO126 (Cat No V1121) and SB203580 (Cat No V1161). From Calbiochem (San Diego, CA, USA): Indomethacin (Cat No 405268) and H89 dihydrochloride (H89, Cat No 371963).

2.1.2 Antibodies

Name/No	Target	Source	Application	Dilution	2°
Schering B	Human and rat generic isoforms PDE4B	Schering-plough	WB,ELISA,IP	1/1000	R
270	Human and rat generic isoforms PDE4A	Scottish antibody production unit (SBTS. Lanark UK)	WB, IP	1/2000	R
93	Human and rat generic isoforms PDE4D	Scottish antibody production unit (SBTS. Lanark UK)	WB, IP	1/2000	R
Anti-Integrin α M (sc6612)	CD-11	Santa Cruz Biotech. (Santa Cruz. CA 95060. US)	WB	1/5000	G
Anti-PKC β	Protein Kinase C isoform β	Transduction Laboratories (Lexington, KY, US)	WB	1/5000	M
Anti-COX-2 (c22420)	Cyclooxygenase 2	Transduction Laboratories (Lexington, KY, US)	WB	1/10,000	M
Anti-ERK1/2 (E17120-050)	Pan -ERK 1 and ERK 2 Mitogen activated protein kinase	Transduction Laboratories (Lexington, KY, US)	WB	1/5000	M
Anti-P-ERK1/2 (T202/Y206, 612358)	Phosphorylated (activated) ERK1/2	Transduction Laboratories (Lexington, KY, US)	WB	1/1000	R
Anti-RACK-1 (TLR20620-050)	RACK-1	Transduction Laboratories (Lexington, KY, US)	WB	1/10,000	M
Anti-iNOS (N39120)	Inducible nitric oxide synthase	Transduction Laboratories (Lexington, KY, US)	WB	1/10,000	M
Anti- mouse/rat TNF α (mo46423)	Tumour necrosis factor α	Pharmingen	ELISA		M
Anti-CREB (sc186)	Camp response element binding protein	Santa Cruz Biotech. (Santa Cruz. CA 95060. US)	WB	1/400	R

Anti-P-CREB (sc7978)	Phosphorylated (activated) CREB (P- Ser133)	Santa Cruz Biotech. (Santa Cruz, CA 95060, US)	WB	1/400	G
Anti- <i>rap1</i> (R22020)	Human and mouse <i>Rap1</i>	Transduction Laboratories (Lexington, KY, US)	WB	1/10,000	M
Anti-rabbit HRP (A6154)	Rabbit IgG (Horse radish peroxidase conjugated antibody)	Amersham Pharmacia	WB ELISA	1/10,000	N/A
Anti-mouse HRP (NA-931V)	Mouse IgM (Horse radish peroxidase conjugated antibody)	Amersham Pharmacia	WB ELISA	1/10,000	N/A
Anti-B (sc9002)	Raf Human B Raf	Santa Cruz Biotech. (Santa Cruz, CA 95060, US)	IP, WB	1/5000	M
Anti C Raf	Human C Raf	Santa Cruz Biotech. (Santa Cruz, CA 95060, US)	IP, WB	1/5000	M

Table 2.1 Antibodies used in the following research. (WB, Western Blot; IP, Immunoprecipitation; ELISA, Enzyme-linked Immunosorbant Assay; 2⁰, species of secondary antibody used; M, Mouse; G, Goat; R, Rabbit)

2.1.3 Primers

The following oligonucleotides were used in the following research.

PDE4 Isoform	Forward primer	Reverse Primer	Fragment size (bp)	Cycling conditions:		
				Dn	An	Ex
PDE4A4B – specific N-terminal region	CGGAAAGGAGCCTGTCTCTG	AGTGCCATG GAAGGACGAGG	257	94 °C 30 s	60 °C 30 s	72 °C 1 m
PDE4A10 – specific N-terminal region	AGATCTGTCTCAGCTTCGAGGCAG	AGTGAGAAG TTGCTACGG ACGGC	281	94 °C 30 s	60 °C 30 s	72 °C 1 m
HIV-tat-PDE4B2 – specific N-terminal region	GAGCTCTATGGCAGGAA GAAGCGGAGACAGCGAC GAAGACGGCGGCGGCGG CGGCGGCGGATGCCTTG AGATGGCAAAGCACTC	AATCACAGT GGTGCTCTG CCTGAGCTC	270	94 °C 1m	68 °C 45 s	72 °C 1 m
HIV-tat-PDE4B2 – full length	GAGCTCTATGGCAGGAA GAAGCGGAGACAGCGAC GAAGACGGCGGCGGCGG CGGCGGCGGATGCCTTG AGATGGCAAAGCACTC	TTATGTATCC GAGCTC	1861	94 °C 1m	52 °C 45 s	72 °C 1 m
HIV-tat-PDE4D3-specific N-terminal region	GAGCTCTATGGCAGGAA GAAGCGGAGACAGCGAC GAAGACGGCGGCGGCGG CGGCGGCGGATGATGCA CGTGAATAATT	TGGCCAAGA CCTGAGCAA ATGAGCTC	358	94 °C 1m	68 °C 45 s	72 °C 1 m
HIV-tat-PDE4D3-full length	GAGCTCTATGGCAGGAA GAAGCGGAGACAGCGAC GAAGACGGCGGCGGCGG CGGCGGCGGATGATGCA CGTGAATAATT	GATCTACAT CATGTATTG CACTGGCGA GCTC	2088	94 °C 1m	52 °C 45 s	72 °C 1 m

Table 2.2 Primers used in the following research. Oligonucleotides were ordered from Interactiva©, Cycle conditions are as follows: Dn, denaturation; An, annealing; Ex, Extension; S, seconds; M, minutes

2.1.4 Plasmids

Clone (name)	Plasmid/ Restriction site	Description:	Source:	Reference:
PDE4B1 (pcDNA R89)	PcDNA 3.0 / NotI	Native PDE4B1	G Bolger	[233]
PDE4B2	PcDNA 3.0 / NotI	Native human PDE4B2	G Bolger	[233]
PDE4B3	PcDNA 3.0 / NotI	Native human PDE4B3	G Bolger	[233]
PDE4B4	PcDNA 3.0 / NotI	Native Rat PDE4B4	G Bolger	(326)
PDE4B4- S56D	PcDNA 3.0 / NotI	PDE4B4 with Ser56 mutated to Asp, mimicking the phosphorylated conformation.	G Bolger	(326)
PDE4B4- S56A	PcDNA 3.0 / NotI	PDE4B4 with Ser56 mutated to Ala preventing the phosphorylation at this site.	G Bolger	(326)
PDE4B4- S14D	PcDNA 3.0 / NotI	PDE4B4 with Ser14 mutated to Asp, mimicking the phosphorylated conformation.	G Bolger	(326)
PDE4B4- S14A	PcDNA 3.0 / NotI	PDE4B4 with Ser14 mutated to Ala preventing the phosphorylation at this site.	G Bolger	(326)
PDE4B4- FLAG	PcDNA 3.0 / NotI	Native Rat PDE4B4 tagged with FLAG peptide sequence	G Bolger	(326)
PDE4B4- S56D	PcDNA 3.0 / NotI	PDE4B4 with Ser56 mutated to Asp, tagged with FLAG peptide sequence.	G Bolger	(326)
PDE4B4- S56A	PcDNA 3.0 / NotI	PDE4B4 with Ser56 mutated to Ala tagged with FLAG peptide sequence.	G Bolger	(326)
PDE4B4- S14D	PcDNA 3.0 / NotI	PDE4B4 with Ser14 mutated to Asp, tagged with FLAG peptide sequence.	G Bolger	(326)
PDE4B4- S14A	PcDNA 3.0 / NotI	PDE4B4 with Ser14 mutated to Ala tagged with FLAG peptide sequence.	G Bolger	(326)
PDE4A4	PcDNA 3.0	Native human PDE4A4 sequence	In house	[76]

PDE4A10	PcDNA 3.0	Native human PDE4A10 sequences	In house	[234]
PDE4D3	PcDNA 3.0	Native human PDE4D3 sequence	In house	[66]
Rap1A	PcDNA3 / Not1	Native Rap1A	In house	[235]
Rap1A-S180A	PcDNA3 / Not1	Rap1A with Ser180 mutated to Ala preventing PKA phosphorylation	In house	[235]
Rap1A-S180D	PcDNA3 / Not1	Rap1A with Ser180 mutated to Asp mimicking PKA phosphorylation	In house	[235]
Rap1A-Ser12-Val	pEXV3	Rap1A with Ser12 mutated to Val resulting in a constitutively active conformation	J Bos et al	[204]
Rap1A-T17N	pEXV3	Rap1A with Thr17 mutated to Asn resulting in a dominant negative conformation.	J Bos et al	[204]

Table 2.3 Plasmids used in the following research. Various plasmids were used in the course of this project. Some were cloned sequences generated in our laboratory, while some were gifts from kind collaborators. Prof G Bolger provided many of the PDE4 constructs in particular the PDE4B4 constructs. The Rap1A activation mutants were kind gifts from Prof J Bos.

Plasmids were transformed into E Coli bacteria and stored as glycerol stocks at -70 °C.

2.2 Buffers and Solutions

2.2.1 Cell Culture

2.2.1.1 Cell Culture Medium

DMEM

Dulbecco's modified Eagles Medium (GibCo Life technologies, Paisley, UK. Cat No 11965). This medium supports the growth of a broad range of mammalian cell lines.

RPMI 1640

Roswell Park Memorial Institution 1640 (GibCo Life Technologies, Paisley, UK. Cat No 11875). This medium supports mammalian cell lines and was originally developed to support growth of leukaemic cells.

Complete medium

Cell culture medium with the addition of 10% (v/v) fetal calf Serum, 2mM L-Glutamine, 1 unit/ml penicillin and 1mg/ml streptomycin.

Serum free medium

As complete but excluding fetal calf Serum

Transfection medium

5ml	Complete medium (replacing fetal calf Serum newborn calf Serum.)
100 μ M	Chloroquine

2.2.1.2 Cell culture buffers

Wash Buffers

Phosphate Buffered Saline (PBS)

2.7mM	KCl
137mM	NaCl
4mM	Na ₂ PO ₄

Tris Buffered Saline (TBS)

137mM	NaCl
20mM	Tris pII 7.6

Transfection Buffers

T E Buffer

10mM	Tris-HCl pH 7.2
1mM	EDTA

DNA adhesion buffer

100mg	DEAE Dextran
10ml	PBS

Shock Buffer

10%(v/v)	DMSO/PBS
----------	----------

Lysis Buffers

KHEM lysis Buffer

50mM	Hepes KOH, pII7.4
50mM	KCl
10mM	EGTA
1.92mM	MgCl ₂

3T3 – Lysis Buffer

50mM	HEPES, pH 7.2
10mM	EDTA
100mM	NaH ₂ PO ₄ ·2H ₂ O
1% (v/v)	Triton X-100

Nuclear Buffer A

10mM	Hepes pH 7.5
1.5mM	MgCl ₂
10mM	KCl
0.5mM	DTT

Nuclear Buffer B

20mM	Hepes pH 7.5
20%(v/v)	Glycerol
0.2mM	EDTA
0.5mM	DTT

Protease Inhibitors

Protease inhibitors were included in all lysis buffers and were added immediately before use to a final concentration of 40µl/ml. Complete EDTA free protease inhibitors were from Boheringer Mannheim, and made up as 2ml H₂O/tablet.

2.2.2 Biochemical Techniques

2.2.2.1 Lactate dehydrogenase (LDH) reaction buffer

150mM	Tris HCl pH 7.4
-------	-----------------

2.2.2.2 LDH reaction mix:

Washed fraction mix:

186µl	LDH reaction buffer
7µl	10mM Pyruvate
7µl	Lysate sample

Occluded fraction mix:

172µl	LDH reaction buffer
7µl	10mM Pyruvate

7 μ l Lysate sample
 14 μ l Triton X-100

2.2.2.3 PDE4 Assay buffer

10mM MgCl₂
 20mM Tris/HCl, pH 7.4

2.2.2.4 PDE4 Assay Dilution Buffer

20mM Tris/HCl, pH 7.4

2.2.2.5 Protein Kinase Assay Buffer (2X)

100mM Tris
 30mM MgCl₂
 30mM β -mercaptoethanol
 20% (v/v) Glycerol

2.2.2.6 Kinase Assay Reaction Mix

500 μ l 2X KAB
 10 μ l [³²P] γ -ATP
 490 μ l H₂O

2.2.2.7 ELISA Binding Buffer

0.1M Na₂PO₄ (pH 9.0)

2.2.2.8 ELISA Blocking Buffer

10% fetal bovine serum in western blot wash buffer

2.2.2.9 ABTS Substrate Solution

150mg 2,2'-Azino-bis-(3-ethylbenzthiazoline-6-sulfonic acid)
 500ml 0.1M anhydrous citric acid in dH₂O

2.2.2.10 5X SDS loading buffer

0.26M Tris/HCl (pH 6.7)
 55.5% Glycerol
 8.8% SDS
 11.1% β -mercaptoethanol

2.2.2.11 2X SDS loading buffer

0.125M Tris/HCl (pH 6.7)
 25% Glycerol

4%	SDS
5%	b-mercaptoethanol

2.2.2.12 Acrylamide resolving gel (6-8%)

6-8%	29:1 Acrylamide:N,N'-methylenebisacrylamide mix
0.375M	Tris/HCl pH8.8
0.1%	SDS
0.1%	Ammonium Persulphate
0.06%	N,N,N',N'-tetramethylethylenediamine (TEMED)

2.2.2.13 Acrylamide resolving gel (10-15%)

10-15%	29:1 Acrylamide:N,N'-methylenebisacrylamide mix
0.375M	Tris/HCl pH8.8
0.1%	SDS
0.1%	Ammonium Persulphate
0.04%	TEMED

2.2.2.14 Acrylamide stacking gel

5%	29:1 Acrylamide:N,N'-methylenebisacrylamide mix
0.125M	Tris/HCl pH8.8
0.1%	SDS
0.1%	Ammonium Persulphate
0.1%	TEMED

2.2.2.15 Tris-Glycine running buffer

192mM	Glycine
25mM	Tris
0.15%	SDS

2.2.2.16 Transfer Buffer

192mM	Glycine
25mM	Tris
20%	Methanol

2.2.2.17 Western Blot Wash Buffer

137mM	NaCl
20mM	Tris pH 7.6
0.05%	Tween

2.2.2.18 Blocking Buffer

137mM	NaCl
20mM	Tris pH 7.6
0.05%	Tween
5%(w/v)	Skimmed milk protein

2.2.2.19 Antibody Dilution Buffer

137mM	NaCl
20mM	Tris pH 7.6
0.05%	Tween
1%(w/v)	Skimmed milk protein

2.2.2.20 Ponceau S stain

0.1%	Ponceau S
3%	Trichloroacetic acid

2.2.2.21 Coomassie stain

0,025%	Coomassie brilliant blue R 250
40%	Methanol
7%	Acetic acid

2.2.2.22 Destain

40%	Methanol
7%	Acetic acid

2.2.3 Molecular Biological techniques

2.2.3.1 Tris Acetate Electrophoresis (TAE) Buffer

2M	Tris
1M	Acetic acid
0.05M	EDTA

2.2.3.2 PCR Reaction mix

50mM	KCl	(10X in Taq polymeRase buffer)
10mM	Tris HCl	(10X in Taq polymeRase buffer)
200μM	dATP	
200μM	dCTP	
200μM	dTTP	
200μM	dGTP	
1.5mM	MgCl ₂	
>1μg	Template DNA	
5 units	Taq polymeRase	
0.5μM	sense/antisense primer	

2.2.3.4 cDNA synthesis mixture (all solutions from kit)

11 μ l	“Bulk first strand cDNA mix”
1 μ l	DTT solution
1 μ l	Not1-d(T)10 (0.2 μ g/ μ l) primer
20 μ l	heat-denatured RNA

2.2.3.5 L-Broth

170mM	NaCl
0.5%(w/v)	Bacto-Yeast extract
1%(w/v)	Bacto-Tryptone
+/-	Antibiotic

2.2.3.6 LB-Agar

170mM	NaCl
0.5%(w/v)	Bacto-Yeast extract
1%(w/v)	Bacto-Tryptone
2%	Agar

2.2.3.7 STE buffer

10mM	Tris pH 8.0
150mM	NaCl
1mM	EDTA

2.2.3.8 Bacterial lysis reagents stocks

Lysozyme	10mg/ml in STE
Sarkosyl	10% in STE
Triton X-100	10% in STE

2.3 Mammalian cell culture

All solutions used in the manipulation of cell culture were heat sterilised by autoclave.

2.3.1 Cell lines

2.3.1.1 Cos 1 cells (ECACC 88031701)

COS 1 cells are an African green monkey renal cell line immortalised with an origin defective mutant simian virus 40 (SV 40). The expression of the SV 40 T antigen in COS cells facilitates the transcription of plasmid DNA containing the SV 40 origin of replication. This characteristic means that COS cells provide an excellent vehicle for transient transfection for analysis of over expressed proteins. COS 1 cells were maintained in complete DMEM unless being prepared for transfection or Serum starved for stimulation. Trypsin EDTA (Sigma Aldrich T4299), solution is required to passage COS-1 cells as they are firmly adherent to plastic.

2.3.1.2 U937 cells (ECACC 85011440)

U937 cells are derived from a human histiocytic lymphoma and continue to express many monocytic markers. U937 is a useful tool to investigate the mechanisms of monocyte inflammatory signalling. They are a suspension cell and were maintained in RPMI medium. U937_{PMA} were U937 cells treated with 4nm PMA for 4 days. Medium was replaced after 2 days.

2.3.1.3 Raw 264.7 cells (ECACC 91062707)

Raw 264.7 monocyte macrophage cells were isolated from a murine lymphoma caused by the Abelson leukaemia virus. They are capable of phagocytosis and have many

characteristics of macrophages. They are adherent and were maintained in complete DMEM.

2.3.1.4 Human Monocytes

Human monocytes were collected to compare with a model based on the U937 cells.

I Donor Selection

Normal healthy volunteers were selected and full ethics approval was obtained from the local ethics committee.

II Monocyte Isolation

Heparinised whole blood was collected and centrifuged over Ficoll-Hypaque at 350 X G for 30 mins. The mononuclear cell layer was removed and washed in Ca^{2+} and Mg^{2+} - free Hanks salt solution and resuspended in RPMI (Section 2.2.1.1). Monocytes were isolated by incubation with paramagnetic beads conjugated to anti-CD14 antibodies (Dynabeads M-450 CD-14) and magnetic separation according to manufacturer's instructions.

III Monocyte Culture

Monocytes were cultured under standard conditions (Section 2.3.2) in plastic 100cm² culture plates. Culture was allowed to proceed for varying lengths of time (0 - 7 days) with frequent changes in culture medium.

2.3.2 Culture Conditions

All mammalian cell culture was performed in incubators maintaining ambient temperature at 37°C and a 5%CO₂ enriched atmosphere. COS and Raw 264.7 cells were grown in continuous culture as a monolayer. U937 cells were grown as a continuous suspension.

Cells were passaged at approximately 90% confluence and were split 1:5. This necessitated passage every 4 days.

2.3.3 Pharmacological treatment

Unless otherwise stated cells were Serum-starved for 4 -12 hours prior to the addition of pharmacological agents. Signal transduction inhibitors were added 30 minutes prior to further stimulation or manipulation. Pharmacological agents were stored at -20°C as 10 X stock solutions. Lipopolysaccharide was used both in the presence and absence of Serum to allow for the presence of LPS binding proteins.

2.3.4 Transfection

Plasmid DNA was prepared for bacterial hosts and diluted in TE buffer (2.2.1.3.1).

2.3.4.1 DEAE Dextran transfection

24 hours prior to transfection 90% confluent COS 1 cells were split 1:2. They were grown overnight until 50-60% confluent. 10µg plasmid DNA per 79cm² cells was diluted to 40ng/ml in sterile TE buffer (2.2.1.3.1), then further diluted in DNA adhesion buffer (2.2.1.3.2) to 40ng/ml. This mixture was incubated at room temperature for 15 min and 5ml transfection medium (2.2.1.1.5) at 37°C was added. This was mixed then added to flasks from which medium had been freshly removed. Following 3-4 hours incubation, DNA solution was aspirated and cells were shocked by the brief (2 min) addition of 2 ml shock buffer (2.2.1.3.3). Cells were washed once with 10 ml PBS and complete DMEM added. Cells were incubated for 72 hours before being harvested.

Where mock transfections were run in parallel all steps were followed, but DNA was omitted.

2.3.4.2 Superfect transfection (Qiagen)– as per manufacturer’s instructions

24 hours prior to transfection Raw 264.7 cells were split to 50% confluence and grown over night. 5µg/ 60mm dish DNA was dissolved in 10µl TE buffer. 130µl Non enriched DMEM was added, followed by 30µl superfect reagent. The solution was mixed then incubated at RT for 10 minutes. 1ml complete DMEM was added to the DNA solution and this was added to cells. Cells were incubated for 3 hours under normal conditions, then the solution was removed and cells washed once with PBS at 37°C. Complete DMEM was added and incubated for 72 hours prior to harvest.

2.3.5 Cell counting

Cell number was calculated using a standard haemocytometer. Suspension cells were diluted in trypan blue 1:1 (v:v), and injected under a cover-slip on an haemocytometer. Cells deemed viable by their ability to exclude trypan blue were counted in 5 defined areas in two regions of the haemocytometer and the mean calculated. This figure was then adjusted for dilution and volume. Where adherent cells (U937_{PMA}) were counted these were grown on gridded cover-slips and counted in the same way.

2.3.6 Disruption

Prior to disruption cells were either washed 3 times in PBS and scraped (adherent cells) or collected from suspension by centrifugation and washed 3 times in PBS.

2.3.6.1 Non-detergent based lysis

Cells were homogenised in KHEM buffer with 0.5mM DTT and protease inhibitors by passage through a 26 gauge needle 10 times. The homogenate was then fractionated by centrifugation at 2,000 rpm for 5 minutes and the supernatant (S1) was removed. The

resulting pellet (P1) was washed in KHEM buffer and kept on ice until resuspension. The S1 was further fractionated by high-speed centrifugation (55,000rpm for 30 minutes), producing a supernatant (S2) and pellet (P2). The P2 fraction was washed in KHEM buffer and both pellets were resuspended in a volume equal to the final volume of the S2 fraction. Lactate dehydrogenase assay was performed to confirm the integrity of each fraction.

2.3.6.2 Detergent based lysis

Washed cells were either scraped into (adherent cells), or added to 313 lysis buffer and incubated end over end for 30 minutes before separating the detergent insoluble fraction by centrifugation at 13,000 rpm for 5 minutes. The detergent soluble supernatant was reserved.

2.3.6.3 Nuclear fractionation

Preparations of enriched nuclei from RAW 264.7 cells were prepared as follows. Washed cells were resuspended in 500 μ l nuclear buffer A to which the detergent NP40 (0.1%v/v) had been added. Cells were mixed and gently pipetted on ice for 10 minutes before being separated by centrifugation at 12,000rpm for 5 minutes. Pellet was retained and resuspended in 300 μ l nuclear buffer B. Enriched nuclei were lysed by sonication on ice at 40W, for 5 seconds. Sonicate was separated by centrifugation at 12,000 rpm for 5 minutes and the supernatant was retained.

2.4 Biochemical Techniques

2.4.1 Sample preparation and storage

Protein samples for western blot analysis were diluted in 5X SDS loading buffer and heated to 100^o C for 5 minutes to denature the proteins.

Protein samples for enzyme assay analysis were frozen in liquid nitrogen and stored at -70°C until use.

Protein samples for other forms of analysis were frozen in liquid nitrogen and stored at -20°C .

2.4.2 Protein quantification (Bradford's assay)

Lysate protein content was measured in 96 well microtitre plates against a standard curve derived from known concentrations of bovine Serum albumin (BSA) 0-5 μM . A series of dilutions of test lysate were made in 50 μl volumes and 200 μl 1:5 Bradford's reagent was added to these and the standard curve protein. Light absorbance at 590nm was measured on a MRX microtitre plate reader (Dynex technologies). All samples were measured in triplicate.

2.4.3 Lactate Dehydrogenase (LDH) Assay

To confirm the integrity of high speed fractionation the activity of the cytosolic enzyme lactate dehydrogenase (LDH) was measured in each fraction. The following reaction allows quantification of NADH oxidation to be measured spectrophotometrically in 96 well microtitre plates using a MRX microtitre plate reader at 340nm wavelength:



The activity of washed and occluded fractions were measured by setting up pre-reaction solutions and the reaction was started by the addition of 10 μl 2mM β -NADH. Readings were taken at 20 second intervals for 10 minutes. The rate of extinguishing was proportional to the LDH activity in the sample, and the difference between washed and occluded fractions represented contamination of pellet fractions by intact cells or S2. (appendix 2 demonstrates the integrity of fractionation measured in this way).

2.4.4 Phosphodiesterase assay

Cyclic AMP was stored at -20°C as a 10mM stock and diluted to 1mM immediately prior to use. Substrate solution was prepared by further diluting the stock cAMP to 2 μM in assay buffer supplemented with $8\text{-}^3\text{H}$ cAMP ($0.003\mu\text{Ci } \mu\text{l}^{-1}$). The reaction was performed in 100 μl volume consisting of 50 μl cAMP (final concentration 1 μM) and 40 μl sample lysate. Rolipram or assay buffer contributed the remaining 10 μl . The solution was mixed by vortexing and the reaction was performed at 30°C for 10 minutes. Where PDE4 activity was less abundant a longer reaction period was used after ensuring this remained in the linear range of the reaction. Placing in boiling water for 2 minutes stopped the reaction and tubes were cooled on ice.

25 μl of 1mg/ml snake venom (*Crotalus atrox* venom) was added to the reaction and mixed by vortexing. This was then incubated for 10 minutes at 30°C and cooled on ice. 400 μl of a 1:1:1 solution of activated dowex : water : ethanol was then added, and thoroughly mixed. This was then incubated on ice for a minimum of 15 minutes with regular agitation before being vortexed and separated by centrifugation at 13,000 rpm for 3 mins. 150 μl of the top soluble layer was then removed and added to 1ml of scintillation fluid and counted on a Wallac 1409 liquid scintillation counter.

Data was processed using the following calculation where X is the mean of the PDE activity measured in triplicate with a value of non-metabolised cAMP subtracted.

$(X / (\text{total activity of } 50\mu\text{l } 2\mu\text{M cAMP solution}) * 391.67 / 150$ (representing the proportion of total reaction supernatant sampled) * $(1 * 10^{-10} / 10)$ (representing moles of cAMP in solution divided by the time of the reaction) * 10^{12} (converting to picomoles)) / quantity of protein in μg tested. This equation produces an activity in terms of velocity

pmol/min/ μ g. Where activity is expressed as pmol/min/mg the figure is multiplied by 1000.

2.4.5 Kinetic analysis of PDE4 isoforms

When characterising the activity of PDE4B4 I modified the assay as follows.

2.4.5.1 Transfection specific activity

For each transfection of active PDE4B4, a mock transfection and a comparison PDE4B isoform were included as controls. To calculate the specific activity for each PDE4B4 assay mock activity for a given [cAMP] was subtracted from the transfected activity under investigation.

2.4.5.2 Relative transfection efficiency

Comparison of relative activities between two transfections requires assessment of enzyme expression for each. Quantative analysis was performed by ELISA using antisera raised against the C-terminal region of PDE4B isoforms or by semi-quantitative western blot analysis. In the latter analysis increasing quantities of protein from two transfection lysates were western blotted beside each other. Densitometry using Kodak 2.0 software was then used to construct protein Vs density plots. The gradient of these plots reflects the amount of transfected protein present. The ratio of these gradients was used to adjust activities against each comparative experiment.

2.4.5.3 Relative activity determination

To define the K_{m} of PDE4B4, data from PDE assays over a range of cAMP concentrations 0.1, 0.2, 0.4, 0.6, 0.8, 1, 2, 4, 6, 8, 10, 15, 20, 25, 30 μ M, were plotted and analysed using

computer modelling of the parabolic form of the Michaelis-Menton equation. This equation ($y=(M1*M0)/M2+M0$, where $y = V_{obs}$, $M1 = V_{max}$, $M0 = [cAMP]$ and $M2 = K_m$), was used to calculate the K_m . Each assay was performed in triplicate and each experiment was performed on three transfected samples. Equal amounts of enzyme were used to generate V_{obs} and V_{max} was calculated for $1\mu M$ cAMP. Relative V_{max} calculations were calculated by comparing V_{max} for PDE4B4 and comparing it against V_{max} for a known PDE4B control.

2.4.5.4 IC₅₀ Rolipram

IC_{50} of an enzyme for its inhibitor is calculated by measuring the activity of an enzyme at a set substrate concentration in this case $1\mu M$ cAMP, in the presence of varying amounts of inhibitor. I used 10, 5, 2, 1, 0.5, 0.2, 0.1, 0.05, 0.02, 0.01 and 0 μM rolipram and $3\mu g$ lysate protein. IC_{50} was then calculated by using a least squares log fitting algorithm.

2.4.6 Preparation and running of Tris-Glycine gel

Both mini-gels and standard 25cm gel kits (Bio-RAD, Hemel Hempstead) were used for SDS-Poly-acrylamide gel electrophoresis (SDS-PAGE) during this work. The gel apparatus was assembled as per the manufacturer's instructions. A resolving gel (2.2.2.11, 2.2.2.12) appropriate for the molecular weight of the protein under investigation (see table 2.4) was prepared and poured between the plates. A protective layer of deionised water was poured on top to exclude oxygen during polymerisation. The gel was left for a minimum of 30 minutes at room temperature. One hour before use a stacking gel was prepared and poured on top of the resolving gel (2.2.2.13). Once poured a comb was inserted to make wells in the stacking gel. Running buffer was used to clean the individual wells of non-polymerised gel solution. Samples prepared in SDS sample buffer (2.2.2.10) were warmed to $40^{\circ}C$ prior to being loaded into wells. The gel was then immersed in a

tank containing tris-glycine running buffer (2.2.2.14). A hood connected to an electrical supply was connected and electrophoresis was performed for 1-4 hours (40 V / gel) or 16 hours (8 V/gel).

Acrylamide content (%)	Molecular weight (kDa)
8	40-200
10	21-100
12	10-40

Table 2.4 Range of protein separation on SDS PAGE

2.4.7 Transfer to nitrocellulose

Once SDS-PAGE was complete the gel was removed and layered on a pre-soaked nitrocellulose membrane (Bio-RAD X μ M). This was then immersed in transfer buffer and sandwiched between two protective non-insulative plates bound by 3mm blotting paper (Whatman, UK). This assembly was slotted in a transfer tank and proteins were electrically transferred to nitrocellulose at 1 A, for 1 hour. To confirm adequate transfer and equal loading of lanes, membranes were washed in Panceau red stain to visualise proteins (2.2.2.19).

2.4.8 Immunostaining of proteins

Membranes were blocked in 5% milk protein blocking buffer (2.2.2.17), for 1 hour and washed in wash buffer three times (2.2.2.16). Proteins were visualised by incubation with antibodies raised against the proteins selected, at the pre-determined concentrations in 1% blocking buffer. Incubations were performed for 4 hours at room temperature or o/n at 4°C. Membranes were washed 3 times in wash buffer and incubated with peroxidase-conjugated secondary antibody (0.00001%), appropriate for the species of the primary antibody in 1% blocking buffer (see table 2.1). After 1 hour membranes were washed and

treated with ECL-reagent (Amersham Ltd) prior to development on blue light sensitive film (KODAK, UK).

In all cases positive controls were recombinant proteins expressed in COS cells (SAPU, PDE4 isoform antibodies) or well characterised cell conditions supplied with antibodies (commercial antibodies).

2.4.9 Quantification of western blot analysis

Where quantification of expressed protein was required radiographs were scanned and densitometry of expressed band was performed using kodak ID software. A control band of recombinant sample, from transfected COS cells was used as a blank value and different quantities of cell lysate were compared to generate a range of values. A mean of these values was used for comparison with a similarly calculated mean for an opposing set of conditions.

In the specific case of phospho-ERK antibodies, the ratio of P-ERK band density was compared with total ERK band density and ratios are expressed.

2.4.10 PDE4B2 Back Phosphorylation

Six confluent flasks of RAW264.7 cells were treated with LPS for a range of time intervals. Cells were washed in ice cold PBS and lysed in 3T3-lysis buffer. Immunoprecipitation of PDE4B isoforms was performed as described below. After 2 hours incubation with antibody captured PDE4B was isolated on protein A-beads, beads were collected and washed 3 times in 3T3-lysis buffer containing protease inhibitors. Beads were then washed once in PBS and once in kinase assay buffer (2.2.15).

To 1ml of kinase assay reaction buffer, 1 μ l 0.2mM ATP-P³² was added. Where phosphorylation was to be performed, 1 μ l (21.4mU) recombinant ERK kinase was added to the immunoprecipitates in a micro-tube, followed by 50 μ l reaction buffer. These were mixed and incubated for 30 minutes at 30°C. Beads were collected by centrifugation, and supernatant removed. Beads were then boiled in 2X sample buffer collected and supernatants were loaded onto an SDS-poly acrylamide gel.

Following SDS-PAGE, proteins were transferred to a nitrocellulose and incubated on a phosphoimage plate and images were quantified on a phosphoimager (Bio-Rad LTD, UK).

2.4.11 Immunoprecipitation and Co-immunoprecipitation

Immunoprecipitation was performed using antisera, raised against cell signalling molecules in non-immune animals. Pre-immune serum is serum from the animal used to raise the antisera, prior to exposure to the antigenic portion of the molecule. Ranging experiments were performed to assess the optimum ratio of cell protein to antisera to immunoprecipitate all active target molecule.

Cells lysates were prepared in 3T3-lysis buffer and protein content quantified. A volume of cell lysate equivalent to the required amount of protein was incubated with a volume of preimmune serum equal to the volume of immune serum to be used for immunoprecipitation. Incubation was allowed to continue for 1 hour at 4°C end over end. During incubation, 60 μ l of protein A beads per immunoprecipitate sample were prepared by repeated centrifugation at 13,000rpm and washed in 100 μ l 3T3 lysis buffer with protease inhibitors. Immediately prior to use these beads were washed again, distributed to micro-tubes and immunoprecipitate samples were added. Protein A binds to the Fc portion of IgG antibodies allowing these to be isolated from solution. Further incubation was allowed to continue for 30mins at 4°C.

Preimmune antibodies bound to protein A coated beads were removed by centrifugation, and antiserum was added to the resulting precleared lysate. Incubation with antiserum was allowed to continue for 2 hours at 4°C, before being added to protein A beads prepared as above. Further incubation was allowed to continue for 30 mins at 4°C and beads were collected by centrifugation at 13,000rpm.

Protein A beads were washed in PBS with 1µM DTT, and protease inhibitors, twice and transferred to a new microtube. Where immunoprecipitates were to be analysed by western blot, beads were washed once more in 3T3 lysis buffer with protease inhibitors, collected by centrifugation and resuspended in 1X SDS loading buffer. These samples were boiled for 5 mins and the bead free supernatant was collected and loaded onto polyacrylamide gel. Where immunoprecipitates were to be analysed by phosphodiesterase4 assay, beads were washed once in PDE4 assay buffer with 1µM DTT and protease inhibitors, before being resuspended in 120µl PDE4 assay buffer and distributed evenly between three microtubes.

2.4.12 Enzyme-linked Immunosorbant Assay (ELISA)

ELISA was performed to quantify the amount of protein in cell lysate or cell culture medium. All ELISA was performed with test samples in parallel with standards of known quantity, by which a standard curve was generated. Four different quantification protocols were followed. Where cell culture medium was being assayed, standards were prepared in the culture medium used. Where cell lysate was prepared all samples were diluted in lysis buffer to a range of protein concentrations (Appendix 1, presents the standard curves prepared).

2.4.12.1 "In-house" TNFα assay

Anti- TNFα capture antibody, was diluted in ELISA binding buffer to 2µg/ml and 50µl of the resulting solution was added to each well of a 96 well ELISA plate. Plates were sealed

with wax paper and incubated for 18 hours at 4°C. Plates were warmed to room temperature and excess capture antibody removed by washing twice with PBS. Non-specific peptide binding was blocked by incubating each well for 2 hours at room temperature with 100µl ELISA blocking buffer. Blocking buffer was removed by 3 washes with western blot wash buffer.

Samples and standards were prepared in DMEM 100µl. TNFα standards were prepared by multiple dilutions from 200ng/ml to 0.195ng/ml. 100µl samples and standards were added to each well the plate was sealed with wax paper and incubation was allowed to continue overnight at 4°C. Following incubation plates were allowed to rewarm to room temperature and wells were washed 4 times with western blot wash buffer.

Biotinylated anti- TNFα was diluted to 1µg/ml in western blot wash buffer, and 100µl was added to each well. Incubation was allowed to continue for 1 hour at room temperature and plates were washed with 100µl wash buffer per well 4 times. Avidin-horse radish peroxidase conjugate (Av-HRP) was diluted to 2µg/ml in ELISA blocking buffer and 100µl was added to each well. Incubation at room temperature was allowed to continue for 30 minutes before each well was washed in western blot wash buffer 4 times.

ABTS substrate solution was thawed immediately prior to use and 100µl H₂O₂ added to 11mls solution. 100µl of prepared substrate solution was added per well and incubated at room temperature in the dark until colour change occurred. Plates were read in a microtitre plate reader at 405nm over a range of time. Standard curves were calculate from the standards and samples were measured by reference to this standard curve. Appendix 1.2 presents a typical example of a cytokine standard curve.

2.4.12.2 Commercial TNF α ELISA (Chemicon International, Inc, CA, USA)

For TNF α assay in RAW 264.7 cells transfected with Rap-1 mutants the commercial mouse TNF α enzyme immunosorbant assay (EIA) kit (Chemikine, mouse TNF α EIA kit, Cat CYT140) was used. This kit is a competitive EIA using wells precoated with TNF α antiscrum to which samples and standards were added. Following washing biotinylated TNF α was added to occupy free antibody sites. Streptavidin-alkaline phosphatase was bound to the biotin and colour reaction was achieved with commercial solutions and quantified by absorption at 490nm. In contrast to the in-house TNF α ELISA, a high reading indicates free antibody and therefore a low TNF α content in the test solution.

2.4.12.3 Recombinant Protein ELISA

Where relative transfection efficiencies were compared by cell lysate ELISA for PDE4 isoforms the volumes of cell lysate representing a range of protein quantities, prepared in KHEM were allowed to bed in 96 well ELISA plates at 4 $^{\circ}$ C overnight. PDE4B content of this embedded lysate was detected by incubating each well with PDE4B antiserum diluted 1/5000 in ELISA blocking buffer. Incubation was allowed to continue for 1 hour at room temperature and antibody was removed by washing 4 times with western blot wash buffer. HRP conjugated anti-rabbit antibody was diluted to 0.5 μ g/ml in ELISA blocking buffer and 100 μ l was added to each well. Incubation was allowed to continue for 1 hour at room temperature and antibody was removed by washing 4 times in ELISA wash buffer.

ABTS substrate solution was prepared as for cytokine detection, and 100 μ l was added to each well and incubation was continued for a range of time periods at room temperature in the dark. Protein was quantified by optical density measurement at 405nm and relative protein quantities were plotted by O.D. against protein quantity. A representative assay is presented in appendix 1.2 (p249).

2.4.12.4 Prostaglandin E2 (PGE2) EIA

PGE2 production from RAW264.7 cells was quantified using the commercial EIA kit from Cayman chemicals CO, USA. This competitive EIA uses 96 well ELISA plates coated with goat anti-mouse antiserum to which a mixture of sample or standard, mouse anti-PGE2 antiserum and alkaline phosphatase conjugated PGE2 is added and incubated at room temperature for 2 hours. This mixture is washed and colour reagent added. The resulting colour change is quantified by light absorption at 490nm and a plot of known standard against OD_{490nm} was used to generate a standard curve. Test samples were calculated from this standard curve (appendix 1.3, p250).

2.5 Molecular biology techniques

2.5.1 Plasmid / DNA preparation

Glycerol stocks of *E Coli* transformed with plasmids encoding recombinant proteins were maintained at -70 °C. Prior to bulk preparation a sample of stock was smeared on antibiotic selective agar plates, and grown o/n at 37 °C. One colony was selected to inoculate a 10 ml (mini-prep) or a 400ml (maxi-prep) flask of L-Broth with appropriate antibiotic added. After incubation for 24 hours, bacteria were collected by centrifugation. Plasmid preparation was performed using either Qiagen's QIAprep maxiprep kit or QIAprep spin miniprep kit. Manufacturer's instructions were followed at all times.

Recovery of cDNA from agarose gels was achieved using Qiagen's QIAquick gel extraction kit following manufacturer's instructions.

2.5.2 RNA extraction

Cells were collected by centrifugation and homogenised in Tri-reagent (1ml/10⁷ cells) using a 12 guage needle. Homogenates were incubated at room temperature for 5 minutes, transferred to sterile eppendorph tubes and centrifuged at 13,000rpm for 5 minutes to remove cell debris. Supernatants were transferred to fresh tube, 0.2ml RNase-free chloroform was added and solutions were mixed by vortexing for 15 seconds. RNA and DNA were phase separated by incubating the mixed solutions at room temperature for 3 minutes, then centrifugation at 13,000 rpm for 15 minutes. The aqueous (clear) phase was removed to a sterile tube and 0.5ml isopropanol/ml of Tri-reagent used was added to precipitate RNA. Incubation at room temperature for 10 minutes then centrifugation at 13,000 rpm and 4 oC for 10 minutes collected precipitated RNA. The pellet of RNA was washed with 75% ethanol and RNA stored before quantification immediately prior to use.

2.5.3 Quantification of DNA and RNA

A known volume of dissolved RNA or DNA was quantified spectrophotometrically by measuring absorbance at 260nm and 280nm on a Shimadzu UV-1201 UV-VS spectrophotometer blanked against distilled water. Estimates of nucleic acid quantity and purity were made from the following assumptions:

1. Absorbance of 1 at 260nm (A_{260}) is equivalent to:
 - 50 μ g/ml double stranded DNA
 - 37 μ g/ml single stranded DNA
 - 40 μ g/ml RNA
2. $A_{260}:A_{280}$ ratio of pure DNA equals 1.8
- $A_{260}:A_{280}$ ratio of pure RNA equals 2

2.5.4 First strand cDNA (Pharmacia kit)

First strand cDNA synthesis uses poly dT primers to amplify poly adenylated mRNA from total cell RNA. 5µg total RNA is diluted to 20µl in DEPC treated H₂O, heated to 65 °C for 10 minutes and transferred to ice. This was added to first strand cDNA mix (section) and gently mixed by pipetting. The solution was incubated at 37 °C for 1 hour then stored at -70 °C.

2.5.5 Polymerase chain reaction (PCR)

Where the PCR template was cDNA from total cell RNA PCR is known as reverse transcriptase PCR. The PCR reaction subsequently is equivalent to that using plasmid DNA as a template. Briefly the PCR mix was assembled (section) and cycled through a Techgene thermocycler PCR machine. Cycling conditions varied for different PCR reactions as determined by the melting temperature of the specific primer used and ranging experiments where necessary.

2.5.6 Restriction digest

Restriction enzymes were used to digest plasmid DNA to isolate an incorporated fragment or to screen for a cloned cDNA. Restriction enzymes were purchased from promega along with the appropriate buffers. Restriction digest was performed in volumes of 10µl in diluted buffers with 1µl enzyme at 37°C.

2.5.7 Agarose gel analysis

Agarose gels were used to resolve nucleic acids of different molecular weight. Agarose content was selected based on the molecular weight of the nucleic acid of interest. The

desired amount of agarose was added to 20ml 1 X TAE and this mix was microwave heated until the agarose was dissolved. Once hand warm 1.7 μ l ethidium bromide was added and mixed by swirling. Molten agarose was poured into the gel mould and allowed to set. The tank was filled with TAE, and wells were filled with samples mixed with loading dye (promega), and the gel run at 75V until the desired distance was run out. Gels were now visualised under UV light by virtue of ethidium bromide incorporated into nucleic acid fluorescence.

2.5.8 Plasmid/insert Ligation

Ligation of PDE4-HIVtat fusion cDNA into linearised PGEX 5.3 for synthesis of a GST fusion protein was achieved using the rapid DNA ligation kit (Roche). Manufacturer's instructions were followed. Briefly, DNA to be ligated (XXX linearised pGEX-5.3 and insert cDNA) was purified from agarose gel quantified. Various molar ratios of vector DNA: insert cDNA were dissolved in DNA dilution buffer to a volume of 10 μ l. The optimum molar ratio was measured for each ligation reaction performed using the following ratios in ranging experiments 1:7, 1:5 and 1:3. 10 μ l of 2 X T4 DNA ligation buffer was added and the solution was mixed. 1 μ l T4 DNA ligase was added, mixed and incubated at room temperature for 5 minutes. The ligation reactions were used immediately for transformation into bacterial hosts.

2.5.9 Bacterial Transformation

Cloned plasmids were transformed into either TOP-10 (Invitrogen) chemically competent *E Coli* for plasmid amplification, or BL 21 chemically competent *E Coli* for protein expression. In each case transformation was carried out in the same manner. 50 μ l chemically competent bacteria were thawed on ice and 1-5 μ l of ligation reaction was added and gently mixed. Mixtures were incubated on ice for 30 minutes before heat

shocking at 42°C for 30-45 seconds before removing to ice. 250µl of pre-warmed SOC medium was added to the transformations, incubated for 1 hour at 37°C and spread on appropriate antibiotic selection agar plates. These were incubated inverted o/n at 37°C and sample colonies selected for screening by restriction digest and sequencing analysis.

2.5.10 Induction of recombinant proteins

Cultures of *E Coli* (BL 21), transformed with a plasmid encoding a recombinant HIV-tat fusion protein were incubated o/n at 37°C in 10ml L-broth containing 100µg/ml ampicillin (LB amp). These cultures were used to inoculate 400ml cultures of LB amp, which were grown at 37°C with agitation and frequent sampling. Once the OD 600nm was 0.6-1.0 protein expression was induced by addition of 4ml 10mM isopropyl β-D-thiogalactoside (IPTG) (final concentration 0.1mM). Incubation was continued at temperatures ranging from 37°C to 4 °C for between 4 hours and 18 hours respectively (see text chapter 6). Finally bacteria were harvested by centrifugation at 2500g for 5 minutes. Harvested bacteria were resuspended in PBS containing protease inhibitors and 1mM DTT and stored at -20 °C until use.

2.5.11 Protein purification PBS/sonification

Frozen bacteria were rapidly thawed and kept on ice. Where lysis buffers were used these were added to the bacterial solution to the desired dilution. Bacteria were lysed by sonication in 30second bursts separated by 30 second rests. The sonicate was separated by centrifugation at 13,000rpm for 1 minute and pellet P1, and lysate S1 were reServed. These were sampled for recombinant protein by addition of 2X SDS sample buffer heated to 40 °C and subjected to SDS-PAGE analysis.

2.5.12 Protein purification Lysosyme/ sarkosyl

Bacteria were prepared as above. Thawed bacteria were washed in STE buffer, resuspended in STE Lysosyme 100µg/ml and incubated on ice for 15 minutes. DTT was added to a final concentration of 5mM, and cells lysed by addition of Sarkosyl in varying concentrations (see chapter 6). Lysates were centrifuged at 10,000 rpm for 5 mins and the supernatant reserved. Triton X-100 was added to 2%(v/v) and protein isolation continued as below.

2.5.13 Sepharose isolation of GST-fusion proteins

Glutathione-sepharose beads equilibrated in the lysis solution required, containing protease inhibitors and 1mM DTT were added to solutions shown to contain GST-fusion protein. These were incubated end over end for 4-12 hours at 4 °C, before beads were collected by centrifugation at 13,000 rpm in a bench top refrigerated centrifuge. Beads were held on ice and washed in PBS containing protease inhibitors and 1mM DTT 3 times. Beads were then aliquoted and one aliquot was heated in 2X sample buffer and analysed for protein content by SDS-PAGE analysis, with coomassie blue identification.

2.5.14 Protein identification and preservation

Expressed proteins were resolved by SDS-PAGE on mini-gel apparatus as described above. Proteins were fixed and stained by incubation in 100ml Coomassie stain and gentle agitation at room temperature for 2 hours. Proteins were visualised by subsequent incubation in destain for 1-4 hours at room temperature. Destained gels were rehydrated by incubation in 1% glycerol for 30 minutes with agitation.

Finally gels were dried for preServation. The stained gel was layered on the drying surface of a gel drier (Bio-Rad, LTD). The cover sheet was sealed by a vacuum and the gel was dried at 65°C for 2 hours.

2.6 Statistical analysis

Statistical analysis was performed on studies where n=3 or more. When comparing the PDE4 profile between two cellular populations Student's paired t-Test was performed on measures of activity or on densitometry derived from western blot analyses. Where the effect of rolipram on a LPS driven effect was analysed, the significance of the difference between LPS alone and basal conditions and LPS + rolipram and basal conditions. In these studies of TNF α or PGE2 production, Student's paired t-Test was performed.

Chapter 3 Characterisation of PDE4B4

Introduction

PDE 4 genes encode a variety of isoforms by virtue of mRNA splice variation and differential use of multiple promoters [4]. Each PDE4 gene family exhibit almost 100% sequence homology within regions downstream of their unique N-terminal regions. The conserved domains of UCR1, UCR2 and the catalytic site demonstrate 95% sequence homology across mammalian species and to the *Drosophila dunce* gene [50]. Each PDE4 isoform is unique however at the extreme N-terminal region. Regulatory and targeting domains in this region allow individual PDE4 isoforms to exhibit non-conserved behaviour, [68] [73]. The human PDE4B gene has been localised to chromosome 1 and the rat PDE4B gene to chromosome 5, [236, 237]. To date, three gene products have been described in both species [233]. PDE4B1 and PDE4B3 are both long forms, distinguished from the short form PDE4B2 by the presence of the N-terminal UCR1 region [50].

A new member of the PDE4B family was recently discovered by our collaborator, Dr G Bolger. A rat cerebral cortex cDNA library obtained from Stratagene (La Jolla, CA, USA), was probed with cDNA corresponding to the PDE4B UCR1 using a technique previously described [233]. A novel cDNA named rPDE90, reflecting the novel PDE4B4 isoform, was identified and cloned. As has been discussed, [4], the existence of multiple isoforms of PDE4 suggests functional specificity and an understanding of the physical and biochemical characteristics of each isoform can be expected to give clues to its function and regulation

My aim in the work described in this chapter was to demonstrate the biochemical properties, the physical distribution and the regulation of PDE4B4. By comparing each characteristic against other PDE4 isoforms I will demonstrate how individual members of each PDE4 family are related and yet exhibit distinct characteristics from each other.

Results

Section 1

3.1.1 Sequence Confirmation of plasmid and transfection efficiency.

PDE4B4 is a 659 amino acid protein containing both UCR1 and UCR2, making it a “long form” PDE4. Fig 3.1.1 demonstrates the characteristic regions common to all PDE4 isoforms. PDE4B4 has considerable homology to the other known long form PDE4Bs, namely PDE4B1 and PDE4B3, over the C-terminal 642 amino acids. The N-terminal 17 amino acids of PDE4B4 show no sequence homology to other PDE4B sequence. However remarkable similarity is seen between the unique N-terminal region of PDE4D3 and PDE4B4, with 12 amino acids being conserved, including a PKA phosphorylation target domain. This domain includes Ser14 of PDE4B4 which correlates with Ser13 of PDE4D3, Fig 3.1.1.

The transcript of PDE4B4 was cloned from a rat (*Rattus Norwegensis*; Sprague Dawley strain) cerebral cortex library (Stratagene) and inserted into the Not1 site of pcDNA3 mammalian expression vector (Invitrogen). This brings the ORF under the control of the cytomegalovirus immediate early promoter allowing, for example, expression in COS cells (Fig 3.1.2A). Plasmids were transformed into E.Coli and kept as glycerol stocks as described in the methods section. Plasmids were purified as described in and restriction digest analysis using Sac1 and Not1 restriction enzymes confirmed the integrity of the clone (Fig 3.1.2B). Not1 cut the insert coding PDE4B4 from the plasmid revealing a very high molecular weight band and a fragment of 2Kba representing PDE4B4. Sac 1 cut the plasmid twice and the insert once resulting in one small 700 base fragment, a larger 1Kbase fragment and the plasmid remnant.

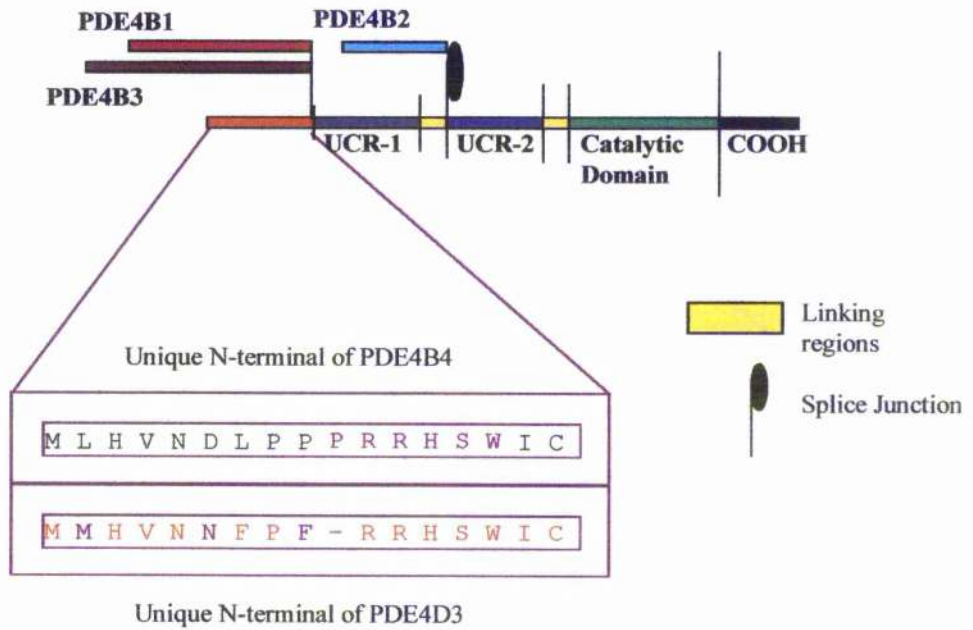


Fig 3.1.1 Schematic representation of PDE4B4

This diagram (not to scale) represents the amino acid sequence of PDE4B4 and illustrates the modular nature of the protein. All domains other than the red shaded region are shared by the long forms PDE4B1 and PDE4B3. One of the two PKA phosphorylation sites (Ser14), of PDE4B4 is highlighted. The second at Ser53, lies within the shared long form common region. The splice junction shown marks the point of divergence between long form and short form PDE4B isoforms. Thus PDE4B2 lacks the region N-terminal of this junction containing UCR1 and LR1. The long forms finally diverge after UCR1 where distinct N-terminal sequence is under the control of specific promoters. The extreme N-terminal sequence of PDE4D3 is presented beneath the sequence of PDE4B4, illustrating the sequence homology between these two molecules. Red letters represent shared residues while purple letters are non-conserved.

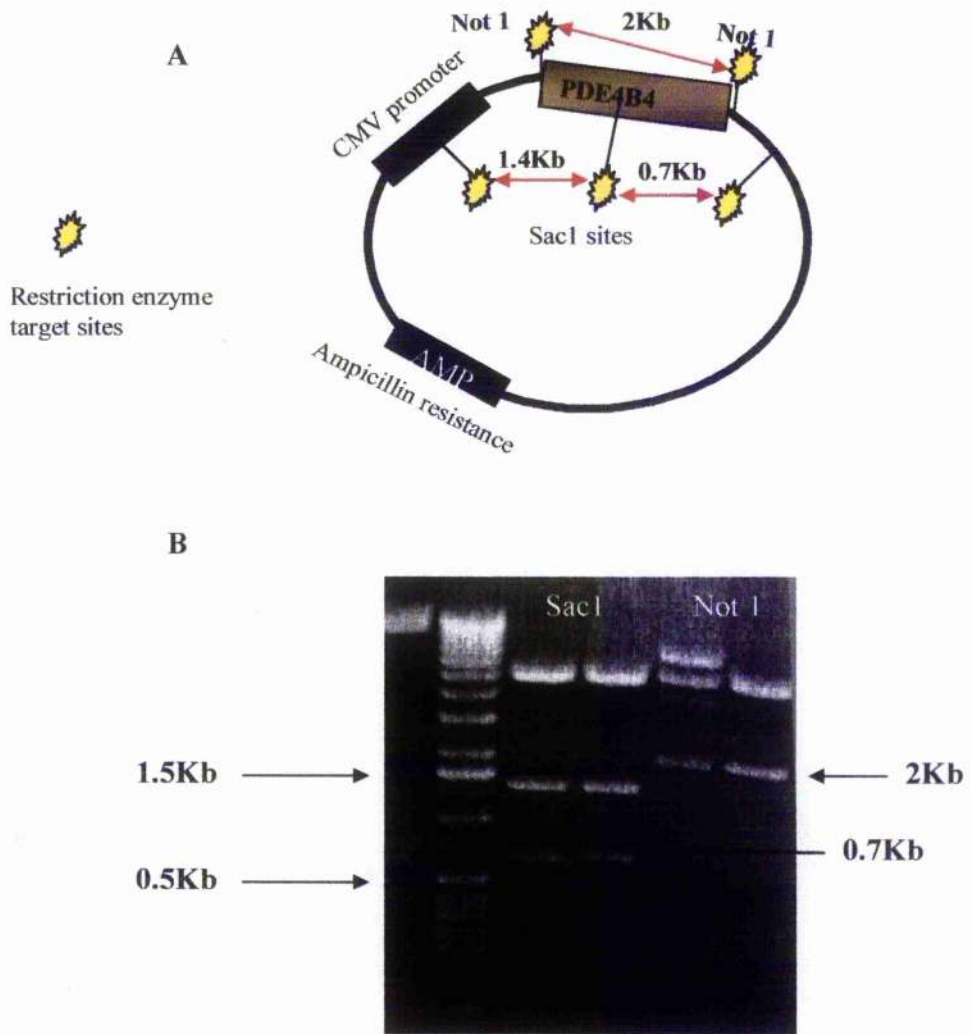


Fig 3.1.2 Restriction digest of PDE4B4 confirms plasmid integrity

cDNA coding for PDE4B4 was cloned into pcDNA3 plasmid vector between the Not1 sites in the poly-linker region. A; a schematic representation of the subsequent plasmid, demonstrating the restriction enzyme sites. B; To confirm that the clone used to characterise the kinetic behaviour of PDE4B4 was intact a restriction digest using Not1 and Sac1 restriction enzymes was performed. Sac1 was used as restriction sites exist within both the plasmid and the sequence of the cloned insert. The predicted restriction map resulted with bands of 0.7Kb and 1.4Kb following Sac1 digestion, and an insert band of 2Kb appearing after Not1 digestion. The plasmid was thus proven to be intact.

3.1.2 *Specific activity of over-expressed PDE4B4*

Our laboratory has employed over-expression of PDE4 isoforms in COS cells as a useful means to analyse their biochemical properties [76]. This compensates for the low abundance of these enzymes in nature and the difficulty in analysing a single PDE4 isoform distinct from other endogenously expressed species. PDE4 activity was measured over a range of protein quantities for transfected and mock transfected cell lysates.

Both Mock transfected and PDE4B4 transfected COS-1 cell extracts exhibited a linear relationship between protein content and PDE4 activity (Fig 3.1.3). PDE4B4 transfected cells, however exhibited considerably higher activity with a range of 0-3.4 pmol/min, corresponding to between 0 and 10 μ g of lysate protein. Mock transfected cells on the other hand achieved a maximum PDE4 activity of 0.09 pmol/min/ μ g over the same range of protein. As can be seen the activity/protein curve eventually forms a plateau, as no further substrate is available for hydrolysis. Using data from the steep, linear part of the curve, PDE4B4 transfected lysate is shown to have an activity of 0.6 pmol/min/ μ g with a specific activity for PDE4B4 of 0.58 pmol/min/ μ g.

To ensure kinetic analysis can be compared between experiments and previous reports, I performed all PDE4B4 characterisation at 1 μ M cAMP. I elected to perform all further kinetic analysis using 3 μ g of protein lysate as this falls on the linear part of the activity/protein curve measured at 1 μ M cAMP. An equivalent time ranging experiment was performed to ensure that assaying PDE4B4 at 1 μ M cAMP for 10 minutes also fell on the linear part of the activity/time curve.

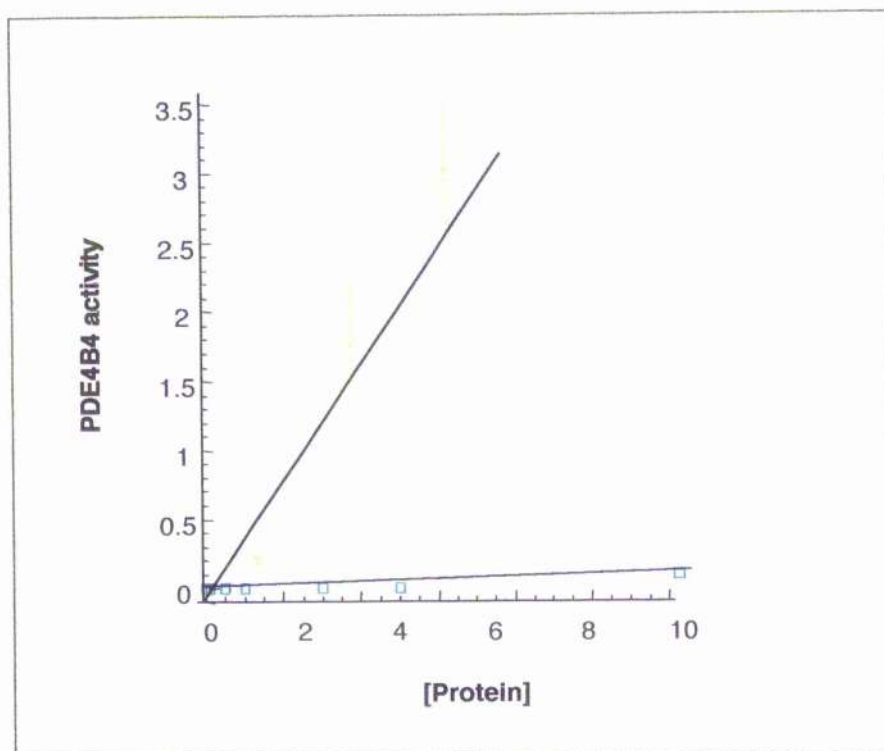


Fig 3.1.3 PDE4B4 protein ranging experiment

COS-1 cells transfected with plasmid coding for PDE4B4 protein and mock transfected COS-1 cells were lysed and PDE4 activity was calculated for a range of protein concentrations at $1\mu\text{M}$ cAMP. PDE activity was plotted against protein to find the linear range within which to analyse PDE4B4 activity. As can be seen $3\mu\text{g}$ of transfected protein lay within the linear part of the curve and corresponded to 1.8 ± 0.3 pmol/min/ μg . In contrast mock transfected COS-1 cells exhibited a cAMP PDE activity of 0.05 ± 0.01 pmol/min/ μg .

Section 2

3.2.1 Calculation of molecular size

The predicted molecular size for PDE4B4 based on primary amino acid sequence is 73kDa. The experimentally derived molecular weight is calculated from the distance migrated on SDS-PAGE gel compared to "markers" of known molecular weight. This experimental determination gives an apparent molecular weight of 85 +/- 3 kDa. (fig 3.2.1).

3.2.2 Subcellular distribution of PDE4B4

It has been shown that certain PDE4 isoforms expressed in COS cells are targeted to specific regions within the cell. For example while PDE4A1 is restricted to the cell membrane fraction, PDE4D1 and PDE4D2 exist in the soluble compartment [73, 77]. I set out to explore the localisation of recombinant PDE4B4 in COS-1 cells lysed in KHEM buffer and subjected to high speed fractionation. The three subcellular compartments Pellet1 (P1), Pellet2 (2) and Soluble (S2), were examined for PDE4B4 content by PDE4 assay and western blot analysis.

Two methods of comparing PDE4B4 content can be used. In the first, the PDE4B4 content per unit protein of each fraction can be examined. This analysis allows the specific PDE4 activity of each fraction to be compared (Fig 3.2.2A). By this form of analysis the greatest PDE4B4 activity in transfected COS-1 cells occurs in the S2 fraction. Different subcellular fractions may contain different quantities of protein. This means that specific activities do not reflect proportional activities at a cellular level. Thus 3µg of P1 protein is likely to be extracted from a different number of cells than 3µg of S2 protein. To compare compartments that represent proportionally, a single cell, each fraction must represent the

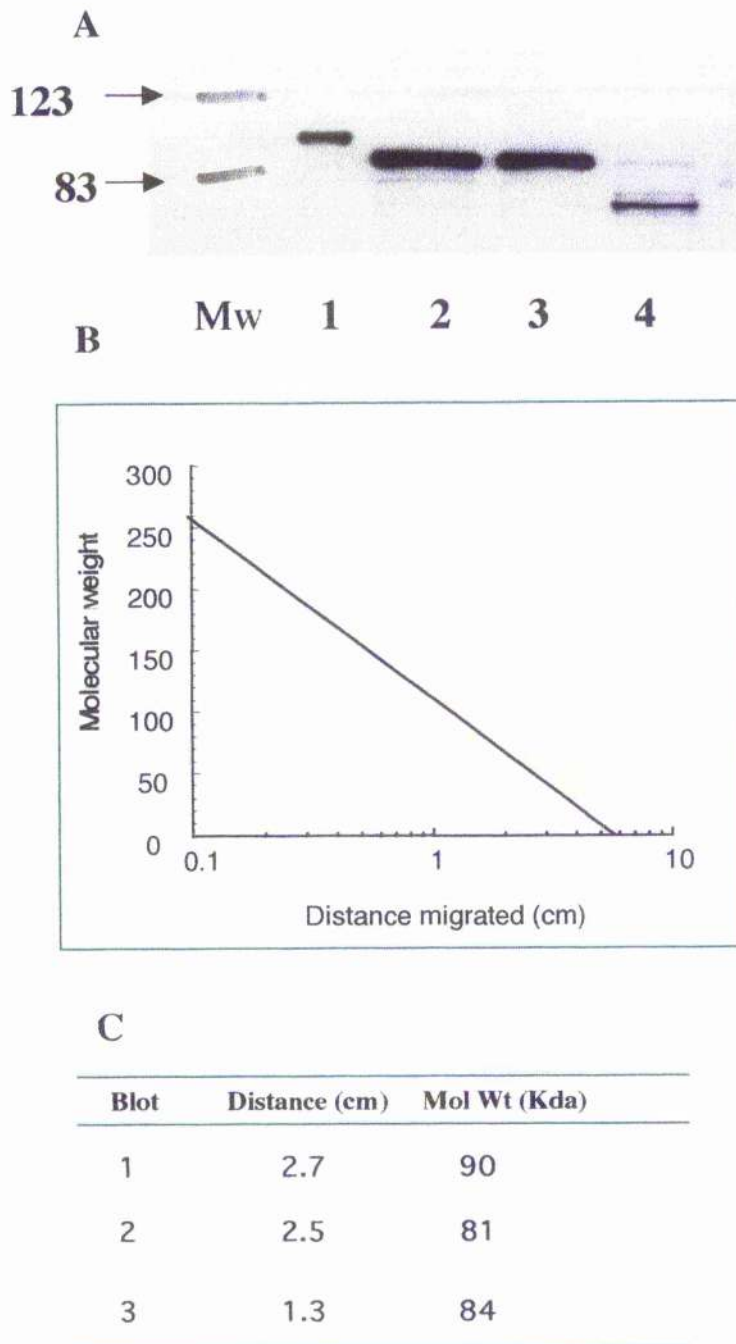


Figure 3.2.1 Molecular weight of PDE4B4

Recombinant PDE4B isoforms were expressed in COS-1 cells and resolved by 8% SDS PAGE fig 3.2.1A. A typical western blot was probed with polyclonal anti-PDE4B antibody (Schering). (lane 1 PDE4B1, lane 2 + 3 PDE4B4 and lane 4 PDE4B2). PDE4B4 migrates in a position between the long form PDE4B1 and the short PDE4B2. B. The log₁₀ of the distance migrated by pre-determined was markers plotted against molecular weight. A representative graph is presented. C. The line linking these distances was used to calculate the weight of recombinant PDE4B4 from the same blots. Three analyses from different transfections are presented. The average of these molecular weights was calculated. Thus the molecular weight of PDE 4B4 was calculated to be 85 +/- 3 Kda.

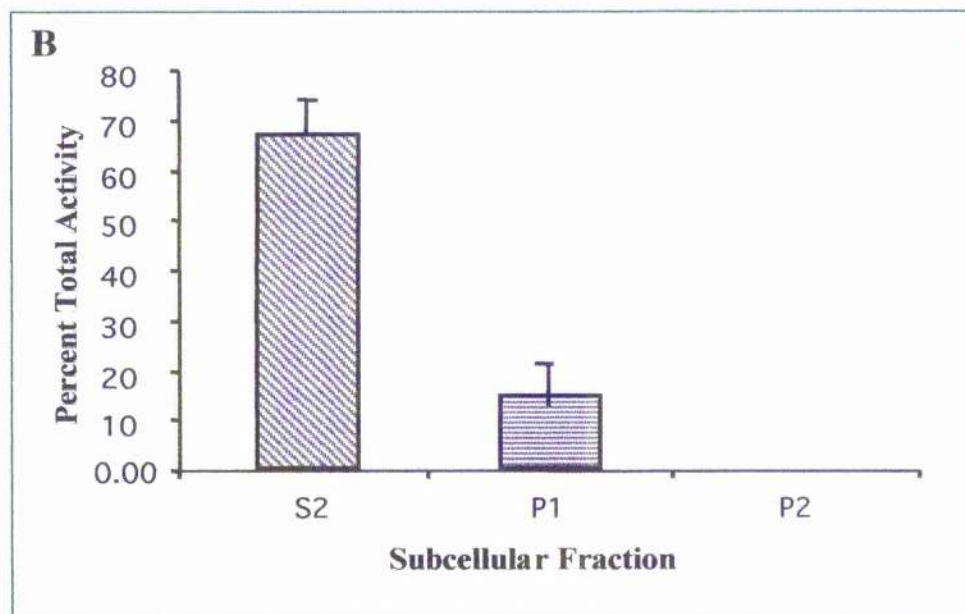
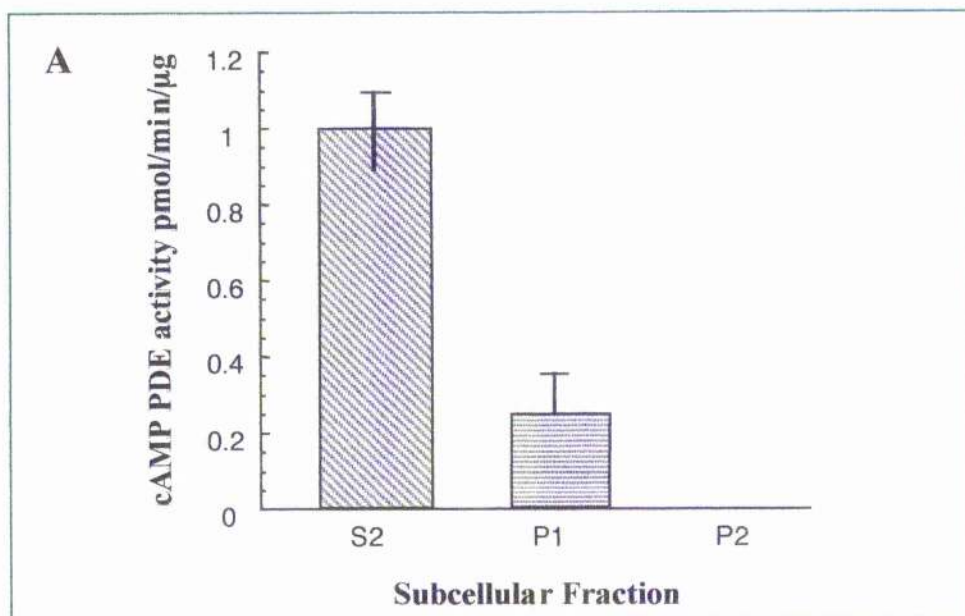


Fig 3.2.2 Sub cellular distribution of PDE4B4 activity

Low speed fraction (P1) and high speed fractions (P2) and (S2) of recombinant PDE4B4 expressing COS-1 cells were prepared in KHEM buffer as described. A; Specific cAMP PDE activity of S2 and P1 was calculated for 3 μ g of protein. Specific activity of P2 is estimated by adjusting the volume based distribution activity described below by mean protein content of the fraction. B; Fractions were equalised for volume to represent equivalent cell numbers per lysate fraction. PDE4 activity was measured for a given volume representing 3 μ g of S2 lysate. The majority (68%), of PDE4B4 activity was found in the S2 cytosolic compartment. With 23% in the P1. In each figure data represents three experiments and are expressed with standard errors.

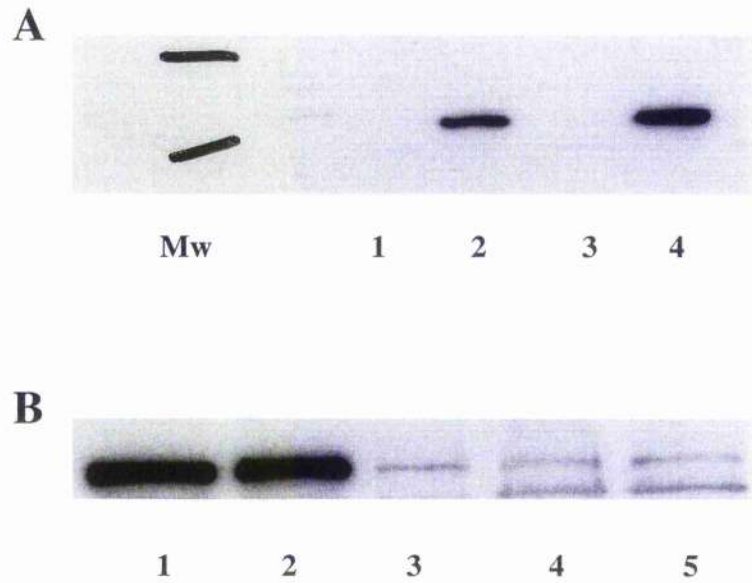


Fig 3.2.3 Sub cellular distribution of PDE4B4 protein

Low speed (P1) and High-speed (P2 and S2) fractions of recombinant PDE4B4 expressing COS-1 cells were prepared as described. Each fraction was reconstituted to an equal volume. Equal volumes of lysate corresponding to 30 μ g S2 protein were resolved on 8% SDS PAGE gel and western blot analysis performed. (A, lanes 1 and 2 P2 fraction, lanes 2 and 4 S2 fraction: B lanes 1 and 2 S2 fraction lanes 3, 4 and 5 P1 fraction). The majority of PDE 4B4 was found in the cytosolic, S2 fraction. The P2 fraction contains no PDE 4B4 while P1 contains very little.

same number of cells. To achieve this, fractions prepared by high speed centrifugation were reconstituted in equal volumes of PDE4 assay buffer. This volume was equal to the volume of collected S2 and all kinetic analysis was performed on volumes of cell lysate equal to that volume of S2 lysate containing 3 μ g of protein. This analysis allows proportional comparisons between subcellular fractions and using this method 62% of PDE4 activity was found in the S2 fraction with a further 23% in the P1 fraction. Quantifying LDH activity in each fraction estimates the degree of contamination (Appendix 2). Thus LDH is mainly cytosolic and if LDH activity is measured in P1 in the presence of detergent it suggests contamination with whole cells. Performing this assay suggested that around 30% of P1 protein was from unbroken cells and adjusting the activities described above reduces the particulate bound proportion of PDE4B4 still further. Little activity was found in the P2 fraction (fig 3.2.2.B).

Western blot analysis was performed in a similar way to the comparison described above. Equal volumes of fraction lysate, corresponding to 30 μ g of S2 lysate protein, were compared for immunological detection of PDE4B. Figure 3.2.3 demonstrates that the majority of immunologically detectable PDE4B4 lies in the S2 fraction, while a small quantity is present in the P1 and no band was resolved in the P2 fraction lanes.

Section 3

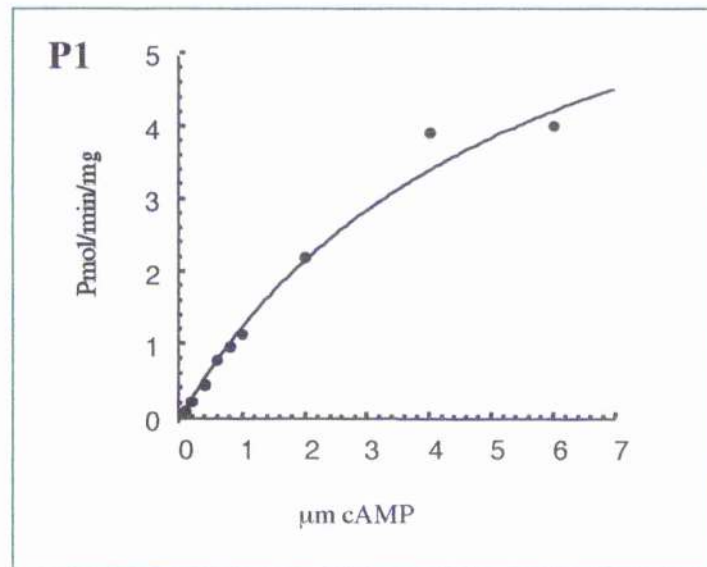
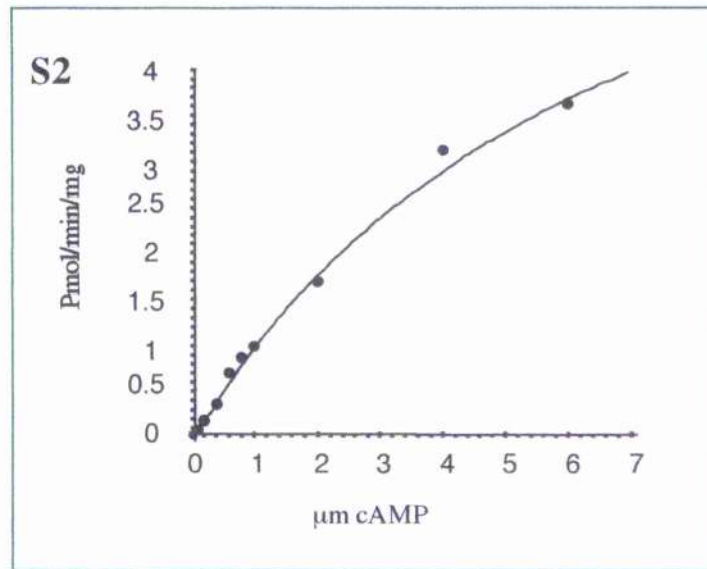
3.3.1 K_m value for PDE4B4.

The Michaelis constant (K_m) represents the concentration of substrate at which an enzyme is half maximally active. Representative plots of the parabolic form of the Michaelis-Menton equation are presented for the S2 and P1 of PDE4B4 (Fig 3.3.1). Using the Michaelis-Menton equation ($V=V_{max}*[cAMP]/ K_m +[cAMP]$), a plot of PDE4B4

activity/[cAMP] was generated, from which the K_M was calculated. The K_M was derived for three transfected lysates and the mean \pm 1 standard error is presented. The K_M value for cAMP of PDE4B4 S2 fraction is $5.4 \pm 0.7 \mu\text{M}$, while that of the P1 fraction is $6.0 \pm 0.5 \mu\text{M}$. Figure 3.3.1 also presents the K_M for recombinant PDE4B1 derived from experiments run in parallel to those described above. This produces a value of $2.0 \pm 0.1 \mu\text{M}$, which serves as an internal control for my system.

3.3.2 V_{max} value for PDE4B4

V_{max} represents the maximal activity for an enzyme measured at a saturating substrate concentration. I derived the V_{max} by calculating the activity (V_{obs}) for a range of protein quantities from COS-1 cells expressing recombinant PDE4B4. Using the mean of these activities I derived the apparent V_{max} for PDE4B4 from the Michaelis-Menton equation defined above. The apparent V_{max} for recombinant PDE4B4 was $8.6 \text{ pmol/min}/\mu\text{g}$ and $2.7 \text{ pmol/min}/\mu\text{g}$ for the S2 and P1 fractions respectively. The apparent V_{max} of an enzyme will depend on the quantity of enzyme present, thus the absolute V_{max} for PDE4B4 would be expressed as $\mu\text{M cAMP/mol enzyme}$. Meaningful comparison between PDE4 isoforms thus requires some means of quantifying the amount of enzyme present. I wished to use PDE4B1 as a comparison as this has served as comparative enzyme in the past [76]. In order to compare enzyme quantities I performed ELISA on a range of lysate volumes and identified recombinant enzyme using PDE4B antibody and a mock transfected cell lysate as a blank. Figure 3.3.3 illustrates one such ELISA, demonstrating that in each case a significant amount of enzyme was present in transfected cell lysates, but that PDE4B1 transfections contained more immunological enzyme than PDE4B4 transfections. The gradient of the line connecting the linear part of the absorption/protein curve reflects the quantity of PDE4B isoform present and was used to adjust the apparent V_{max} values for PDE4B4. This adjustment produces a relative V_{max} ratio (relative to S2PDE4B1) for



PDE4 Isoform/Fraction	$K_m(\mu M)$	Std Error
PDE4B4/S2	5.4	0.7
PDE4B4/P1	6.0	0.5
PDE4B1/S2	2.0	0.1

Fig 3.3.1 K_m calculation PDE4B4.

Recombinant PDE4B4 expressing COS-1 cells were subjected to high speed fractionation in KHEM buffer. 3 μ g of cell lysate from both S2 and P1 fractions were assayed against a range of cAMP concentrations. Representative plots from both S2 and P1 are presented. This data was analysed using the parabolic form of the Michaelis plot. The equation $y = m_1 * m_0 / (m_2 + m_0)$ where $m_1 = V_{max}$, $m_2 = K_m$ and $m_0 = [cAMP]$, defines the Michaelis Menton equation, and can be used to interrogate enzyme activity data to calculate K_m for an enzyme. A mean K_m for these experiments ($n=3$), was calculated and is presented with standard error. Mean K_m for PDE4B1 assayed in parallel is provided for comparison.

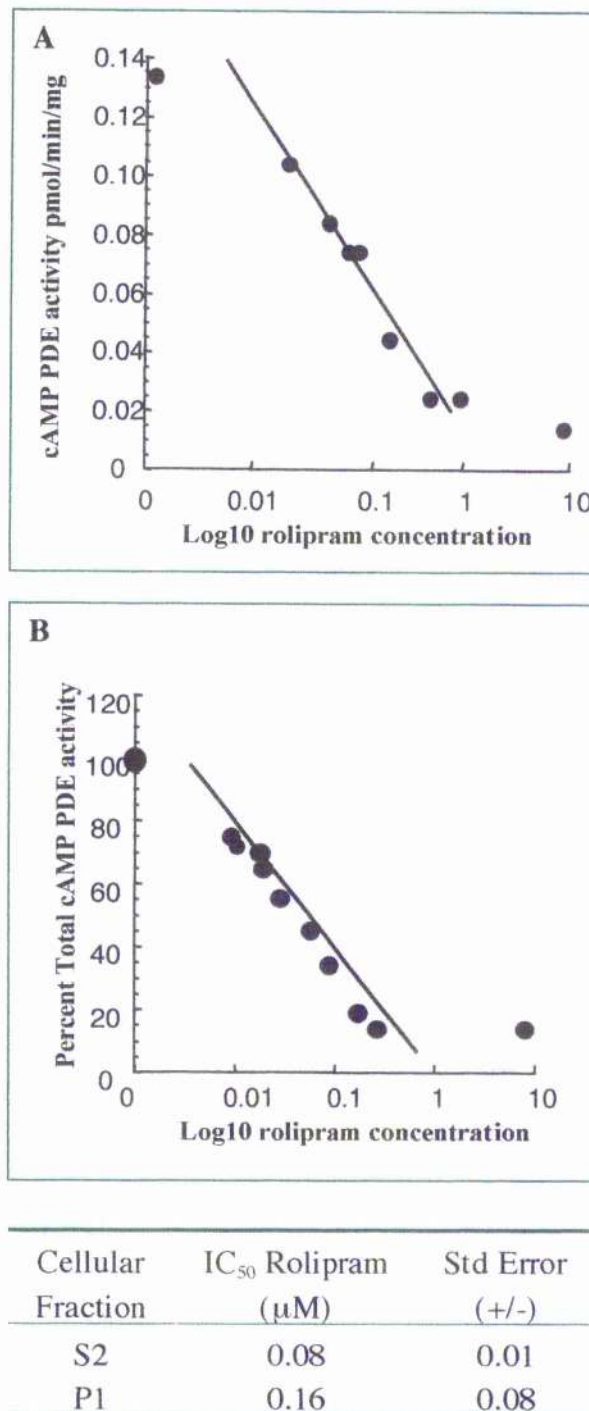


Fig3.3.2 IC₅₀ Rolipram of PDE4B4

The cAMP PDE activity at 1μM cAMP of 3μg cell lysate from Cos-1 cells expressing recombinant PDE4B4 was measured in the presence of a range of rolipram concentrations. Activity was plotted against the Log of the rolipram concentration interrogated using Kaleidograph, and IC₅₀ calculated. A; A sample IC₅₀ plot is presented. B; The mean inhibition of cAMP PDE activity from a number of transfections was used to calculate percent inhibition. This was then plotted against Log rolipram concentration. Presented is the plot representing the S2 fraction (n=3). C; This table summarises the IC₅₀ rolipram for Cox-1 cells expressing recombinant PDE4B4 in the P1 and S2 fractions.

PDE4B4 of 2.1 and 0.54 for the S2 and P1 fractions of COS-1 cells expressing recombinant PDE4B4 respectively.

3.3.3 Rolipram sensitivity of PDE4B4

A defining property of PDE4 enzymes is their capacity to be inhibited by the compound rolipram. It has been proposed that two conformations of PDE4 activity occur that can be detected by virtue of their rolipram binding affinity. Thus “high affinity, (HARB) and “low affinity” (LARB) conformations are said to exist [91]. Combined to this variable property is the range of IC_{50} values observed for different PDE4 isoforms. These range from 1.2 μ M rolipram for the particulate fraction of RNPDE4A5 to 20nM for the soluble fraction of PDE4B2 [50]. Therefore individual PDE4 isoforms are believed to interact with rolipram with isoform specific kinetics. The IC_{50} of an enzyme describes the concentration of an inhibitor that causes 50% reduction in activity at a particular substrate concentration.

The value for IC_{50} Rolipram inhibition was ascertained by incubating recombinant PDE4B4 expressing COS-1 cell lysates with increasing concentrations of rolipram and measuring PDE4 activity at 1 μ M cAMP as before. Fig 3.3.3 illustrates an example of the IC_{50} rolipram curves generated by such an approach. A mean of 4 experiments was used to calculate a final IC_{50} value. The IC_{50} value for the S2 fraction of PDE4B4 was 0.08 \pm 0.01 μ M, while for the P1 fraction IC_{50} value was 0.16 \pm 0.04 μ M. Table 3.1 presents previously described kinetic values for other PDE4 isoforms.

Section 4

3.4.1 PKA activation of PDE4B4

Long form PDE4 isoforms are characterised by the presence of UCR1 in their N-terminal regions. UCR1 contains a PKA phosphorylation target site defined by RRESW, with Ser54

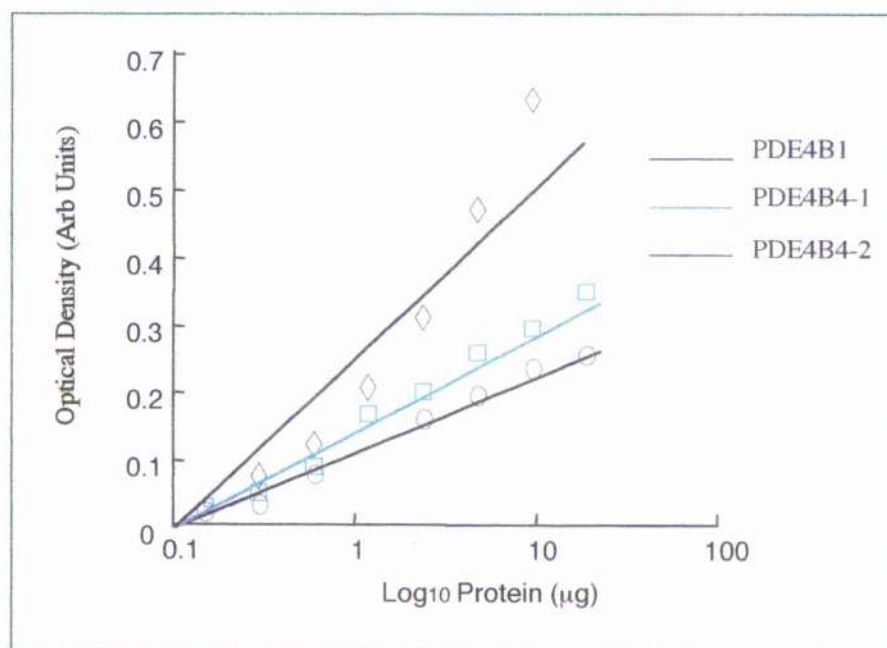


Fig 3.3.3 PDE4B ELISA contrasting recombinant protein expression

In order to calculate the V_{max} of PDE4B4 relative to a known standard (in this case PDE4B1), the apparent activity of each isoform was compared and adjusted for protein expression. To calculate relative enzyme expression ELISA was performed using anti-PDE4B antibody (Schering) to immunologically detect recombinant protein. Data is presented as optical density (arbitrary units) against the Log_{10} of the quantity of protein. Presented is one ELISA demonstrating that while two separate PDE4B4 transfections result in similar enzyme expression, these differ considerably from PDE4B1.

Gene Family	Rat homologue	Molecular Wt (kDa) Pred / Obs	Km(μ M) Cytosol	Vmax		IC ₅₀ Rolipram P C	Distribution %			Regulation	
				P	C		P1	P2	S2	Pka	ERK1/2
PDE4B1	RnPDE4B1	84 / 104	2	1	0.05/0.08	17	11	71	+	-	-
PDE4B2	Rnpde4B2	64 / 80	3	4	0.21/0.02	26	12	61	+	+	+
PDE4B3	Rnpde4B3	82 / 103	1.5	2	0.1 / 0.05	23	17	58	+	-	-
PDE4B4	Rnpde4B4	73 / 84	5.4	3	9 0.16 / 0.08	23	15	62	+	-	-

Table 3. 4 Table demonstrating the physical properties of the PDE4B family after the addition of PDE4B4.

being the Serine Target Residue (STR) in PDE4D3 [238]. This sequence is present in PDE4B4 with the STR being Ser56. A second PKA target site is present in PDE4B4 around Ser14 as shown in figure 3.1.1. The context of this site is very similar to that of a second PKA target site in the N-terminal region of PDE4D3, around Ser13. While phosphorylation of Ser54 of PDE4D3 appears to result in activation of this isoform the role of Ser13 phosphorylation is not clear [68].

Phosphorylation of an amino acid residue alters the charge of that residue by -1 . Conformational changes resulting from this can lead to activity or functional alterations in proteins containing these residues. Substituting an aspartate or a glutamate residue for the STR at a PKA target site adds a -1 charge to the protein and can be used to mimic the conformational changes resulting from phosphorylation. Conversely if an alanine substitution is made for the serine residue, no phosphorylation is possible and a dominant negative phosphorylation mutant results. Mutations of the STR in UCR1 in various long form PDE4 isoforms have been made and Ser-Asp mutants were found to be constitutively activated, while Ser-Ala mutants were resistant to PKA activation.[239]

I wished to examine the role of PKA in the activation of PDE4B4. I used a combination of IBMX and forskolin to increase cAMP and thus activate PKA. I measured the activity of PDE4B4 in the presence and absence of this treatment and demonstrated a 57% increase in activity (Table 3.4.1). PDE4D3 has previously been used as a model of PDE4 long form activation by PKA and I included a parallel experiment using recombinant PDE4D3 in these studies [238]. I demonstrated a doubling of PDE4 activity in COS-1 cells overexpressing PDE4D3. A second property of PKA phosphorylation of PDE4D3 is an alteration of mobility on SDS-PAGE. It is not clear why this change in electrophoretic mobility should occur, but it appears to be related to phosphorylation of Ser13 in the N-terminal STR of PDE4D3. I hypothesised that PDE4B4 would behave in a similar fashion due to its N-terminal sequence homology with PDE4D3. Figure 3.4.1, is a representative

PDE4Isoform	Control activity (pmol/min/ μ g)	Forskolin/IBMX (pmol/min/ μ g)	Percent Change
PDE4B4	10 \pm 1.5	16 \pm 3	+57 %
PDE4D3	4	8	+100%

Table 3.4.1 Effect of PKA activation on PDE4B4

COS-1 cells over-expressing recombinant PDE4B4 or PDE4D3, were pretreated with IBMX 10 μ M for 20 mins before forskolin 10 μ M was added for 15 mins. Cells in each treatment group were taken from a single transfections and multiple transfections were used. PDE4 activity was measured in cell lysate representing 3 μ g of cellular protein prepared in KHEM buffer. Activity is presented with standard error. PDE4B4 activity was seen to increase by 57% under treatment conditions, consistent with positive regulation by PKA (n=3). Also presented for comparison is a single experiment performed on recombinant PDE4D3. This isoform is known be activated by PKA and serves as an internal control.

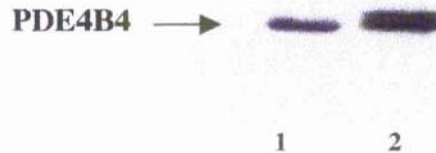


Fig3.4.1 PKA activation alters PDE4B4 migration on SDS PAGE gel.

Cell lysates prepared as described above were subjected to western blot analysis on 10% SDS-PAGE gel. Equal amounts of protein were loaded in each lane. Lane 1; Control (untreated) cell lysate, Lane 2; IBMX/Forskolin treated cell lysate. As has been previously described for PDE 4D3, migration of forskolin/IBMX treated PDE 4B4 is retarded leading to an apparent 'band shift' on western blot.

western blot demonstrating that a change in electrophoretic mobility does occur when COS-1 cells over expressing recombinant PDE4B4 are treated with IBMX/forskolin.

To investigate this behaviour further PDE4B4 cDNA sequences were mutated to contain aspartate and alanine residues at both the STR sites described above. In order to allow comparison these constructs also had a FLAG sequence tag added to the C-terminal. Recombinant mutant FLAG tagged PDE4B4 were expressed in COS-1 cells and activity was measured in the presence and absence of IBMX/Forskolin. In order to overcome differences in transfection efficiency when comparing between constructs and treatments, immuno-activity of PDE4B was measured by densitometry on western blot for a range of protein amounts. Plots of densitometry against protein (μg), were constructed and the linear relationship was derived. The gradient of this line reflects the transfection efficiency of the recombinant protein and activity values were adjusted to allow for these differences.

3.4.2 Ser14 – Ala substitutions

Mutant PDE4B4 containing a Ser14-Ala mutation proved to be sensitive to PKA. PDE4 activity in COS-1 cells overexpressing this mutant form of the enzyme rose by 90% when treated with IBMX/forskolin (fig 3.4.2). Unfortunately expression of the equivalent mutation of Ser56 resulted in a dramatic reduction in cell viability, and cell extracts contained very variable quantities of immunoreactive PDE4B. As a result no comparable experiments could be performed on the effect of Ser56-Ala mutation.

3.4.3 Ser – Asp substitutions

As described above the effect of Ser-Asp mutation at a STR for PKA reflects phosphorylation of this residue. Asp mutations of both Ser14 and Ser56 were made and PDE4 activity was measured in COS-1 cell extracts overexpressing these mutants. Activity

PDE4B4mutant	Control activity (pmol/min/ μ g)	IBMX/Forskolin (pmol/min/ μ g)	Percent increase
Wild Type	10 \pm 2	16 \pm 3	60
Ser14 -Ala	8 \pm 4	14 \pm 1	90

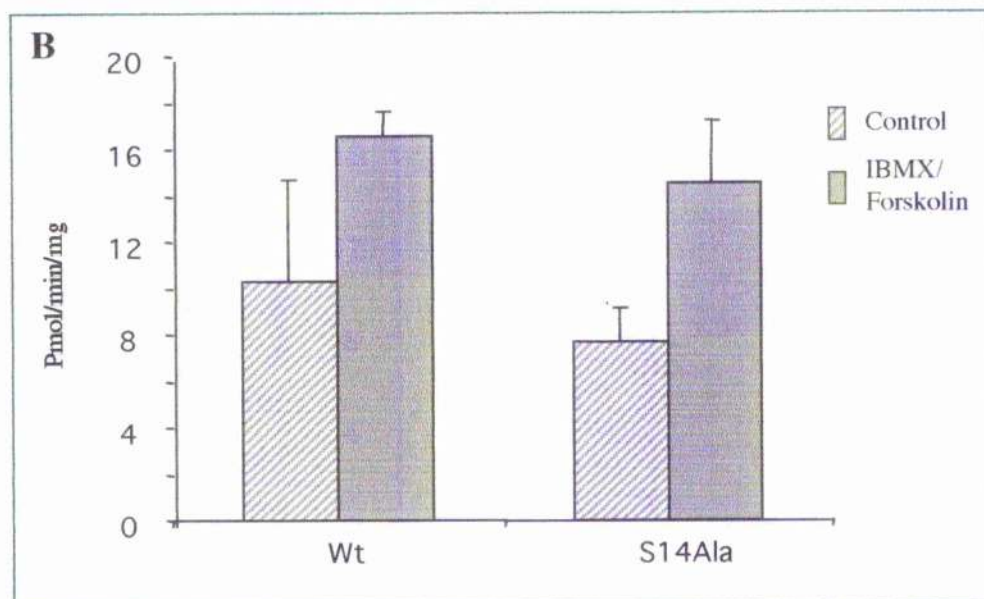


Fig 3.4.2 Effect of Ser14 - Ala mutation on PKA activation of PDE4B4

PDE4B4 cDNA was mutated by quick-change to produce an Ser14-ALA mutation. This mutation prevents phosphorylation by PKA from taking place. This mutant protein was overexpressed in Cos-1 cells and the effect of IBMX/Forskolin treatment was compared to untreated (control) PDE4 activity. To allow for transfection efficiency western blot was performed on increasing quantities of lysate protein and densitometry was used to assess PDE4B isoform expression. A; table presenting change in PDE4 activity with IBMX/forskolin treatment (\pm Standard error). B; graphic representation of the same data (n=3). Control activity was less than wild type PDE4B4 suggesting a role for Ser14 in regulating latent activity. The effect of IBMX/Forskolin treatment was not altered by the Ala14 mutation, suggesting that Ser14 is not involved in PDE4B4 activation by PKA.

A

PDE4B4 Mutant	PDE4 Activity (pmol/min/ μ g)	Percent Wild Type
Wild Type	10.3 \pm 1.5	100
Ser14 - Asp	8.0 \pm 1.6	78
Ser56 - Asp	13.8 \pm 3.7	145

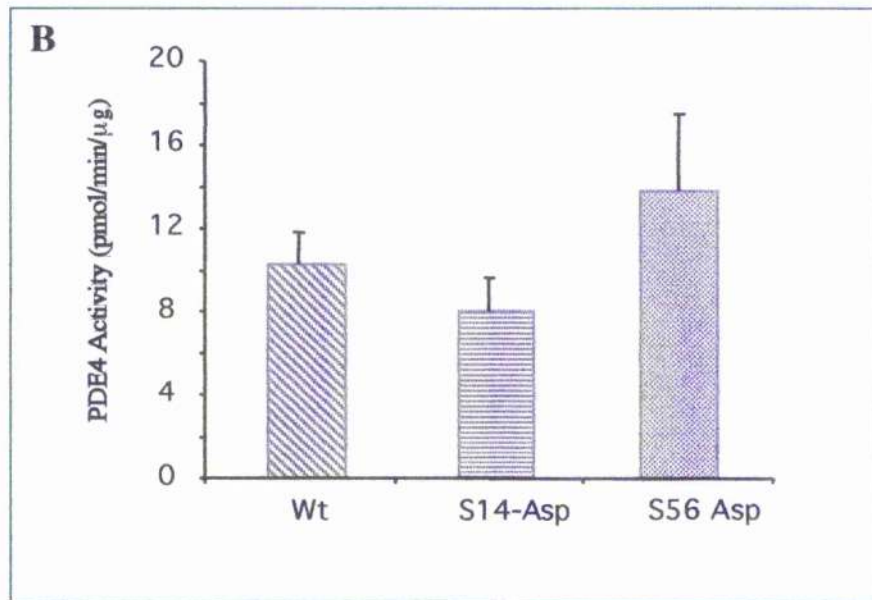


Fig3.4.3 Effect of Ser-Asp mutations in PKA activation sites in PDE4B4

Ser - Asp mutations were made using quickchange technology at both PKA phosphorylation sites (Ser14 and Ser56), in PDE4B4 cDNA with a "Flag" peptide tag. Aspartate substitution adds a negative charge to a protein reflecting a phosphorylation event. Cos-1 cells expressing recombinant PDE4B4 containing each of these mutations, were lysed and PDE4 activity was measured using wild type PDE4B4 as a control. To compare activities relative transfection efficiency was measured using densitometry of western blots probed with anti-FLAG antibody. A; Table showing the relative activity differences between both Asp mutants and wild type PDE4B4. B; Graphic representation of these differences. In each case three transfections were made using each mutation or wild type isoform. As can be seen a "phosphorylation" mutation at Ser56 resulted in increased PDE4 activity.

of Ser14-Asp mutant PDE4B4 was 22% lower compared with wild type enzyme. The Ser56-Asp mutant PDE4B4 had an activity 45% higher than wild type enzyme.

Discussion

A novel member of the PDE4B family was cloned from a cDNA library. Use of a complimentary probe based on the PDE4B UCR2 sequence confirmed the gene source of this novel clone. PDE4 isoforms can be classified by the presence or absence of UCR1 into long and short forms [63]. This structural distinction is based on a mRNA splice junction near the N-terminal region of UCR2 (fig 3.1.1). Splicing of mRNA at this site leads to short form PDE4 isoforms, of which PDE4B2 is the only PDE4B representative [233]. Comparison of the sequence of the novel PDE4B4 and the two other long form PDE4B isoforms, PDE4B1 and PDE4B3, shows 100% sequence homology downstream of the N-terminal 17 amino acids. Thus PDE4B4 contains UCR1 confirming its identity as a long form PDE4. The importance of these structural distinctions can be inferred by the evolutionary conservation between mammalian PDE4 and the drosophila dunce gene [59, 63]. Groups examining the regulation of PDE4 isoform activity have shown the functional significance of long form and short form distinctions. Thus Baillie et al, demonstrated that ERK2 phosphorylation of PDE4 isoforms, increased the activity of the short form PDE4B2, having previously shown reduction in the activity of the long form PDE4D3 [66] [67]. PDE4B4 would be expected to share the regulatory properties of long form PDE4 isoforms.

Further examination of the cDNA sequence of PDE4B4, PDE4B1 and PDE4B3 highlights divergence after UCR1. Thus the extreme N-terminal 17 amino acids are unique to PDE4B4 among the PDE4B family. Such unique N-terminal identity is common to PDE4

isoforms [50]. N-terminal diversity is achieved by differential use of multiple start sites regulating isoform specific transcription. Further analysis of the 17 N-terminal amino acid residues of PDE4B4 demonstrates remarkable homology to an equivalent region of PDE4D3. 13 of the 17 residues are conserved between these regions including the PKA S/TR Ser13 (PDE4D3). Analysis of the primary amino acid sequence thus identifies PDE4B4 as a long form PDE4 isoform, sharing sequence homology at the N-terminal region with PDE4D3.

Based on the primary amino acid sequence, predicted molecular weights of PDE4B1, PDE4B2 and PDE4B3 are 84, 64 and 82 KDa while they have been determined to be 104, 78 and 103 KDa based on SDS-PAGE migration [233]. It is not surprising therefore that PDE4B4, with a predicted molecular weight of 73KDa, migrates at 84 \pm 5KDa on SDS-PAGE. As proteins are fully denatured before electrophoresis is performed means that secondary structure is unlikely to affect electromobility. Whether interaction between SDS and regions of charged amino acids in the primary sequence of PDE4 isoforms results in retarded migration is not known. The influence of phosphorylation on the electromobility of PDE4D3 suggests that this may be the case.

Sixty eight percent of recombinant PDE4B4 activity is found in the soluble (S2) fraction of disrupted COS-1 cells. This distribution is similar to other PDE4B isoforms as 71%, 61% and 58% of expressed activity is found in the S2 fraction of recombinant PDE4B1, PDE4B2 and PDE4B3 lysates respectively [233]. Of the remaining activity the majority (23%) was localised to the P1 fraction (fig3.2.2). It is possible that in an over-expressed system, the membrane-binding sites were saturated and excess enzyme was left free in the cytoplasm. However the integrity of the method for demonstrating particulate association has been shown for other enzymes such as RD1 [240]. While western blot analysis does not suggest any immunoreactive PDE4B4 outwith the S2 portion, activity analysis demonstrates PDE4 activity in the P1 fraction. P1 fraction integrity was confirmed by LDH

assay analysis, described in appendix 1. P1 fractions used in both western blot and PDE4 activity analysis were prepared in the same way. It is not clear why this discrepancy exists, but confocal microscopy of real time subcellular distribution of PDE4B4 would help to clarify this issue.

The kinetic analysis of PDE4B4 is summarised in table 3.4, with previously reported kinetic variables for other PDE4B isoforms presented. As can be seen the K_m value for PDE4B4 lies close to the range set by the other PDE4B isoforms. Soluble PDE4B4 V_{max} relative to soluble PDE4B1 V_{max} is greater by 9 fold. Association with the particulate fraction P1 reduces this difference to a third. Differences in kinetic variables associated with particulate association have previously been reported for PDE4A4 [76]. In this study particulate PDE4A4 had a relative V_{max} that was 56% that of the soluble enzyme. This study also described a difference in the IC_{50} for rolipram between particulate PDE4A4 and soluble PDE4A4. Such a distinction was also demonstrated in my study for PDE4B4, where a P1 IC_{50} rolipram of $0.16\mu M$, was double the S2 fraction ($0.08\mu M$).

Differences between the K_m and V_{max} values for different PDE4B isoforms may not seem large. Small differences in regulatory properties between PDE4B isoforms may allow tight control of cAMP concentrations. Thus PKA activation of PDE4 isoforms increases activity by 50%. If the local concentration of cAMP is set to around the activation threshold of PKA, then small increases in concentration will result in PKA phosphorylation of PDE4 isoforms. The resulting increase in cAMP PDE activity will lower cAMP, limiting the scale and duration of the effect. Differential expression of PDE4 isoforms with small differences in V_{max} may then be used to regulate the response to cAMP.

Particulate association might influence PDE4 isoform activity, by altering the conformation of the protein. Protein-protein interaction sites on the N-terminal regions of

PDE4 isoforms have been described [72]. Interaction of SH3 domains on src family tyrosine kinase enzymes and proline rich domains in the N-terminal region of RNPDE4A5, HSPDE4A4 and PDE4D4 have been demonstrated [82, 83, 241]. Altered conformation of the PDE4 isoforms was demonstrated by a change in the sensitivity to rolipram. Thus interaction of PDE4B4 with as yet undetermined protein partners may explain the differences in P1 and S2 kinetics.

Regulation of PDE4 isoforms by protein kinase enzymes results in cross talk between different cascades. Thus PKA activates PDE4D3 by phosphorylation at Ser54 [238], while ERK2 inhibits long form PDE4s by phosphorylation [66, 67]. PDE4B4 contains the common UCR1 PKA STR at Ser53, equivalent to Ser54 of PDE4D3, a residue shown to be essential for PKA activation of PDE4D3 [238]. I have demonstrated that elevating intracellular cAMP with IBMX/forskolin treatment of COS-1 cells activated PDE4B4 as would be expected by the structural homology with other long form PDE4 isoforms. I have further suggested that Ser53 is the residue responsible for this activation as Ser53-Asp mutants had increased activity over wild type PDE4B4, while Ser14-Asp mutants exhibited reduced activity. Unfortunately the confirmatory Ser53-Ala mutant experiment was unable to be performed due to toxicity and loss of cellular viability.

Conclusion

The novel PDE4 isoform PDE4B4 has been cloned and characterised. It is a long form PDE4B isoform with largely soluble localisation in overexpressing COS-1 cells. K_m and IC_{50} closely resemble the other long form PDE4B isoforms, while the soluble V_{max} was 9 times greater than PDE4B1. Particulate association reduced the sensitivity of PDE4B4 to rolipram and lowered the V_{max} relative to PDE4B1. PKA activation increased PDE4B4 activity and mutation of PKA STR amino acids suggested this was due to phosphorylation

of Ser56. Phosphorylation of Ser14 resulted in electrophoretic mobility changes, but no apparent change to enzyme activity.

Chapter4 PDE4 isoform expression during U937 differentiation

4.1 Introduction

Tissue macrophages derive from circulating blood monocytes and transform through a series of stages to the mature cell,[145]. Macrophages are involved in disease progression, chronicity and resolution so understanding the biochemical changes associated with this phenotypic switch may suggest therapeutic targets. Hunninghake et al for instance showed that PKC β expression was dramatically reduced when macrophage differentiation occurred, [147].

Cyclic AMP is a crucial second messenger in macrophages and monocytes. It is involved in regulating apoptosis [242], maturation and motility [243] of these cells. The role of cAMP in the regulation of cytokine expression is becoming increasingly clear. For example TNF α and IL-12 production are inhibited when lipopolysaccharide treated macrophages are exposed to agents that increase cAMP [244] [194]. On the other hand elevating cAMP increases LPS induced IL-10 production [245].

In 1976 Thompson et al demonstrated that PDE4 represents the greatest cAMP hydrolysing activity in inflammatory cells [221]. Subsequently, many groups have shown 60-70% inhibition of cAMP PDE activity by rolipram in monocytes taken from peripheral blood [119, 246]. Whereas Thompson found little PDE3 in monocytes [221] others have consistently found that PDE3 comprises the greatest proportion of the remaining cAMP PDE activity. Estimates of its contribution range from 9 – 40 %. While the majority of PDE3 activity in monocytes was found to be associated with particulate fractions 90 – 100

% of PDE4 is soluble. This physical compartmentalisation suggests PDE isoforms are targeted to specifically regulate cAMP in these fractions.

Gantner et al demonstrated that PDE isoform expression profile changes upon monocyte to macrophage maturation [119]. While many groups have examined the PDE subfamily profiles of inflammatory cells, few have investigated the individual PDE4 isoforms. This may be related to the low abundance of these enzymes in cells combined with the relatively poor yields associated with cell isolation. Where PDE4 isoforms have been investigated RT-PCR has generally been employed revealing the presence of PDE4A, PDE4B and PDE4D [223, 246]. Due to the potential for post-transcriptional degradation of mRNA it has been previously advised that cellular profiling should include analysis of the enzyme protein itself [50].

Attempts to study macrophage development are hampered by the low abundance of tissue available for study. Attempts to measure PDE4 isoform activity in cells isolated from sputum proved unrewarding due to the small number of cells and the difficulty in achieving uncontaminated pure-lineages (see Appendix 2). Monocytes from human blood cultured on plastic have been shown to phenotypically represent tissue macrophages, but the small numbers of cells produced makes analysis of low abundance signalling proteins difficult [119]. Increasing use of cell lines representing monocytes has shown that they can be made to take on the characteristics of macrophages [154].

The U937 promonocytic cell is a suspension cell line that under certain conditions can take on the characteristics of macrophages [154]. This model has been used to identify the key stages in macrophage differentiation and the signalling systems involved [154, 156]. Previous investigators have studied the PDE4 activity of U937 cells [226, 247, 248]. Before using such a model to investigate a specific aspect of biochemical behaviour, it is

essential to verify that the model approximates the original with regards to the behaviour to be analysed.

I hypothesised that tight regulation of PDE4 isoform expression would occur during the development of mature macrophages. Understanding how PDE4 isoform expression changes might offer insights into the roles each isoform plays in cellular behaviour. I also wanted to verify the U937 cell model with regards to PDE activity by comparing it to an ex-vivo model of macrophage development.

Results

Section 4.1 U937 differentiation

Previous reports have suggested that treatment of U937 cells with 4nM PMA (U937_{PMA}) results in a phenotypic switch similar to that undergone by monocytes cultured on plastic [154]. One of the earliest changes to occur on transfer of peripheral blood monocytes to plastic is surface adhesion[119]. To assess the capacity of U937 cells to mimic this behaviour I incubated suspension monocytic U937 cells in flasks containing gridded glass cover-slips, with or without PMA and counted adherent cells after 96 hours. Cells from both adherent and suspension compartments were lysed and the protein quantified. The relative proportion of total cell lysate protein in the suspension and adherent populations was quantified and used to examine the expression of various surface phenotypic markers, signalling molecules and PDE activities.

4.1.1 PMA increases the adherence index of U937 pro monocytic cells

Table 4.1.1 demonstrates that U937_{PMA} cells are 10 fold more adherent. Total protein is increased in U937_{PMA} cells by a factor of 3.8. The proportion of the total protein found in the adherent compartment in treated cells (71%), is greater than that in control U937 cells (2%). Thus treatment of U937 cells with 4nm PMA leads to greater surface adherence than in control cells. Visually, U937_{PMA} looked larger and more spread out than control cells.

4.1.2 PMA causes the increased expression of β -2 integrin (CD-11)

In view of the increased adherence and previous reports that cultured monocytes express a macrophage like profile of adhesion molecules, I assessed the expression of the β 2 integrin CD11b[155, 156]. Figure 4.1.2 demonstrates expression of CD11b protein in U937_{PMA} but not U937 cells.

4.1.3 PMA reduces the expression of PKC β and increases the expression of COX 2

To assess the effect on functional markers of macrophage behaviour I chose to examine PKC β and COX-2. PKC β has been shown to be down-regulated with alveolar macrophage development [147], while COX-2 is believed to be expressed primarily by macrophages in human lung .The expression of both of these proteins is represented in fig 4.1.3. In U937_{PMA} cells, PKC β expression was dramatically reduced while COX 2 was transcriptionally activated.

	Control U937	U937 _{PMA}
No of Cells per hpf	39 +/- 20	468 +/- 98
Total Protein (µg/ml)	47 +/- 4	178 +/- 14
Percent Solution (%)	97	28
Percent Adherent (%)	2	71

Table 4.1. PMA treatment increases the surface adhesion of U937 cells.

U937 cells were incubated for 96 hours with 4nM PMA, in flasks containing circular coverslips. After incubation coverslips were removed washed three times with ice cold PBS. Adherent cells were counted in 4 high power fields (hpf) per coverslip using a standard haemocytometer. Culture medium was removed from each flask and cells in suspension were collected by centrifugation these were washed and lysed in buffer containing 0.1% TritonX100. Remaining adherent cells were washed and similarly lysed. Protein quantification was carried out and the total protein calculated for each flask. Number of adherent cells per treatment is presented as a mean (n=4). Total protein represents the combined protein quantification of adherent cells and cells in solution. Proportion of the protein from each compartment is presented.

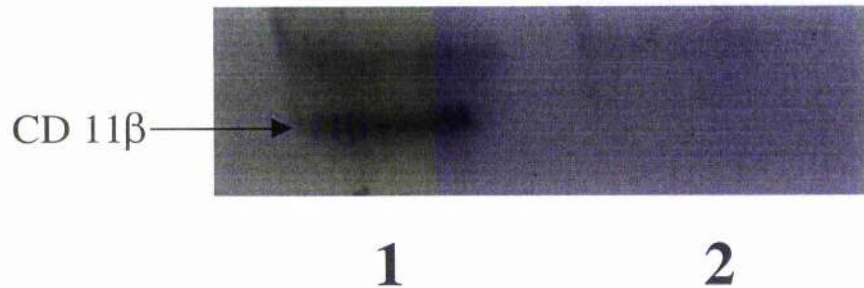


Fig 4.1.2 PMA induces the expression of $\beta 2$ integrins in U937 cells.

U937 cells were treated with 4nM PMA for 96 hours and non adherent cells were removed. Remaining cells were washed and lysed in 3T3 lysis buffer. Untreated U937 cells were lysed and used as control cells. Proteins were separated using SDS-PAGE ensuring equal protein loading in each lane. Western blot analysis was performed on the cell lysates and nitrocellulose was probed with anti CD-11b monoclonal antibody. Lane 1; U937_{PMA}, lane 2; U937 cells. As can be seen, 96 hours of 4nM PMA induces CD-11 integrin expression in U937 cells.

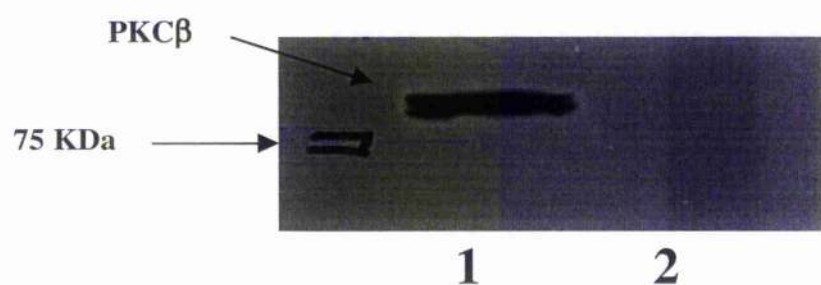
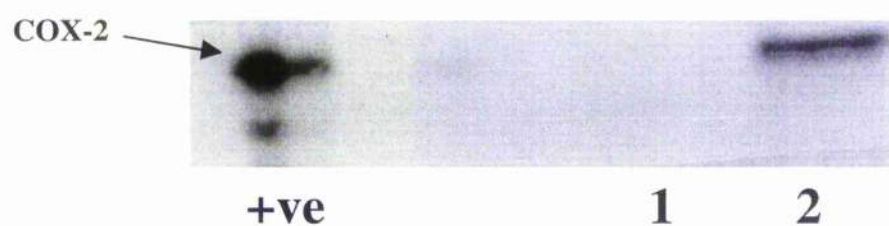
A**B**

Fig 4.1.3 Changes in the expression of PKC β and COX -2 with differentiation

U937 cells and U937_{PMA} were lysed and equal amounts of protein were separated by SDS-PAGE. Western blot analysis was performed and proteins identified immunologically with antibodies raised against PKC β and COX-2. Lane1; control U937 cells, lane2; U937_{PMA}. Fig 4.1.2.A, demonstrates that a striking reduction in PKC β expression occurs with macrophage differentiation. Fig 4.1.2.B, shows that COX 2 expression is induced with differentiation. Both changes correspond to previously reported changes with macrophage development and are believed to contribute to the phenotype stability.

4.1.4 Changes in PDE isoform activity occur with macrophage differentiation

I compared the effect of PMA induced differentiation of U937 cells on PDE3 and PDE4 activities. PMA treatment results in a fall in the total cAMP phosphodiesterase activity (fig 4.1.3A,B). While the proportion of PDE3 to the total activity rises from 11 to 28% on 96 hours of PMA treatment that of PDE4 falls. There is also a significant fall in the actual PDE4 activity in U937_{PMA} cells, from 132pmol/min/mg to 66pmol/min/mg. To ensure that this conformed to the peripheral blood monocyte model we compared the same parameters in cultured monocytes from human volunteers. Fig 4.1.3C demonstrates that while PDE3 activity rose from 20 pmol/min/mg to 51pmol/min/mg with 5 days of culture, PDE4 activity fell from 73pmol/min/mg to 47pmol/min/mg. Plastic cultured monocytes therefore reflect the PDE isoform changes seen in U937_{PMA} cell development.

4.1.5 Changes in PDE isoform activity in U937_{PMA} cells on a per cell basis

The data presented above suggests that PDE4 activity falls in line with total cAMP PDE activity. These data were calculated on a total protein basis as has previously been reported for macrophage differentiation studies [119]. I have also shown that the cellular protein content changes with U937_{PMA} development. To measure the changes in PDE isoform activity at a cellular level I recalculated the activity making a correction for cellular protein content to give activity on a per cell basis. Figure 4.1.4 shows that while total PDE4 activity falls on per mg protein basis, it rises when calculated on a cellular basis. Both PDE3 and PDE4 activity rise in a similar fashion.

A

Cyclic AMP PDE activity	U937 (pmol/min/mg)	U937 _{PMA} (pmol/min/mg)
Total	149 +/- 38	92
PDE3	18.0 +/- 3.0	26 +/- 4
PDE4	132 +/- 6	66 +/- 5 **

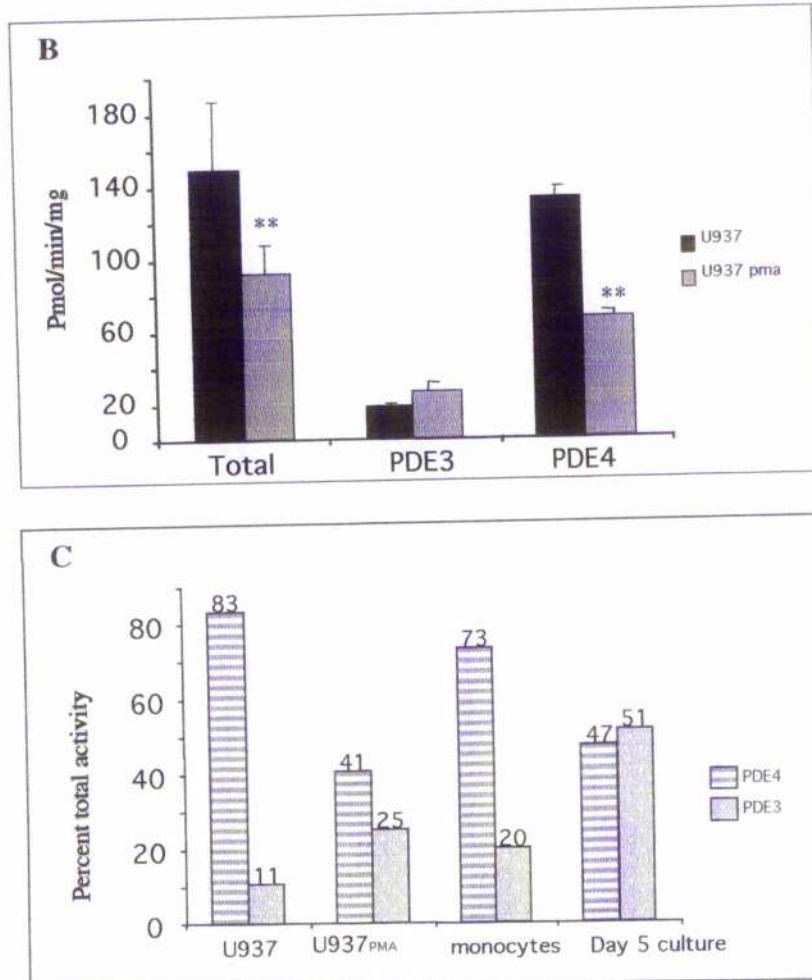


Fig 4.1.4 Effect of PMA on PDE isoform expression in U937 cells and plastic differentiation on ex-vivo monocytes.

U937 cells and ex-vivo monocytes, were differentiated as described in materials and methods. U937 cells and U937PMA were counted and lysed in KHEM buffer. PBMC from normal volunteers were cultured on plastic for up to 5 days and washed and lysed in KHEM buffer. Total cAMP PDE activity was measured at $1\mu\text{M}$ cAMP. PDE3 and PDE4 activities were measured using the specific PDE inhibitors cilostamide $1\mu\text{M}$ (PDE3) and rolipram $10\mu\text{M}$ (PDE4) and subtracting the resulting activity from total activity. A, table expressing the Total PDE, PDE4 and PDE3 activity for U937 and U937_{PMA}. Protein per cell was calculated and used to adjust the activity per unit protein. Both activity per unit protein and activity per million cells are presented ($n=3$); B, graphic representation of changes in each cAMP PDE activity with differentiation; C, graphic representation of the percent total activity represented by both PDE3 and PDE4 in both U937/U937_{PMA}, and ex-vivo monocytes/macrophages ($n=1$). (**, $P=0.002$ Student's paired T Test).

A

Cyclic AMP PDE activity	U937 (pmol/min/mg)	U937 (pmol/min/10 ⁶ cells)	U937 _{PMA} (pmol/min/mg)	U937 _{PMA} (pmol/min/10 ⁶ cells)
Total	149 +/- 38	6.8 +/- 1.8	92	16.5
PDE3	17.7 +/- 2.6	1 +/- 0.2	26 +/- 4	4.6 +/- 0.2
PDE4	132 +/- 6	6.2 +/- 0.5	66 +/- 5	12 +/- 0.9

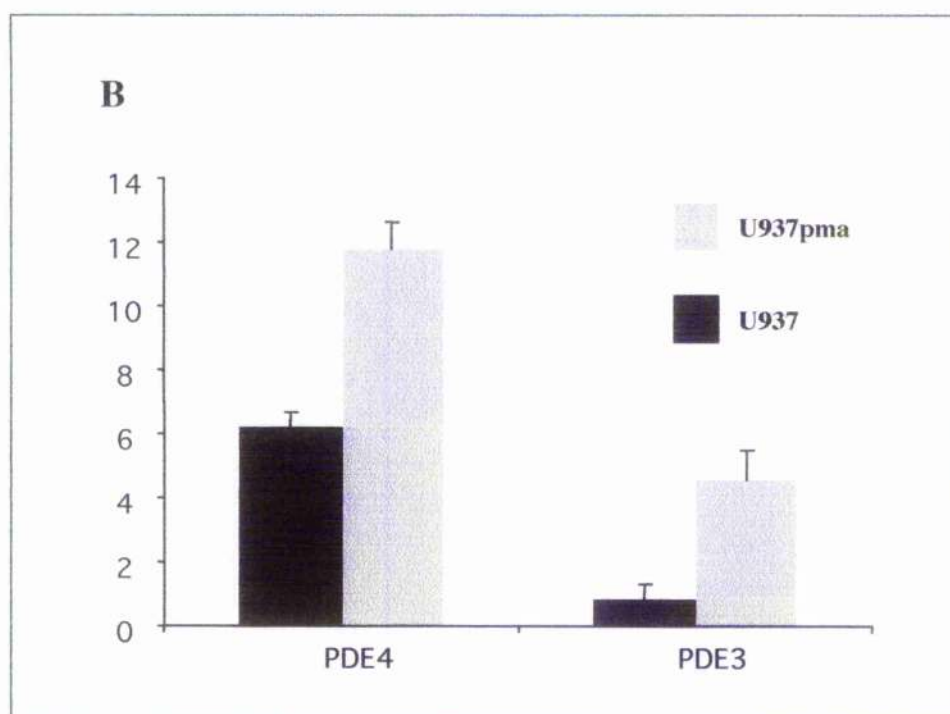


Fig 4.1.5 Activity of cellular PDE4 and PDE3 activity in U937 and U937_{PMA} cells.

U937 cells and U937_{PMA} were counted and lysed in KHEM buffer. Total cAMP PDE activity was measured at 1 μ M cAMP. PDE3 and PDE4 activities were measured using the specific PDE inhibitors cilostamide 1 μ M (PDE3) and rolipram 10 μ M (PDE4) and subtracting the resulting activity from total activity. Protein per cell was calculated and used to adjust the activity per unit protein. A; both activity per unit protein and activity per million cells are presented (n=3); B; graphic representation of the PDE3 and PDE4 activity per million cells in both U937/U937_{PMA} (n=3).

Discussion Section 4.1

Cell lines have been used previously to reflect mature inflammatory cells, [154] [155, 249]. U937 differentiation to U937_{PMA} reflects changes of monocyte to macrophage differentiation. I developed this model to measure changes in PDE4 isoform expression. To verify this model I measured adhesion index by comparing protein content and cell count in the suspension and adherent compartments of cultured U937 and U937_{PMA} cells. Increased adhesion to plastic is a recognised behaviour of both directly isolated and ex-vivo differentiated macrophages [119, 145]. Observing U937_{PMA} cells demonstrated significant phenotypic changes typical of macrophages. In comparison with their progenitor cells U937_{PMA} are flat large cells. Such an increase in the plasma membrane may be associated with an increase in the protein content. I used the data described above to calculate the amount of protein per cell and found a significant increase in this index with differentiation. (47 +/- 4 Vs 179 +/- 14 per 10⁶ cells). Again this reflects the ex-vivo model described by Gantner et al who reported an increase from ~50 to ~150 µg/ 10⁶ cells [119]. It is likely that such an increase in protein and membrane reflects, among other things, the expression of cell surface molecules associated with cell adhesion [250, 251].

CD11b expression reflects macrophage development and is a surface adhesion molecule important in cell-cell interactions in developing inflammation [149, 251]. In combination with CD18 it forms the complex integrin Mac-1. Hass' group have demonstrated that surrogate cell lines induced to differentiate to macrophage like cells express increased CD11b [154]. This group have recently demonstrated that eliminating expression of CD11b, using antisense oligo-nucleotides, prevents the full expression of the differentiated phenotype, [156]. Fig 4.1 shows increased expression of CD11b in U937_{PMA}, consistent with a macrophage phenotype. Hunninghake et al showed reduced PKCβ expression in

AM compared to progenitor monocytes and I have demonstrated a similar change in U937_{PMA} compared to U937 cells (Fig 4.1.2) [147]. Thus key signalling molecules other than PDE isoforms that are known to change during macrophage development also change during U937_{PMA} development. Finally COX-2 expression takes place as macrophages mature [242, 252]. It has been proposed that COX-2 products such as PGE2 and TXA2 maintain the phenotype of mature AM. I have demonstrated that in U937 cells no basal expression of COX-2 is present while in U937_{PMA} COX-2 expression is seen.

The markers used above to confirm the developmental stage of U937 cells on the granulocytic lineage were all effectively "on-off" markers. Using such markers protects to some extent against bias related to protein content. Thus comparing equal quantities of protein from each cell type may bias the result if each cell type contains different amounts of protein per cell. In fact by comparing two markers of macrophage activation I have weighted the bias in favour of the null hypothesis, that no significant change has occurred. That is 100µg of U937 protein reflects almost four times as many cells as 100µg of U937_{PMA} cell protein. This strengthens my results in favour of U937_{PMA} cells reflecting macrophage biochemistry.

Having demonstrated that the U937_{PMA} model accurately reflects macrophages I compared PDE3 and PDE4 activity in each stage of development. This follows Gantner et al, who found a fall in PDE activity with a co-incident fall in PDE4 and a rise in PDE3 activities with AM development [119]. Other reports have also demonstrated that monocytes have different PDE profiles than macrophages [126, 127]. Excitingly Fig 4.1.3 demonstrates that PDE3 activity rises while PDE4 activity falls on the background of falling total PDE activity with the development of U937_{PMA}. These data reflect the activity derived for expressed protein in cell lysate. As U937_{PMA} contain more protein per cell I recalculated the activities for total cell number (fig 4.1.4). Interestingly total PDE4 activity per 10⁶ cells does not fall as noted above. To confirm that this reflected the previously reported work by

Gantner et al I re-calculated their data as presented and found that they too found an effect of protein content. Doing this shows a fall in PDE4 activity from ~ 100 pmol/min/mg in monocytes to ~ 20 pmol/min/mg in day 6 differentiated macrophages. This converts to 6.2 pmol/min/ 10^6 cells and 4.5 pmol/min/ 10^6 cells respectively. Thus in both cell marker expression and signalling molecule activity the U937_{PMA} model appears to reflect the changes taking place when macrophages develop. I could now examine which PDE4 isoforms changed in activity or expression.

Section 4.2 Changes to PDE4 isoforms when U937 cells differentiate with PMA.

To compare the expression and activity of various PDE4 isoforms I used western blot, RT-PCR and immunoprecipitation to isolate specific PDE4 families.

4.2.1 PDE4A activity is increased by PMA treatment of U937 cells

Our group previously reported that PDE4A4 is present in resting U937 cells [247]. Immunoprecipitation using antiserum raised against the common PDE4A C-terminal allows isolation of all active PDE4A isoforms expressed. The PDE4 activity of these immunoprecipitates can be measured to compare the relative activities between control U937 cells and U937_{PMA} cells. Figure 4.2.1A, shows PDE4A contributes a greater (81%) proportion of the total cellular PDE4 activity in U937_{PMA} cells than in U937 cells (2%) when activity is equalised for protein concentration. This increase in activity does not reflect the reduction in total PDE4 activity seen in section 4.1, as actual PDE4A activity is seen to increase from 1.1 pmol/min/mg to 53 pmol/min/mg, (fig 4.2.1B). The change in

protein content with U937_{PMA} cells would tend to limit any increase in PDE4A activity per cell, as PDE4A isoforms are “diluted” by other proteins. Calculating the activity per 10⁶ cells, however shows the increase in PDE4A activity to be preserved with U937 cells having 0.02 pmol/min/10⁶ cells and U937_{PMA} cells having 9.6 pmol/min/10⁶ cells.

4.2.2 Change in PDE4A expression in U937_{PMA}

To test if the increased PDE4A activity was related to a change in enzyme content, I examined protein expression by western blot. Fig 4.2.2 clearly shows that a band identified by PDE4A C-terminal anti-Sera is increased in U937_{PMA} cells. Figure 4.2.2A, compares equal cell numbers, while Fig 4.2.2B compares increasing amounts of U937 and U937_{PMA} lysate protein. Both blots demonstrate an increase in the intensity of the protein band developed with anti-PDE4A antiserum and this is quantified by densitometry in fig 4.2.2C. This demonstrates a profound increase in the intensity of staining for PDE4A consistent with the activity data described in 4.2.1.

4.2.3 Novel appearance of PDE4A10 mRNA in U937_{PMA}

Unfortunately two long forms of PDE4A, PDE4A4 and PDE4A10 both run at a similar weight on SDS PAGE. To attempt to identify which isoforms are being expressed I performed RT-PCR using RNA from each cell type as template. Primers designed to complement the unique N-terminal regions of PDE4A4 and PDE4A10 were used and conditions and sequences are presented in materials and methods section 2.1.4. Figure 4.2.3, shows that PDE4A10 is only expressed in U937_{PMA} cells while PDE4A4 is expressed in both cell types. This suggests that PDE4A10 expression is transcriptionally activated with maturation. Interestingly an intense RT-PCR product band is found in U937 cells although relatively little protein is identified on western blot or immunoprecipitation.

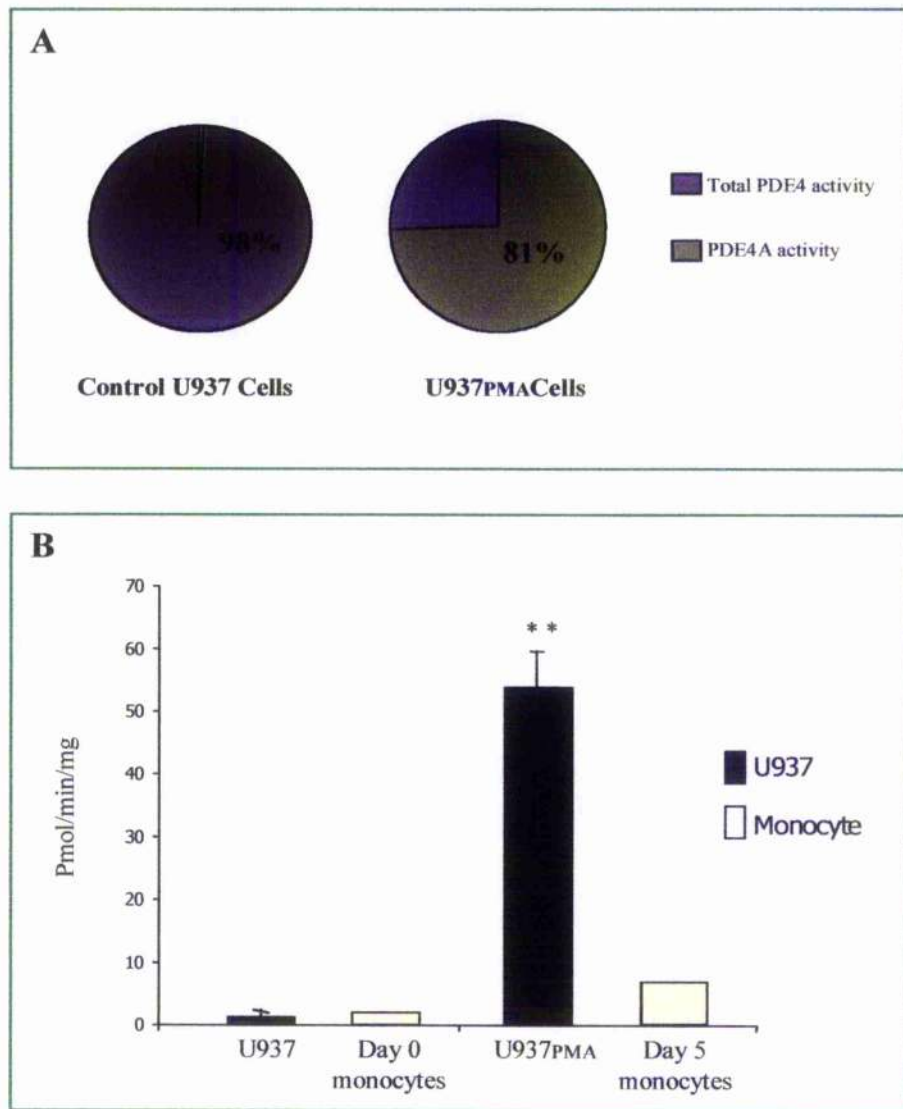


Fig 4.2.1 Changes in PDE4A activity when U937 cells and monocytes differentiate towards macrophage like cells

U937 cells were differentiated for 4 days with 4nm PMA. Adherent human monocytes were differentiated on plastic for 5 days. Control cells (Day 0), and differentiated (U937_{PMA}, Day 5 monocytes) cells were lysed and PDE4A isoforms were immunoprecipitated using an anti-sera raised against the PDE4A C terminal. Immunoprecipitates were assayed for PDE4 activity. Fig 4.5 A demonstrates that the proportion of PDE4A to the total PDE4 activity rises dramatically from 1.94% to 81%. Fig 4.5 B demonstrates that in both the U937 model and in ex-vivo monocytes the PDE4A activity increases. (** P = 0.002, Student's T test).

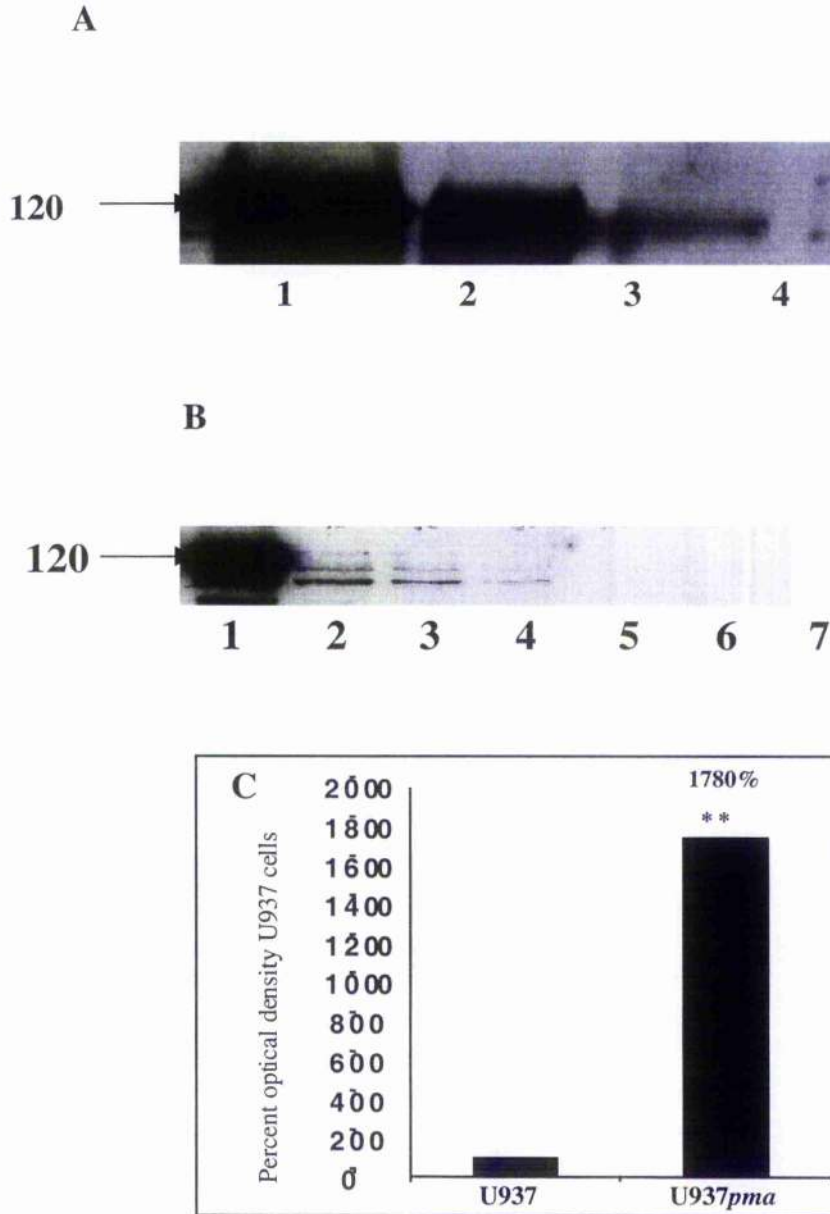


Fig4.2.2 Differentiation is associated with an increase in expression of PDE4A protein

U937 and U937_{PMA} cells were lysed in 3T3 lysis buffer and lysate protein was resolved by SDS-PAGE, followed by western blot analysis using antisera raised against the C-terminal of PDE4B. Fig4.2.2A, protein from 1×10^5 cells was loaded in each lane: Lane 1 PDE4A4; Lane 2 PDE4A10; Lane 3 U937_{PMA}; Lane 4 control U937. Fig 4.2.2B, equal quantities of protein was loaded in each lane: Lane 1 PDE4A4; Lanes 2 - 4 100, 60 and 40 μ g of protein from U937_{PMA} cells; lanes 4 - 7 equivalent protein quantities from control U937 cells. Both PDE4A4 and PDE4A10 run at the same weight making them difficult to distinguish on a western blot. Figure 4.2.2C, autoradiographs were subjected to densitometric analysis, and the intensity of PDE4A bands relative to control U937 cells are presented ($n=3$). Note that consistent with previous activity data, PDE4A protein expression is significantly increased on differentiation. ($P = 0.007$, Student's T test).

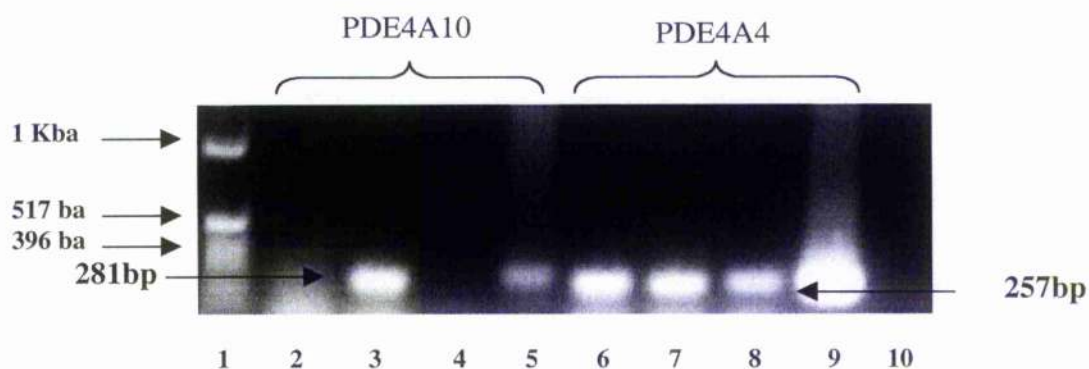


Fig.4.2.3 Differentiation is associated with an increase in transcription of PDE4A10.

RT-PCR analysis of RNA isolated from U937 cells and U937_{PMA}. Equal amounts of RNA was isolated and cDNA was prepared as described in materials and methods. This cDNA was used as template for PCR using primers directed against the specific N terminal regions of PDE4A4 and PDE4A10. Lane1 contains markers, lane 2 - 5 contain the PCR product following pcr using PDE4A10 primers, lanes 6 - 10 contain pcr products from reactions using PDE4A4 primers. Lanes 2, 6 and 7 contain template cDNA from control U937 cells, while lanes 3 and 8 contain template from U937_{PMA} cells. Lanes 5 and 9 are positive controls and lanes 4 and 10 are negative controls. As can be seen while PDE4A4 is expressed under both control and differentiation conditions PDE4A10 expression appears only after 4 days of treatment with 4nM PMA.

4.2.4 Peripheral blood monocytes show increased PDE4A activity with plastic differentiation

Immunoprecipitation of active PDE4A was performed on cell lysates derived from peripheral blood monocytes cultured for increasing periods of time on plastic. Figure 4.2.4 demonstrates that a similar increase in activity as seen with U937_{PMA} development occurs in plastic cultured ex-vivo monocytes suggesting that these changes normally occur in macrophage maturation.

4.2.5 PDE4D expression falls upon macrophage differentiation

Cell lysates derived from U937 and U937_{PMA} were analysed by western blot, with antisera raised against the C-terminal of PDE4D. Figure 4.2.5A, shows that while PDE4D3 and PDE4D5 are expressed in control U937 cells 4 days of incubation with 4nM PMA leads to a fall in the expression of both isoforms. PDE4D3 is absent from U937_{PMA} cell lysate, while PDE4D5 can be found only when large quantities of protein are resolved. Figure 4.2.5B, expresses the PDE4D5 data in terms of intensity of protein band using U937 cells as a reference point. This shows that PDE4D5 expression in U937_{PMA} cells is 18% of U937 cell expression.

4.2.6/4.2.6.1 PDE4D activity falls with U937_{PMA} and day 5 macrophage development

In contrast to the increased activity of PDE4A, immunoprecipitation of PDE4D isoforms demonstrates a fall in activity of this family in U937_{PMA} cells. Figure 4.2.6A shows that as a proportion of total PDE4 activity PDE4D falls from 60% to 25%, while fig 4.2.6B expresses this in terms of actual activity showing a fall from 80 +/- 14 pmol/min/mg to 17 +/- 7 pmol/min/mg in U937_{PMA} cells. With the change in cellular protein content a fall in

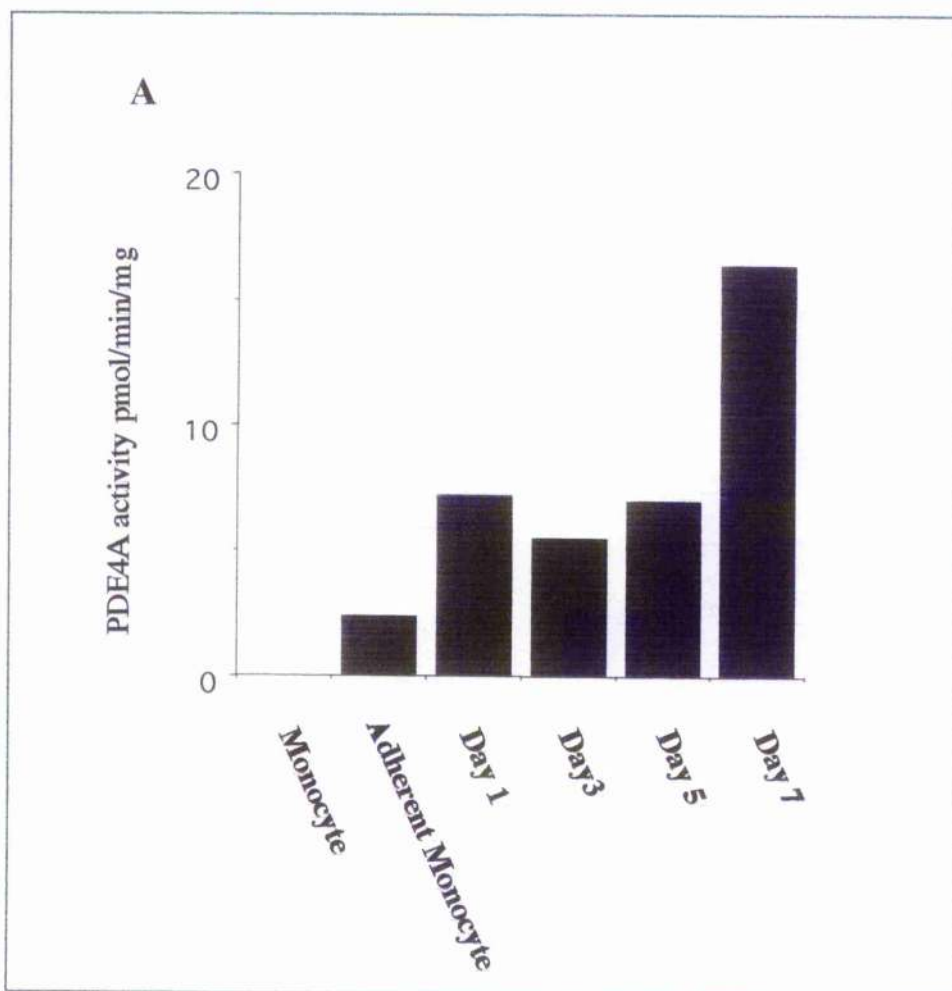


Fig 4.2.4. PDE4A activity in ex-vivo monocytes.

PBMC from normal volunteers were cultured on plastic for 2 hours then non-adherent cells were washed off. Differentiation on plastic was allowed to progress for a range of periods. Cells were then washed and lysed in KHEM buffer. PDE4A isoforms were isolated by immunoprecipitation using antisera raised against the C terminal of PDE4A. PDE4 assays were performed on the immunoprecipitates. It can be seen that progressive culture resulted in the increasing expression of PDE4A activity.

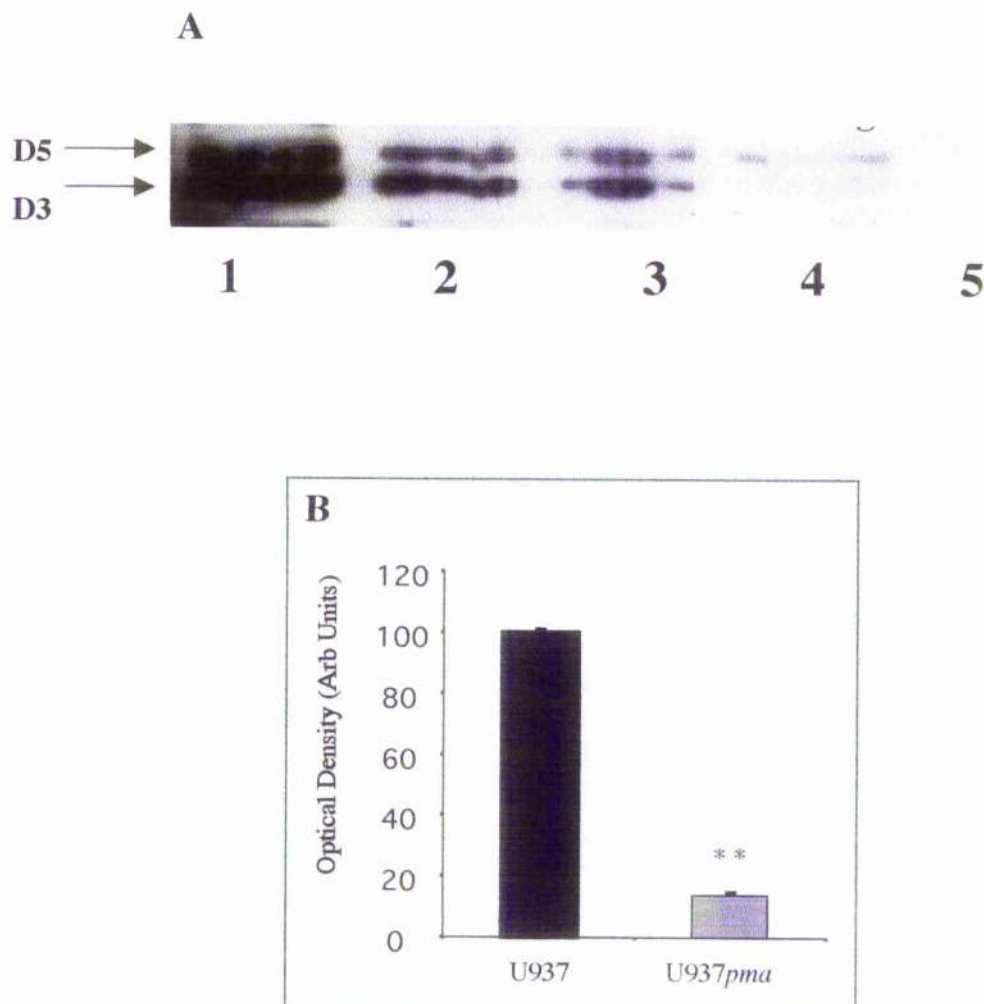


Fig 4.2.5 The changes in PDE4D expression in U937 cells differentiated with 4nM PMA

U937 cells and U937_{PMA} cells were lysed in 3T3 lysis buffer and equal amounts of protein were resolved by SDS-PAGE and analysed by western blot Fig 4.2.5A: Lane 1 positive control recombinant human PDE4D3 & 5; Lanes 2 and 3 correspond to 100µg and 60µg of control U937 cell lysate; Lanes 4 and 5 contain the same protein quantities from U937_{PMA} cells. As can be seen differentiation causes the complete disappearance of PDE4D3 from U937 cells, while PDE4D5 undergoes a significant but smaller drop in expression. Autoradiographs from these western blots were subjected to densitometry and the amount of detectable PDE4D5 relative to control U937 is presented (fig 4.2.5B). As PDE4D3 completely disappeared no value is presented for this isoform, however PDE4D3 expression in U937 cells was equivalent to PDE4D5. As can be seen there is a dramatic reduction in the expression of PDE4D isoforms with macrophage differentiation. (**, $P = 0.007$, Student's T test)

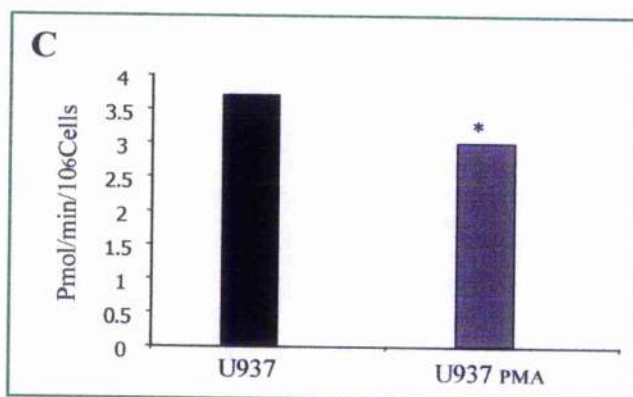
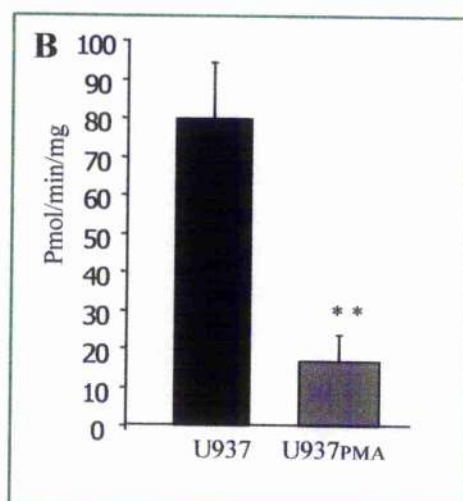
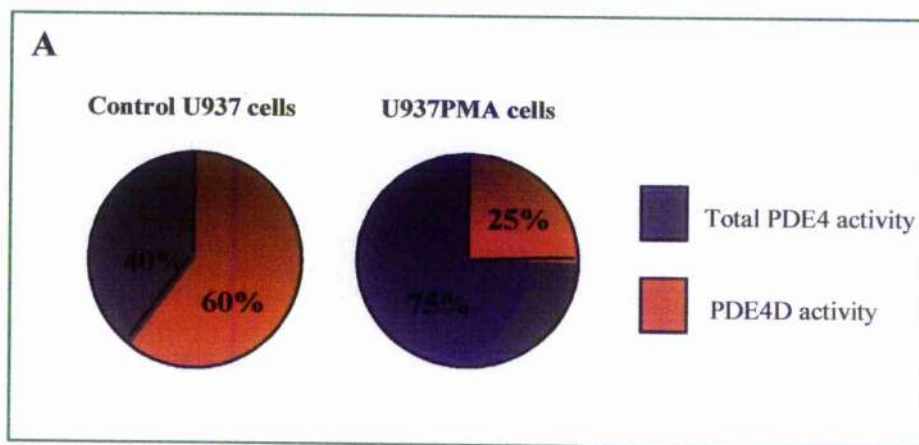


Fig 4.2.6A The changes in PDE4D expression in U937 cells differentiated with 4nm PMA

U937 cells and U937_{PMA} were lysed KHEM buffer and a volume of lysate representing 600 μ g protein was subjected to immunoprecipitation using antiserum raised against the common C terminal of PDE4D. Immunoprecipitates were analysed for PDE4 activity at 1 μ M cAMP. Figure 4.2.5A, the proportion of PDE4D activity relative to total PDE4 activity is presented. As can be seen the relative contribution of PDE4D to total PDE4 activity falls from 60% to 25% in U937_{PMA}. Figure 4.2.5B, The actual PDE4D activity per unit protein is presented reflecting a substantial fall in overall PDE4D activity (n=3). Fig 4.2.5C, The PDE4D activity per million cells is presented. Again activity per cell also falls. (** P=0.049, * P>0.5, Student's Paired T Test)

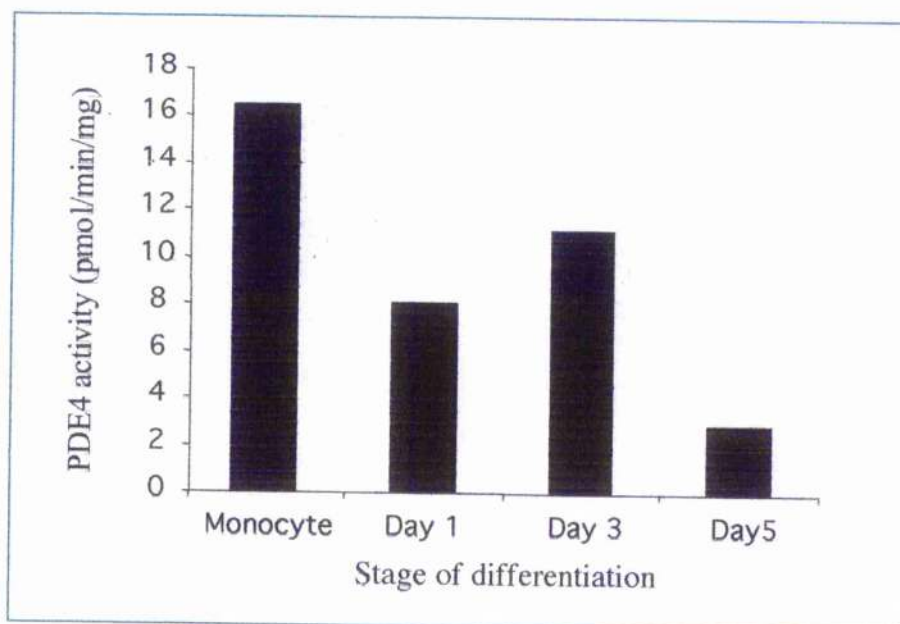


Fig 4.2.6.1 The changes in PDE4D expression in plastic adherent peripheral blood monocytes

Monocytes were cultured on plastic for up to 5 days. Day 1, day 3, day 5 and undifferentiated monocytes were lysed in KHEM buffer and a volume of lysate representing 600 μ g protein was subjected to immunoprecipitation using antiserum raised against the common C terminal of PDE4D. Immunoprecipitates were analysed for PDE4 activity at 1 μ M cAMP. PDE4D activity fell with time spent in culture from a initial activity of 17.1 pmol/min/mg to 2.7 pmol/min/mg. This reflects the changes seen with U937 cell differentiation.

activity could represent a dilution effect of other proteins, thus I recalculated the activity on a per 10^6 cell basis. Figure 4.2.6C, shows that the reduction in activity seen on per mg protein basis is less marked at a cellular level. This is inconsistent with the western blot data on protein expression. Figure 4.2.6.1 expresses the PDE4D activity immunoprecipitated from lysates prepared from fresh peripheral blood monocytes and monocytes cultured on plastic. PDE4D activity again falls confirming the physiological relevance of the U937_{PMA} model.

4.2.7 PDE4B expression increases with U937_{PMA} development

Cell lysates from U937 and U937_{PMA} cells were analysed by western blot and PDE4B isoforms identified using antisera raised against the C-terminal of the PDE4B family. As previously reported only PDE4B2 is expressed in U937 cells and remains present in U937_{PMA} cells (fig 4.11) [247]. Differentiation to U937_{PMA} is associated with a substantial increase in the intensity of the band shown in fig 4.2.7A. Three experiments are presented in a disordered sequence to improve densitometry. This analysis is presented in fig 4.2.7B, and clearly shows a 180% increase in the intensity of the PDE4B2 band with U937_{PMA} development.

4.2.8 PDE4B activity increases with U937_{PMA} development

Figure 4.2.8 presents data derived from immunoprecipitation of PDE4B isoforms and subsequent PDE4 assay on the immunoprecipitates. Figure 4.2.8A and 4.2.8B, demonstrate that both the activity of PDE4B and the contribution to total PDE4 activity rose considerably with U937_{PMA} maturation. Thus in U937 cells PDE4B activity was 8 ± 4 pmol/min/mg representing 6% of total PDE4 activity, while in U937_{PMA} cells PDE4B activity was 29 ± 10 pmol/min/mg, representing 44% total activity. Again the activity was calculated on a per cell basis and the increase in activity was preserved.

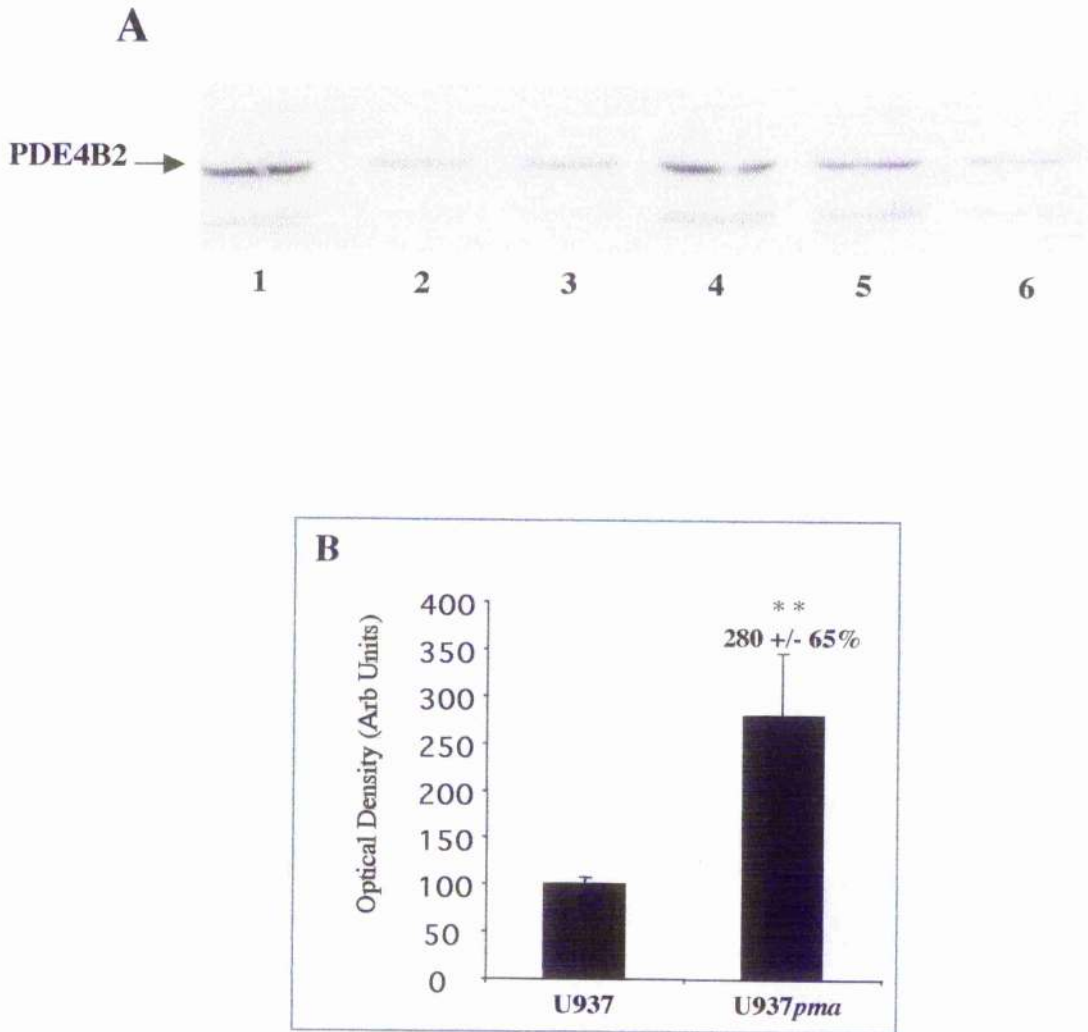


Fig 4.2.7 The changes in PDE4B expression in U937 cells differentiated with 4nM PMA

U937 cells and U937_{PMA} were washed and lysed in 3T3 lysis buffer and equal quantities of protein from each cell type were resolved by SDS-PAGE. PDE4B isoforms were identified by anti-PDE4B antisera on a western blot fig 4.2.6A. Lanes 1,4 and 5, U937_{PMA} cell lysate. Lanes 2, 3 and 6, control U937 cells. Autoradiographs were subjected to densitometric analysis and the relative intensities of each PDE4B band compared to control U937 was calculated and are presented (fig 4.2.6B). Control U937 cells express only PDE4B2, of the PDE4B family. Differentiation with PMA causes a substantial increase (+180%) in the band for PDE4B2 in U937_{PMA}. (** P = 0.02, Student's Paired T test)

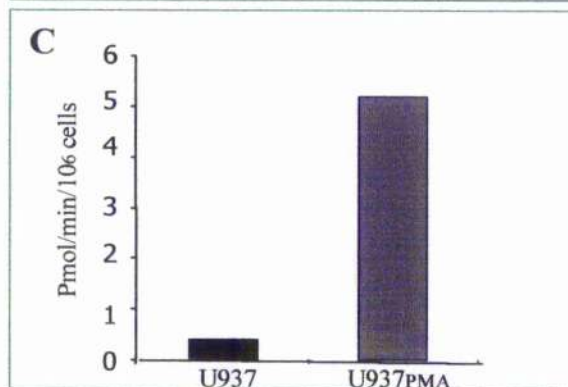
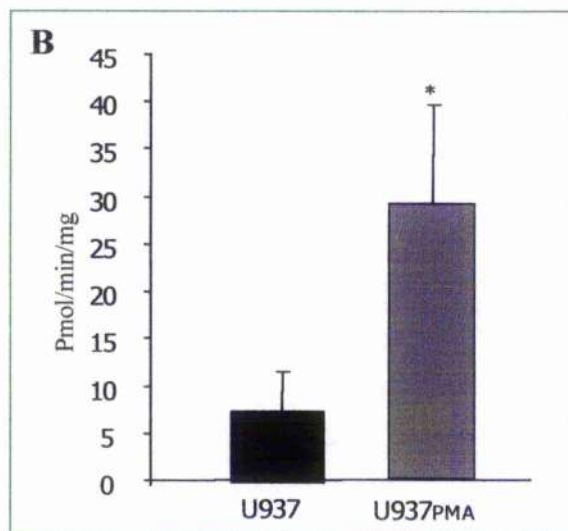
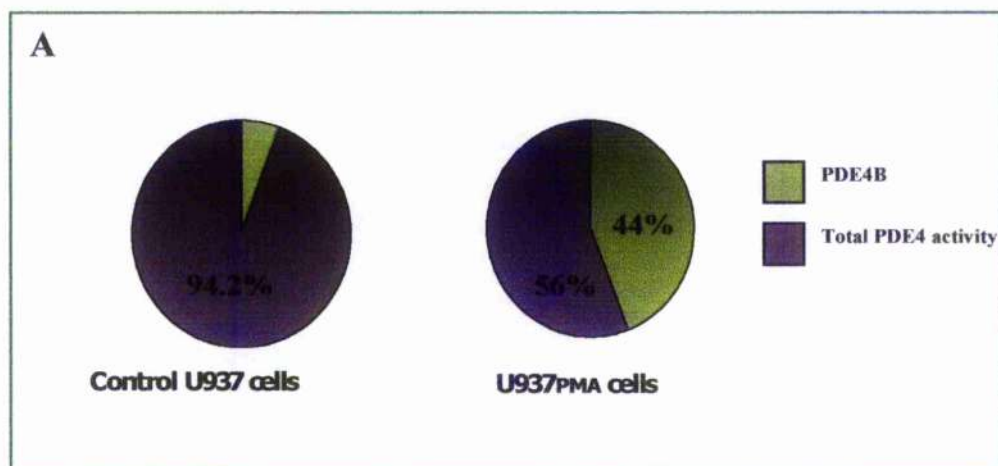


Fig 4.2.8 Changes in PDE4B activity in U937 cells differentiated with 4nM PMA.

U937 cells and U937_{PMA} cells were counted and lysed in KHEM buffer. A volume of cell lysate equal to 600 μ g was subjected to immunoprecipitation using antisera raised against the common C terminal of PDE4B. These lysates were analysed for PDE4 activity. Fig 4.2.7A, a pie chart representing the proportion of total PDE4 activity represented by PDE4B before and after differentiation. Fig 4.2.7B, The absolute activity per unit protein is presented \pm standard error (n=3). Fig 4.2.7C, The activity per million cells is presented. As can be seen an absolute increase in PDE4B activity is seen both in terms of absolute activity and activity per cell. (* P = 0.09, Student's Paired T test)

4.2.9 Densitometric analysis of western blot

Throughout this detailed profiling of the PDE4 isoform content of U937 and U937_{PMA} cells, I have presented data showing both activity per cell and activity per mg protein. This reflects the changes in cellular protein content found with differentiation. The densitometric analysis of band intensity from western blot was performed on equal quantities of protein, however and may result in bias. Figure 4.2.9 presents the densitometry data as optical density units with additional calculation of expected band intensity for equal cell numbers. As can be seen where an increase in expression occurs, as with PDE4A and PDE4B comparing equal numbers of cells would increase the difference described in my work. Thus it is likely that a greater quantity of PDE4A and PDE4B are expressed in U937_{PMA} cells than my data suggest. In terms of PDE4D, my data again underestimates the changes at a cellular level. Thus although PDE4D content of U937 cells is higher in my experiment than predicted for a per cell analysis, the fall is less marked. Thus it is likely that actual PDE4D expression at a cellular level in U937_{PMA} cells is lower than suggested in this work.

Discussion section 4.2

Having shown that U937_{PMA} cells represent mature macrophage development I measured the changes in PDE4 isoform expression. U937 cells expressed PDE4D3, PDE4D5, PDE4B2 and small quantities of PDE4A4. This is in agreement with MacKenzie et al [247]. I demonstrated a large increase in PDE4A activity and expression in U937_{PMA}. Increases in activity and PDE4A expression were found at both total protein and cellular level and were not an artefact of the changing protein content of cells. This increase was at least in part due to new expression of PDE4A10 a recently described long form PDE4A

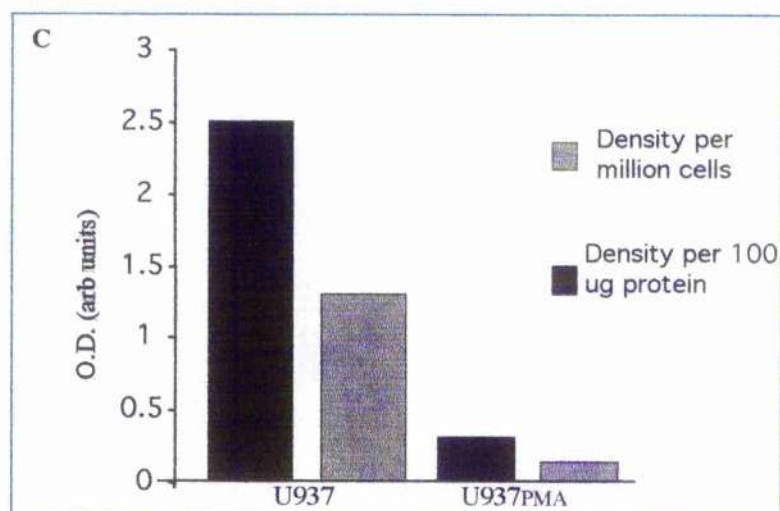
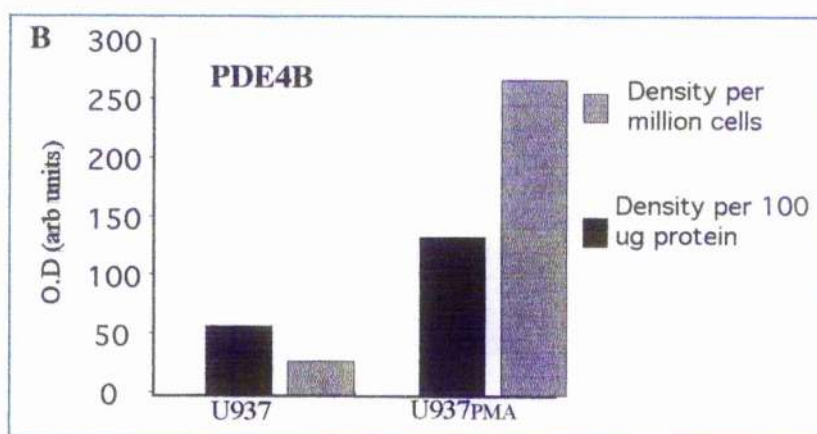
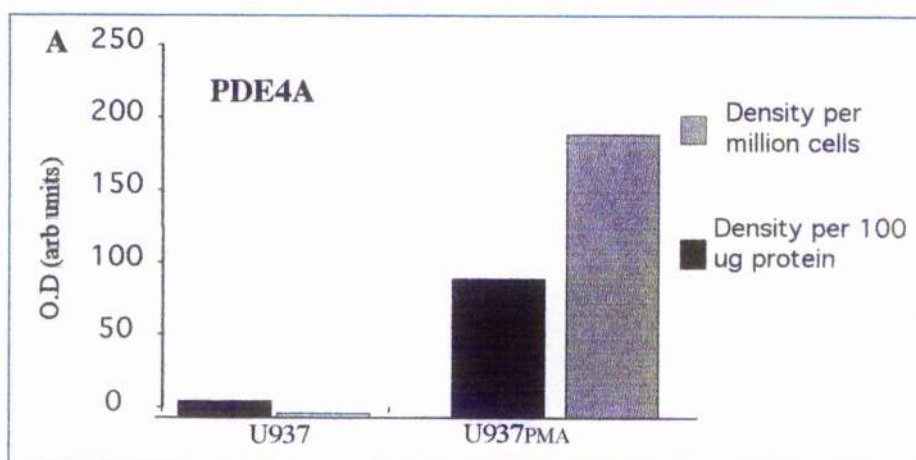


Fig 4.2.9 Expression of PDE4 isoforms in U937 and U937_{PMA} cells

U937 and U937_{PMA} were lysed and western blot analysis was performed on equal quantities of lysate protein (100 μ g). Proteins were visualised with antisera raised against the C-terminal regions of PDE4 isoforms. Quantification of isoform expression was performed using Kodak Digital Science 1D densitometry software. Data presented here demonstrates the difference between the density observed using equal quantities of protein and that predicted by expression per cell number. As can be seen the patterns of expression per cell number exaggerate the relative expression expressed per 100 μ g protein. (n=3 per experiment (arb units = arbitrary units)).

isoform [234]. As a novel gene expressed with a phenotypic switch PDE4A10 may play a role in macrophage specific regulation. On the other hand it seems likely that PDE4A4 is also increased in U937_{PMA} cells over U937 cells.

Wang et al suggested that in human monocytes PDE4B2 was the key cAMP PDE isoform in controlling inflammatory behaviour[253]. Another group found a linear correlation between the ability of a range of cyclohexyl amine compounds' to selectively inhibit PDE4A or PDE4B as opposed to inhibiting PDE4D and their capacity to limit T cell proliferation or TNF α production in response to house dust mite antigen [253, 254]. Using a knock out mouse model Jin et al demonstrated the importance of PDE4B2 in inflammation by demonstrating failure to produce TNF α in knock out mice exposed to LPS,[255]. I demonstrated a trebling of the PDE4B2 content and activity in U937_{PMA}. These data is consistent with the reports described above and strengthens the likelihood of PDE4B2 having important immunomodulatory roles.

In contrast to PDE4A isoforms and PDE4B2, PDE4D3 and PDE4D5 expression falls in U937_{PMA}. This finding was consistent in all western blot analyses performed. The level of reduction in expression was greater than the fall in PDE4D activity found using immunoprecipitation of U937 and U937_{PMA} lysates. Although the trend was for a fall in PDE4D activity it was not consistent with the western blot data. Increasing the stringency of the washing steps of the immunoprecipitation, led to a complete loss in all PDE4 isoform activity, and thus could not be used to correct PDE4D activity. The western blot data was more consistent than the immunoprecipitation data. In the latter greater variability was found between experiments suggesting more error. The same antibody was used for both forms of analysis and it seems unlikely that the error lies with the antisera. The immunoprecipitated PDE4D may have been isolated along side another PDE4 isoform in a molecular complex that then contributed to the activity recorded. No such additional PDE4 isoform was found when immunoprecipitates were blotted with antisera raised against the

other PDE4 isoforms. I believe the data from the western blot is a more correct reflection of the cellular changes that occur with U937_{PMA} development due to the consistency of these data.

To confirm that the findings in U937_{PMA} reflected changes seen in peripheral blood monocytes my colleague Dr George Baillic examined the activity and expression profiles of ex-vivo monocytes differentiated on plastic. He demonstrated that PDE4A isoforms increased alongside PDE4B2 while PDE4D3 and PDE4D5 were reduced in expression. Again my U937 model closely reflected the ex-vivo model.

Section 4.3 A switch in long form/ short form dominance has functional significance in ERK 1/2 signalling.

PDE4B2 is a short form PDE4 and its activity is increased by ERK2 phosphorylation[67]. PDE4D3 and PDE4D5 are long forms and their activity is reduced by ERK2 phosphorylation [66, 67]. The changes outlined in section 4.2 demonstrate a switch from long form PDE4D dominance to a short form PDE4B2 dominance with U937_{PMA} development. I hypothesised that PDE4 regulation by ERK2 would be altered by this change in isoform expression.

4.3.1 Changes in PDE4 response to EGF

Figure 4.3.1 demonstrates that when control U937 cells are treated with EGF the total PDE4 activity falls implying a long form-dominant response. U937_{PMA} cells however show an increased PDE4 activity consistent with a short form-dominant response.

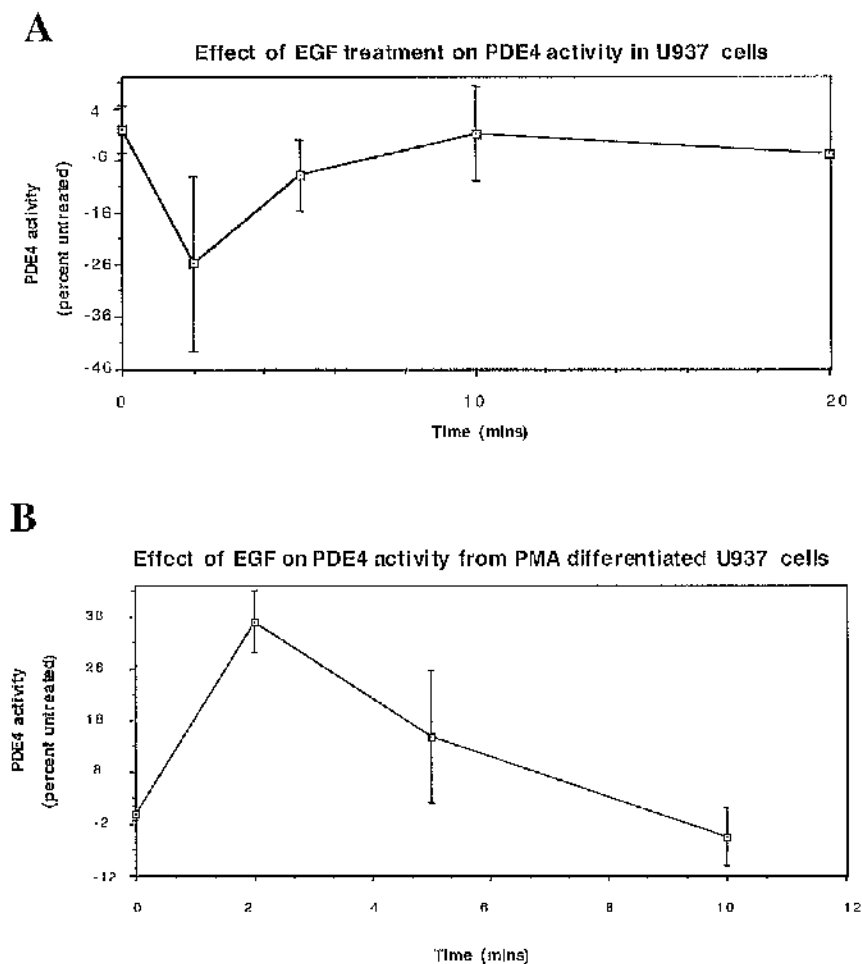
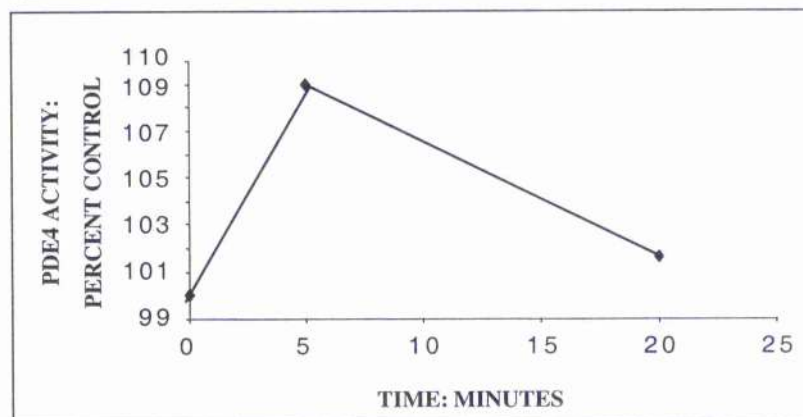


Fig 4.11 PDE4 responses to EGF treatment varies with PMA treatment

Control and PMA treated U937 cells were exposed to EGF for increasing periods of time. Cells were washed and lysed and the PDE4 activity measured. As can be seen EGF caused a rapid 26% decrease in the PDE4 activity of U937 cells. In PMA treated, differentiated cells however a rapid increase in activity was recorded. This difference probably corresponds to the ability of EGF to rapidly activate MAPKinase series of signal transduction kinases. These are known to exert opposite effects on the long and short isoforms of PDE4.

A



B

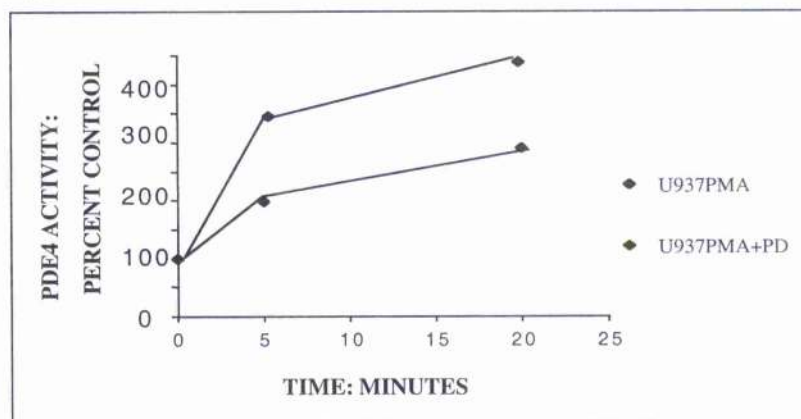


Fig 4.3.2 PDE4 responses to salbutamol in U937 and U937 PMA cells

Control and pma treated U937 cells were exposed to 10 μ M salbutamol for up to 25 minutes. Cells were washed and lysed and the PDE4 activity measured. A. U937 PDE4 activity rose by around 10% by 5 minutes and returned to normal by 25 minutes. B. U937pma cell PDE4 activity continued to rise unchecked. The presence of the MEK inhibitor PD98059 leads to an increased elevation in activity and demonstrates that MAPkinase may become activated by salbutamol.

4.3.2 Changes in response to β_2 agonists

Figure 4.3.2 shows the PDE4 activity in response to treatment with salbutamol in U937 and U937_{PMA} cells. Although representing only two experiments these data suggests that PDE4 activity in U937 cells initially increases then falls while in U937_{PMA} the activity continues to rise.

Discussion Section 4.3

I used EGF to activate ERK2 in U937 cells because other pro-inflammatory signals such as LPS or TNF α activate ERK by multiple different pathways. Such 'dirty' signals might have changed PDE4 activity by other pathways that are hard to isolate in a living system. My data suggested that a switch in long form-dominance to short form-dominance was reflected by a change in crosstalk between ERK2 and cAMP signalling. This exciting result suggested that PDE4B2 could play a significant role in the development of inflammatory signals. Cyclic AMP is believed to have anti-inflammatory behaviour on cell signalling and my data suggests that increased PDE4B2 activity will reduce local cAMP levels and permit signalling to progress.

Conversely I measured the activity of PDE4 in response to a β_2 agonist. These are important therapeutic agents in asthma. It is known that salbutamol increases PDE4 activity in monocytes [226]. This may result in reduced activity of the receptor in a process called heterologous desensitisation. β_2 agonists are G-protein coupled receptors that activate adenylyl cyclase by release of G α_s . It is believed however that prolonged receptor occupancy results in a switch in downstream signalling to a G α_i activation of ERK1/2. Thus I was interested to observe changes in this complex receptor system in terms of PDE4 activity. Initial results showed an early an increase in PDE4 activity in U937 cells perhaps reflecting PKA phosphorylation of PDE4 isoforms. Following activation, however a

gradual decrease in activity occurs. Whether this represents a dephosphorylation event or a ERK2 related inactivation is not clear. In U937_{PMA} however activation continues unchecked. This suggests that a subsequent activation of ERK2 downstream of the β 2 receptor may cause short form activation in differentiated macrophages.

Conclusions

In this chapter I have demonstrated that while tissue fixed macrophages are hard to acquire *in vivo*, the U937_{PMA} model is a useful surrogate for the study of phosphodiesterase 4 activity. Macrophage differentiation is associated with significant changes in the expression and activity of PDE4A, PDE4B2 and PDE4D. In particular the new expression of PDE4A10 may offer a "cell specific" PDE4 isoform to target therapeutically. PDE4B2 is also highlighted as an important PDE4 in macrophages. The overall switch from a long form dominant to a short form dominant profile of PDE4 may have important implications for our understanding of crosstalk in inflammation based signalling cascades involving cAMP.

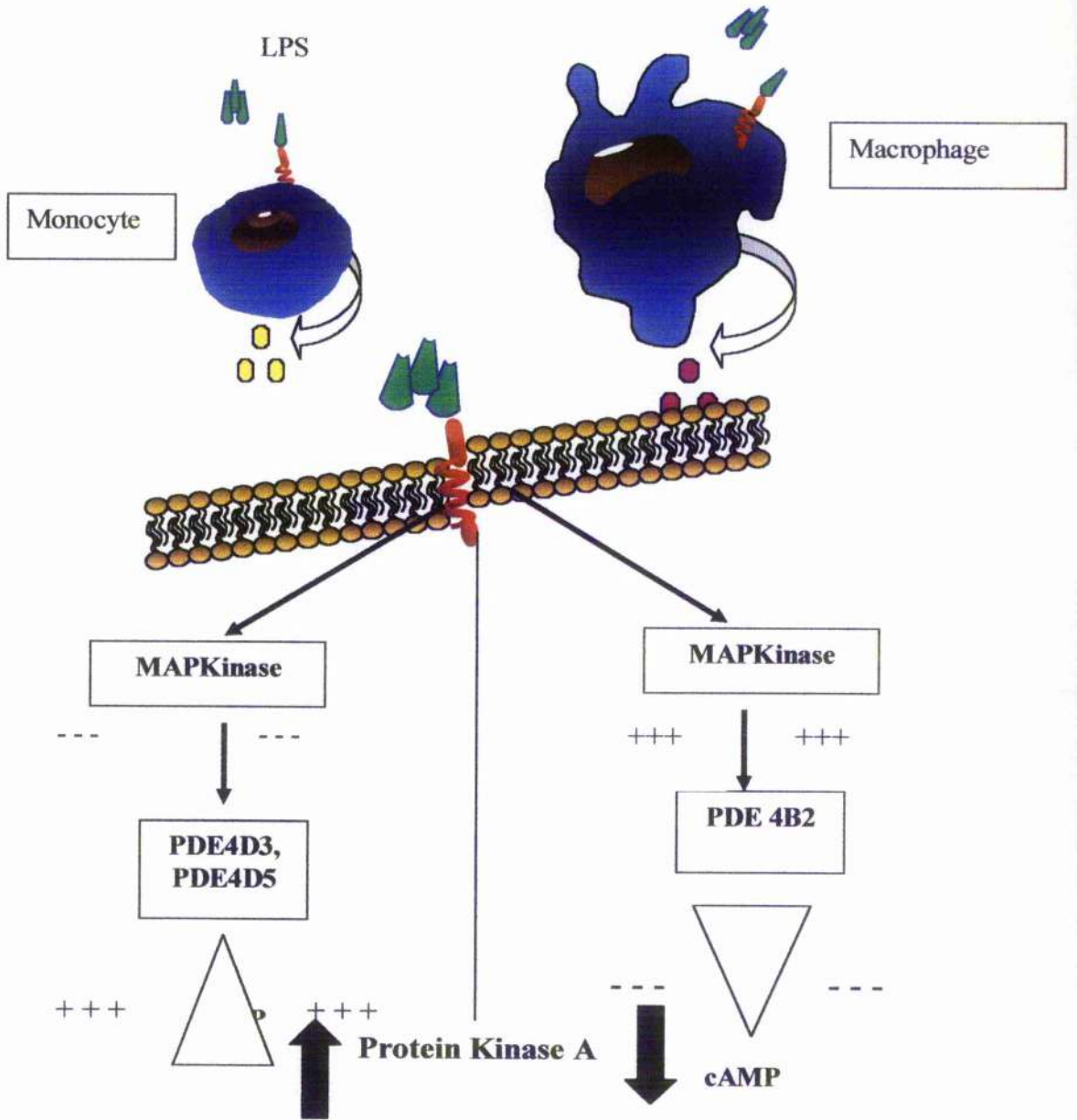


Fig 4.3.3 Diagram representing the effect of macrophage development on cAMP crosstalk with MAP Kinase

Monocyte

/

Macrophage

Chapter 5 Lipopolysaccharide regulation of PDE4 isoforms and PDE4 inhibition in activated RAW 264.7 cells

Introduction

In chapter 4 I demonstrated differential regulation of PDE4 isoforms in macrophage development suggesting that different PDE4 isoforms might regulate specific functions. Support for PDE4 dependent regulation of macrophage function comes from studies demonstrating specific inhibition of PDE4 alters macrophage behaviour. For example PDE4 inhibitors have been shown to prevent LPS stimulated TNF α and IL-12 production [256, 257]. The association of rolipram with PDE4 occurs with two distinct kinetics, a high affinity rolipram binding site (HARBS) and a low affinity rolipram binding site (LARBS) [223] leading to a proposal that different conformations of PDE4 isoforms interacting with rolipram in specific ways [91]. Inhibition of TNF α production by rolipram occurs with kinetics more akin to PDE4 activity inhibition than H³rolipram displacement from HARBS, suggesting that different conformations of PDE4 may have different roles in regulating cellular cAMP [223]. Mackenzie et al demonstrated in U937 cells that cAMP dependent phosphorylation of CREB (PCREB), showed stepwise increases with rolipram dose [247]. This work suggests that rolipram may inhibit PDE4 with multiple kinetics and thus regulate cell function in an isoform or conformation specific fashion.

By what mechanism cAMP inhibits LPS stimulated TNF α production is unclear although indirect inhibition by IL-10 has been proposed. Cyclic AMP can increase the production of the "anti-inflammatory" cytokine IL-10 [245] and removing with anti-IL-10 antiserum,

prevented the inhibition of TNF α by rolipram [163]. Procopio et al, on the other hand demonstrated that in an IL-10 knock out mouse model, cAMP was still capable of preventing LPS stimulated TNF α arguing for an alternative method of inhibition [194]. While Kambayashi et al did not find a change in TNF α mRNA levels from rolipram treatment alone, many groups have found cAMP dependent TNF α regulation occurs at transcriptional and post translational stages [206]. Cyclic AMP inhibition of LPS induced TNF α production therefore may occur in a direct or indirect manner.

Many groups studying rolipram inhibition of cytokine production have found that the effect is enhanced by the presence of a cAMP elevating signal. Thus while rolipram alone will not elevate intracellular cAMP the addition of for example, a β 2 adrenergic agonist or PGE2 along with PDE4 inhibition causes changes in cellular behaviour [258]. Whether LPS can provide such a cAMP stimulus is not clear[244].

LPS activates ERK1/2 [259, 260] and cAMP is known to inhibit the classical Ras-Raf-1 pathway of ERK1/2 activation by PKA mediated phosphorylation of Raf-1 [261]. Cyclic AMP generated by PDE4 inhibition is therefore well placed to prevent LPS generated ERK1/2 activation if LPS uses the Ras-Raf-1. Guthridge et al demonstrated that both LPS and constitutively active Raf-, activated ERK1/2 in RAW 264.7 cells [262]. LPS however did not cause Raf-1 activation. Indeed both LPS and Raf-1 were mutually antagonistic. Other groups have demonstrated Raf-1 independent activation of ERK1 in myeloid cells [263]. Controversial work recently presented proposes that Rap1 can activate B-Raf and thus activate ERK1/2 [264, 265]. Rap 1 is activated by a number of second messengers including cAMP [266]. A family of guanine nucleotide exchange factor (GEFs) called EPAC have been shown to activate Rap1 in a cAMP dependent, PKA independent fashion [38]. Rap1 could resolve the puzzle posed by Guthridge et al, in that if Rap1 was activated by LPS then it might activate ERK1/2 in a Raf-1 independent manner (Fig 5.1). Carron et

al recently showed that LPS induces β integrin induced macrophage spreading in a process that involves rap1 activation [204].

Although many studies have investigated the effects of inhibiting PDE4 on cytokine generation few have looked at LPS modulation of PDE4 activity. I hypothesised that cAMP regulation would take place in a PDE4 isoform specific manner and that this might influence inflammatory behaviour. Thus I proposed to measure the response of PDE4 to LPS and look for functional outcomes of PDE4 inhibition. Finally I investigated what role if any Rap-1 might play in transducing the cAMP signal generated by PDE4 inhibition

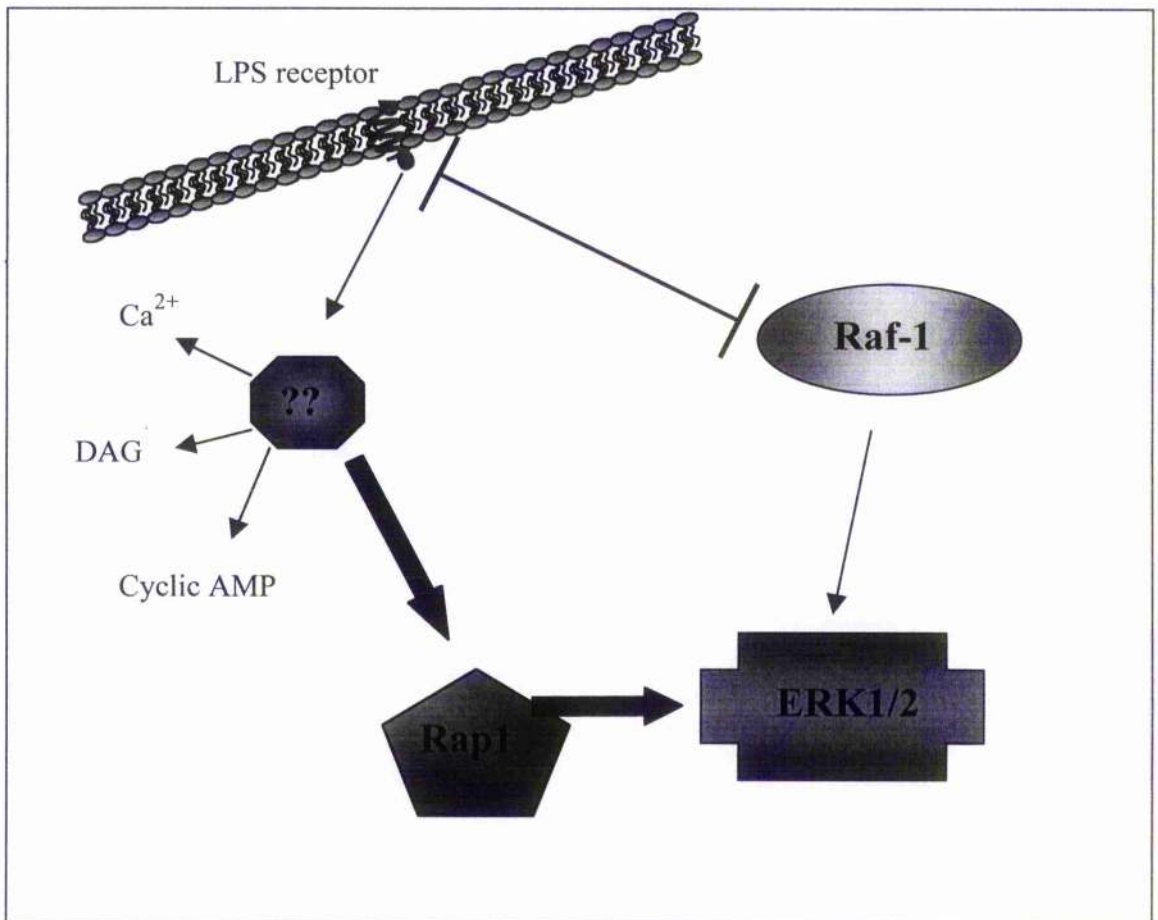


Fig 5.1 Proposed mechanism of cAMP crosstalk in LPS activation of MAPKinase.

(Ca^{2+} , calcium; DAG, diacyl glycerol;)

Results

Section 5.1

5.1.1 Lipopolysaccharide activates PDE4 but reduces PDE3 activity

I hypothesised that increases in cAMP phosphodiesterase activity would be required to “permit” proinflammatory signals to be transduced. 10ng/ml LPS was used to activate RAW 264.7 cells and PDE activities were measured over 90 minutes exposure (Figure 5.1.1) (n=2). PDE4 activity climbs from 10 minutes, peaks at 50 minutes with normal activity regained by 90 minutes (figure 5.1.1.A). In contrast PDE3 activity, which contributes around 30% of cAMP PDE activity in resting cells, is rapidly reduced following LPS stimulation.

LPS stimulates the production of various mediators from macrophages. To avoid a secondary autocrine effect, I selected an early time point to analyse the activation further (figure 5.1.1.B). By 30 minutes I found a significant increase of 39.8% +/- 4.2% activation of PDE4 (n=4). The data presented is pooled from various experiments and percent change is quoted to minimise the effect of cellular variability between experiments.

5.1.2 Wortmannin and PKA inhibitors significantly reduce LPS activation of PDE4

Gene transcription and phosphorylation by PKA and ERK2 can regulate PDE4 activity. I employed a battery of signal transduction inhibitors to try and identify the pathways leading to PDE4 activation by LPS. Actinomycin 3µg/ml, did not significantly affect the activation of PDE4 suggesting that new protein production does not underlie the increase in activity at 30 minutes. Inhibition of the MEK-ERK axis reduced PDE4 activation by

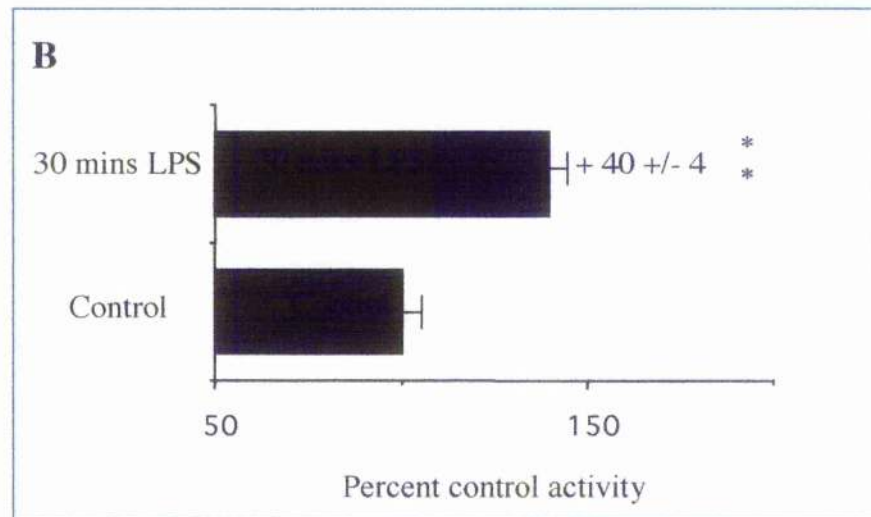
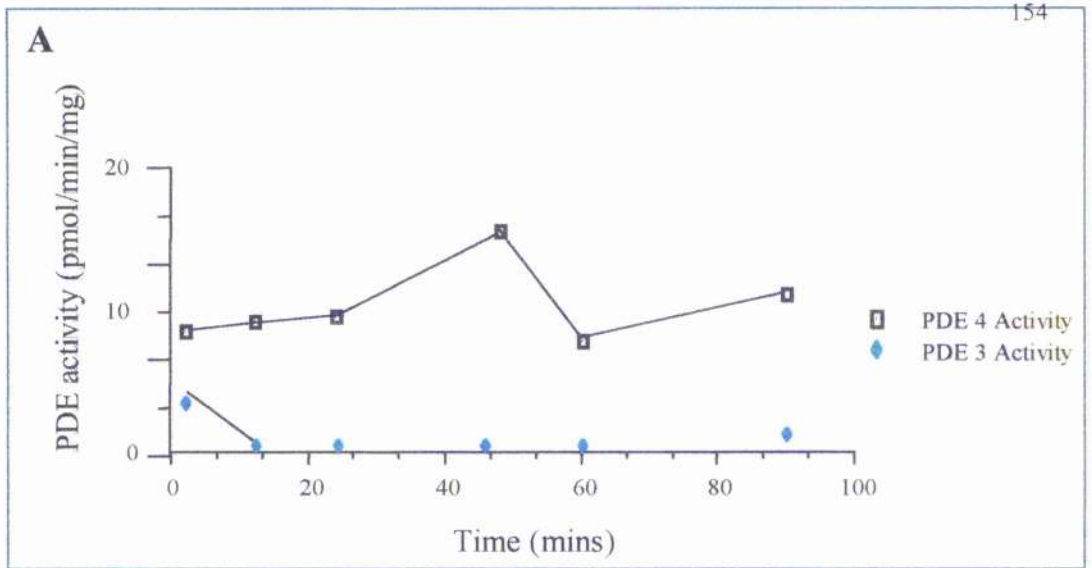


Fig 5.1.1. LPS increases PDE4 activity while reducing PDE3 activity

Raw 264.7 cells were incubated with 10ng/ml LPS for various periods. Cells were harvested, lysed in KHEM buffer and PDE3 or PDE4 activity was measured. Fig5.1.1A demonstrates that while PDE3 activity is rapidly reduced, PDE4 activity is preserved and increases from around 25 mins until 50 mins (n=2). Fig5.1.1 B presents data from repeated experiments looking at 30 minutes of LPS stimulation (n=4). LPS appears to increase PDE4 activity by 40% +/- 4% after 30 minutes. (** indicates P = 0.05, calculated by paired T test of treated and non treated cells).

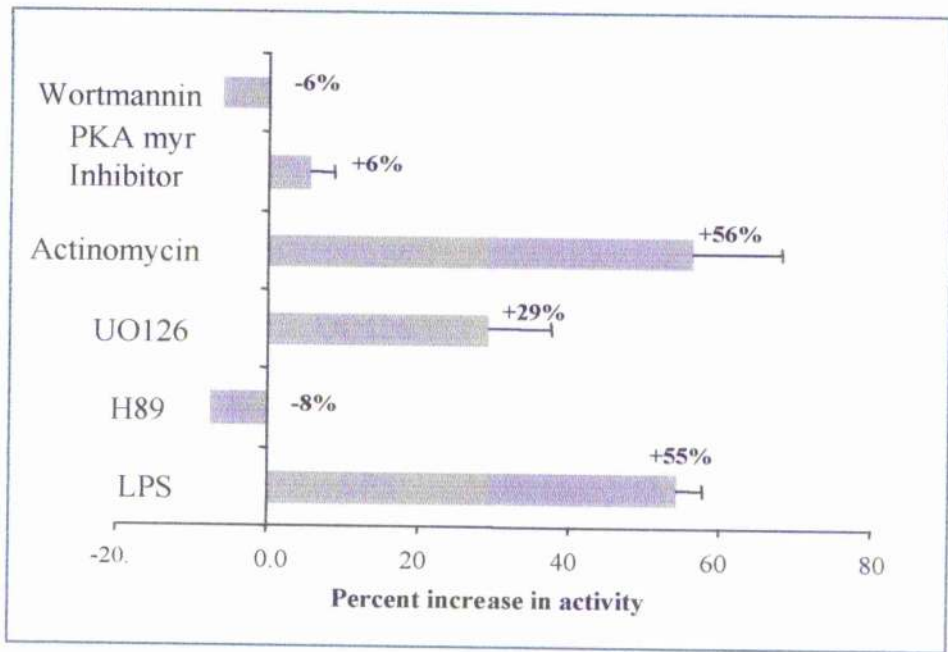


Fig 5.1.2 The effects of various compounds on the increase in PDE4 activity produced by 20 minutes treatment with LPS.

Raw 264.7 cells were pre-incubated with various signal transduction inhibitors for 30 minutes, prior to 20 minutes incubation with 10ng/ml LPS. Cells were lysed in KHEM buffer and the PDE4 activity to $1\mu\text{M}$ cAMP was measured. The data is presented as percentage change in the treated cells compared to the untreated cells. As can be seen little difference is recorded in the presence of actinomycin ($3\mu\text{g/ml}$). MEK inhibition only inhibits 16% of the activation seen with LPS. The greatest effects were seen in the presence of H89 ($10\mu\text{M}$) and the myristylated PKA inhibitor peptide ($10\mu\text{M}$) and wortmannin ($10\mu\text{M}$). These molecules abolished PDE4 activation by LPS and reduced resting PDE4 activity.

50%. The greatest inhibition of PDE4 activation by LPS was seen with wortmannin and H89, both of which reduced PDE4 activity overall.

5.1.3 RAW 264.7 cells contain PDE4A1, PDE4A6, PDE4B2 and PDE4D3 and PDE4D5

On the basis of inhibitor studies it appeared that MEK was involved in the activation of PDE4 by LPS. ERK2 can activate short form PDE4 isoforms and inhibit long forms and so I investigated which long and short forms exist in these cells using western blot analysis. PDE4D5 is expressed to a greater degree than PDE4D3. The short form, PDE4B2 is the only member of the PDE4B family to be expressed. Two representatives of the PDE4A family, rPDE4A1 and rPDE4A6 are seen.

5.1.4 Lipopolysaccharide activates PDE4B2

Next I used immunoprecipitation to isolate PDE4 isoforms before and after LPS treatment and measured the PDE4 activity in the resulting immunoprecipitates. Figure 5.1.4 demonstrates that while PDE4A and PDE4D immunoprecipitates did not appear to increase in activity PDE4B activity rose by around 50%.

5.1.5 Inhibition of PDE4B in LPS treated RAW 264.7 cells

Using a range of signal transduction inhibitors I identified the pathways involved in activating PDE4B. While the SB203580 compound inhibiting P38 MAPKinase, did not affect the activation of PDE4B, UO126 does abolish the activation completely. Again actinomycin does not alter the activation arguing against a gene transcription event.

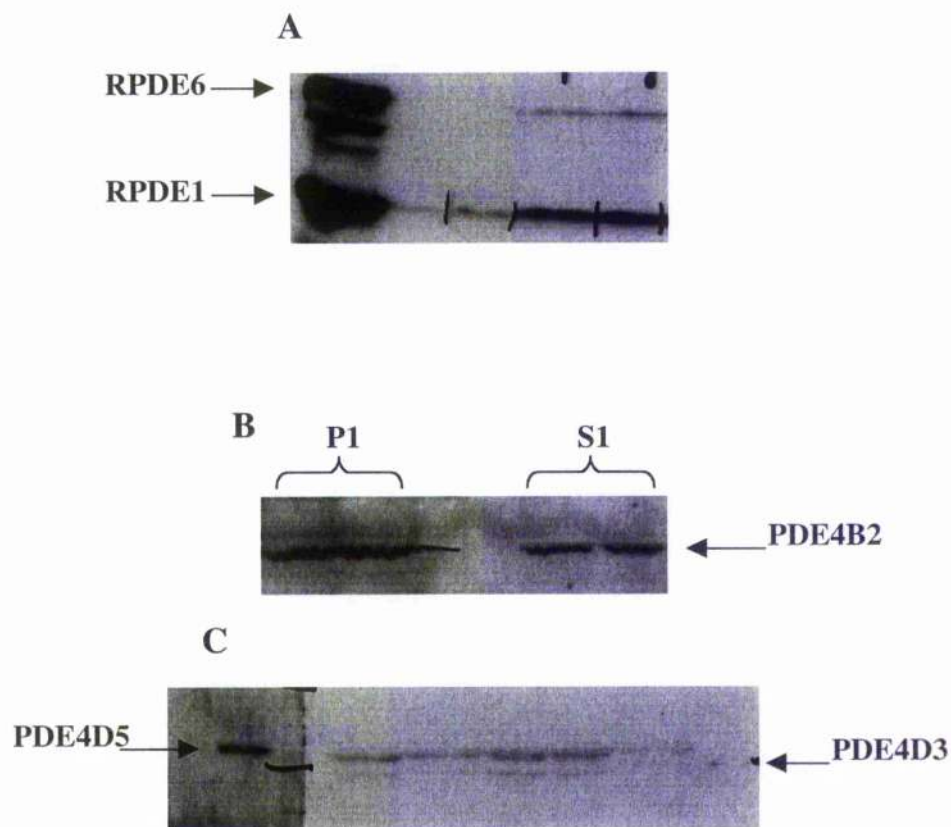


Fig 5.1.3. PDE4 isoform expression in RAW 264.7 macrophage cells.

Raw 264.7 cells were lysed in either 3T3 lysis buffer (A and C) or KHEM and subjected to high speed fractionation (B) and proteins were resolved on SDS-PAGE. Nitrocellulose membranes were probed with antibodies raised against the common C-terminal of PDE4 gene families. Within each experiment equal amount of lysate protein were loaded onto each lane. Fig 5.1.3A, PDE4A isoforms. Two immunobands appear co-migrating with rat PDE4A1 and PDE4A6. Fig 5.1.3B, PDE4B isoforms. One band co-migrating with PDE4B2 appears in both soluble and particulate fractions fraction. Fig 5.1.3C, PDE4D isoforms. Two bands co-migrating with PDE4D3 and PDE4D5 appear. There is a clear excess of PDE4D5.

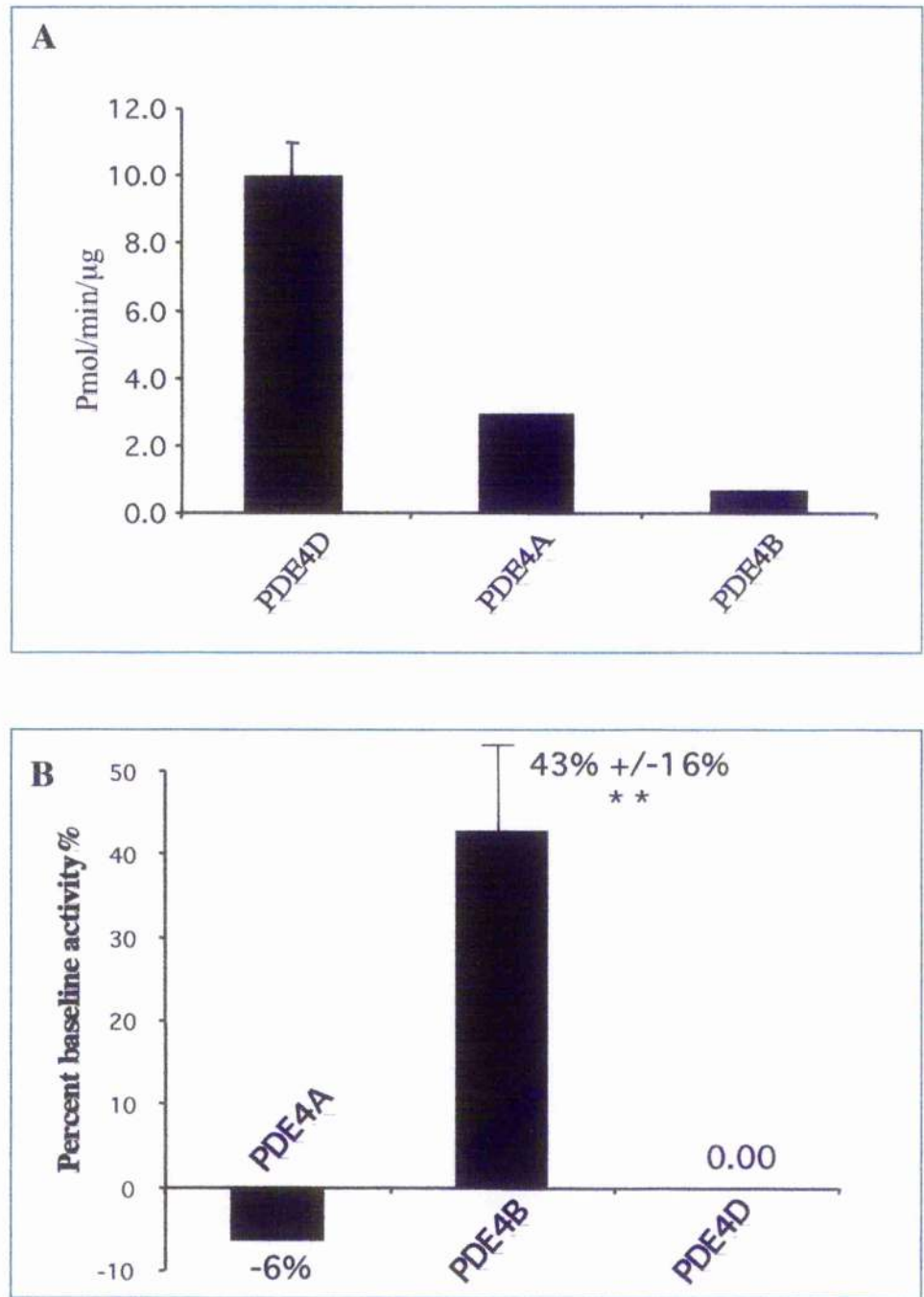


Fig 5.1.4 PDE4B is activated following LPS treatment of RAW macrophages

RAW 264.7 cells before and after treatment for 20 minutes with 10ng/ml LPS treatment were lysed in KHEM buffer. PDE4 isoforms were isolated by immunoprecipitation using antiserum raised against PDE4A, PDE4B and PDE4D. PDE activity of immunoprecipitates was measured (n=3). Fig 5.1.4A, the majority of PDE4 activity in RAW 264.7 cells is accounted for by PDE4D, while 5% is accounted for by PDE4B. Fig 5.1.4B, LPS increases PDE4B activity but does not increase PDE4A or PDE4D activity (n=3). (**, P = 0.00, Paired T test of immunoprecipitates before and after LPS treatment).

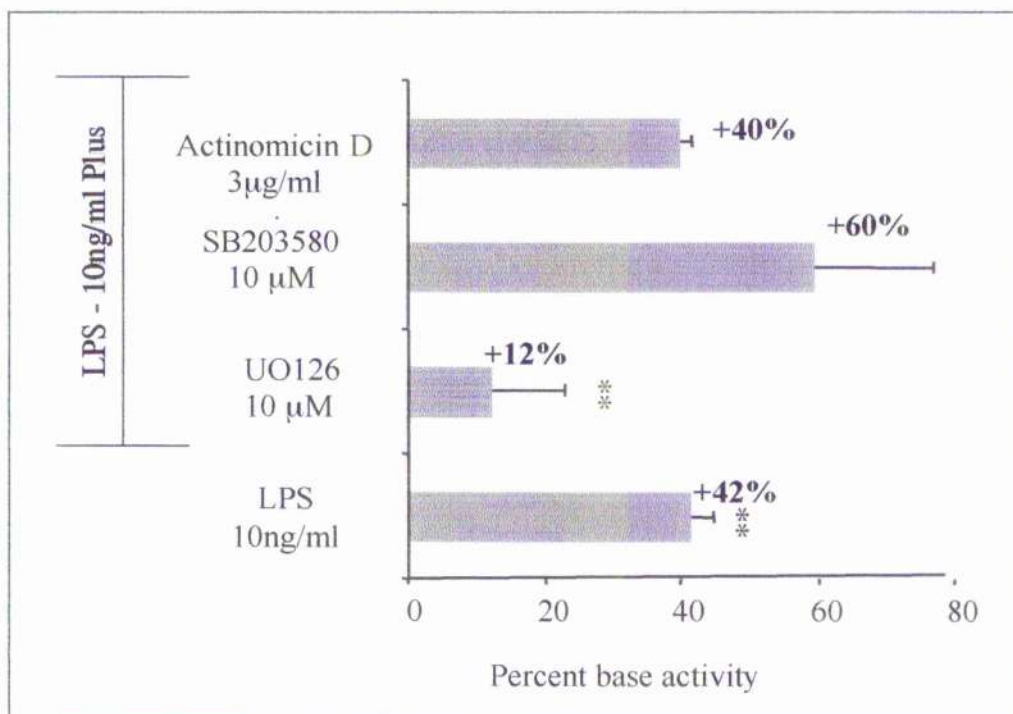


Fig 5.1.5 Inhibition of the activation of PDE4B

Serum starved RAW 264.7 cells were pre-treated with various inhibitors of signal transduction cascades, prior to incubation for 20 minutes with 10ng/ml LPS. PDE4B was immunoprecipitated from cell lysates and the PDE activity of these extracts was measured. LPS increased PDE4B activity by 42%. As can be seen gene transcription does not appear to explain the increase in activity of PDE4B as actinomycin has no significant effect on PDE4B activation. MEK inhibition by the UO126 compound results in a loss of activation. Inhibiting P38 MAPkinase with the SB203580 compound does not alter PDE4B activation. (**, $P < 0.05$, Student's paired T test of the difference between LPS and LPS + inhibitor from base).

Discussion Section 5.1

Lipopolysaccharide's capacity to activate of RAW 264.7 murine macrophage has been shown to equate with toxicity in vivo [267]. An extensive literature exists on pathways downstream of the LPS receptor complex yet surprisingly little is known about the effect of LPS on PKA activity or intracellular cAMP levels [259, 268]. Indirect studies using inhibitors of PKA on LPS stimulated macrophages suggest that PKA is not activated [269]. Other groups have shown PKA inhibition to reduce LPS responses. H89, a PKA inhibitor, can inhibit the activity of MSK 1 and Caivano et al have demonstrated that some effects attributed to PKA on the basis of H89 inhibition may be due to bystander effects on this kinase [216].

I have shown that LPS causes an increased PDE4 cAMP hydrolysis in macrophages. This increase in activity would be expected to lower intracellular cAMP levels, as I hypothesised. PDE3 and PDE4 show contrasting responses to LPS in a similar fashion to other examples of functional compartmentalisation. Ahmad et al, demonstrated that while GM-CSF, an important macrophage survival factor was capable of activating PDE3 and PDE4, IL-3 specifically activated PDE4 [102]. Dousa demonstrated in kidney mesangial cells, PDE3 inhibitors inhibit proliferation, while PDE4 inhibitors prevent oxide radical release [98]. Thus biochemical compartmentalisation may explain distinct functional responses to anti-inflammatory agents.

The greatest effects on PDE4 activation came with PI3Kinase and PKA inhibition. Baseline PDE4 activity was decreased implying that a degree of constitutive activation of PDE4 is present in these cells. PKA can activate PDE4 isoforms and PI-3Kinase has been shown to activate PDE4A in pre-adipocytes through a p70S6 Kinase mediated pathway

[112, 238]. LPS is known to activate PI-3kinase in macrophages [231]. I have also found partial reduction in PDE4 activity with MEK inhibition. ERK2 has been shown to affect PDE4 isoform activity in an isoform specific manner [67]. I wished to try and tease out which isoform was being activated as this might suggest which pathway was dominant in the LPS activation.

RAW cells express one PDE4B and two PDE4A isoforms (fig 5.1.3). This pattern reflects the mature macrophage phenotype described in chapter 4. PDE4D5 is also expressed differing from our U937 model. It is possible that this isoform reflects the immortalisation process. Immunoprecipitated PDE4A activity did not change with LPS treatment of RAW 264.7 cells. This argues against a direct role for the PI-3kinase – p70S6 kinase pathway described in preadipocytes. If PDE4D was the predominant isoform responsible for controlling the inflammatory response LPS would be expected to inhibit PDE4 activity by MAPkinase activation. Thus MEK inhibition would activate PDE4. This was not seen, and immunoprecipitated PDE4D did not respond to LPS.

PDE4B2 is the only 'short-form' PDE4 isoform present in RAW cells making it the likely subject of ERK 1/2 activation downstream of LPS [67]. Immunoprecipitation studies support this hypothesis as PDE4B2 is activated. The contribution of PDE4B2 to total PDE4 activity is not sufficient to explain the change in PDE4 activity recorded. This may reflect an artefact of immunoprecipitation where isoforms are stripped from their molecular partners, altering their constitutive function. Again MEK inhibition reduces the activation of PDE4B2 further supporting its contribution to the overall activation of PDE4 seen.

Section 5.2

Evidence for multi-molecular signalling complexes is accumulating [79]. Physical compartmentalisation of individual PDE4 isoforms may explain some of the differences between the response of PDE4B2 and PDE4D5 to LPS described above. This suggests differential activation of that ERK1/2 physically associated with PDE4B2, but not that associated with PDE4D.

Evidence for the incorporation of PDE4 isoforms in multi-molecular complexes is lacking. Yarwood et al demonstrated that RACK-1 binds PDE4D5 tightly [84] and RACK-1 was shown to be important in determining macrophage integrity [270]. Corsini et al have also shown that senility in murine macrophages could be overcome by replacing reduced RACK1 expression [230].

I next attempted to identify roles for PDE4B2 and PDE4D5 by demonstrating a direct physical relationship between PDE4 isoforms and components of the B-Raf – ERK 1/2 pathway and RACK 1.

5.2.1 PDE4B2 appears to co-immunoprecipitate with Phospho - ERK1/ERK2 and B-Raf

I attempted to demonstrate physical association between PDE4B2 and activated ERK1/2 by co-immunoprecipitation. I used PDE4B antiserum to isolate PDE4B2 and performed western blot analysis of the immunoprecipitate. These were probed with antibodies raised against the phosphorylated residues of activated ERK1 and ERK2. Figure 5.2.1.A shows that a band co-migrating with phospho-ERK2 appears associated with PDE4B2. As it is believed that the members of the MAPkinase signalling pathway form multimolecular complexes, I predicted that other members of this pathway should co-localise with

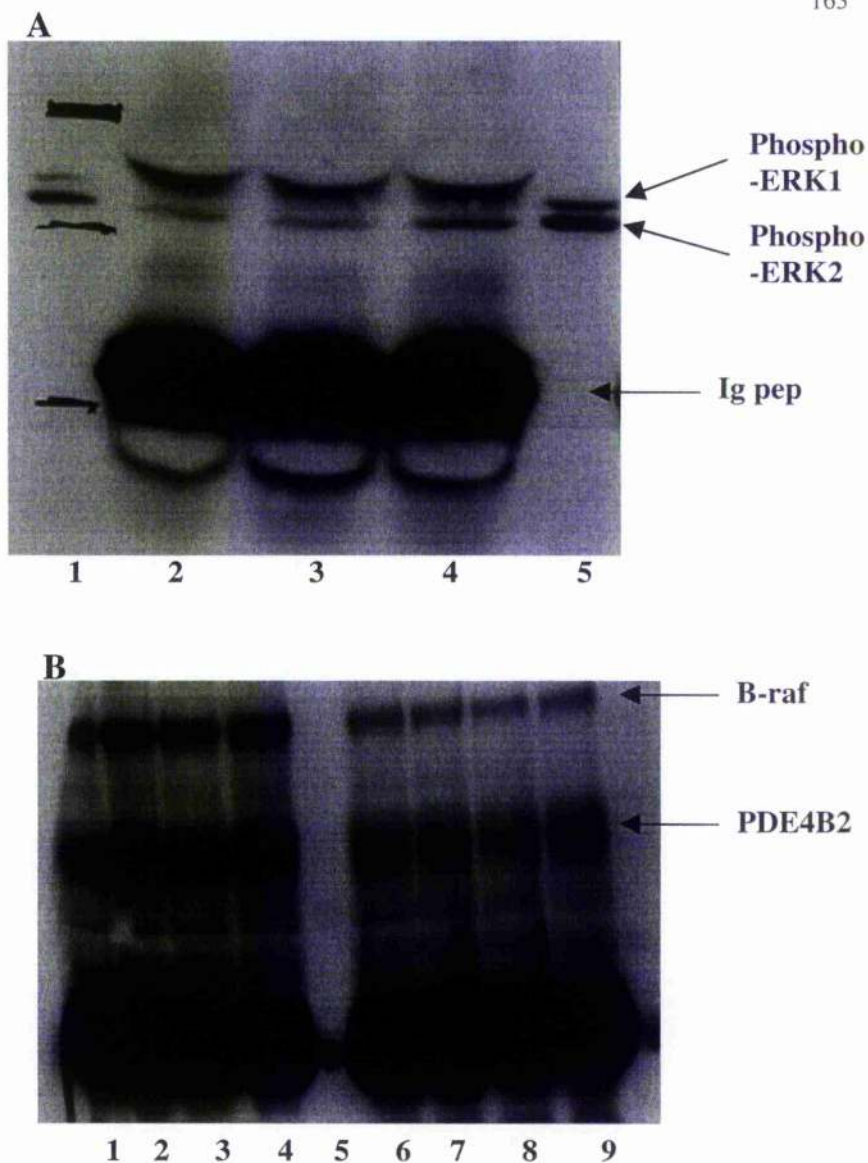


Fig 5.2.1 Co-immunoprecipitation of IP-Band signalling proteins of the ras-ERK1/2 pathway

Raw 264.7 cells treated with Ips for various times were lysed and Immunoprecipitation was performed from 1mg of lysate protein using antiserum raised against PDE4B (Schering, UK). Immunoprecipitates were resolved by SDS-PAGE. Immunobands were developed with antibodies raised against B-raf and phospho-ERK1/2 proteins. Fig 5.2.1A, ERK1/2: lane 1 molecular weight markers and ERK1/2 control; lane 2 IP-PDE4B from untreated cell lysate, lanes 3 and 4 IP-PDE4B from raw cells treated with Ips (10ng/ml) for 10 and 20 minutes respectively. Lane 5 positive ERK1/2 control. Fig 5.2.1B, B-raf blot. Lanes 1 - 4 immunoprecipitates from lysates of control and Ips treated RAW cells. Lanes 6 - 9 contain pre-clear 'pull-down'. It can be seen that although initially promising, the results of the pre-clear studies suggest non-specific association of B-raf and anti-serum is taking place.

PDE4B2. Figure 5.2.1.B demonstrates an equivalent immunoprecipitation experiment probed with antibodies against B-Raf. Unfortunately the right side of this blot shows B-Raf appearing in the Serum taken from pre-immunised rabbits that were subsequently used to raise the PDE4B antibody. Thus the validity of the co-immunoprecipitation studies is poor.

Despite altering the stringency of the washing stages of immunoprecipitation I was unable to produce conditions where B-Raf did not appear in the preclear supernatant.

5.2.2 Back phosphorylation of Immunoprecipitated PDE4B2

I used a back phosphorylation method to time the phosphorylation of PDE4B2. PDE4B immunoprecipitates were used as substrates for 'hot' phosphorylation studies using recombinant active-ERK2 and radiolabelled phosphate (^{32}P) as a label. PDE4B2 endogenously activated by phosphorylation will resist further phosphorylation and inactive PDE4B2 will be labelled. Figure 5.2.2 demonstrates that although a weak band corresponding to PDE4B2 can be made out, the degree of phosphorylation is too slight to distinguish it above background 'noise'.

5.2.3/5.2.4 PDE4D5 and RACK-1 in LPS treated RAW 264.7 cells

I investigated a physical association of PDE4D5 and RACK-1. Figure 5.2.3 demonstrates expression of both these molecules in RAW 264.7 cells. In each case high speed fractionation was performed and Fig 5.2.3A, demonstrates that PDE4D5 is distributed to all fractions with a greater proportion in the particulate than the cytosolic fraction. Figure 5.2.3B demonstrates that RACK-1 is excluded from the cytosolic compartment, with the majority being found in the nuclear fraction. To investigate if activation of Raw 264.7 cells altered RACK-1 or PDE4D5 distribution, they were treated with LPS for up to 30 minutes. Figure 5.2.4 shows that no significant shift of either protein from the P1 compartment to the S2 takes place within this time frame.

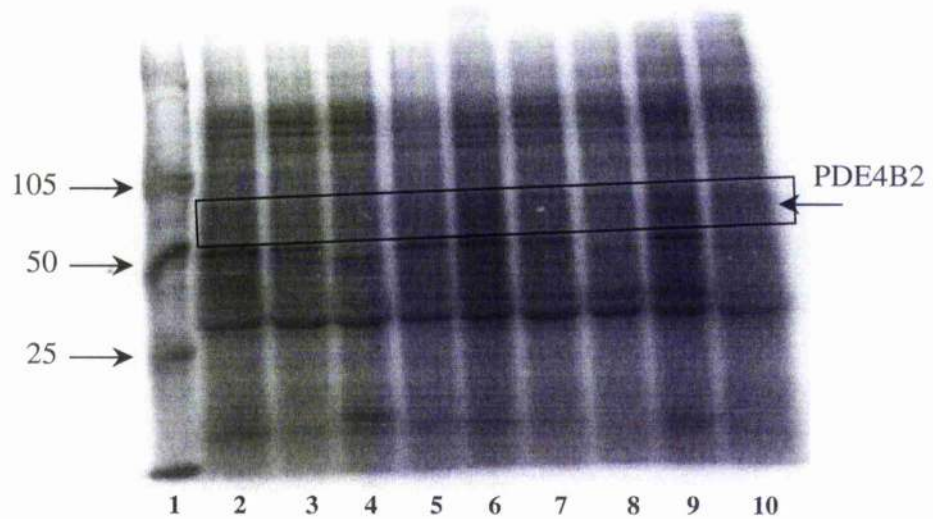


Fig5.2.2 Back phosphorylation of immunoprecipitated PDE4B2 from LPS treated RAW 264.7 cells

RAW 264.7 cells treated with LPS (10ng/ml) for a range of times were lysed and antiserum raised against PDE4B was used to immunoprecipitate PDE4B2 from lysates. Immunoprecipitates were incubated with recombinant active ERK kinase fragment in the presence of ^{32}P -ATP. Immunoprecipitates were resolved by SDS-PAGE, and acrylamide gels were transferred to a nitrocellulose membrane and exposed on a phosphoimager (Bio Rad LTD, UK). The resulting image is presented. Lane 1 phospho-markers, molecular weight markers (Amersham-Pharmacia); Lane 2 No treatment; Lanes 3-6 and Lanes 7-10, LPS 10ng/ml for 2, 5, 10 and 20 minutes respectively. The level of PDE4B2 is marked on the image, but as can be seen only a faint band is detectable. Insufficient protein is therefore present to make an estimate of the degree of phosphorylation compared to basal conditions.

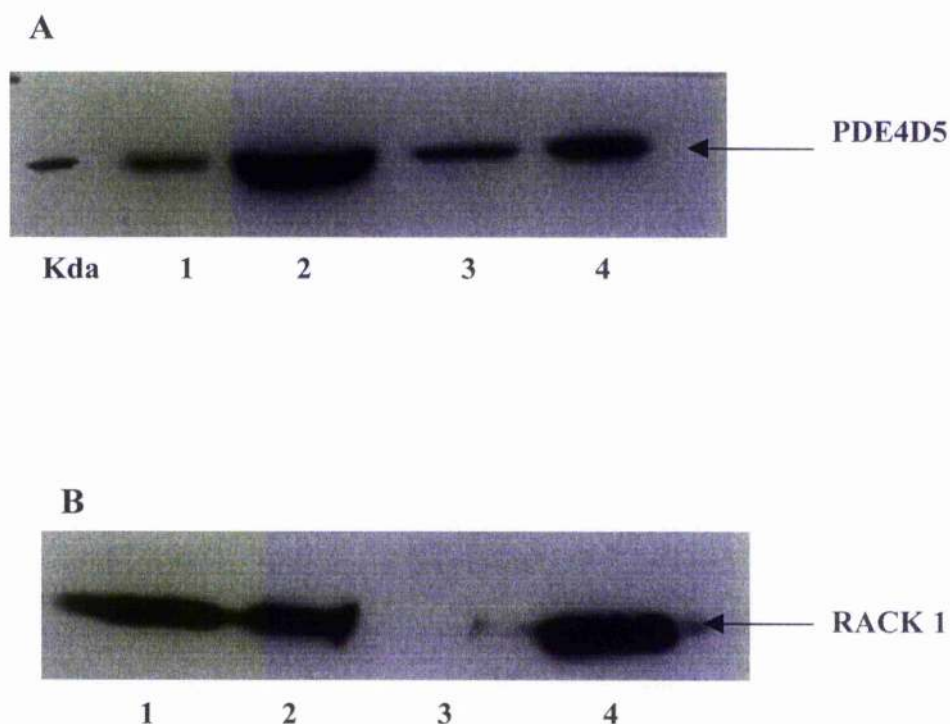


Fig 5.2.3 PDE4D5 shares a similar distribution as RACK 1 in RAW 264.7 cells

RAW 264.7 cells were harvested and subjected to high speed fractionation as described in materials and methods. Fractions were resuspended in equal volumes and PDE4D5 and RACK 1 were visualised by western blot analysis. Equal volumes of fraction, equivalent to 40 μ g S2 lysate protein, were loaded in each lane. Fig 5.2.3A PDE4D5: lane 1 +ve control; lane 2 P1 fraction; lane 3 S2 fraction and lane 4 P2 fraction. Fig 5.2.3B RACK 1: lane 1 +ve control; lane 2 P2 fraction; lane 3 S2 fraction and lane 4 P1 fraction. As can be seen the majority of both PDE4D5 and RACK 1 is distributed between the particulate fractions with a greater proportion in the P1 fraction. RACK 1 appears to be excluded from the S2 compartment while a small fraction of PDE4D5 appears here.

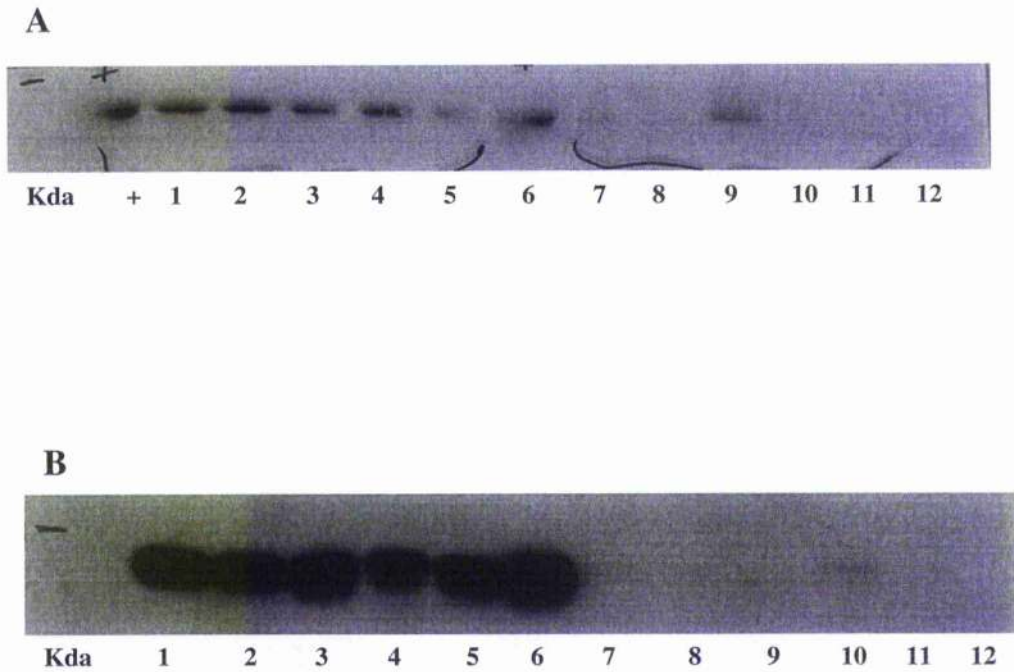


Fig 5.2.4 Activation does not affect PDE4D5 or RACK 1 distribution in RAW 264.7 cells

RAW 264.7 cells were incubated with 10ng/ml LPS for given time periods. Cells were subjected to high speed fractionation and PDE4D5 and RACK 1 were visualised in the S2 and P1 fractions, by western blot. Equal volumes of cell fraction were loaded on each lane, equivalent to 40 μ g of S2 protein. Fig 5.2.4A PDE4D5: lane + and 6 +ve control; P1 fraction lanes 1 - 5, lps 10ng/ml 0, 1, 5,10, 30 minutes respectively; S2 fraction lanes 7 - 11, lps 10ng/ml 0, 1, 5,10, 30 minutes respectively. Fig 5.2.4B RACK 1 P1 fraction lanes 1 - 6, lps 10ng/ml 0, 1, 5,10,15, 30 minutes respectively; S2 fraction lanes 7 - 12, lps 10ng/ml 0, 1, 5,10,15, 30 minutes respectively. No significant changes in distribution occurred with lps treatment. This does not rule out a translocation between particulate fractions.

Discussion Section 5.2

These studies were carried out in order to investigate PDE4B2 activation by ERK1/2 following LPS treatment of macrophages and to identify a role for PDE4D5 in macrophage activation. Although I was able to demonstrate physical association between PDE4B2 and both Erk 2 and B-Raf molecules, I also found these molecules associated with pre-immune Serum. Figure 1.3 illustrates that two ERK2 docking domains exist in PDE4D3. I predicted that direct association between long form PDE4 and ERK2 would take place. While this invalidates the experiment it does not refute the hypothesis that the molecules do associate. My next attempt to demonstrate 'back-phosphorylation' of immunoprecipitated PDE4B2 failed due to low signal-noise ratio. This probably reflects the low abundance of PDE4B2 isoforms in RAW 264.7 cells in common with most PDE4 isoforms. Again this unsuccessful experiment does not refute my hypothesis that ERK1/ ERK2 activates PDE4B2 and that this requires physical association. In order to demonstrate this activity I would have liked to develop stable RAW 264.7 cell lines over-expressing PDE4B2. By increasing the substrate for ERK 1/2, I would hope to improve the sensitivity of both these experiments. Unfortunately time restraints coupled with difficulty in successful transfection of these cells meant this work was not completed.

To demonstrate a role for PDE4D5 in activated RAW 264.7 cells I looked for co-localisation of PDE4D5 and the scaffold protein RACK-1. Both molecules localised to the nuclear compartments of lysed RAW 264.7 cells. RACK-1 was completely excluded from the cytosolic compartment. This co-localisation was exciting and led me to attempt co-immunoprecipitation experiments. Unfortunately this work was inconclusive. The nuclear distribution of RACK-1 in RAW 264.7 cells was intriguing as it has previously been described as a cytosolic protein [84]. One explanation for the nuclear distribution of PDE4D5 is stimulation by components of the serum in cell culture medium causing

proliferation of RAW 264.7 cells. To investigate this serum starvation of these cells was performed, however this failed to cause any change in the distribution.

Lipopolysaccharide is known to activate macrophages and inhibit proliferation. To see if LPS stimulation led to a shift of PDE4D5 or RACK-1 out of the nucleus RAW 264.7 cells were treated with LPS. While LPS did not increase the S2 content of either PDE4D5 or RACK-1 (Fig 5.2.4), a movement between the particulate compartments cannot be ruled out. To further clarify this I would have liked to measure the PDE4 content of each compartment over the time course. To further clarify the role of PDE4D5, I would have liked to treat RAW 264.7 cells with other activators of ERK1/ ERK2. It may be that restricted pools of ERK1/ ERK2 are activated by different agents. Valledor et al showed that timing of MAPKinase activation was linked to different outcomes [271]. Thus physical compartmentalisation of PDE4D5 and ERK1/ ERK2 means that different activators may lead to different PDE4 isoforms being affected and that different downstream effects may result.

As my attempts to clarify LPS' action on PDE4 were unsuccessful, I chose to investigate the result of PDE4 inhibition on cellular behaviour. Thus I measured RAW 264.7 inflammatory responses to LPS in the presence and absence of rolipram.

Section 5.3

Functional outcomes of PDE4 inhibition on LPS stimulated RAW cells.

5.3.1 PDE4 inhibition increases LPS stimulated iNOS expression

To assess what role PDE4 plays in regulating macrophage behaviour I examined the expression of various inflammatory mediators and proteins in the presence of rolipram. As

rolipram potently inhibits the production of TNF α in LPS stimulated macrophages and both TNF α and iNOS are described as being present in asthmatic airways I examined iNOS expression in the presence of rolipram. Figs 5.3.1A, demonstrates that iNOS expression is increased by PDE4 inhibition in the presence of LPS at a dose of rolipram between 10-50 μ m. To confirm that this was a PDE4 specific phenomenon, I compared the effect of cilostamide with rolipram. As can be seen in fig 5.3.1B, inhibition of PDE3 failed to increase the expression of iNOS to the same degree.

5.3.2 Indomethacin abolishes the increased iNOS expression

Next I co-incubated the stimulated RAW cells with indomethacin (100nM) to exclude a prostanoid driven cAMP effect. As can be seen in fig 5.3.2, Indomethacin abolished the increase in iNOS expression caused by rolipram.

5.3.3 Rolipram causes an increase in LPS stimulated COX-2 expression

Figure 5.3.3 shows that resting RAW 264.7 macrophages express little COX-2, but when exposed to LPS an immunoband corresponding to COX-2 appears. When the cells are co-incubated with rolipram and LPS this expression is dramatically increased. Fig 5.3.3 B & C shows rolipram's effect is dose dependent.

5.3.4/5.3.5 Rolipram enhanced COX-2 expression is resistant to indomethacin and results in increased PGE2 production

COX-2 expression is under partial cAMP control. To exclude a positive feedback of PGE2 derived cAMP on COX-2 I included indomethacin in the medium. Fig 5.3.4 demonstrates that the increased COX 2 expression occurs despite the presence of indomethacin (100nM). Rolipram appears to be exerting a direct effect on COX-2 transcription. To ensure that the effect of rolipram on LPS induced COX 2 expression was translated into a

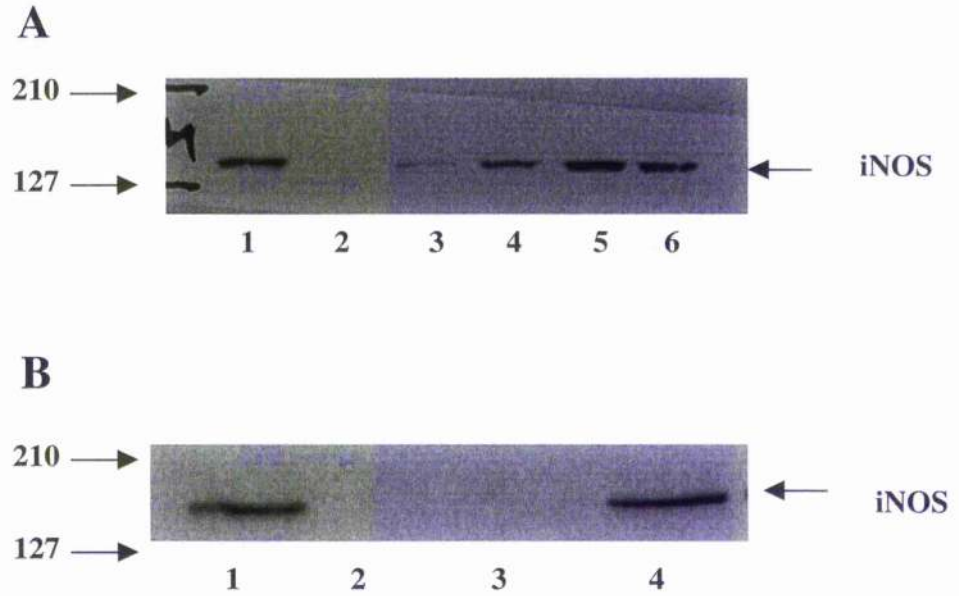


Fig 5.3.1 Rolipram enhances the transcriptional activation of iNOS by LPS in RAW 264.7 cells.

Raw 264.7 cells were incubated for 16 hours in serum free DMEM with LPS (10ng/ml) with or without rolipram or cilostamide. Cells were lysed and western blots prepared from these cell lysates were probed with iNOS monoclonal antibody. Equal amounts of protein were loaded in each lane. Fig 5.3.1A Lane 1 +ve, Lane 2 - 6 LPS + rolipram 0.1 μ M, 1 μ M, 10 μ M, 100 μ M, 1mM respectively. This experiment clearly showed the dose dependent increase in iNOS expression that occurred when rolipram was co-incubated with LPS in RAW cell cultures. Fig 5.3.1B. Lane 1 +ve control, Lane 2 Rolipram 10 μ M alone, Lane 3 cilostamide 2 μ M alone and Lane 4 LPS + cilostamide 2 μ M. This data demonstrates that neither rolipram or cilostamide alone is capable of causing the transcription of iNOS alone in serum free medium. Cilostamide, a PDE3 inhibitor, does not enhance LPS stimulated iNOS expression similar to Rolipram.

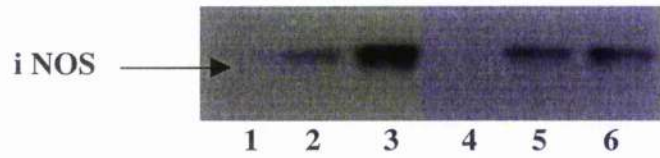


Fig 5.3.2 Indomethacin reduces rolipram's augmentation of iNOS expression in the presence of lps.

Raw 264.7 cells were incubated in the presence of LPS, rolipram(10 μ M) and indomethacin (100nM). Cells were lysed and equal amounts of protein were resolved by SDS-PAGE. Nitrocellulose membranes were immunoblotted using antiserum raised against iNOS. Lane 1 no treatment, lane 2 lps alone, lane 3 lps + Rolipram. Lanes 4 - 6 as lanes 1 - 3 with the addition of indomethacin. While rolipram enhances LPS iNOS expression the addition of indomethacin abolishes the increase in iNOS expression caused by rolipram.

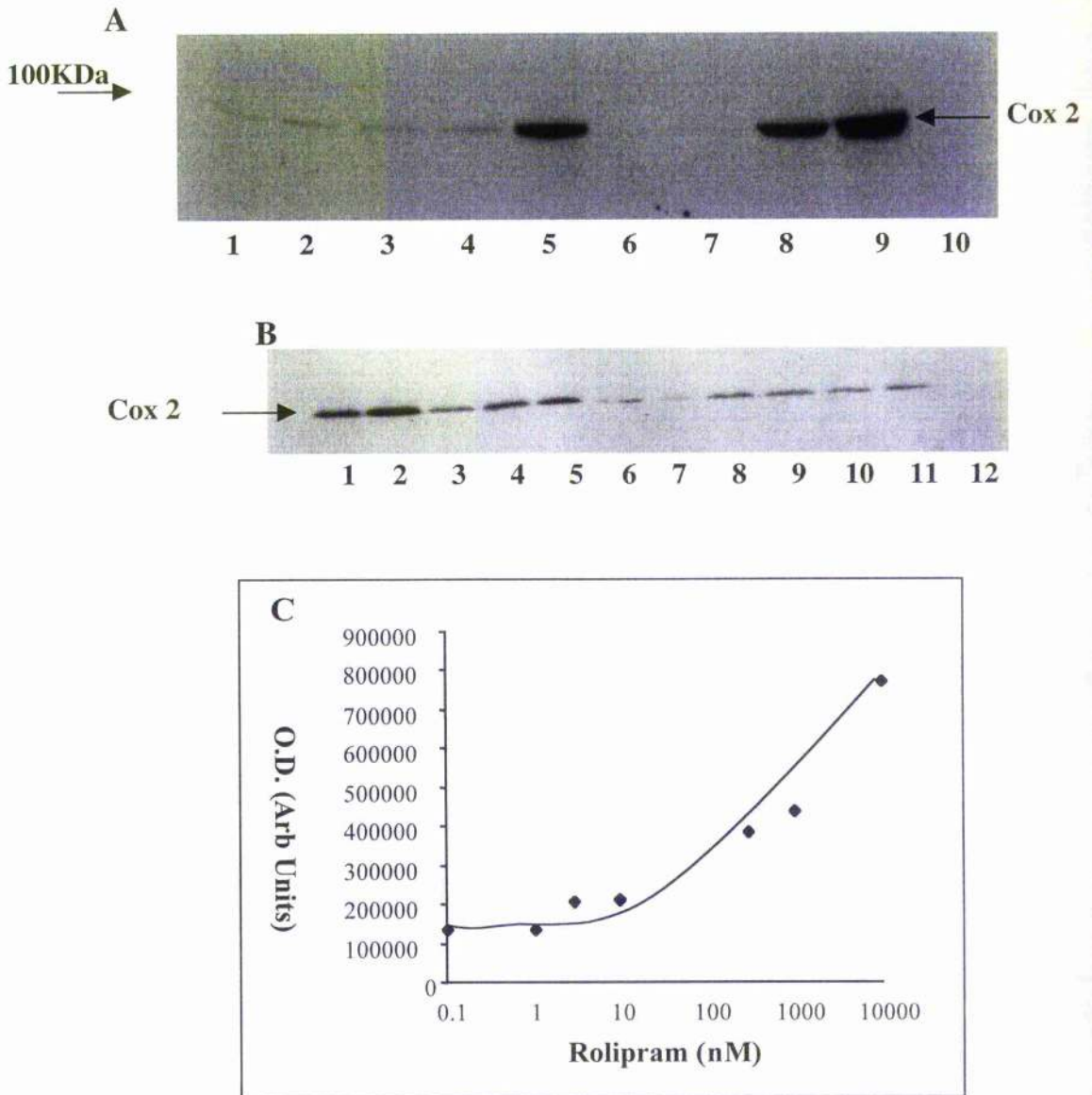


Figure 5.3.3 Rolipram but not cilostamide increases LPS stimulated cox-2 expression.

Raw cells were incubated with LPS (100ng/ml) +/- a range of rolipram concentrations, +/- cilostamide 10 μ M +/- forskolin 100 μ M. Cell lysates were prepared and subjected to western blot analysis with 40 μ g of protein loaded in each lane. Blots were probed with monoclonal antibody raised to COX-2. Fig 5.3.3A, Rolipram does not cause COX-2 expression and enhances LPS induced COX-2 expression. Cilostamide has no effect on LPS mediated COX-2 expression. Forskolin, does not mimic the effects of rolipram alone. (lane 1 no treatment, lanes 2-4 rolipram 1 μ M, 5 μ M and 10 μ M respectively, lane 5 LPS 100ng/ml, lanes 6-7 cilostamide 1 μ M and 10 μ M respectively, lane 8 LPS + cilostamide 10 μ M, lane 9 LPS + rolipram 10 μ M, lane 10 forskolin 100 μ M). Fig 5.3.3B Rolipram increases LPS stimulated COX-2 expression in a dose dependent manner. (lanes 1 to 10 LPS 100ng/ml + rolipram 30 μ M, 10 μ M, 3 μ M, 1 μ M, 0.3 μ M, 0.1 μ M, 0.03 μ M, 0.01 μ M, 0.003 μ M, 0.001 μ M, respectively. Lane 11 LPS 100ng/ml, lane 12 no treatment). Fig 5.3.3C Band intensity was measured from representative blots illustrated in fig 5.3.3B and a graph of intensity against Log₁₀ rolipram concentration was plotted.

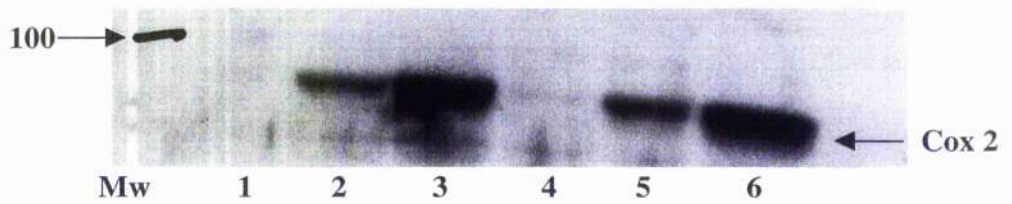


Figure 5.2.4 Rolipram enhances COX-2 expression in an indomethacin resistant fashion

Raw 264.7 cells were incubated for 16 hours in the presence or absence of LPS (100ng/ml) +/- rolipram (10 μ M) +/- indomethacin (100nM). Cell lysates were prepared and equal quantities of protein were resolved by SDS-PAGE. Immunobands were visualised using antiserum raised against COX-2. Lane 1 no treatment, lane 2 LPS alone, lane 3 LPS + rolipram, lane 4 indomethacin alone, lane 5 LPS + indomethacin, lane 6 LPS + indomethacin + rolipram. This figure demonstrates that the enhanced expression of COX-2 by rolipram does not represent an exaggeration of a autocrine feedback loop by PGE₂.

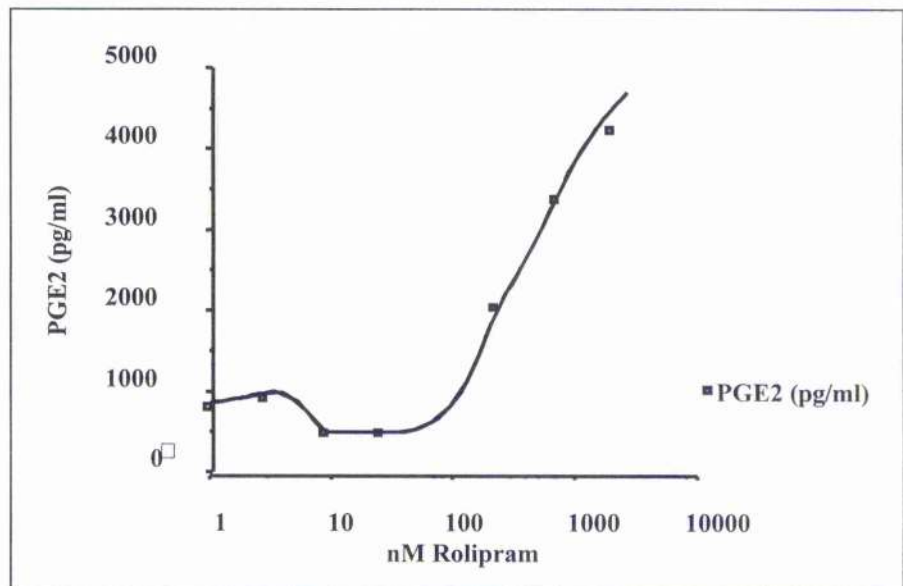


Fig 5.2.5 Rolipram dose dependently increases PGE₂ production by RAW 264.7 macrophages.

Raw 264.7 cells were incubated with LPS and rolipram in increasing concentrations for 16 hours. PGE₂ EIA was performed on cell free medium. Rolipram causes a dose dependent increase in PGE₂ production.

functional effect I demonstrated an increase in PGE₂ production. Fig 5.3.5 clearly shows a dose dependent increase in PGE₂ production when macrophages are activated by LPS in the presence of rolipram.

5.3.6 Indomethacin does not alter the ability of rolipram to inhibit TNF α .

COX-2 derived PGE₂ could exert anti-inflammatory activity and partially explain rolipram's negative control of TNF α . Fig 5.2.6 demonstrates that Raw 264.7 cells produce large amounts of TNF α when activated by 10ng/ml LPS. Rolipram reduces this significantly, confirming that my model system behaves in a similar fashion to other groups'. Indomethacin introduced to the system has no significant effect on the ability of rolipram to inhibit TNF α production, implying that this effect is not driven by PGE₂.

Discussion Section 5.3

PI3K is believed to have pro-inflammatory activity by virtue of its ability to reduce intracellular cAMP and the anti-inflammatory activity of rolipram. I have demonstrated increases in iNOS and COX-2 expression in the presence of rolipram. This apparently paradoxical work suggests that NO and PGE₂ may exert anti-inflammatory behaviour. Increasing evidence supports this view and my work offers further explanations for rolipram's anti-inflammatory role [167, 244, 272, 273]. Several groups have shown these proteins to be under transcriptional control by cAMP [274] although both transcriptional activation and repression have been reported [275]. Inducible nitric oxide synthase regulation by rolipram was secondary to COX-2 activation, suggesting either PGE₂ or TXA₂ increases iNOS expression. Thus, COX-2 causes a PGE₂ autocrine activation of adenylyl cyclase and cAMP production. In the presence of rolipram this cAMP is enhanced and a powerful signal to iNOS expression is produced.

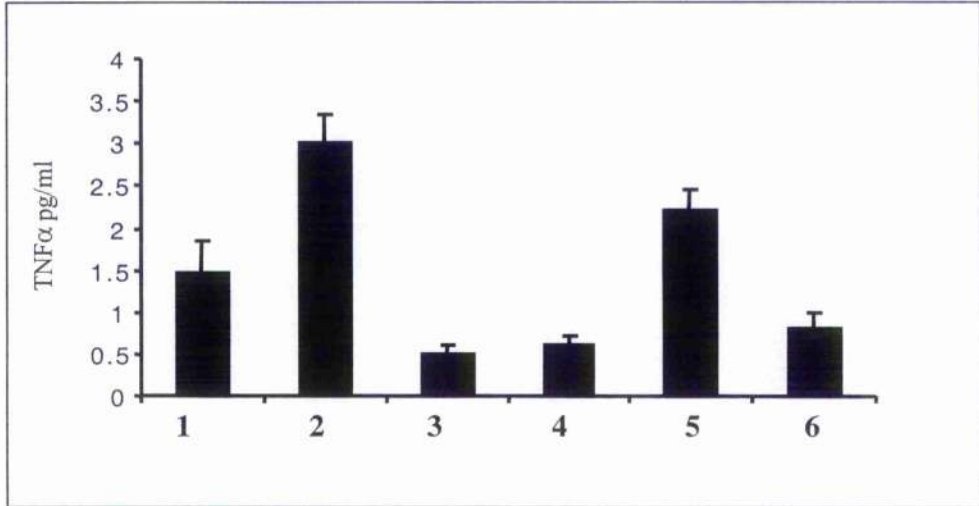


Fig 5.3.6. Indomethacin does not prevent rolipram inhibiting LPS induced TNF α in RAW macrophages.

RAW cells were cultured as described in the presence of LPS, rolipram 10 μ M and indomethacin (100nM). Cell free medium TNF α content was measured by ELISA. Column 1 no treatment, column 2 LPS 10ng/ml, column 3 LPS + rolipram, column 4 indomethacin alone, column 5 LPS + indomethacin and column 6 LPS + indomethacin + rolipram. As can be seen rolipram powerfully inhibits LPS stimulated TNF α production. While indomethacin appears to slightly reduce TNF α production from LPS stimulated macrophages, it has no significant effect on rolipram.

The indirect effect of rolipram on iNOS through COX-2 is reminiscent of its reported indirect effect on TNF α through IL-10. I have demonstrated that indomethacin did not affect the increased expression of COX-2 in the presence of rolipram. Rolipram appears to affect the expression of COX-2 in the absence of an additional positive cAMP stimulus. This suggests that PDE4 normally exerts a negative regulatory effect on COX-2 expression following LPS stimulation. Rolipram may then act in this circumstance by elevating cAMP slightly, possibly in a local region of the cell, or simply preventing the negative effect of increased PDE4 activity following LPS stimulation. PDE4 activity increases then falls following LPS exposure, lowering cAMP then restoring it. This dip could allow cAMP inhibited signals to propagate transiently. The effect of rolipram on COX-2 expression is not therefore straight forward and requires further investigation. It is of note that cilostamide did not cause the same effect on iNOS expression as rolipram, which may seem unlikely given a non-PDE source of cAMP such as PGE2. I propose that the reduction in PDE3 activity seen with LPS treatment leads to the abolition of any PDE3 inhibitor activity.

In view of the increase in PGE2, a cAMP elevating stimulus, following rolipram I hypothesised that PGE2 might be responsible for TNF α inhibition. Figure 5.3.6, clearly demonstrates that COX-2 activity is not responsible for TNF α inhibition by rolipram in RAW cells. The precise role of cAMP in regulating TNF α production is not clear, with some groups disputing IL-10's role and suggesting a post-translation effect instead. The anti-inflammatory behaviour of PGE2 and rolipram requires further investigation.

Section 5.4

LPS is a powerful activator of ERK1/2, a signal transduction pathway that is characteristically inhibited by cAMP. I was surprised by the apparent ability of rolipram to increase LPS signalling in terms of COX-2 expression. I hypothesised that rolipram, by

increasing cAMP was enhancing the signal transduction cascade downstream of LPS. This counter-intuitive theory suggests that differential activation of signal transduction elements could take place. I chose to investigate rolipram's effect on LPS activation of the ERK1/ERK2 family of molecules.

5.4.1 LPS activates a restricted pool of ERK 1/2 in RAW cells

To confirm that LPS activated MAPkinase I stimulated RAW cells with various activators of ERK1/2. Using monoclonal antibodies raised against the phosphorylated residues of activated ERK 1/2 I compared immunoblots of activated versus total ERK 2. Fig 5.4.1 shows the effects of different compounds on ERK-1/2 phosphorylation. As can be seen PMA causes a substantial and early (1 minute)s activation of ERK 2 while TNF α and LPS cause a sequentially less profound and delayed activation.

5.4.2 Rolipram increases the phosphorylation of ERK 2 over LPS alone

I measured the effect of LPS on ERK-2 phosphorylation in the presence and absence of rolipram. Fig 5.4.2 shows that the presence of rolipram leads to an earlier and more profound phosphorylation. Fig 5.4.2, B uses figures derived from densitometry to calculate the effect of rolipram on the activation of ERK 2.

5.4.3 Rolipram activates CREB in an H89 sensitive manner

So far I have demonstrated apparently paradoxical effects of rolipram on RAW 264.7 cells. To confirm that PDE4 inhibition can function in a classical manner in these cells, I examined the role of rolipram on the transcription factor CREB. CREB activation conforms to its phosphorylation status, and fig 5.3.4 demonstrates that rolipram increases CREB phosphorylation in a PKA dependent manner.

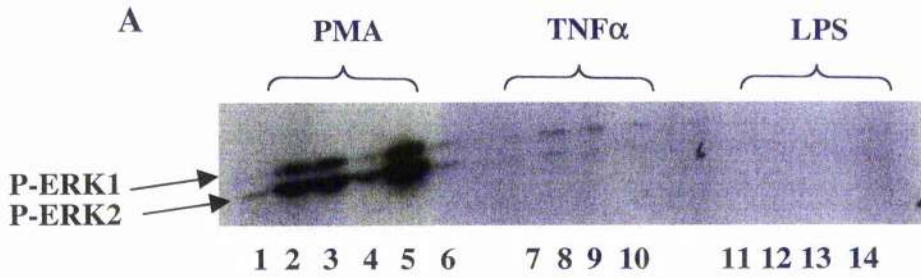
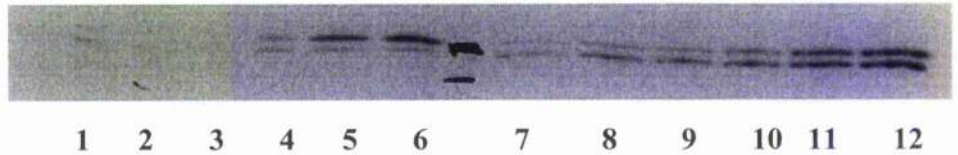


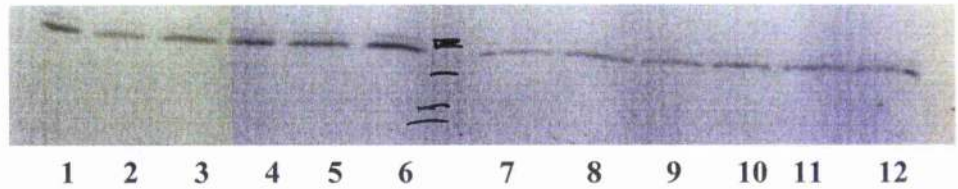
Fig 5.4.1 Different compartments of ERK1/2 are activated by different stimulators of RAW 264.7 cells

Raw 264.7 cells were incubated in the presence of three different agents for varying lengths of time. Lysates were prepared and equal quantities of lysate protein were resolved by PAGE and subjected to western blot analysis. Immunodetection of activated ERK 1/2 was achieved using phospho-ERK1/2 antibodies. Lanes: Lanes 1, 7 and 11, no stimulation; Lanes 2 - 5 PMA 4 μ M for 1, 3, 5 and 10 minutes; 8 - 10 TNF α 10 μ M 5, 10 and 20 minutes; lanes 12 -13 LPS 10ng/ml 5, 10 and 30 minutes. As can be seen while all agents are known to activate ERK 1/2, they do so in different time frames and to different degrees.

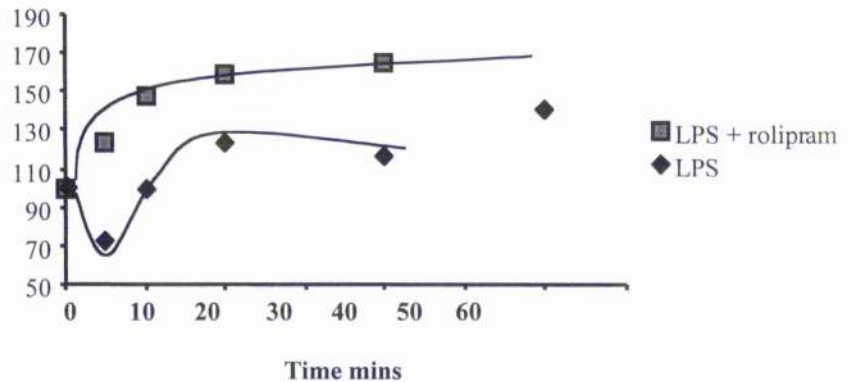
A



B



C



D

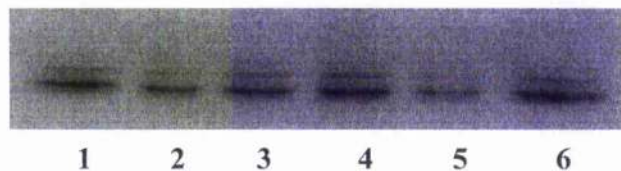


Fig 5.4.2 Effect of rolipram on LPS induced ERK 1/2 phosphorylation.

Raw 264.7 cells were incubated with LPS (10ng/ml) with (lanes 7-12, 40 μ g protein per lane) or without (lanes 1-7 60 μ g protein per lane) rolipram 10 μ M, for various times. Lanes 1 + 7 0 minutes, lanes 2 + 8 5 minutes, 3 + 9 10 minutes, 4 + 10 20 minutes, 5 + 11 40 minutes, 6 + 12 60 minutes. As can be seen LPS causes the phosphorylation of ERK1 by 20 minutes. In the presence of Rolipram, however this activation event occurs more rapidly and to a greater degree. The effect is particularly marked in ERK2. Fig 5.3.2.B shows ERK1 staining to demonstrate protein loading. Slightly more protein was loaded in the lanes without rolipram to allow a reasonable visualisation. This would be inclined to bias the experiment against showing any significant difference with rolipram. Fig 5.3.2.C, shows the results of this experiment subjected to densitometric analysis (n=2). This data confirms the more rapid and greater phosphorylation that occurs in the presence of rolipram. Fig 5.3.2.D Demonstrates that no effect on ERK phosphorylation was seen in the presence of rolipram alone, (lane 1 ctrl, lanes 2 - 6, 5, 10, 15, 20 and 25 mins respectively).

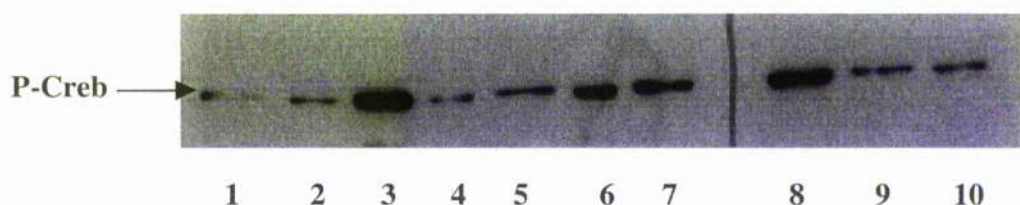


Fig5.4.3. LPS phosphorylates CREB in a MEK dependent manner, while rolipram acts through PKA.

Raw cells were treated with various compounds and the cell lysates were subjected to western blot analysis, using an antibody raised against the phosphorylated residue of activated CREB transcription factor. Lane 1 no treatment, Lane 2 LPS 10ng/ml, Lane 3 LPS + rolipram 10μM, Lane 4 LPS + rolipram + H89 10μM, Lane 5 LPS + H89, Lane 6 rolipram alone, Lane 7 cilostamide 10μM alone, Lane 8 cilostamide + LPS + H89, Lane 9 LPS + UO126 10 μM and Lane 10 UO126 μM alone. This data shows that LPS causes phosphorylation of CREB in a UO126 sensitive fashion. This confirms Cohen et al's work, that demonstrated MSK dependent activation of CREB. In their hands H89 inhibited MSK, but here H89 did not affect LPS phosphorylation of CREB. On the other hand H89 did reduce the marked phosphorylation caused by rolipram in the presence or absence of LPS. This suggests firstly that rolipram is capable of activating Pka in RAW cells, but also that a basal level of PDE4 activity is generally controlling the level of intracellular cAMP.

Discussion Section 5.4

To demonstrate that ERK1/2 can be differentially activated in RAW 264.7 cells I used various agonists, chosen to elicit different functional effects. Valledor et al working with RAW 264.7 cells demonstrated the outcome of ERK1/2 activation varied with the timing [271]. While M-CSF, PMA, GM-CSF and IL-3 cause proliferation of macrophages and induce a very rapid (5min) maximal activation of ERK1/2, LPS reduced proliferation with a slower (15min) peak activation. It is interesting to speculate if this differential response depends on spatial as well as temporal compartmentalisation. I confirmed this using phosphorylation of ERK1/2 as a surrogate marker of ERK 1/2 activation. Thus LPS treatment of resting RAW 264.7 cells causes delayed activation of a restricted pool of ERK1/2 when compared to PMA, consistent with its recorded anti-proliferative activity. Such differential activation supports the notion of compartmentalised pools of signalling molecules. Next I demonstrated that rolipram alters the manner in which ERK activation occurs. Thus in the presence of rolipram phosphorylation occurred earlier and to a greater degree than in its absence. If differential ERK activation affects cell behaviour differently then rolipram would alter the response to LPS and may suggest a mechanism for some of the anti-inflammatory effects seen with rolipram.

Having demonstrated a number of unexpected effects of rolipram on RAW 264.7 cell function I ensured that more 'classical' activity was taking place. I measured the effect of elevating cAMP by rolipram on the phosphorylation of the transcription factor CREB. I demonstrated H89 inhibited this pathway and thus confirmed that the mechanics of 'classical' cAMP signalling were present in RAW 264.7 cells.

Section 5.5

PDE4 inhibition led to increased COX 2 expression and altered ERK1/2 activation I next looked for a mechanism to explain these effects. A new GEF called EPAC has recently been described that allows cAMP to activate the small G protein Rap-1[276]. Rap-1 has been controversially reported to cause ERK 1/2 activation by B-Raf [277]. Rap-1 has been shown to be important in macrophage behaviour, with Carron et al showing a role in macrophage response to β -integrin binding [204]. Using activation and regulation mutant forms of Rap-1 transfected into RAW 264.7 cells I looked for changes in inflammatory mediator production.

5.5.1 Successful transfection of RAW 264.7 cells using Superfect (Qiagen)

Attempts to transfect RAW 264.7 cells using the DEAE/Dextran method proved difficult and I used the Superfect (Qiagen) system to successfully express the Rap-1A mutants. Figure 5.5.1 demonstrates that although transfection efficiency varies between mutants, each transfection expresses more Rap-1A than mock transfected cells.

5.5.2 Over expression of Rap-1A activation mutants does not alter rolipram inhibition of LPS-stimulated TNF α

To investigate if rolipram activates Rap-1A to inhibit LPS stimulated TNF α production, I created temporary transfections of mutant Rap1 constructs in RAW 264.7. These have previously been described [204] and are designed to represent the conformation of active (GTP-bound, Ser12/Val mutation) or constitutively inactive (Dominant negative, GDP-bound, Thr17/Asn mutation) Rap1 conformations. Cells were treated with 10ng/ml LPS in the presence and absence of 10 μ M rolipram. I measured the TNF α production in each case. Fig 5.5.2 suggests that constitutively active Rap-1A transfects produced less TNF α .

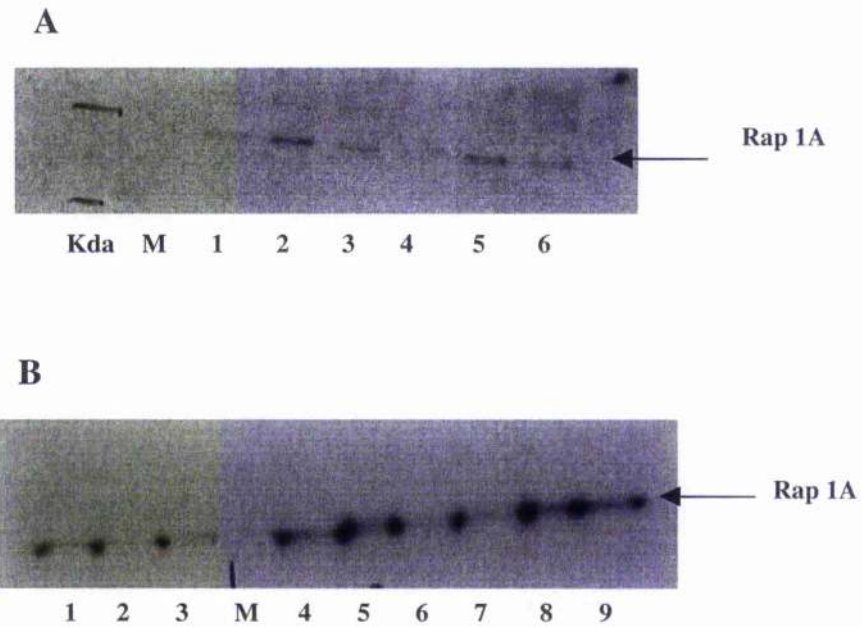


Fig 5.5.1 Success of superfect transfection of RAW 264.7 cells

Raw 264.7 cells were transfected using the superfect method (Qiagen). Activation and PKA phosphorylation mutants of rap-1A were prepared and transfected. Equal quantities of cell lysate were loaded on each lane and resolved by PAGE. Immuno-detection of recombinant Rap1 was achieved using antisera raised against Rap1 protein. M=Mock transfections. Fig 5.5.1.A: lanes 1 and 4, Wild type; lanes 2 and 5, Dom Neg; lanes 3 and 6, Cons Active. Fig 5.5.1.B: Lanes 1-3, Wild type; lanes 4-6 Aspartate mutants; lanes 7-9, Alanine mutants. As can be seen transfection efficiency varied between cells, but in each case rap-1A expression in transfected cells exceeded non-transfected 'mock' cells. (Dom Neg, dominant negative mutation, Cons Act, Constitutively active, Aspartate mutants, Alanine mutants)

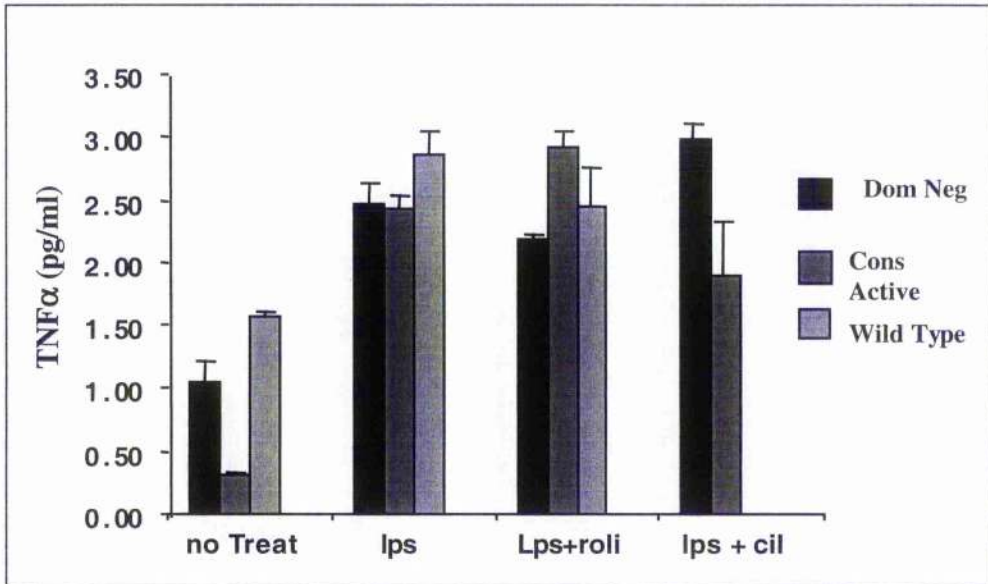


Figure 5.5.2 *Rap-1A* activation mutants alter the effect of rolipram on *lps* induced $TNF\alpha$ production

Raw 264.7 cells transfected with *Rap-1A* activation mutants were treated with 10ng/ml *lps* and the $TNF\alpha$ production was measured in cell free medium by ELISA. Cons Active = Constitutively active: Ser12/Val mutation; Dom Neg = Dominant negative: Thr17/Asn mutation. As can be seen constitutively active mutants led to reduced $TNF\alpha$ production at base. No significant differences were seen* between the different mutants in terms of *lps* or rolipram on $TNF\alpha$ production. Note in all transfections the inhibitory effect of rolipram was lost by transfection. No difference was seen with cilostamide 10 μ M (Cil). (*Paired T test of differences between treatment groups and control).

than controls in a resting state. No significant difference was seen, however between different activation mutants when treated with LPS. In each case a substantial increase in TNF α was found. Rolipram failed to inhibit LPS stimulated TNF α in any of the cells regardless of the mutant form transfected. I have previously shown a significant reduction of TNF α production in the presence of rolipram and these data suggests that transfection itself may subvert the mechanics of rolipram inhibition.

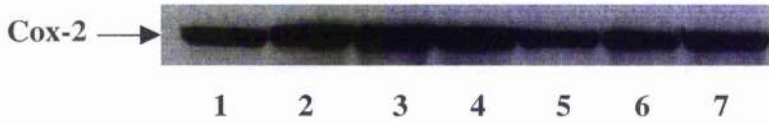
5.5.3 Over expression of Rap-1A activation mutants affects rolipram induced increase in COX-2 expression and PGE2 production

Next I used the same transfects and measured PGE2 production and COX-2 expression when LPS was administered in the presence and absence of rolipram. Fig 5.5.3 shows that dominant negative rap-1A appears to abolish the effect of LPS on these cells. When transfected with constitutively active mutants LPS was able to cause an increase in PGE2 production but no additional effect of rolipram was seen. In wild type transfects LPS effects were abolished, but rolipram caused activation of the COX-2 gene. In each transfection no significant difference was seen in the level of COX-2 protein expression. There was greater expression of COX-2 between transfected cells and mock transfected.

5.5.4 Protein Kinase A activation mutants effect on TNF α production in LPS stimulated RAW 264.7 cells

As the effects of Rap-1A activation mutants were equivocal, I reasoned that cAMP may involve Rap-1A by the more classic PKA route. Our laboratory had previously made constructs of Rap-1A mutated at the PKA phosphorylation domains. Thus a Ser180/Asp has a 'phosphorylated' conformation while a Ser180/Ala results in a 'non-phosphorylated

A



B

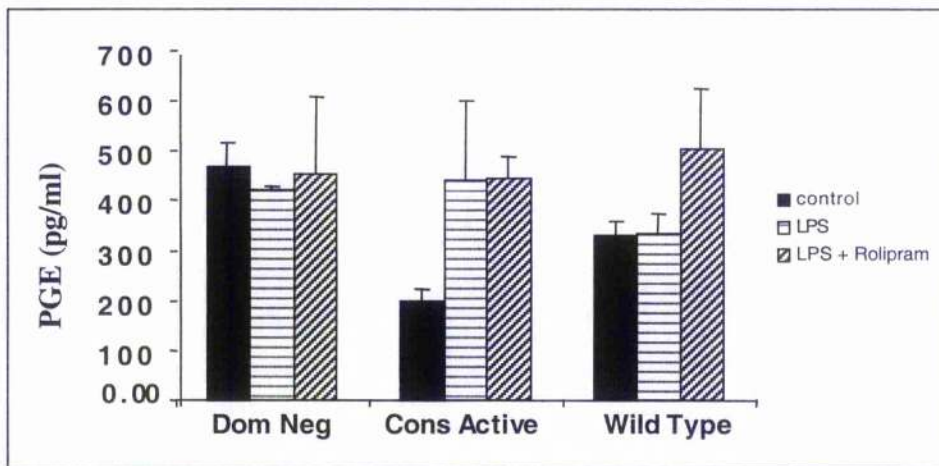


Fig 5.3.3 Effect of RAP-1 activation mutants on COX - 2 expression and PGE2 production by LPS stimulated RAW cells.

Raw 264.7 cells were transfected with various RAP-1 activation mutants. (Dom Neg, Dominant Negative Thr17/Asn; Cons Active, Constitutively active Ser12/Val.) Fig 5.3.4A. Western blot analysis of equal protein quantities for COX-2 expression when various activation mutants are treated with lps (10ng/ml) and rolipram 10 μ M. (Lanes 1+5 mock transfection, 2+ 6 wild type, 3 constitutively active, 4 wild type, 7 dom neg.) Fig 5.3.4B, PGE2 production from various treatments of the above transfected RAW cells. No consistent patterns are seen. No significant effect of either lps or Rolipram are evident. This data may suggest an important role for RAP-1 or may illustrate experimental difficulties when using transfected cell models.

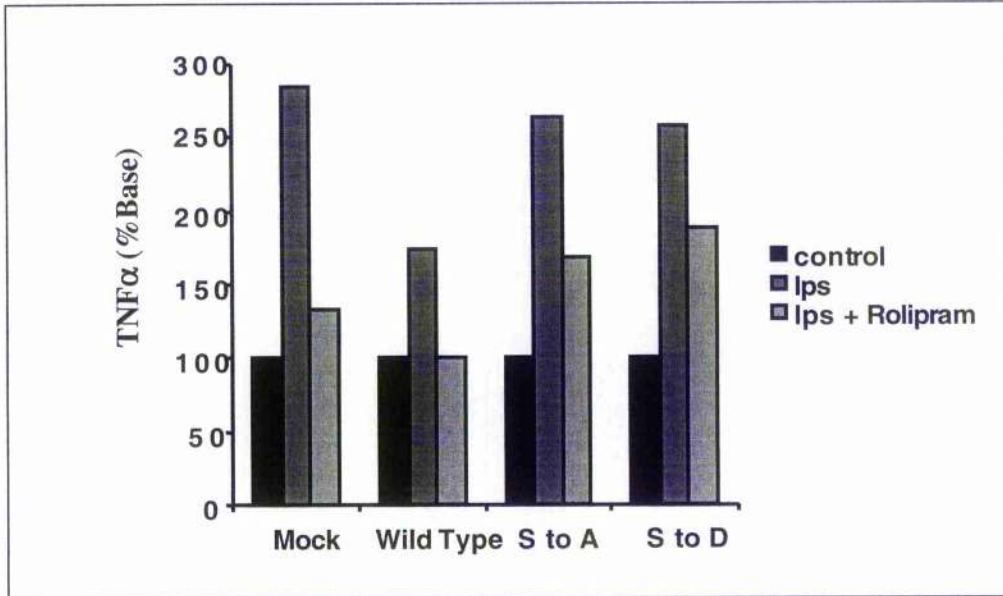


Figure 5.5.4 Rap-1A PKA phosphorylation mutants effect on lps stimulated TNF α production

Raw 264.7 cells were transfected with rap-1A mutated for the PKA phosphorylation domains. Wild type represent non-mutated over-expressed Rap-1A, S to A, Ser180/Asp activation mutants and S to D, Ser180/Ala phosphorylation negative mutants. Cells were treated with 10ng/ml lps and TNF α was measured in cell free culture medium by ELISA. As can be seen wild type rap-1A transfects behave similarly to non-transfected cells. In both the gain of function and loss of function mutants lps behaved normally, however rolipram did not inhibit this effect to the same degree.

non-phosphorylatable' mutant. I made RAW 264.7 cell transfects over expressing these mutants and treated them as above. Fig 5.5.4 shows the effect of rolipram in mock transfections to be maintained with a significant reduction in $\text{TNF}\alpha$ production. The effect of PKA mutants however is again less clear. While the peak $\text{TNF}\alpha$ produced by wild type transfects is muted, the effect of rolipram is retained, suggesting transfection alone may alter LPS signalling.

Discussion Section 5.5

I decided to investigate the role of the novel cAMP signalling pathway EPAC-Rap1A in transducing rolipram's effects in macrophage inflammation. There are two strategies available to measure Rap-1A activity in cells. Firstly activated Rap-1A is a powerful ligand for its partner ral in a GTP bound form (ral-GDS). Ral GDS can be synthesised in fusion with GST allowing Rap-1A to be 'fished' out of lysate using this construct as 'bait'. Several reports have suggested difficulty with this technique in immune cells [278]. The other technique relies on G-protein's being activated by conformational change when bound to GTP. This active conformation can be mimicked by mutation and thus conformationally active and in-active forms can be made for most G proteins. Over expressing these mutants and measuring the effects biochemically in comparison to each other allows some inferences to be drawn. Our lab received mutant forms of Rap-1A as a gift from J. Bos et al, and we made a Series of PKA domain mutants by Quickchange (Qiagen). I successfully developed a method of transfecting these immune cells that have traditionally been difficult to manipulate.

I have not seen consistent effects of Rap 1A mutants on either LPS or rolipram's effect on RAW 264.7 cells. If rolipram functioned through Rap-1A I would expect constitutively active mutants to cause a diminished response to LPS and an exaggerated response to rolipram. Thus LPS would cause a smaller $\text{TNF}\alpha$ effect and a larger COX-2/PGE2 effect.

On the other hand dominant negative Rap-1A mutants should take the brake off TNF α production and prevention of rolipram inhibition. Neither of these effects was consistently seen.

There are several possible methodological problems with my strategy. Firstly transfection efficiency varied between experiments. I attempted to split all transfections into triplicates 24 hours before treatment to avoid internal variation of transfection efficiency. Adjusting for Rap-1A expression based on western blot density did not alter the results. Transfection efficiency is less than 100%. This means normal cells remain that are capable of normal responses to LPS and rolipram. If these normal cells constitute a large proportion of the population any effects of mutant transfection will be swamped. My data does not conclude that this is occurring, as the effects seen in transfected cells do not match that seen in mock transfections. To avoid this problem in the future, pure stable cell lines should be created using cytotoxic selection strategies to produce pure strains of over-expressing cells.

Transfection of foreign material into a cell can be a toxic procedure to cells. Cells responses vary, but a pro-inflammatory effect in macrophages would not be surprising. Such a response would certainly invalidate my data. Including mock transfections, positive and negative controls partially get round this problem but not entirely.

Conclusion

I have extended my studies of PDE4 in macrophage cells by investigating biochemical and functional roles of PDE4 isoforms and PDE4 inhibition. I have demonstrated increased PDE4 activation following LPS stimulation of RAW cells. The complex signalling mechanisms activated by LPS make this global effect on PDE4 difficult to interpret. Certainly the effects of signalling inhibitors suggest that constitutive activation of PDE4 occurs in RAW cells and thus changes to total PDE4 activity is likely to reflect the balance

of activation and de-activation of individual isoforms. I have shown that PDE4B2 is activated by LPS stimulation and MEK inhibitors reduce that this. This agrees with Wang et al, who showed PDE4B2 to be the key isoform regulating monocyte behaviour in ex-vivo cells[253]. Unfortunately I have not been able to consistently demonstrate a physical association between PDE4B2 and members of the MAPKInase signalling pathway.

Rolipram is an anti-inflammatory compound and its behaviour varies with its ability to cleave cAMP and I have demonstrated two new anti-inflammatory behaviours. Firstly in the presence of rolipram LPS generates increased amounts of iNOS and COX-2 protein. These are functionally active enzymes producing nitric oxide and PGE2 respectively. The role of these mediators has come under scrutiny recently and it has been postulated that they may reflect an attempt to dampen an inflammatory response in diseased airways. That the increase in iNOS expression is dependent on COX-2 production of PGE2 suggests that this latter is the key anti-inflammatory molecule. Thus I have demonstrated a new secondary pathway for rolipram's physiological activity. I have also shown that this is not responsible for inhibition of TNF α production.

The second anti-inflammatory effect is a change in macrophage response to LPS. Rolipram causes an increased and early phosphorylation of ERK 1/2, an event that closely correlates with activation. The pattern of ERK 1/2 phosphorylation changes in the presence of rolipram from an 'activated' profile to a 'proliferative' one as described by valledor et al. This would significantly alter the cells response to LPS and may effect the inflammatory outcome.

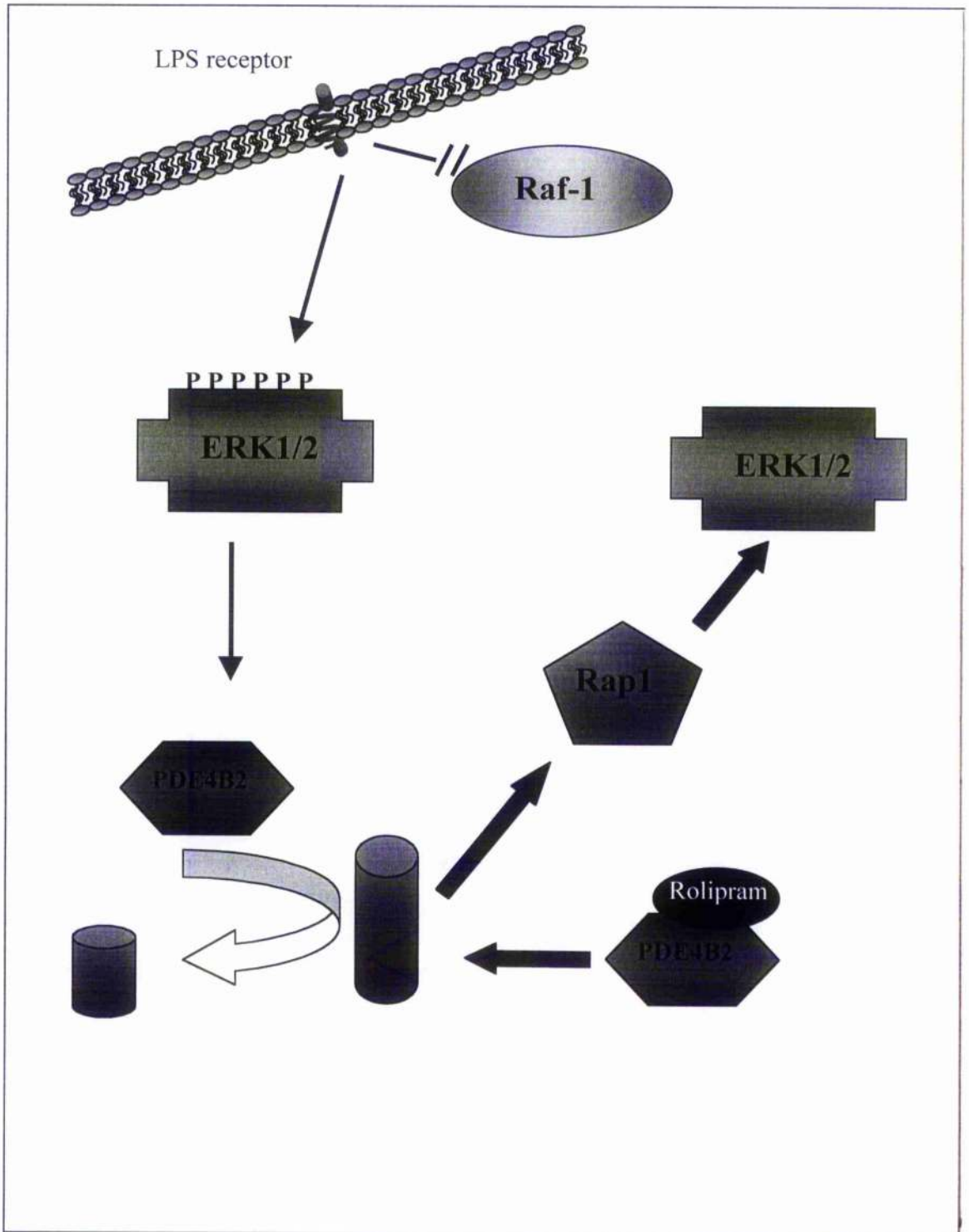


Fig 5.5.5 Revised proposal for cAMP/ERK1/2 crosstalk: Incorporation of rolipram

Chapter 6 The synthesis of HIV-Tat fusion protein

PDE4D3 and PDE4B2

Introduction

I have demonstrated regulation of PDE4 isoform expression in macrophage development, and suggested certain isoforms may have function-specific roles in inflammatory signalling. Compartmentalisation suggests that such specificity may reflect spatial isolation of individual isoforms to restricted areas of the cell or to multi-protein signalling modules. Protein-protein interactions governing such physical organisation also underpin kinase and kinase target association essential in functional regulation. Producing 'mock' peptides mimicking the protein interaction sites on PDE4 isoforms may thus inhibit both targeting and regulation by enzymes. These mock peptides must occur in the correct context to reduce "bystander" effects on proteins with similar modules.

There is no entirely 'clean' way to introduce peptides into cells. Transfection of DNA coding for the desired regions may lead to changes in cell behaviour as seen in chapter 5, while infection of immune cells with adenovirus containing coding DNA has similar or more devastating effects. In any case both of these strategies have proven difficult in macrophages, which are professional phagocytic cells and very resistant to the introduction of active foreign material.

Various methods of transducing protein into intact cells have been attempted. Tagging peptides with lipid groups has been shown to allow small molecules to enter cells, but in a very variable manner. In 1999 Schwarze et al [279] described a novel method for delivery of a fully active enzyme into all cells of a live mouse. This group utilised the property of

the N-terminus of the HIV twin arginine transactivation enzyme (Tat) that allows it to pass through bi-lipid membranes. This small portion of the enzyme is known as HIV-Tat, and Schwarze et al showed that recombinant, denatured full length β -galactosidase protein in fusion with HIV-Tat was not only delivered into cells, but was renatured and active once internalised.

My aim was to synthesise four such fusion proteins coding for full length and N-terminal fragments of PDE4 isoforms linked to HIV-Tat. I chose PDE4B2 since I had previously shown this molecule to be important in the development of inflammatory signalling, and PDE4D3 as this molecule was shown to be absent from these cells and would function as a negative control. Although unsuccessful in my attempt this process was a useful methodological experience.

Results

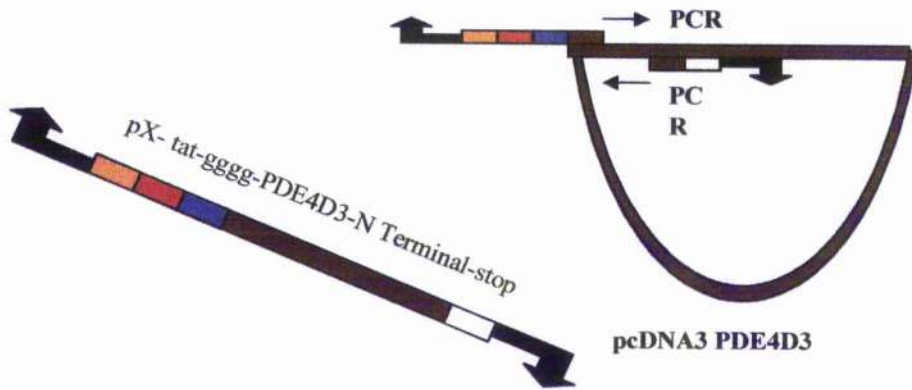
Section 1

Strategy employed

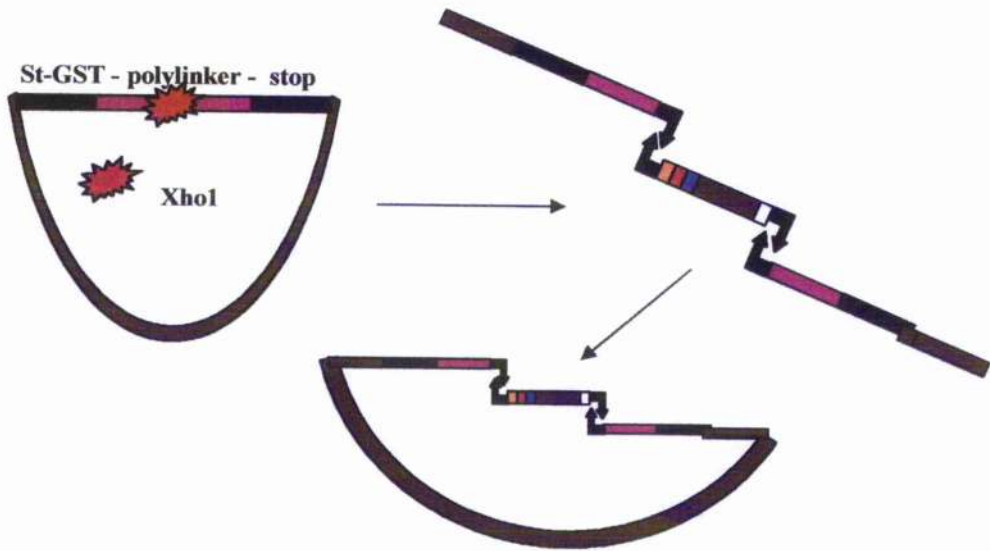
Following standard protocols reported in materials and methods, I planned to produce full length and N-terminal PDE4 isoform-HIV tat fusion proteins. A schematic illustration of the method I employed is shown in figure 6.1.1. The sequence for HIV-TAT was retrieved by interrogating the complete HIV genome as published in the NCBI genome database, using the sequence published by Schwarze et al as a search tool [279]. This peptide sequence was connected to the PDE4 fragment of choice by a poly-glycine linker region. This allows free rotation of the combined proteins once synthesised preventing inhibitory interaction. A seven amino acid length sense primer for the PDE4 was added to the glycine linker. An antisense primer for the C-terminal region of the PDE4 sequence to be cloned was created. Figure 6.1.2 describes the various elements of the primers used. Each cDNA had reciprocal open restriction enzyme sites ends encoding the complimentary sequence of a restriction site of the poly-linker region of P_{gex} precision plasmid vector. I used Not-1 sites for the majority of these constructs. This vector contains the sequence of GST and a peptidase target domain allowing recombinant proteins to be purified on sepharose beads then cleaved off. By using this plasmid I intended to utilise the Kozak initiation sequence included. While simplifying the method, this strategy requires careful planning to ensure that the subsequent fusion protein 'insert' cDNA lies in-frame for that Kozak.

Prior to ligation the vector plasmid was linearised by incubating with a restriction enzyme designed to cut the plasmid within the poly-linker region. The insert cDNA was then ligated into the linearised poly-linker region. A plasmid was identified by RLFP and sequence analysis was performed to ensure correct alignment and the integrity of the DNA

A/ insert synthesis



B/ Clone into expression vector



C/ Transformation and amplification

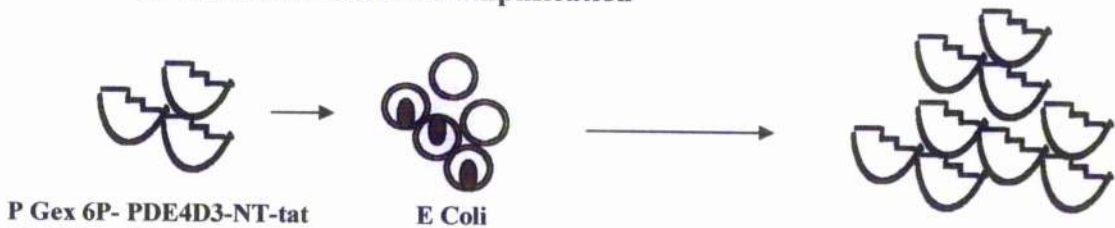


Fig 6.1.1 Schematic representation of PDE4D3 N terminal HIV tat fusion protein

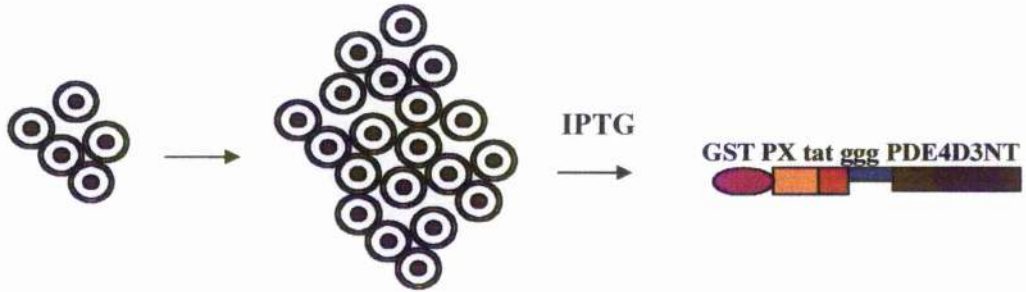
PCR primers designed to recognise N terminal sequence of PDE4D3 and coding for HIV-tat and restriction enzyme binding sites were used in PCR reactions with pre-cloned PDE4D3 in pcDNA3 plasmid vector, A. The resulting cDNA was used as an insert for a ligation reaction into the poly-linker region of Eco-R1 linearised P-Gex 5X expression vector, B. These expression clones were transformed into standard E Coli for amplification and screening, C. Screening was performed by restriction digest using *pst*-1 with three resulting cDNA fragments confirming correct sequence cloning, D. Formal confirmation was made by sequence analysis

continued.....

D/ Restriction digest screening



E/ Growth and stimulation



F/ Isolation of protein

Recombinant PDE4D3NT-GST lysate

Sepharose coated beads

Precision protease

G/ PDE4D3-N Terminal -HIV tat fusion protein

PDE4D3-NT - GlyGlyGly - HIV tat



Fig 6.1.1 Continued.

A clone with confirmed sequence was selected and plasmid isolated and purified. This was transformed into BL 21 E Coli, a strain selected for its ability to produce recombinant proteins. A successfully transformed colony was identified on ampicillin selection media. This colony was cultured at optimised temperature and stimulated to produce the fusion protein by the addition of IPTG, E. Bacteria were harvested by centrifugation and lysed. Protein rich supernatant from lysed bacteria were incubated with sepharose coated beads, F. Sepharose binds the GST of the fusion protein allowing purification from the supernatant. Finally precision protease was used to cleave the recombinant PDE4D3-N Terminal - HIV tat fusion protein from the GST which was removed by bead centrifugation, D. Finally a cartoon representation of the desired fusion protein, E.

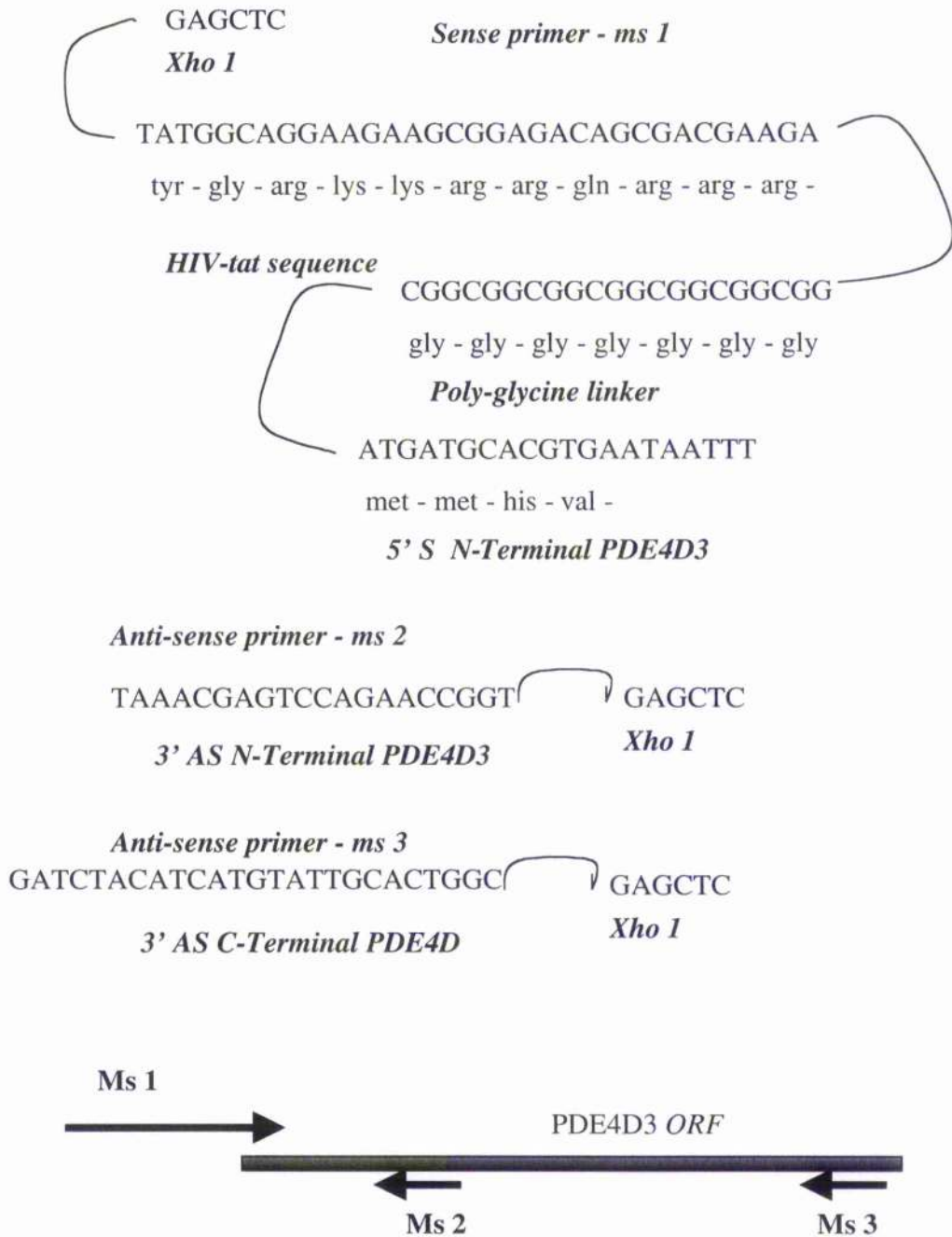


Fig 6.1.2 sequence of the PDE4D3 N-Terminal HIV tat fusion primer

Schematic representation of the primers used to generate the insert from a cloned stock PDE4D3 full length sequence. Sense primer codes the fusion peptides to be included in the cloned sequence. These are detailed as HIV-tat and the poly-glycine linker. A region coding for the specific N-terminal of PDE4D3 is included in the sense sequence. For other PDE4 isoforms the specific N-terminal sequence could be substituted at this point. Two anti-sense primer sequences are described. MS2, codes N-terminal truncated PDE4D3 while ms3 encodes the generic C-terminal PDE4D. By including this latter sequence full length PDE4D3 fusion protein could be synthesised. Finally a schematic diagram demonstrating how these primers related to full length sequence is provided.

sequence. A plasmid containing verified coding sequence for HIV-tat-PDE4 was amplified and purified as described. This was transformed into the BL-21 E Coli expression system. These bacteria were stimulated to synthesise protein, using IPTG. Harvested bacteria were solubelised and the protein extracted from the supernatant fraction using beads coated with sepharose. Finally precision protease was used to cleave the peptide from the beads to produce a purified peptide.

I attempted to make HIV tat fusion proteins for a variety of PDE4 isoforms. Unless otherwise noted I will describe PDE4D3-N-terminal fusion protein to illustrate the problems encountered. Figure 6.1.2 illustrates the primers I designed to code for HIV-tat PDE4D3-Nterminal fusion.

Section 2

Optimising the method

6.2.1 Optimising PCR methods HiFi Vs Taq

I set out first to compare a variety of PCR agents as successful ligation depends on having optimum quality cDNA product. Optimal PCR conditions were assessed by varying the cycling temperature and times over a range of values. Optimum cycling conditions based on these experiments are presented in table 2.3, (materials and methods). Figure 6.2.1 demonstrates two agents, Taq (Promega), High Fidelity (Roche) and High Fidelity2 (Roche, with a mix containing twice the template DNA). Taq is a thermostable DNA polymerase, while the high fidelity mixes Taq and Pwo DNA polymerases. These latter enzymes contain intrinsic 3'-5' proof reading capacity that increases the fidelity of the PCR product. In this experiment I used HIV-tat-PDE4D3 N-terminal sense primer and a PDE4D3 C-terminal primer, thus cloning a full length PDE4D3-HIVtat fusion coding for

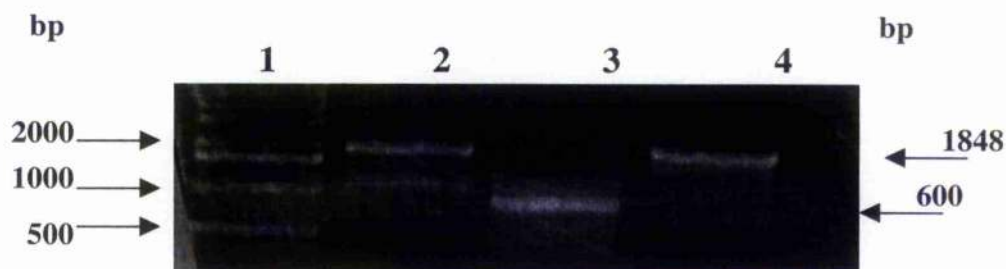


Fig 6.2.1 Optimisation of PCR technique

Primer pairs encoding the HIV-tat-N-terminal PDE4D3 fusion [GAGCTCTATGGCAGGAAGAAGCGGAGACAGCGACGAAGACGGCGGGCGGC GGCGGGCGGCGGATGATGCACGTGAATAATTT] and the extreme C-terminal of PDE4D3 [GATCTACATCATGTATTGCACTGGC] were incubated using a variety of PCR reagents. An cDNA of ~1848 bp was expected. Lane 1 molecular weight markers, lane 2 High Fidelity(Roche), Lane 3 Taq (Promega) and Lane 4 High Fidelity (Roche, double template DNA). As can be seen the conditions selected were satisfactory for use with High Fidelity, PCR reagents and this was selected for further experiments.(values molecular size, bp: base pairs)

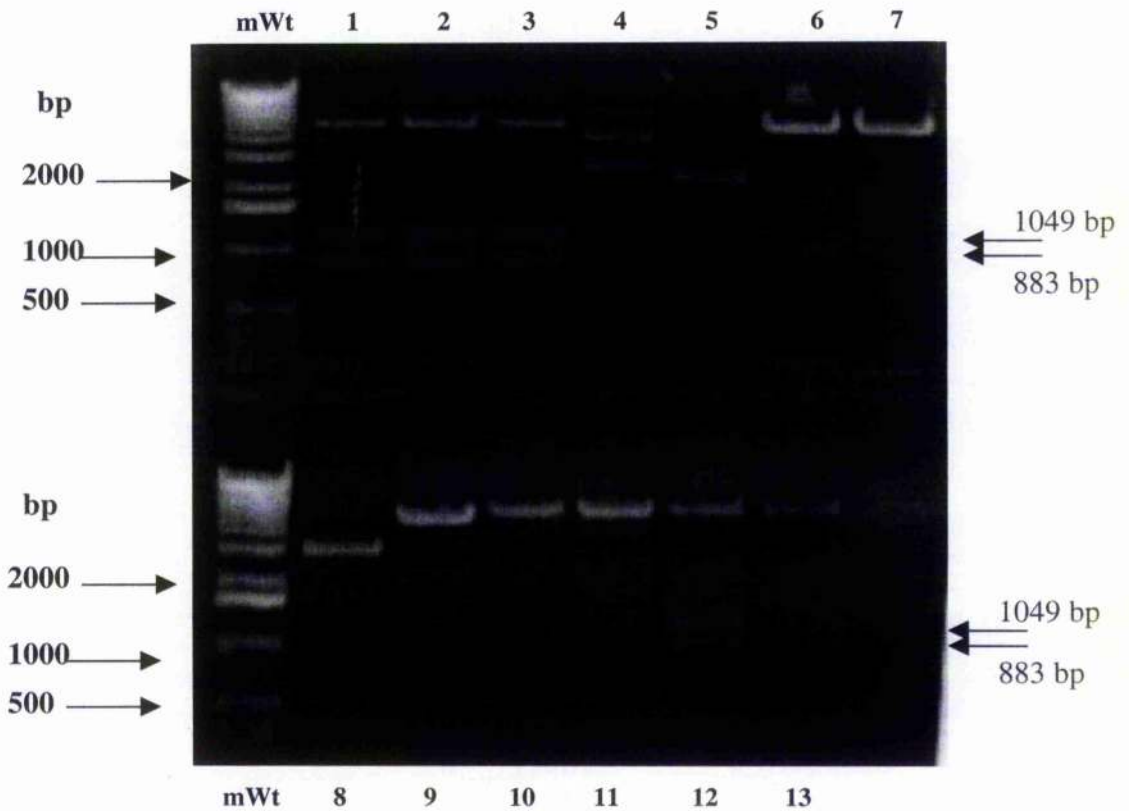


Fig 6.2.2 Restriction fragment (rFLP) analysis of ligated plasmids

PGEX 5.3X plasmids into which cDNA encoding PDE4D3 N-terminal - HIV tat fusion protein had been ligated using a range of molar ratios of insert to plasmid, were incubated with *pst*I restriction enzyme as described in materials and methods. The cDNA was resolved on a 1% agarose gel containing ethidium bromide and visualised under UV light. Lanes 1 -4 vector/insert (v/i) ratio of 1/7, 5-8 v/i ratio 2/7 and 9-13 v/i ratio of 3/7. Expected fragments of 5040Kba, 1049Kba and 883Kba were seen in lanes 1, 2, 3 and 12. These plasmids were selected for further analysis by commercial sequencing.

1.8 Kba. On the basis of this early optimisation I used HiFi (Roche) for all further PCR steps.

6.2.2 Screening for transformed vectors – restriction digest

Complimentary DNA encoding a PDE4 sequence fused to HIV-tat was purified from agarose gel and quantified by spectrophotometry. This cDNA became the “insert” DNA for plasmid ligation. Ligation of insert cDNA was completed as described in the materials and methods, and different ratios of insert to plasmid were compared to ensure optimum ligation. Successful ligation of insert into most linearised plasmid led to some re-circularised plasmid that did not contain the insert and possibly some inverted sequence insertion. This led to false positive resistant colonies when transformed E-Coli were grown on selection media. To avoid selecting bacteria with non-ligated or misaligned plasmids, restriction digest was performed on purified plasmid from randomly selected samples from bacterial colonies. Figure 6.2.2 demonstrates the successful incorporation of insert in only 4 of 13 colonies selected. Three of the 4 successful clones were ligated with a ratio of insert cDNA to vector plasmid of 1/7 based on molarity. When other ratios were used the resulting number of colonies on selection media was small. Thus for future ligations this ratio was used. Clones suggested by digest screening were commercially sequenced to confirm their integrity.

6.2.3 Optimising expression

Following successful cloning and amplification of the expression vector containing fusion cDNA I transformed the plasmid into BL 21 E Coli. This strain is used as an expression vehicle as it is less likely to make inclusion bodies with recombinant proteins than other E Coli. These complexes of bacterial proteins form when ‘foreign’ proteins are improperly processed by bacteria and are prepared for destruction [280]. Growing the bacteria under

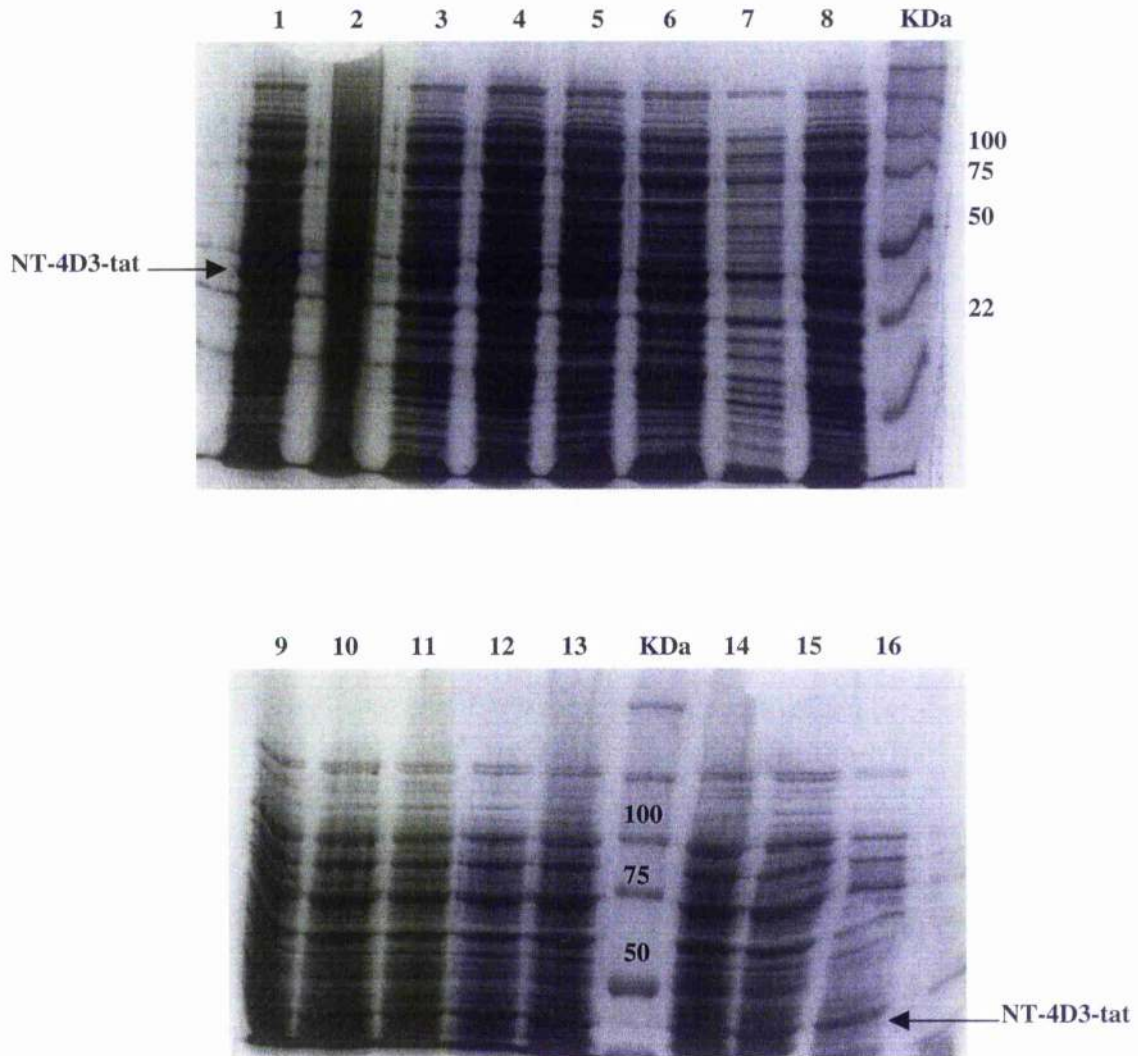


Fig 6.2.3 Optimisation of expression of PDE4D3-NT-tat in BL 21 E Coli

BL21 E Coli transformed with PDE4D3-N Terminal-HIVtat cDNA P Gex vector were grown to optimum density (0.7 abs units) and IPTG added. 4 colonies were selected and incubated at different temperatures. Bacteria were harvested, lysed and particulate free lysate was boiled in 2XSDS sample buffer. Lysate was applied to an 8% SDS-PAGE gel as follows: Lanes 1-4, 37°C; 5,6,8 and 9, 22°C; 10-13,4°C and lanes 7 and 16 non-stimulated E Coli. Gels were stained with coomassie blue stain and dried. As can be seen different colonies appear to express protein optimally at different temperatures. Further analysis was performed on colonies represented in lanes 6 and 8, grown at 22°C.

conditions favouring slow production of protein reduces the formation of inclusion bodies. Different growth conditions were tested to optimise protein production free from IB, by resolving particulate free cytoplasm on SDS-PAGE. Figure 6.2.3 demonstrates that different colonies produced protein optimally under different conditions. This is well recognised and means that for any given recombinant protein optimising growing conditions is necessary. It was still clear that a large proportion of the expressed protein existed in inclusion bodies. This may be explained by the tendency of PDE4 N-termini, to form oligomers by UCR1 – UCR2 interaction. It is also known that GST can form dimeric forms, thus large complexes of peptides may develop within the E Coli. I next attempted to vary the lysis buffer to improve solubility of peptide in the supernatant.

6.2.4 Optimising isolation

To optimise the solubility of the expressed peptide I attempted to lyse the BL 21 E Coli in a range of lysis buffers. These included two different lysozyme buffers (Ly1 and Ly2 – section MM) and a sucrose buffer (Su1). Figure 6.2.4 demonstrates that lysozyme based bacterial lysis results in a greater proportion of protein in the supernatant fraction. I next attempted to isolate the soluble protein on sepharose beads to maximise purification. Unfortunately despite achieving a high supernatant to pellet protein ratio I was unable to isolate the fusion protein on sepharose beads. Various conditions were tried, to enhance sepharose binding but the protein remained in the supernatant following collection of beads by centrifugation. This suggests that little active GST was present to bind and that soluble protein was not an active fusion protein. I assumed therefore that most of the expressed protein was contained in the form of inclusion bodies (IBs).

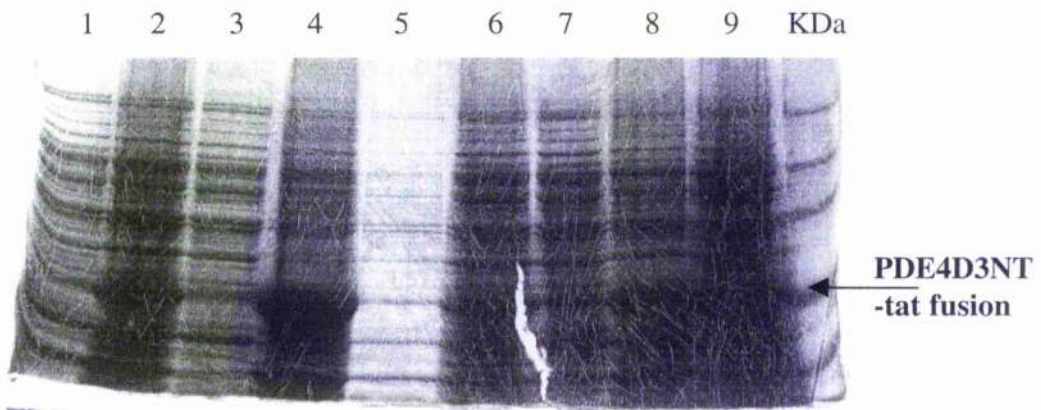


Fig 6.2.4 Optimisation of bacterial lysis

BL21 E Coli transformed with P Gex plasmid containing the fusion cDNA coding for PDE4D3N-Terminal-HIVtat, were treated with IPTG and grown at 22°C for 6 hours. Bacteria were harvested and lysed in a range of lysis buffers Ly 2, Ly1 and su1(section Materials Methods). Supernatant and pellet fractions were boiled in 2X SDS sample buffer and resolved on an 8% SDS-PAGE gel. Gels were stained with coomassie blue stain and dried. Lane 1 and 2 Ly 1, lane 3 and 4 Ly 2 and 5 and 6 Su 1. Lanes 8 and 9 represent full bacterial cells boiled in lysis buffer. Even lanes supernatant fractions while odd lanes pellet fractions. Lysozyme (Ly) based buffers were selected for further analysis as a greater proportion of expressed protein is found in the supernatant fraction.

6.2.5 Sarkosyl detergent based lysis of BL 21 E Coli

In an attempt to denature IB during bacterial lysis, I used a strategy involving the ionic detergent Sarkosyl. This causes IB disruption by denaturing protein-protein interactions. The supernatant collected from centrifugation of bacteria lysed in 10% sarkosyl contained a relatively high supernatant/pellet recombinant protein ratio, (fig 6.2.5.1). In lane 6, it is clear that no association between sepharose beads and recombinant GST-fusion protein took place. It is likely that the 10% sarkosyl buffer used to produce protein denaturation and inclusion body solubilisation also denatures GST causing failure to associate with sepharose.

To combat this problem I attempted to minimise the concentration of sarkosyl in the lysis buffer (fig 6.2.5.2). As can be seen, although recombinant protein appears in the supernatant from low dose sarkosyl lysed bacteria (fig 6.2.5.2,A) little difference was seen at reducing sarkosyl concentrations when protein was collected on sepharose coated beads P2 (fig 6.2.5.2, B). I attempted to re-nature GST by adding the ionic detergent triton X-100. As can be seen (Fig 6.2.5.3) while some re-natured protein was collected on beads (P2), a large proportion remains in the supernatant (S2).

6.2.6 Urea denaturation of inclusion bodies

Inclusion bodies can be denatured in 8M urea, and I attempted fusion protein isolation with this method. Lysozyme lysed bacterial pellet fraction (P1), was solubilised in 8M Urea and gradually renatured by osmotic replacement of Urea using dialysis. Figure 6.2.6 demonstrates a significant concentration effect of sepharose beads suggesting that dialysis based re-naturation of GST has allowed successful isolation of fusion protein. Unfortunately lane 4, shows loss of fusion protein with peptidase cleavage of P2.

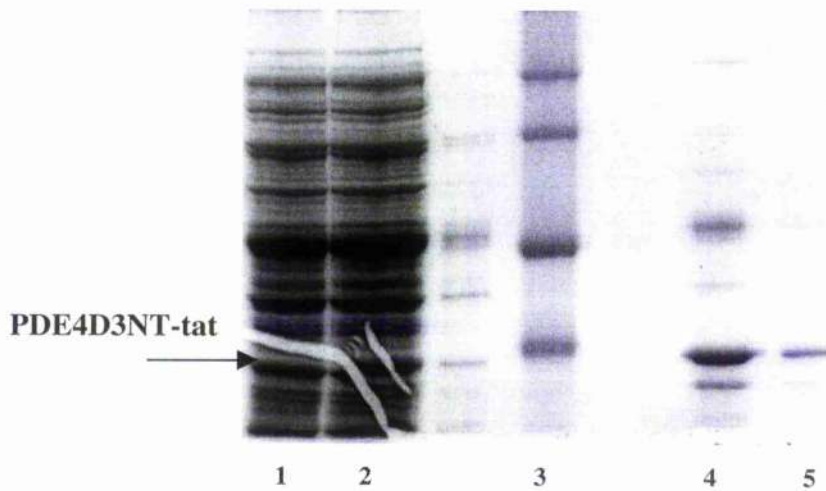


Fig 6.2.5.1 Comparison of 'GST-pull down' to pellet fraction in sarkosyl lysed transformed E Coli

BL 21 E Coli transformed with P Gex containing the fusion cDNA coding for PDE4D3N Terminal-tat, were treated with IPTG and grown at 22°C for 6 hours. Bacteria were harvested and lysed in 10% sarkosyl lysis buffer (section MM). Pellet fraction (P1) and supernatant S1 were collected by centrifugation. Sepharose coated beads were added to S1 and incubated at 4°C for 2 hours. Beads were collected and washed and collected by centrifugation. Collected beads (P2) and wash buffer (W1) were retained. All fractions were boiled in 2XSDS sample buffer and applied to an 12% SDS-PAGE gel as follows: lane 1 and 2 S1, Lane 3 molecular weight markers, lane 4 P1, lane 5 W1 and lane 6 P2. Despite a significant amount of recombinant protein appearing in the P1 fraction none appears to be collected on the beads. This is likely to be due to the denaturing effect of 10% sarkosyl on GST.

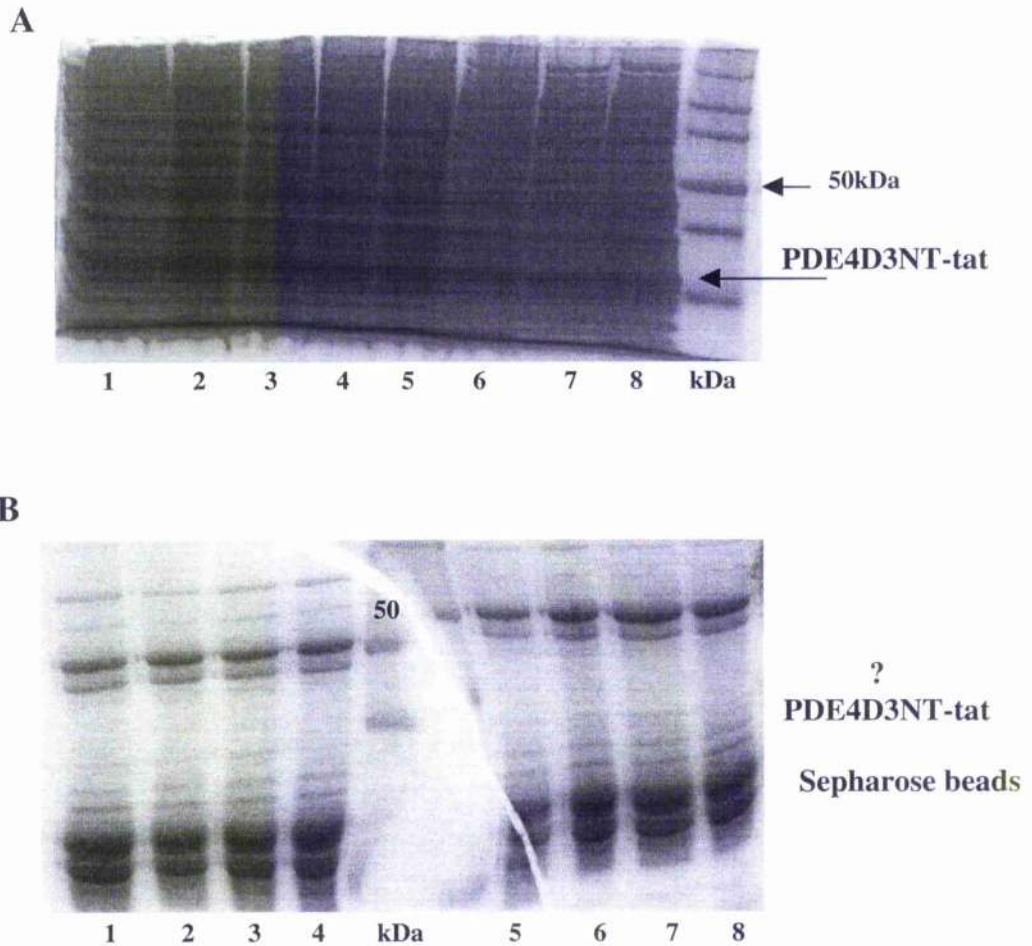


Fig 6.2.5.2 Effect protein solubilisation and GST denaturation of minimising sarkosyl concentration

BL 21 E Coli transformed with P Gex containing the fusion cDNA coding for PDE4D3N Terminal-tat, were treated with IPTG and grown at 22°C for 6 hours. Bacteria were harvested and lysed in buffer containing a range of sarkosyl concentrations (section MM). Supernatant S1 was collected by centrifugation. Sepharose coated beads were added to S1 and incubated at 4°C for 2 hours. Beads were collected and washed and collected by centrifugation (P2). P2 and S1 were boiled in Laemmli buffer and applied to an 12% SDS-PAGE gel as follows: lanes 1 - 8, 0.025, 0.05, 0.1, 0.15, 0.2, 0.3, 0.4 and 0.5 % respectively. Significant quantities of protein were found in the S1 fraction from buffers containing 0.05 - 0.2 % sarkosyl, A. No significant sepharose bead isolation of GST fusion protein was seen at any concentration of sarkosyl. Thus minimising the concentration of sarkosyl did not prevent the inhibition of GST function.

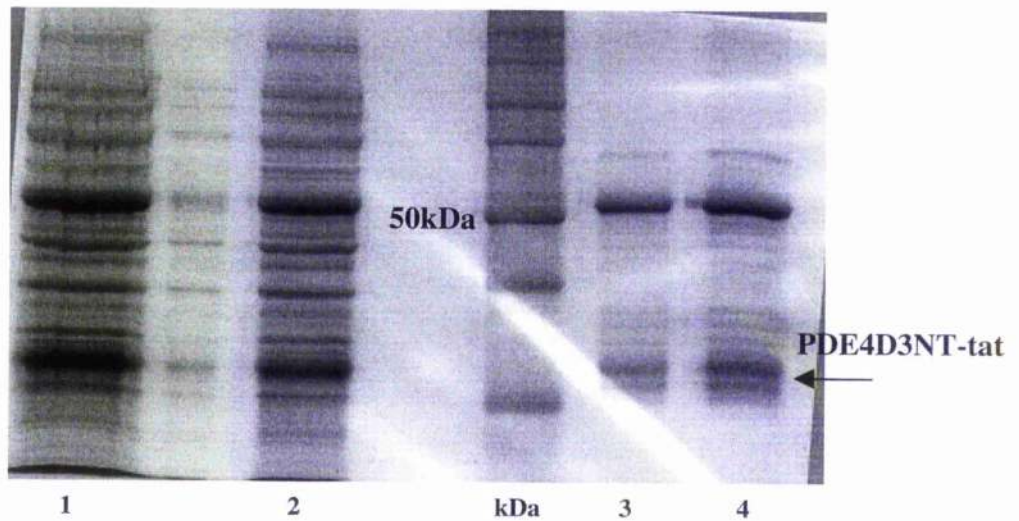


Fig 6.2.5.3 Effect on GST function of adding triton X 100 to sarkosyl lysed E Coli.

BL 21 E Coli transformed with P Gex 5X containing the fusion cDNA coding for PDE4D3N-Terminal-tat, were treated with IPTG and grown at 22°C for 6 hours. Bacteria were harvested and lysed in buffer containing 1% sarkosyl to which 1% triton was added (section MM). Supernatant S1 was collected and sepharose coated beads were added and incubated at 4°C for 2 hours. Beads were collected and washed by repeated centrifugation (P2), while remaining supernatant from bead pull down (S2) was retained. P2 and S2 were boiled in Lamelli buffer and applied to an 12% SDS-PAGE gel as follows: S2 lanes 1 and 2; P2 lanes 3 and 4. S2 contains the majority of expressed recombinant protein, while a proportion appears associated with the P2 bead fraction. This proportion appears little different when triton X 100 is included compared to no triton buffers.

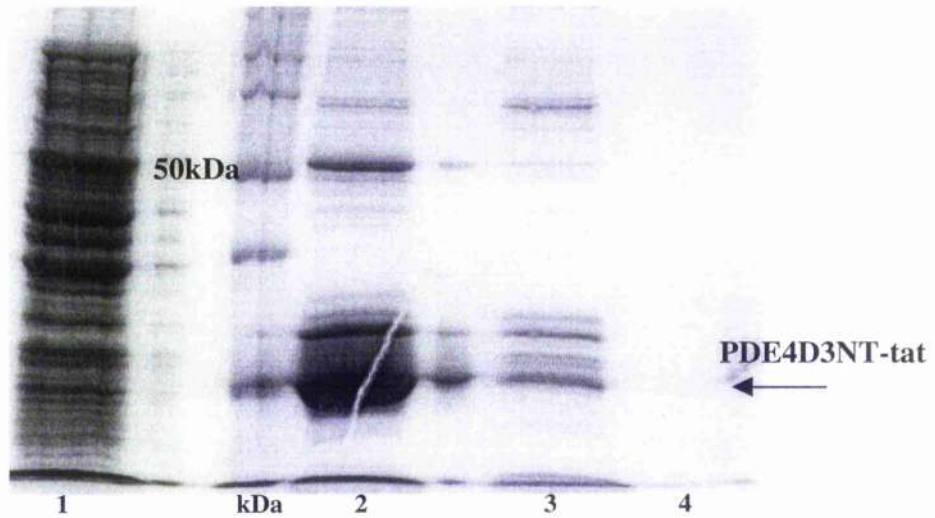


Fig 6.2.5.4 Urea denaturation of inclusion bodies allows more efficient extraction of recombinant protein

BL 21 E Coli transformed with P Gex 5X containing the fusion cDNA coding for PDE4D3N-Terminal-tat, were treated with IPTG and grown at 22°C for 6 hours. Bacteria were harvested and lysed 8M Urea at 4°C (section MM). Supernatant S1 was collected and dialysed through graduated osmotic saline solutions. Sepharose coated beads were added to the reconstituted lysate and incubated at 4°C for 2 hours. Beads were collected and washed by repeated centrifugation (P2). Half P2 was retained while half was incubated with precision protease to cleave the recombinant protein from the beads. Beads were collected by centrifugation (P3) and the remaining protease buffer was denatured using protease inhibitors. This supernatant (S3), contains the full length recombinant fusion protein. All fractions were boiled in Lamelli buffer and applied to an 12% SDS-PAGE gel as follows: lane1 S1; lane 2 P2; lane 3 S3 and lane 4 wash 1. P2 demonstrates the concentration of renatured GST-fusion protein bound to sepharose beads. S3 is contaminated by other protein bands suggesting an impure collection.

Chapter 6: Discussion

The ability to transduce proteins or peptide fragments into live mammalian cells offers the opportunity to interfere with protein activity in a highly specific fashion. In this way information about the functioning of individual members of the PDE4 family could be gained. If successful, such work would allow development of rational therapeutic targets engineered to inhibit individual members of the family and hopefully reduce adverse effects associated with non-specific inhibitory action. Unfortunately mammalian cells are highly resistant to internalising such foreign material. The development of HIV-tat fusion proteins and allied strategies appears to offer an opportunity to overcome cells' natural resistance to invasion.

Various strategies are available when synthesising fusion proteins. A full-length insert encoding cDNA for the entire fusion protein can be made as I have done. Alternatively small sections can be made independently and inserted by ligation. The advantage of the latter is that the cDNA fragments are relatively short and easier to synthesise and ligate, however the main disadvantage is the number of ligation reactions required. My strategy requires careful planning in advance to ensure all the protein remains in frame, but requires only one ligation step. The main disadvantage of this method is that the primers required to produce the fusion cDNA are very large. This makes PCR more difficult to perform due to the development of secondary structure and leads to more errors as primers are less inclined to bind target DNA due to the large areas of 'overhang'.

I selected a Glutathione S-Transferase (GST) fusion system to ease isolation. GST is a short 26Kda peptide originally isolated from *Schistosoma Japonicum*. It reversibly binds sepharose containing matrices allowing elution in increasingly ionic buffers. I used PGex

5.3 X which contains a protease cleavage domain sensitive to the precision protease from Pharmacia.

In designing primers to synthesise the fusion insert cDNA, I had to bear in mind 3 important principles. Firstly, bacterial expression of proteins requires the presence of upstream sequences of initiation called Kozak sequence [281]. This sequence provides the start of transcription and all downstream sequence including the HIV tat, PDE4 sequences and the terminal stop codon must be in frame with this sequence. By using the pre-engineered plasmid PGex 5.3 I already had a Kozak sequence present. Secondly the choice of restriction sites for insertion is critical to allow correct alignment for transcription to continue and to prevent the unintentional production of new restriction sites. Finally because the length of overhang will reduce the strength of binding of the primer to the plasmid sequence I tried to make the shortest possible primers. This process is complicated by the need to have a long overlap section for binding to firmly attach to the plasmid. Thus these two factors mean that the optimum length of primer is hard to assess prior to performing PCR. A final aspect of length is that long primers tend to form secondary structure or primer oligomers, which reduces the efficiency of PCR. In the process of optimising the PCR reaction briefly detailed in results section 6.2.1, I encountered some of the problems associated with primer design and PCR. The final proof of successful insert synthesis comes with protein production thus poor primer design can waste considerable time and resources before becoming apparent.

Optimising conditions of reaction are critical to successful recombinant protein production. Optimum protein expression requires optimal cDNA synthesis, successful ligation, efficient transformation and bacterial growth conditions. Each of these aspects has competing factors which require careful consideration. PCR requires optimal primer design, and correct melting and annealing temperatures. Different Taq systems cope better at different temperatures and under different conditions and errors can be incorporated into

cDNA when using long primers. I optimised the PCR system used and the reaction conditions over several weeks to produce the purest and greatest quantity of insert cDNA possible. High Fidelity PCR reagent (Roche), has a 'proof-reading', capacity that seeks errors in cDNA sequence. I found that this system produced the purest PCR product, and subsequent sequence analysis confirmed the integrity of the reaction. Ligation requires the correct plasmid to insert ratio to increase the chances of insertion and correct orientation. Again I spent some time assessing the correct ratios to use and chose 1 insert/7 plasmid molar ratios. Most importantly the successful production of recombinant protein in bacteria requires consideration be given to conditions of growth, replication, nutrient supply, stimulation and time for protein production. I have detailed the conditions I experimented with during this phase of protein production.

The greatest problem I encountered while attempting to synthesise recombinant fusion proteins was the development of inclusion bodies (IBs). In mammalian systems a complex system of chaperones and proteases exist to eliminate misfolded proteins. When this system breaks down amyloid plaques form. These are highly organised fibrillar proteinaceous complexes that lead to degenerative disease especially in the central nervous system. Inclusion bodies represent the bacterial equivalent of amyloid plaques. These complexes contain proteases and over expressed proteins along with proteolytic fragments and chaperones. Carrio et al recently demonstrated that IB are highly organised and contain active enzymes, including proteases and often the recombinant protein artificially expressed [280]. It was initially assumed that GST fusion proteins would be soluble, however it has been widely reported that even short peptides often form inclusion bodies [282]. Slowing growth conditions by reducing the incubation temperature or the dose of IPTG have all been tried with varying success. I tried manipulating the growing conditions to improve the solubility of the fusion protein but these strategies largely failed.

The standard lysis buffers used in the purification of soluble protein contain the non-ionic detergent Triton-X 100. This detergent allows the GST to maintain its activity and bind sepharose. Unfortunately it has been shown that these do not enhance the solubility of IBs. I attempted to use different buffers to maximise the solubility of the over expressed protein. Although I met with some success when using buffers containing lysosyme, I found that the resultant soluble protein was not active in terms of sepharose binding. Frangioni et al reported that the ionic detergent sarkosyl could solubilise IB proteins containing GST and described renaturation. Thus I decided to pursue a method of IB purification solubilisation and renaturation. I initially used high percentage (10%) sarkosyl buffers and confirmed both the solubility of IB protein and the denaturation of GST when sepharose binding was attempted. I attempted to minimise sarkosyl concentration and found that equivalent solubilisation was possible at between 0.05 and 0.5% sarkosyl. These concentrations are less than reported by Frangioni (~ 1%), but GST-Sepharose binding was still inhibited. Next I included 1% Triton X-100 in the buffer and demonstrated some isolation on sepharose beads, but this proportion was still small compared to the unbound protein.

Finally I attempted a method described by Wey-Jinq Lin et al [283]. They used 8M urea to solubilise isolated IBs and renatured them slowly by gradual dialysis in salt buffers. While this produced the purest samples of sepharose bound protein the quantity of product was too small to use in experimental analysis.

While I was unsuccessful in producing sufficient quantity of pure fusion protein, I learned a lot from the attempt. The main problem encountered after conditions of plasmid production had been optimised was inclusion body formation. This problem has previously been described by Richter et al who attempted to make His tagged PDE4A truncates for enzyme analysis [284]. They showed that C-terminal truncates formed dimeric forms, while if the C termini were included larger aggregates were formed. This tendency for

oligomeric aggregation may well increase the tendency for IB formation. Beard et al demonstrated that UCR 1 and UCR 2 regions tend to form multimeric units when expressed [69]. Thus even though I was working with N-terminal fragments I may have produced multimeric IB complexes.

In the future various alterations to the method might be tried to prevent this happening. Firstly the choice of purification may have increased the tendency to form inclusion bodies. Thus GST tends to form oligomers which will compound the problems described above. To get round this problem other tags could be used. Successful recombinant PDE4 isoforms have been made in fusion with M(?? major basic protein) by using the P MAL vector. This can then be isolated by virtue of binding to beads coated with. The original authors of the HIV tat fusion protein system described isolating their proteins by tagging them with HIS tag. Richter et al also successfully used His tagging in PDE4A truncate preparation, [284]. The tendency of the UCR-1 and UCR-2 regions of PDE4 N-terminals to form protein protein interactions results in another source of oligomer formation. Curtailing the region of PDE4 in fusion with HIV tat may reduce the efficacy of the final protein product as an inhibitor, but may increase the probability of successful production.

I did not experiment with the full range of expression bacteria available. It may be that some are more inclined to form IBs with certain recombinant proteins than others. In the future I would include an optimisation step using other E Coli such as the JM 21 strain.

Although Schwarze et al reported that proteins isolated in a denatured state were renatured in live cells, it is possible that alternative strategies of transducing DNA into cells may provide a better solution [279]. Thus the development of reverse transcriptase containing viruses capable of transfecting immune cells may aid DNA transduction.

Conclusion

I attempted to synthesis a series of PDE4 isoform HIV-tat fusion proteins. I encountered various problems. Eventually time was the primary limiting factor. Careful planning of each stage improved the success at each point. Optimising conditions for each reaction helped ensure a succssful outcome.

Chapter 7 Discussion

Given the evolutionary pressure for conserving resources it is remarkable that nature has developed families of signalling proteins whose family members each express the same activity. Cyclic AMP phosphodiesterases are one such family and PDE4 constitutes one subfamily of enzymes exhibiting this behaviour. The PDE4 family itself consists of an extensive range of enzymes with around 16 family members. Studying PDE4 is of interest to biological scientists, as understanding the reasons for such variety within one enzyme family may shed light on basic principles of cellular regulation [4]. PDE4 enzymes are also of considerable interest to medicine, and pulmonary medicine in particular, as inhibitors of PDE4, by virtue of elevating cAMP levels, act as both anti-inflammatory and bronchodilatory agents [117]. Understanding the functions of individual PDE4 isoforms may help to illuminate the reason for such molecular diversity and suggest specific therapeutic targets whose inhibition will lead to precise changes in cellular behaviour with a low incidence of adverse effects. A large volume of current PDE4 research is therefore aimed at identifying specific roles for individual PDE4 isoforms.

Macrophages are a useful model for investigating PDE4 isoform specific function as they exhibit well-characterised behaviour that is relatively easily measured. As key cells in the regulation of both the innate and specific immune systems they present a target for therapeutic manipulation to control inflammatory disease. As a result macrophage signal transduction has been intensively investigated in the hope that therapeutic targets will be discovered [285]. PDE4 regulation of macrophage cAMP levels has frequently been found to alter cellular function with important consequences for inflammation [195, 286].

I have here firstly characterised the properties of a novel PDE4 isoform and subsequently investigated the importance of individual PDE4 isoforms to macrophage function in order to identify possible therapeutic targets. In analysing macrophages I began by monitoring

the changes in PDE4 isoform expression with macrophage development from monocytes and by measuring the response of individual PDE4 isoforms to macrophage stimulation. In order to investigate the molecular mechanisms behind PDE4 inhibitor regulation of inflammation I investigated the outcome of rolipram treatment on activated macrophages. To illuminate these molecular mechanisms I investigated crosstalk between PDE4 and ERK1/2 systems and the effect of the small GTPase Rap1 on rolipram manipulation of macrophage function. Finally I attempted to develop reagents that could be administered to cells to disrupt specific isoform function.

7.1 The new PDE4B isoform PDE4B4

The complexity of PDE4 gene regulation means that further PDE4 isoforms are likely to be discovered. An understanding of the structure of PDE4 genes coupled with the sequence of rodent and primate genomes will allow new isoforms to be found. Identification can be done using bio-informatics approaches, looking for conserved 5' regions across species that may reflect exons of novel PDE4 isoforms. Also molecular techniques can be used employing probes that recognise regions of homology between members of PDE4 gene families. These can be used to interrogate cDNA libraries in order to identify novel molecules sharing this sequence. The attractive aspect of this strategy is that by using cDNA derived from expressed cellular mRNA it is likely that the cDNA identified will encode an expressed and therefore functional protein. Such a strategy was used in the discovery of the new PDE4B isoform PDE4B4.

A region of the common domain UCR2 from the PDE4B gene sequence was used to probe a rat cerebral cortex library and thus identify a molecule of different molecular size to other known PDE4B isoforms. It is rather surprising that no human homologue to this species has been identified given the high degree of cross species conservation that exists between other PDE4 isoforms [50]. However inspection of the murine genome indicates an

authentic exon encoding the unique 5' region of PDE4B4, supporting the notion that this is a genuine PDE4B isoform found in rodents. Other PDE4 isoforms for which such conservation has yet to be identified include rnPDE4A6, but whether this is a species specific phenomenon or a gap in our understanding is not clear [50].

Kinetic analysis of PDE4B4 reveals a cAMP hydrolysing enzyme with similar characteristics to other PDE4B isoforms that are summarised in table 3.4. Thus the sensitivity to inhibition by rolipram (IC_{50}) and an approximation of the affinity for cAMP (K_m), for PDE4B4 lie within a range that includes other PDE4B isoforms. The apparent V_{max} for PDE4B4 derived from a range of observations of activity at $1\mu M$ cAMP, relative to PDE4B1 is however 9 times greater. The actual activity that this represents at a cellular level will depend on the levels of expression, but such a range of V_{max} for one species of PDE4 family demonstrates the capacity to control cellular response to cAMP by varying expression levels. The effect of regulation on PDE4 isoforms may shed light on this. Phosphorylation of PDE4 enzymes by PKA leads to around a 50% increase in activity (refs check), while phosphorylation by ERK2 reduced PDE4D3 the activity by 75% [66]. These changes in cAMP hydrolysing activity is achieved by increasing V_{max} while leaving K_m unaltered [68]. By setting the intracellular cAMP concentration close to the threshold for PKA activation a cell can control the propagation of a cAMP dependent signal by controlling PDE4 isoform activity within these relatively tight limits. Having different PDE4 isoforms with similar affinities for cAMP but different activities may allow differential expression to control cAMP signals in a cell specific manner.

Particulate bound PDE4B4 V_{max} differs from soluble PDE4B4 (Table 3.4). Thus while soluble PDE4B4 V_{max} was 9 times that of soluble PDE4B1, particulate bound PDE4B4 V_{max} was only 3 times higher. This is similar to the difference in V_{max} between particulate and soluble fractions of PDE4A4 expressed in COS-1 cells [76]. It is suggested that conformational changes associated with particulate fraction binding lead to a change in

the kinetic characteristics of PDE4 isoforms, evidenced by the increased sensitivity of particulate PDE4A4 to rolipram [82]. This change in IC_{50} was mimicked by association with Src tyrosine kinase isoforms and lost when the Src binding domain was deleted from PDE4A4 [232]. PDE4B4 displays the opposite characteristic as the IC_{50} for rolipram is greater in the P1 fraction than the S2 fraction and therefore PDE4B4 is similar to other long form PDE4B isoforms, but differs from the short form PDE4B2 [233]. It may be that the interaction of UCR1 and UCR2 described by Beard et al, alters the effect of particulate binding in a PDE4 family specific manner [69] such that PDE4B isoforms behave in a different way to PDE4A isoforms. Alternatively particulate association of PDE4B long forms may involve different regions of the molecule that lead to specific conformational changes resulting in a different conformational switch to that described for PDE4A4. It is interesting that Baroja et al described association of a PDE4B isoform with the T cell antigen receptor molecule CD3 ϵ [287], confirming the ability of PDE4B isoforms to associate with specific membrane proteins.

Analysis of the cDNA sequence of PDE4B4 reveals coding regions for UCR1 and UCR2 revealing it to be a third long form PDE4B isoform along side PDE4B1 and PDE4B3 [233]. Long form status confers certain regulatory properties on PDE4B4. For example, a recent observation that PKA activation of long form PDE4 isoforms was due to phosphorylation of a Serine residue in the UCR1 region was investigated in the context of PDE4B4 [239]. I have shown that Ser53 of PDE4B4 is critical for the PKA dependent activation of this molecule. Thus PKA activation led to a 57% increase in activity while the Ser53-Asp mutant displayed a 45% increase in activity. This degree of activation is similar to that seen with PDE4D3 where Ser54 is the equivalent Serine Target Residue (STR) [68].

Finally examination of the unique N-terminal region of PDE4B4 reveals structural homology to the long form PDE4 isoform PDE4D3. Of particular interest is the conservation of a PKA STR around Ser14 of PDE4B4. The equivalent residue in PDE4D3

can be phosphorylated by PKA, but the function of this modification is not known. One observation in PDE4D3 that is conserved in PDE4B4 is that PKA phosphorylation results in retarded mobility on SDS-PAGE. It has been suggested that Ser13 in PDE4D3 (Ser14 PDE4B4) is responsible for this mobility shift. Consistent with data described for PDE4D3 Ser14 in PDE4B4 does not appear to be important for PKA dependent activation.

I have investigated the kinetic characteristics of a new long form PDE4B isoform. It shares many properties with other long form PDE4B family members and differs from other PDE4 isoforms. It displays remarkable N-terminal homology with PDE4D3 (fig3.1.1). This region is believed to allow association between PDE4D3 and AKAP450 and MAKAP and it would therefore be interesting to see if PDE4B4 also displays protein interactions with these targeting molecules.

7.2 PDE4 inhibition in macrophages

Macrophages have served as a useful model for examining PDE4 inhibition in inflammatory systems. Two important principles have been described. Firstly inhibitors of PDE4 by virtue of causing elevations in intracellular cAMP have anti-inflammatory activity [118]. Secondly the cAMP generating capacity of PDE4 inhibition is increased in the presence of a positive stimulus for cAMP such as PGE2 or a β 2 agonist such as isoprenaline [142, 223]. The functional outcome of PDE4 inhibition is also partially dependent on adenylyl cyclase stimulation. This was demonstrated by Seldon et al in monocytes who found that although PDE4 inhibition elevated cAMP in a synergistic fashion, with both PGE2 and albuterol, increased TNF α suppression was only seen with PGE2 [142]. This work suggests a degree of functional compartmentalisation of monocyte cAMP and it raises the possibility that different pools of cAMP may control different cellular functions. As previous reports have found PDE4 inhibitors are effective in preventing LPS stimulated cytokine production from macrophages I was interested to

investigate how LPS, which is not known to activate adenylyl cyclase could combine with rolipram to cause macrophage inhibition.

I elected to investigate macrophage production of inducible nitric oxide synthase (iNOS) along side $\text{TNF}\alpha$ as this is the enzyme responsible for nitric oxide (NO) production at sites of inflammation [288]. Nitric oxide and iNOS have been found to be increased in the airways of active and quiescent asthmatics [219, 289], and macrophages have been shown to be responsible for a large proportion of lung NO production in response to inhaled endotoxin [290]. Inducible NOS is thus an interesting marker for macrophage activation and is of relevance to diseases of the lung. Together with this iNOS expression has recently been found to be under partial control by cAMP. The response of the iNOS gene to elevations in cAMP, however appear to depend on the cell type and the source of adenylyl cyclase activation. For example Pang et al, found that forskolin and PGE2 both suppressed LPS induced iNOS transcription in J774 macrophages [275], Nusing et al, however found that db-cAMP potentiated the expression of iNOS in response to interferon γ ($\text{IFN}\gamma$) in microglial cells [220].

7.2.1 Rolipram increases LPS stimulated iNOS expression in RAW264.7 cells

I have found that rolipram dose dependently increases the expression of iNOS in LPS treated RAW 264.7 macrophages (fig 5.3.1A) while cilostamide, an inhibitor of PDE3 did not (fig 5.3.1B). PDE3 represents substantial (~30%) cAMP PDE activity in resting macrophages (figure 5.1.1) and peripheral blood monocyte derived macrophages [119], but I found rapid reduction in activity following LPS stimulation. Thus failure of cilostamide to cause an up regulation of iNOS may simply reflect a cAMP dose response, or may suggest functional compartmentalisation of PDE3 and PDE4. Previous studies of alveolar macrophages have found that while PDE4 inhibition has displayed anti-inflammatory behaviour PDE3 inhibition has not [291].

Increasing doses of rolipram alone did not cause iNOS expression while synergism with LPS was found at low doses of rolipram. It is not known if LPS causes activation of adenylyl cyclase allowing synergism with PDE4 inhibitors. Jeon et al studying the cannabinoid receptor CB2 in macrophages found that CB2 dependent inhibition of AC prevented LPS stimulated expression of iNOS [292]. Other studies not specifically directed at iNOS expression have found little effect of PKA inhibition following LPS treatment of macrophages. Thus circumstantial evidence points to a role for AC downstream of LPS stimulation in the activation of iNOS, but the precise nature of this role remains to be understood.

On the other hand LPS can cause PGE2 production from macrophages by transcriptional activation of COX-2. Prostaglandin E2 can activate AC and the resulting intracellular cAMP has been shown previously to partly mediate the anti-proliferative effects of PDE4 inhibitors [202]. Indomethacin prevented the increase in iNOS transcription with rolipram (fig5.3.2), suggesting that a product of COX-2 was promoting the effect of rolipram. Although cAMP is known to upregulate iNOS expression in some cell systems and PGE2 acts with rolipram as described above this effect was interesting, because the body of work detailed below suggests PGE2 does not increase macrophage iNOS expression while cAMP from other sources can. Thus Rutherford found in bone marrow derived macrophages that PGE2 did not affect nitrite production [293]. A group studying thermal injury using splenic macrophages found PGE2 reduced NO products from LPS treated resting macrophages [294] while Pang et al found PGE2 suppressed LPS stimulated iNOS in J774 macrophages [275]. In contrast to this Lin et al showed that while PGE2 could enhance LPS stimulated iNOS expression and NO production from J774 cells this effect was not observed in RAW264.7 cells [295]. Cyclic AMP from other sources can also decrease iNOS and NO production, thus Delgado et al found that pituitary adenylyl cyclase activating peptide prevented LPS stimulated iNOS production from RAW264.7 cells [296]. Finally Morris et al found that 8-bromo-cAMP prevented the LPS stimulated production of

iNOS from RAW264.7 cells [297] and Hasko et al demonstrated isoproterenol inhibition of LPS stimulated nitrite production in RAW264.7 cells [192]. Considerable evidence therefore suggests that PGE2 is unlikely to cause increased iNOS expression.

On the other hand cAMP has been shown to positively regulate iNOS expression and two groups, one using peritoneal macrophages, [298] and one a macrophage cell line [299] have found exogenous cAMP to increase nitrite and iNOS expression. Kunz et al have investigated this further and found that while IL-1 increases nitrite production 40 fold, cAMP analogues elevate this 2 fold [300, 301]. This group found two pathways regulating nitrite production, thus while the IL-1 signal was transduced through NF κ B, cAMP was not.

The source of the cAMP signal and the context of that signal, therefore appear to affect the outcome in terms of iNOS expression. Few studies have looked at PDE inhibition on iNOS expression. Okado found that IBMX, a non-selective PDE inhibitor able to inhibit both PDE3 and PDE4 increased iNOS protein in LPS stimulated macrophages [302] and Greten et al found that rolipram increased nitrite production in RAW 264.7 cells but did not examine iNOS expression [256]. Beshbay et al however, found that rolipram inhibited NO production from LPS stimulated macrophages [303]. I hypothesise that the source of cAMP determines the functional outcome. Thus it may be that cAMP derived from PGE2 activation of AC is only capable of iNOS stimulation in the presence of a PDE4 inhibitor. This argument for compartmentalisation waits rigorous testing.

7.2.2 Rolipram increases LPS stimulated COX-2 production

While I have discussed how rolipram can increase PGE2 induced cAMP production, a second possibility was that rolipram increased PGE2 production. I have found a dose dependent increase in PGE2 production with PDE4 inhibition of LPS treated RAW 264.7 cells (fig 5.3.5). I have further demonstrated an increase in the expression of COX-2 in

LPS stimulated macrophages treated with rolipram (fig 5.3.4). The evidence supporting a cAMP mediated regulation of COX-2 expression is persuasive. Miller et al found that PKA phosphorylation of CREB was partly responsible for COX-2 regulation in chondrocytes [217] while Hinz et al working with peripheral blood monocytes stimulated with LPS found PGE₂ positively regulated COX-2 expression [215]. Lo et al found db-cAMP enhances COX-2 mRNA and PGE₂ production from LPS stimulated RAW 264.7 cells. In contrast the study by Pang et al referred to above looked at COX-2 in J774 macrophages and found PGE₂ inhibited expression [275]. Mechanistic studies support a role for cAMP and PGE₂ in regulating COX-2 expression. Caivano et al found that LPS led to CREB phosphorylation upstream of COX-2 activation [304] while Hinz found PGE₂ could upregulate its own synthetic enzyme through EP₂/EP₄ receptors [213]. No studies have specifically studied the role of rolipram in regulating COX-2 expression, but two have looked at non-specific PDE inhibitors. Hinz et al found that IBMX enhanced LPS driven COX-2 mRNA and PGE₂ production in monocytes while Juergens et al again working with monocytes showed theophylline increased LPS stimulated PGE₂ production [305].

It seems likely therefore that PGE₂ is capable of upregulating its own synthetic enzyme and that PDE4 is present to provide a braking mechanism to prevent excessive overproduction of PGE₂. If this positive feedback model is true, then I expected to find a similar inhibition of rolipram enhancement of COX-2 expression with indomethacin as I have described for iNOS. On the contrary, enhanced COX-2 expression was found to be conserved in the presence of indomethacin (fig 5.2.4), suggesting that rolipram was not acting in synergy with PGE₂ as predicted.

The only known function of rolipram is PDE4 inhibition, thus increased COX-2 expression must be related to this behaviour. One explanation is that rolipram inhibits PDE4 increasing cAMP and causing COX-2 expression in the absence of LPS co-stimulation. Thus the increased expression in co-stimulation is an additive effect of each compound. I

was not able to demonstrate any COX-2 expression in cells treated with rolipram alone. Another explanation is that PDE4 activity provides a brake to the expression of COX-2. Thus PDE4 activity in LPS treated macrophages is sufficient to keep cAMP levels low and remove the synergistic effects of two pathways described by Kunz et al above. This would suggest either that resting PDE4 levels are set to keep cAMP low enough to prevent COX-2 expression, or that LPS elevates PDE4 activity to allow controlled expression of COX-2.

The absence of a COX-2 signal in the presence of rolipram alone suggests that rather than an additive effect, the cAMP produced by PDE4 inhibition is synergistic with LPS signalling. It is possible that a PDE4 isoform regulates the cAMP level locally to a signalling complex downstream of LPS and elevations in cAMP cause enhanced signal transduction.

7.2.3 Rolipram inhibition of TNF α is not COX-2 dependent

I have demonstrated a prostaglandin dependent increase in iNOS expression and a prostaglandin independent increase in COX-2 expression by rolipram in LPS stimulated RAW cells. Such a dichotomy has previously been observed in vascular cells where COX-2 cAMP led to an inhibition of GM-CSF, but not IL-8 production [306].

Both iNOS and COX-2 are believed to exert anti-inflammatory effects on immune cells. I hypothesised that in a similar manner to the indirect inhibition of TNF α through IL-10 proposed by Kambayashi [245], some antiinflammatory activity of rolipram might be mediated through PGE₂. Thus various groups have found that exogenous PGE₂ is capable of inhibiting LPS driven TNF α from monocytes and macrophages of diverse origin [194, 307, 308]. I have found that although rolipram enhances the production of PGE₂ from LPS stimulated macrophages indomethacin did not prevent TNF α inhibition. This further

supports the view that cAMP alters TNF α production at the level of transcription or translation.

I have demonstrated some effects of PDE4 inhibition in RAW macrophages. I have shown that rolipram increases iNOS production by up regulating COX-2 and PGE2 production. I have also shown that COX-2 up-regulation appears to be mediated by PDE4 inhibition in the absence of an obvious costimulation of adenylyl cyclase. Finally I have found that despite an expected increase in intracellular cAMP through inhibition of PDE4 and increased PGE2 production, TNF α inhibition by rolipram is not mediated through COX-2 activity. Having identified possible compartmentalisation of cAMP signalling governed by PDE4 isoforms I wanted next to address which PDE4 isoforms are important in macrophage function. I did this in two ways, by profiling the expression and by measuring the effects of PDE4 isoforms to macrophage activation.

7.3 U937 differentiation

I sought to identify PDE4 isoforms of importance to macrophage function by recording changes in expression with mature cell development from progenitor cells. By demonstrating novel or altered expression of specific PDE4 isoforms at different stages of differentiation I hoped to propose stage specific roles for these enzymes. Two caveats must be considered before addressing my findings.

7.3.1 Using cell lines as inflammatory cell models

Firstly I used a cell line model to profile the PDE4 isoform changes associated with macrophage development. This strategy has inherent problems and some advantages over freshly isolated "ex-vivo" tissue. These cells are transformed tumour cells and thus some

of their properties may reflect the changes associated with immortalisation rather than simply the cell of origin. Signalling processes associated with cell cycle regulation that would not occur in a freshly isolated cell may influence the precise behaviour in response to stimuli or chemical manipulation. Finally by virtue of the process of transformation it is likely that certain important signal transduction elements will have been deleted or switched off, these might interfere with the normal behaviour of the cell under investigation. Despite these caveats I feel using a cell line is justified. Although monocytes are relatively abundant and easy to harvest, macrophages are much less readily available. Macrophages derived from peripheral blood monocytes are likewise much less abundant than their progenitor cells. At a cellular level individual PDE4 isoforms are low abundance proteins. Thus although PDE isoforms can be measured in "ex-vivo" plastic cultured monocytes [119] individual PDE4 isoforms are less easy to measure or subsequently manipulate.

A wealth of literature describes using inflammatory cell lines as models for mature cell behaviour and development. Hancock et al in the 1980's used the HL-60 cell line to investigate the processes of IL-2 receptor expression [309]. This cell line has been used as a model for neutrophil development and signalling [310, 311]. It appears to be less suitable for studying macrophage responses however. The U937 cell was more attractive to study as it has been well characterised in terms of monocyte to macrophage differentiation by Hass et al [154, 155]. They demonstrated that treatment of suspension monocytic U937 cells with low dose PMA produced an adherent cell with surface receptors that displayed a macrophage phenotype. This cell has subsequently been used as a model for differentiation, most recently by Prudousky et al who demonstrated the importance of CD11b expression in the maturation process [156].

Finally U937 cells have been extensively used as models for understanding the regulation of PDE4 activity. Torphy et al have used these cells to demonstrate PDE4 activity changes

following salbutamol treatment [312], while DiSanto demonstrated rolipram effects on the phosphatidic acid sensitivity of PDE4 isoforms [313]. Of interest to my own work on PGE2 regulation Alvarez et al found that PGE2 increased PDE4 activity in U937 cells through PKA activation of PDE4D3 [314].

Cell lines have therefore been used to model changes in signalling molecule expression in inflammatory cell development, however before any inferences can be made these models must be verified. I have confirmed that the U937_{PMA} cell closely reflects macrophage development by comparing cell surface markers, signalling molecules and behaviour against reports in the literature. Thus as mentioned above CD11b is believed to reflect macrophage development in the context of monocyte differentiation [156]. I have shown novel CD11b expression in U937_{PMA} development from U937 cells (fig 4.1.2). Hunninghakes' group demonstrated loss of PKC β expression in the development of the alveolar macrophage and I have confirmed this in U937_{PMA} cells [147]. Finally Gantner et al found that an "ex-vivo" model of plastic cultured monocytes became more adherent, increased their surface area and protein expressed per cell [119]. I have identified all these behavioural changes in the U937 model. Thus I have verified my U937_{PMA} model against historical precedent and found it closely reflects changes associated with macrophage development.

Gantner et al along with various other groups since Thomson in 1976 have found characteristic PDE isoform expression in monocytes and macrophages [119, 221]. Before I could use my model to measure individual PDE4 isoform expression I had to verify it against these precedents. In these studies of PDE3 and PDE4 activity I compared a model of "ex-vivo" monocytes prepared in our laboratory. I have found the expected fall in PDE4 activity along with the rise in PDE3 (fig 4.1.3). Unfortunately most studies compare PDE activities using protein quantity as a denominator. Although this is a reasonable approach when comparing activity levels between cells or in the same cell following a treatment it is

not satisfactory to compare a mature phenotype with a progenitor cell. This is because as described above the quantity of protein per cell can change by orders of magnitude, meaning that perceived activity losses may simply reflect a dilution effect of increased protein. While an elevation of PDE3 activity thus must reflect a significant rise in activity a loss of PDE4 activity may or may not be an artefact of this effect. I have demonstrated that changing protein content does alter the pattern of PDE4 activity change. Thus for activity expressed on a cellular level PDE4 activity rises in the U937_{PMA} model, while that in the ex-vivo model of Gantner et al does not fall as significantly as reported.

7.3.2 Techniques used to profile cellular PDE4 isoform content

The second caveat to these studies concerns the use of different techniques to quantify PDE4 isoforms. Various techniques are available to measure the expression of PDE4 isoforms. Initial studies of expression in inflammatory cells used chromatography to separate PDE activity by molecular size [221]. While this demonstrated that different PDE activities existed it did not specify individual PDE4 isoforms. RT-PCR using harvested mRNA has been used to profile PDE4 isoform expression in various inflammatory cells [223, 315]. However although gene expression is measured in this way, regulation of protein expression can be achieved at a post translational stage and mRNA transcripts may have specific roles in themselves that do not require protein production. It was with such concerns in mind that Houslay et al recommended that profiling of the expression of PDE4 isoforms in cells should include some attempt at quantifying protein [50]. Protein identification however is not straightforward. One can measure immunological activity based on western blot, quantifying the physical presence of an enzyme, but this does not address isoform activity. PDE4 isoform activity is regulated by changes to tertiary protein structure as well as by transcriptional expression. Quantifying activity is more difficult but can be approximated by immunoprecipitation. This technique takes advantage of the property of IgG Fc portion which has a high binding affinity for protein A. Thus by

incubating a solution containing a PDE4 isoform with a specific antibody, all the antibody can be isolated bringing bound PDE4 with it. Due to the nature of antibody-antigen binding dynamics it is important to immunoprecipitate from the same protein concentration if comparisons are being made. Thus in the case of U937 and U937_{PMA} cells a calculation had to be made to account for cell number. A second consideration is that immunoprecipitation may or may not conserve tertiary structure of a target protein. Endogenous binding partners may be lost, while immunoglobulin binding might alter the conformation of the protein. Bearing these considerations in mind, however it is possible to make comparisons of relative activities between two different cell states for a specific PDE4 isoform if the same quantity of protein has been used with the same amount of antibody.

In my studies I used all three techniques available to quantify and identify different PDE4 isoforms. Thus I used RT-PCR to distinguish between PDE4A isoforms, western blot and immunoprecipitation to identify all individual isoforms.

7.3.3 PDE4 isoform profile changes in U937_{PMA} cell development

7.3.3.1 PDE4A activity rises

Although the observed PDE4 activity fell in U937_{PMA}, PDE4A activity rose. When compared at a cellular level this rise was even more substantial (Fig 4.2.1). The proportion of PDE4A to the total activity measured in different experiments rose from around 2% to 81% suggesting a considerable change in the importance of this gene family to the regulation of cAMP between monocytes and macrophages. Western blot data confirms the rise in PDE4A transcription as no PDE4A is immunologically detected in U937, while two bands are easily seen in U937_{PMA}. Two human PDE4A isoforms migrate at the same weight on SDS-PAGE, and I used RT-PCR to define which were present. Although no

PDE4A activity was found in U937, mRNA for PDE4A4 was seen with RT-PCR (fig 4.2.3). This is interesting and reflects the contention discussed above that the presence of mRNA is not a good guide to the activity of an individual enzyme. In U937_{PMA} cells, considerably more PDE4A4 transcript was present, as was the novel expression of PDE4A10 mRNA. Although I did not quantify the amount of PDE4A4 mRNA, I required 3 dilutions of template cDNA to gain resolution on agarose gel, suggesting a substantial increase in mRNA.

The PDE4A4 isoform has been shown to bind to proteins of considerable relevance to macrophage function. Thus McPhee et al found PDE4A4 bound to the SH3 domains of Lyn tyrosine kinase, one of the Src family of kinase enzymes [82]. The importance of Lyn kinase to macrophages has recently been described [231]. Lyn recruitment and activation has been found following LPS stimulation of macrophages [260]. Apoptosis, a key means of regulating an inflammatory response involves the co-ordinated activation of proteolytic enzymes called caspases. PDE4A4 is a target for the essential caspase3 and cleavage as part of apoptosis removes the LYN-SH3 interaction domain on the N-terminal region of PDE4A4 with a resulting increase in activity [232]. Thus circumstantial evidence points to the possible importance of PDE4A4 in macrophage inflammatory function.

PDE4A10 is a relatively recently identified isoform [234]. It is found in brain tissue and this report is the first to demonstrate regulated expression upon cellular differentiation [316]. As yet little is known about the functional regulation or protein binding partners for PDE4A10, which might point to specific roles for it in regulating cell function. My study however points to a role in macrophage specific regulation as no mRNA was found in U937 cells.

7.3.3.2 PDE4B2 expression is increased in U937_{PMA} and differentiated PBM cells

PDE4B2 expression increases when macrophages develop in both the U937 and ex-vivo models. These data are consistent across both immunoprecipitation and western blot data, however no new PDE4B isoforms were found in differentiated cells. A role for PDE4B in regulating inflammatory cell function has been postulated from work in T lymphocytes, where PDE4B species were found to associate with the CD3 ϵ protein of the T cell antigen receptor [287]. A role for PDE4B in monocyte regulation was also proposed by Wang et al, who found that it could be increased by LPS stimulation [253]. Interestingly PDE4B transcription could be limited by co-stimulation of monocytes with IL-10, reminiscent of TNF α and further supporting a pro-inflammatory role for this isoform [317]. Jin et al have recently used a PDE4B knock out model and demonstrated that TNF α production in response to LPS was absent in contrast to the wild type mouse [255]. Thus my data further supports the role of PDE4B2 in supporting pro-inflammatory signalling in macrophages.

7.3.3.3 PDE4D expression is reduced in U937_{PMA} cells and differentiated PBM cells

Jin et al, having demonstrated that the absence of PDE4B acted to prevent TNF α in response to LPS, then compared PDE4D deficient mice [255]. They found no difference in response to LPS when PDE4D knock out mice were compared with wild type mice. This argues against PDE4D isoforms having important pro-inflammatory activity. This distinction between PDE4B and PDE4D neatly demonstrates a functional compartmentalisation between these isoforms. My data agrees with this hypothesis, as PDE4D expression was severely reduced when western blot data was examined (fig 4.2.5). Immunoprecipitation of PDE4D did not agree with these data however. PDE4D activity per U937_{PMA} cell did not fall despite a large reduction in immunologically detectable

isoform. This difference between the two techniques is difficult to explain. The integrity of the antibody has been confirmed through rigorous assessment in the laboratory and was used in both types of analysis and therefore does not explain the discrepancy. It is possible that in immunoprecipitation studies a species of PDE4 other than PDE4D was 'pulled down' along with a small amount of remnant PDE4D artificially elevating the activity measured. This was not confirmed when western blot analysis of the immunoprecipitate was performed. It is possible that post translational modification of the bound PDE4D, however small was sufficient to artificially increase the measured activity. Thus I am unable to explain why a consistent discrepancy existed between the PDE4D activity found by immunoprecipitation and the immunological activity identified by western blot analysis. I believe that western blot is the more robust form of analysis and this is backed up by the data from peripheral blood monocyte differentiation studies.

7.3.3.4 A change in ERK2 regulation of PDE4 occurs with U937_{PMA} development

A significant change in the relative proportions of PDE4D and PDE4B isoforms takes place in both the experimental models discussed. This has important implications for ERK2 regulation of PDE4 activity and therefore for ERK2 cAMP signal crosstalk. PDE4 isoforms can be distinguished on the basis of their response to ERK2 phosphorylation. Long form isoforms such as PDE4D3 and PDE4D5 present in U937 cells, but reduced in U937_{PMA} cells are inhibited by ERK2 phosphorylation, while the short form PDE4B2 which is upregulated in U937_{PMA} cells is activated [67]. The differentiation of U937_{PMA} cells results in a change from long form dominant PDE4 isoforms to short form dominance. I have shown that this has important outcomes for PDE4 regulation as in U937 cells PDE4 activity is reduced by ERK2 activation, while in U937_{PMA} PDE4 is activated. ERK2 is an important enzyme in the transduction of signals downstream of cytokine and

endotoxin receptors and thus macrophage differentiation is likely to be accompanied by significant changes to ERK/cAMP crosstalk [318].

7.3.4 Summary

I have advanced the understanding of PDE4 in inflammation by demonstrating a change in the expression of isoforms with macrophage development. Thus PDE4A10, PDE4A4 and PDE4B2 were transcriptionally upregulated, while PDE4D3 and PDE4D5 expression was reduced. This suggests that both PDE4A isoforms and PDE4B2 are important for regulating cAMP in pro-inflammatory signal transduction. Cyclic AMP is known to inhibit inflammation but how it achieves this is not clear. One possibility is that cAMP activated PKA can prevent downstream signalling through, for example Raf-1 inhibition. Co-ordinated PDE4 activity local to a signalling complex might therefore be permissive to such a signal, while inhibition by rolipram, by elevating cAMP, may inhibit the signal cascade. The work by Jin et al showing a distinction between PDE4 isoforms in regulating inflammatory signals and my work showing specific isoform expression in specific stages of macrophage maturity proposes that individual isoforms may have specific roles in such cAMP regulation. I wanted to further clarify the role of different PDE4 isoforms by measuring their activity following LPS treatment of macrophages.

7.4 Effect of LPS on macrophage PDE4 isoforms

Only a few studies have addressed the regulation of PDE4 by LPS. Verghese et al found an LPS stimulated increase in PDE4 activity and related this to increased transcription [224]. PDE4B2 expression was found to be up regulated by LPS [317]. My data confirms a rise in PDE4 activity with LPS treatment of RAW macrophages, however this occurs in the context of a fall in PDE3 activity. Such a distinction between PDE3 and PDE4 has been described both in terms of PDE activation, [319] and in terms of function [98]. One

explanation for the elevation in PDE4 activity is that resting intracellular cAMP concentration is sufficient to inhibit LPS stimulated signal transduction. Thus activating PDE4 reduces cAMP and permits signal transduction. An alternative explanation is that LPS activates adenylyl cyclase and PDE4 activation in parallel with this prevents the inhibitory effect of elevated cAMP. The transient nature of the PDE4 activation suggests that reaccumulation of cAMP acts as a brake to ongoing signal transduction. This might support the second theory as cAMP reaccumulation will require a positive activation of AC. The reduction in PDE3 activity further supports the theory of compartmentalisation. Thus while cAMP controlled by PDE4 is reduced that controlled by PDE3 is elevated.

7.4.1 Regulation of PDE4 activation

Previous investigators have found transcriptional regulation underlies increased PDE4 activity in LPS treated monocytes [317]. I found that the inhibition of mRNA translation with actinomycin D did not prevent the increase in PDE4 activity at 30 minutes arguing against new protein expression (fig 5.1.2). This illustrates the need for caution when interpreting RT-PCR, as although increased transcript for PDE4 isoforms may be found it is unlikely that new protein production underlies this early phase of activation. It may be that over a longer time scale, changes in the expression of individual isoforms do occur, my data suggests that this is not associated with a prolonged activation of PDE4 in RAW 264.7 cells.

Inhibitors of PI3kinase and PKA both resulted in the abolition of LPS stimulated activation (fig 5.1.2). Wortmannin and H89 however reduced PDE4 activity to below the basal levels of untreated cells. It is impossible on the basis of these studies to identify a difference between inhibition of constitutive regulation in contrast with LPS stimulated activation. Both PKA and PI3Kinase have been shown to cause up regulation of PDE4 activity [50, 112]. The role for PI3kinase in LPS signal transduction is well documented however,

whereas the role of PKA is less well understood [320]. The effect of MEK inhibition with UO126 was interesting. This compound reduced LPS induced activation by around 50% (fig 5.1.2). While this could equally well represent the constitutive activation of short form PDE4 isoforms the effect is less profound than the previous two inhibitors. The role of MEK and ERK1/2 activation downstream of LPS stimulation is also well documented. The ERK2 dependent activation of short form PDE4 isoforms reflects the U937 data discussed above (section 7.3.3.4). In order to investigate the role of ERK2 in PDE4 activation following LPS treatment of macrophages I investigated the PDE4 short form activity in these cells.

7.4.2 RAW264.7 cells express PDE4A, PDE4B and PDE4D isoforms but only PDE4B2 is activated by LPS

The U937_{PMA} studies described above predicted macrophages to express PDE4A and PDE4B isoforms. Western blot data demonstrates the presence of PDE4D isoforms along with two PDE4A isoforms and PDE4B2 (fig 5.1.3). Thus although PDE4A and PDE4B isoforms closely match the cell model PDE4D5 and PDE4D3 appear but were not expected. Various differences exist between the RAW264.7 and U937 cell lines. The former is a rat cell line while the latter is human derived. More significantly RAW 264.7 cells represent a mature cell that has been transformed whereas U937_{PMA} represent a differentiated immature cell line. It is possible that the expression of PDE4D isoforms reflects the process of transformation and immortalisation that are lost in the differentiation of U937 cells. Weak support for this is found in the nuclear localisation of PDE4D in fractionated RAW 264.7 cells (fig 5.2.3).

I have already provided evidence that PDE4B isoforms are believed to play a role in regulating LPS signal transduction. To investigate a role for each isoform I stimulated RAW264.7 cells with LPS and immunoprecipitated each using PDE4 isoform specific

antibodies. Only PDE4B2 activity increased with LPS stimulation. This agrees with Ma et al [317], actinomycin D however again failed to prevent PDE4B activation arguing against new protein transcription causing the increase. While the P38 mitogen activated protein kinase inhibitor SB3850 –did not affect the increase in PDE4B activity the MEK inhibitor UO126 did reduce it significantly.

I have presented further evidence in support of a role for PDE4B2 in pro-inflammatory signalling in macrophages. Work cited above have suggested that this enzyme is important in cAMP regulation in inflammation [253, 255, 317]. I have found a MEK dependent activation of PDE4B2 occurring some 20 minutes following LPS treatment of RAW 264.7 cells. MEK stimulates the activation of ERK1/2 enzymes and being a short PDE4 isoform, PDE4B2 would be activated by ERK2 phosphorylation. I was not able to demonstrate direct phosphorylation of PDE4B2 in LPS treated RAW264.7 cells due to low abundance of the protein. By using a recombinant active ERK kinase protein and ³²P-labelled ATP I attempted to show that PDE4B2 immunoprecipitated from LPS treated RAW 264.7 cells was less capable of being phosphorylated than PDE4B2 immunoprecipitated from untreated cells. I was unable to demonstrate any signal above noise, due in part to the low abundance of PDE4B2 in RAW 264.7 cells.

The ERK1/2 enzymes are important in the transduction of many cytokine stimulated signalling pathways and it is possible that PDE4B2 plays important regulatory roles in other inflammatory systems. Thus I have illustrated an example of molecular crosstalk between the MEK-ERK1/2 signal cascades and the cAMP-PDE4 pathway that may have important implications for immune cell signalling. I have been unable to demonstrate a direct link between ERK1/2 and PDE4B2 however.

7.5 Raf-MEK-ERK1/2 / cyclic AMP crosstalk

I have provided evidence for the influence of ERK1/2 signalling in regulation of cAMP in macrophages. Firstly I demonstrated a distinction between the effects on cellular PDE4 activity of EGF between U937 and U937_{PMA} cells. Why less mature cells would require an increase in cAMP induced by an inhibition of PDE4 is not clear. However it is possible that PDE4D isoforms control cAMP, which in turn regulates progress through the cell cycle. Several reports have described cell cycle arrest in G1 phase in macrophages stimulated with growth factors and treated with cAMP analogues [321, 322]. On the other hand in mature cells where the cell cycle machinery is not active cAMP may play other roles in regulating pro-inflammatory signalling.

Cyclic AMP can exert both negative and positive regulation on the ras-raf-ERK1/2 signal transduction pathway (Houslay/Kolch). PKA phosphorylation of Ser259 of Raf-1 prevents its interaction with Ras and therefore downstream activation of ERK1/2 [261]. Rap-1 is another ras family GTP-ase that is capable of activating ERK1/2 by association and activation with B-Raf [323]. The effect of cAMP in regulating ERK1/2 activity has been shown to be determined by the relative expression of Raf-1 or B-raf in neurones [324]. Thus where B-raf predominates in neurones cAMP activates ERK1/2 while where Raf-1 is dominant in astrocytes cAMP inhibits ERK1/2 activation.

Molecular crosstalk between cAMP-PDE4 and the ERK1/2 pathways can therefore occur in two directions. I have provided evidence for ERK1/2 having influence over PDE4 activity but wished to demonstrate activity in the opposite direction.

7.5.1 Rolipram increases ERK1/2 phosphorylation by LPS

ERK1/2 are protein kinases that are themselves activated by phosphorylation. Antibodies raised against the phosphorylated residues are thus a useful marker of ERK1/2 activation. I

have found that LPS treatment of RAW264.7 cells in the presence of rolipram leads to a larger and more rapid activation of ERK1/2 than LPS alone (fig 5.4.2). ERK1/2 phosphorylation was seen before the production of inflammatory mediators would be expected, suggesting that PDE4 may regulate ERK1/2 activation immediately downstream of LPS. Valledor et al found that timing of macrophage ERK1/2 activation predicted the cellular response to stimulation [271]. They found agents that induce macrophage proliferation such as PMA and CSF-1 cause an early and more substantial activation of ERK1/2 than LPS, which inhibits proliferation and promotes an activated phenotype. I confirmed that PMA and LPS could activate ERK1/2 in RAW264.7 cells to different degrees and over a different time scale (fig 5.4.1). Thus rolipram, by altering the dynamics of ERK1/2 activation may be expected to alter cellular response to LPS. I have only used phosphorylation as a surrogate marker of ERK1/2 activation and quantified the effect by densitometry. I would like to confirm these data by performing ERK1/2 kinase activity assays.

7.5.2 Co-immunoprecipitation of PDE4, Raf isoforms and ERK1/2

Considerable evidence is accumulating for the formation of complexes of signalling molecules bringing interacting enzymes into proximity with each other and possibly preventing inappropriate "over-spill" of activated enzymes [79, 325]. I predicted that molecular crosstalk between PDE4 and ERK1/2 would require direct interaction between these molecules. This hypothesis is supported by the presence of kinase interaction motif (KIM) and FQF domains on PDE4 isoforms [65]. These motifs serve as enzyme docking sites for ERK2 allowing PDE4 isoforms to become target molecules for phosphorylation. By immunoprecipitating PDE4 isoforms I hoped to isolate all the molecular binding partners including ERK1/2 enzymes if they were present. Although initially it appeared that ERK1/2 were coimmunoprecipitated with PDE4B2, subsequent analysis of B-raf and pre-immune serum suggested this could be an artefact. I was unable to increase the

stringency of the conditions sufficiently to exclude a possible experimental error in this work. Developing RAW264.7 cells that overexpress PDE4B2 fused to a peptide tag that would allow isolation without the need for immunoprecipitation might allow a "cleaner" isolation of PDE4B2 binding partners.

I have provided evidence for crosstalk between cAMP-PDE4 and ERK1/2 in both directions. That is, ERK1/2 can regulate LPS activation of PDE4B2 thus controlling cAMP, while rolipram increases ERK1/2 activation suggesting a role for PDE4 isoforms in regulating this cascade.

7.6 Rap1 mutants in RAW macrophages

One implication of the work described above is that cAMP can activate ERK1/2 in macrophages. As detailed above cAMP can activate Rap-1 and subsequently ERK1/2 by a B-raf dependent mechanism [264]. The immunoprecipitation studies confirmed the presence of B-raf in RAW 264.7 cells which is a precondition for this pathway [324]. Important roles for Rap1 have been described in macrophage function including the regulation of integrin binding [204]. The essential components of a cAMP dependent activation of ERK1/2 are therefore available in RAW 264.7 cells and may have important influence over the regulation of macrophage behaviour.

Two methods for proving a role for Rap1 exist. First the GTPase binding protein Ral-GDS, binds only to activated rap and ras [326, 327]. By fusing this protein to a GST peptide it can be used to "fish" for active species of these molecules [328]. Caron et al used mutant Rap-1 molecules, designed to represent the active conformation or mutated to prevent activation [204]. These mutant Rap-1 molecules were then transfected into macrophages and cellular responses to stimulation were measured. Our Laboratory received plasmids encoding mutant Rap-1 molecules as a kind gift from J.L. Bos.

I used RAW 264.7 cells transfected with these plasmids to measure the effect of Rap-1 activation on TNF α and PGE2 production and COX-2 expression. Although RAW macrophages are difficult to transfect and are resistant to genetic manipulation, I believe that sufficient rap1 expression was achieved. Transfection efficiency was variable between the mutants and all the data presented has been corrected for the relative amount of Rap-1 protein present.

Despite allowing for transfection differences the only significant effect I found was on PGE2 production when RAW 264.7 cells transfected with constitutively active Rap-1 were stimulated with LPS in the presence of rolipram. In the absence of a significant effect of constitutively active Rap-1 on PGE2 production in untreated cells over either dominant negative or wild type mutants it is difficult to draw any conclusions from these data. It is interesting to note that in both the PGE2 and the TNF α experiments transfection of wild type Rap-1 appeared to diminish the effect of rolipram. I hypothesise that the act of transfection results in an activated macrophage that produces many cytokines and mediators through alternative pathways. Finally Rap-1 may itself be a target for PKA mediated inhibition of activity. This is achieved by phosphorylation of a serine residue at position 180 [43, 46]. I used Rap-1 constructs mutated at this residue to reflect either a phosphorylated conformation or a mutant that was unable to be phosphorylated. Transfecting these into RAW 264.7 cells allowed me to measure a potential role for PKA modification of Rap-1 in the production of TNF α . In this case the transfection of wild type Rap-1 did not influence the production of TNF α , while both mutant Rap-1 constructs reduced the inhibition of rolipram. While this argues against the hypothesis that transfection alone affects the rolipram sensitivity of RAW 264.7 cells, it is hard to draw conclusions from the results for two opposing Rap-1 mutations having similar functional effects.

7.7 HIV-tat fusion proteins

I have provided evidence of my own backing up previous reports that PDE4B2 may have important roles in regulating inflammatory cell function. Proof of such a role would come from the development of PDE4B2 specific inhibitors compared with other isoform specific inhibitors. Most PDE4 inhibitors interact with the catalytic region of the enzyme. As this is the most highly conserved region of the cell these compounds suffer from being non-isoform specific. Developing isoform specific inhibitors remains an elusive goal.

Individual PDE4 isoforms differ from each other at their extreme N-terminal region. The functions of the N-terminal regions do not lend themselves to chemical manipulation. These functions include targeting, protein-protein interactions and phosphorylation based regulation. I hypothesised that catalytically inert N-terminal domains would compete with the sites required to express these N-terminal functions and disrupt isoform function in a specific manner. Although attractive this strategy is complicated by the need to get these proteins into cells.

Expressing foreign proteins in cells is difficult and doing so in macrophages is particularly so. Various methods of transducing genetic material into intact cells exist including transfection and infection. Both of these have proven difficult in RAW cells. The recent description by Schwarze et al of denatured HIV-tat fused enzymes being incorporated into cells and renatured offered an exciting solution to this problem [329]. In this report β -galactosidase was successfully introduced into the peritoneum of rats and found to have penetrated every tissue of the body within 12 hours. Importantly the denatured protein was found to be within cells and to have been renatured. I hypothesised that catalytically inert PDE4B2-N-terminal peptide fused with HIV-tat would have anti-inflammatory behaviour. I aimed to compare RAW 264.7 cells response to such a fusion peptide with a PDE4D3 N-

terminal HIV-tat fusion protein as this protein is likely to be less important in regulating LPS signal transduction.

Unfortunately I ran out of time to successfully isolate a fused protein but I learned a lot from the attempt. The various stages of synthesis are described in the text of chapter 6, however some significant lessons were learned. My main problem was the development of inclusion bodies consisting of recombinant proteins. This is likely to be due to the adhesive properties of various molecules included in the GST fusion proteins. Firstly, the N-terminals of long form PDE4 isoforms contain both UCR1 and UCR2 and Beard et al described the physical association of these regions [69]. Although PDE4B2 N-terminal does not contain both of these regions it may be that other bacterial proteins expressed UCR2 related proteins sufficient to cause interaction. The choice of GST as a means of isolating recombinant proteins is complicated by the tendency of this protein to form oligomers. This will further encourage the formation of inclusion bodies.

In the future I would overcome these problems in a variety of ways. Previous attempts at PDE4 N-terminal fusion protein synthesis have been successful using shorter sequences of the protein. I would try to make truncated sections of the entire PDE4B2 N-terminal regions in fusion with HIV-tat that would have the additional attraction that I would be able to pin point the source of any inhibitory effect seen. On the other hand such a strategy might fail due to a lack of appropriate tertiary protein structure. I would use different a isolation system. Thus rather than a GST tag I would include a "His" tag which is smaller, does not form oligomers and is easily isolated by association with methionine. Finally I would construct a plasmid vector containing the HIV-tat sequence and His tag in fusion into which I could clone short sequences of the PDE4 isoforms. In this way I could use smaller PCR primers increasing the integrity of the cDNA product.

Future directions

The work presented raises several questions that should be addressed. Firstly the function, regulation and distribution of PDE4B4 requires to be investigated. What purpose is served by having three separate long form PDE4B isoforms is not clear. It may be that tissues express each isoform under a specific set of circumstances. Thus probing a variety of cDNA libraries or performing northern blot analysis of different tissues might increase our understanding. Identifying and investigating the regulation of the splice junction promoters should offer insights into how each isoform is controlled. Such studies can be done through promoter sequence analysis and electrophoretic mobility shift assay (EMSA). This latter is a functional test of promoter activation and therefore has the additional attraction of being physiologically relevant. ERK1/2 phosphorylation would be expected to inhibit PDE4B4. I would like to confirm that this does occur and investigate the possible interaction of PKA phosphorylation of Ser14 and ERK1/2 inhibition.

The U937 and U937_{PMA} cell model offers considerable scope for investigating PDE4 regulation. As this model is verified it can be used to understand how each PDE4 isoform interacts in generating an inflammatory pattern of behaviour. Sufficient tissue is available to measure the responses of individual isoforms to specific stimuli. Creating stable transfected U937 cells with of active and dominant negative PDE4 isoforms would advance our understanding of the process of differentiation. For example it may be that if PDE4D isoforms are over expressed the process of macrophage differentiation will not occur. On the other hand, a RAW 264.7 cell transfected with a dominant-negative form of PDE4B2 may act like a rolipram treated macrophage and inflammation will be prevented.

The role of cAMP in regulating individual inflammatory mediators is complex and varies between cell and mediator examined. Much work is required to discover the mechanisms by which PDE4 regulates individual pools of cAMP that in themselves regulate specific

cytokines. Targeting of PDE4 requires to be better understood and discovering more molecular partners will illuminate this further. Yeast-2 hybrid analysis can be used to identify new binding partners, and understanding the expressed proteosome of stimulated inflammatory cell will allow an appropriate experiment to be performed.

Molecular crosstalk holds the keys to many complex questions of regulation of cellular behaviour. In particular how the MAPkinase and cAMP pathways interact. I have highlighted various possible mechanisms that require to be illuminated. For example the role of the EPAC/rap1/B-Raf pathway in control of inflammatory processes may offer interesting therapeutic opportunities. Using Ral-GDS to "fish" for activated rap1 and using dominant negative EPAC mutants upstream of inflammatory responses would shed light on this early field of investigation.

The development of new molecular inhibitors of PDE4 isoforms requires a greater understanding of the structure/function relationships at the N-terminals. Development of small peptide inhibitors such as HIV-tat fusion should address some of this.

Appendix 1 Standard curves and quantification

In chapters 3 and 5, I have used various methods to quantify proteins and chemical mediators of inflammation. The solutions from which quantification was performed include cells lysed in KHEM buffer and cell free culture medium. Where appropriate all standard curves were generated using known amounts of the target compound dissolved in the same fluid as test samples were prepared.

App1.1 PDE4B4 quantification

Two methods were used to quantify the relative amount of transfected PDE4B isoforms when assessments of relative activity were calculated.

App 1.1A PDE4B ELISA

Firstly enzyme linked immunosorbant assay (ELISA) plates were constructed as described in materials and methods (section 2.4.12). Thus increasing quantities of protein from cell lysates prepared in KHEM were allowed to adhere to 96 well ELISA plates overnight prior to detection using antiserum raised against PDE4B (Schering). Antibody detection was carried out using HRP conjugated anti-serum raised against rabbit IgG, and visualised using ABTS reagent. Optical density (O.D.) of each well was counted using a multi-well plate reader at 405nm (Dynex technologies). Plots of protein content against O.D. were constructed and the relative PDE4B isoform content of each lysate was estimated from the gradient of the straight line linking the plots (fig App1.1A).

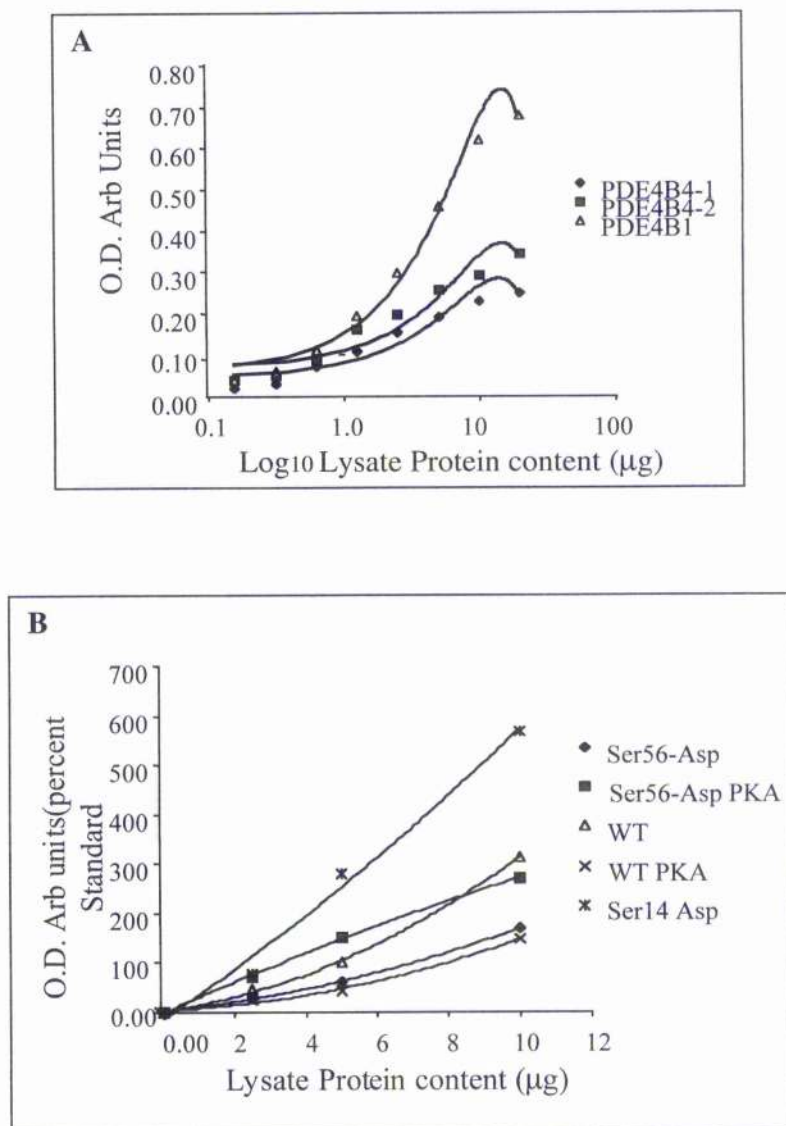


Figure App1.1 PDE4B4 relative transfection efficiency

In order to compare PDE4 activity between different transfected PDE4B isoforms and to compare between different treatment groups, when characterising PDE4B I used two forms of quantitative analysis. Fig App1.1A, Enzyme linked immunosorbant assay (ELISA), was performed using in-house prepared ELISA plates with PDE4B antiserum (Schering). Increasing quantities of lysate protein was incubated in a standard ELISA protocol. The relative steepness of the linear part of the Log protein content/O.D. curve estimates the relative transfection efficiency. Fig App1.1B, western blots were prepared for a range of protein contents for each treatment group in a PKA activation analysis of PDE4B4. The intensity of each band was compared against a standard immunoband. Again the relative steepness of the gradients reflects the relative transfection efficiency. (O.D. Optical density; Arb Units. Arbitrary density units)

App 1.1B Western blot analysis

The second method used to quantify relative transfection efficiencies between different PDE4B transfections was western blot densitometry (section 2.4.9). SDS-PAGE was performed on cell lysates prepared in KIEM and a range of protein quantities from each transfection was resolved on an 8% gel. Net intensity of immunobands visualised using PDE4B antiserum (Schering), HRP-conjugated anti-rabbit antiserum (Sigma UK) and ECL detection reagent (Amersham Pharmacia) was calculated from autoradiographs using KODAK I.D. software. Intensity was adjusted against a standard on each autoradiograph and a plot of intensity against protein content was prepared (Fig App 1.1B). Relative transfection efficiency was calculated from the linear part of each curve plotted from these plots.

App1.2 TNF α quantification

Two ELISA protocols were used when quantifying the content of TNF α from the cell free culture medium of RAW 264.7 cells treated with LPS with or without rolipram.

App 1.2A In House ELISA

ELISA plates were prepared using a standard protocol by bedding mouse TNF α antiserum onto 96 well ELISA plates and incubating with sample medium and a range of known TNF α quantities dissolved in culture medium (Section 2.4.12.2). HRP-conjugated TNF α secondary detection antibody was then added and finally visualisation was performed using ABTS solution. Optical density was measured on a Dynex micro-plate reader (Dynex technologies) at 405nm. A plot of TNF α (pg) against O.D. was prepared and TNF α content of test samples was recorded from the linear part of this standard curve.

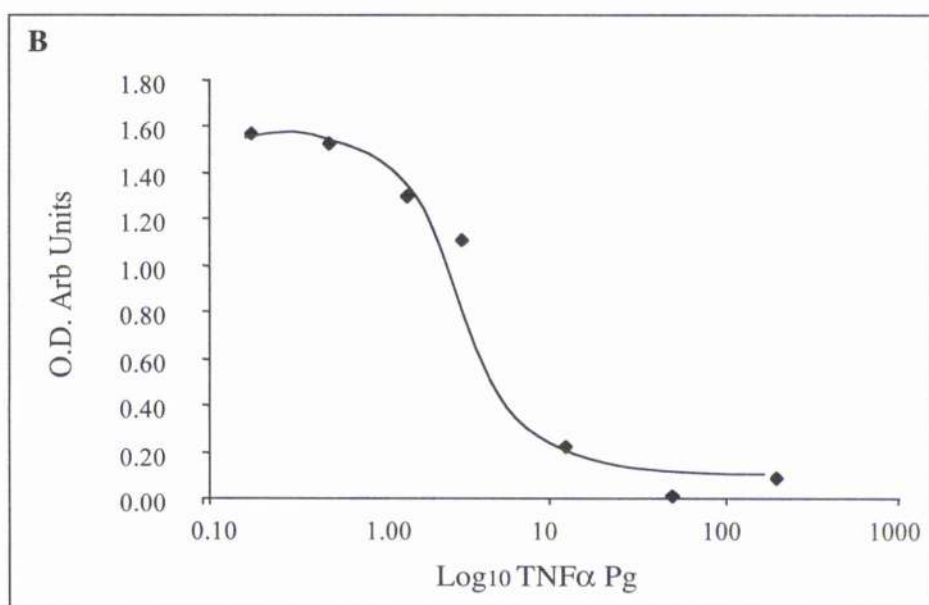
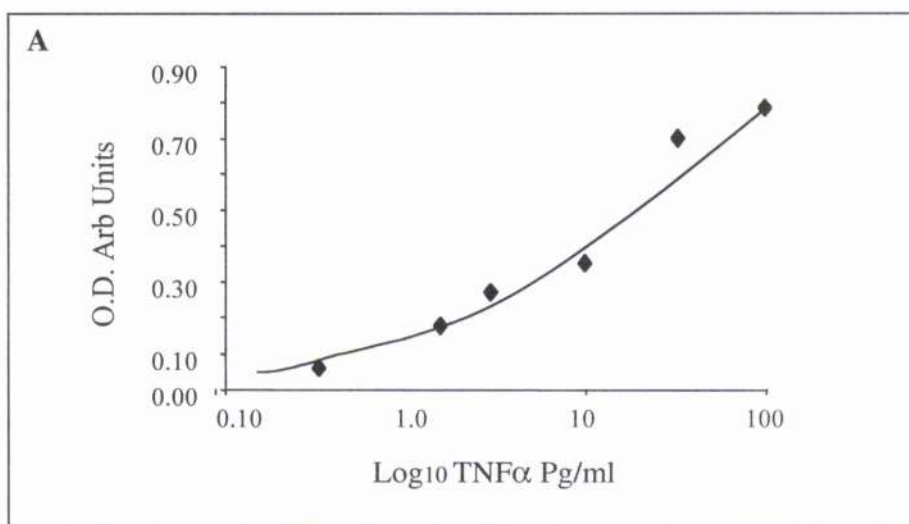


Fig App1.2 TNF α ELISA Standard Curves

To quantify the production of TNF α by RAW 264.7 cells treated with LPS and various inhibitors I used two different ELISA kits. Fig App1.2A, In house ELISA using commercially acquired TNF α antiserum bedded onto standard 96 well ELISA plates. A standard non-competitive ELISA protocol was followed. App1.2B, commercially acquired competitive TNF α ELISA kit. Note in non-competitive ELISA O.D. increases with increasing TNF α content, while in a competitive protocol the reverse is true.

(O.D. Optical density, Arb Units, Arbitrary units)

App 1.2B Commercial competitive TNF α ELISA

A commercial TNF α ELISA kit was also used in this study. This protocol differs from the in-house ELISA in being a competitive ELISA (Section 2.4.12.3). Thus pre-prepared ELISA plates with embedded capture antibodies were incubated with test samples and standards of known TNF α content. Following incubation and washing, HRP-conjugated TNF α was then incubated and washed off. Thus free antibody sites were occupied by HRP conjugate. Colour visualisation was achieved using ABTS as above. In this competitive ELISA a high reading at 405nm is equivalent to a low TNF α content.

App 1.3 Prostaglandin E2 quantification

A commercial competitive assay was used to quantify the PGE2 content of cell free culture medium from RAW 264.7 cells incubated with LPS with or without rolipram. This assay followed a competitive protocol as described above (Section 2.4.12.4). A sample standard curve for this assay is presented (Fig App 1.3).

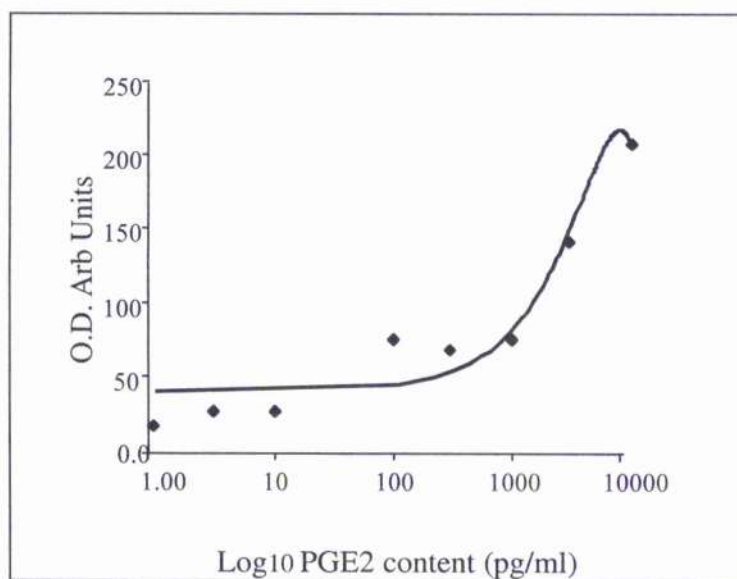


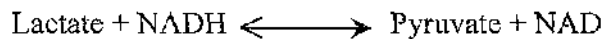
Fig App1.3 PGE2 ELISA Standard Curve

PGE2 content was quantified using a commercially acquired enzyme immunosorbant assay (EIA), (Assay Design Inc). This competitive assay was used to construct a standard curve from which to measure the PGE2 content of cell free culture medium from RAW 264.7 cell stimulated with LPS and various inhibitors.

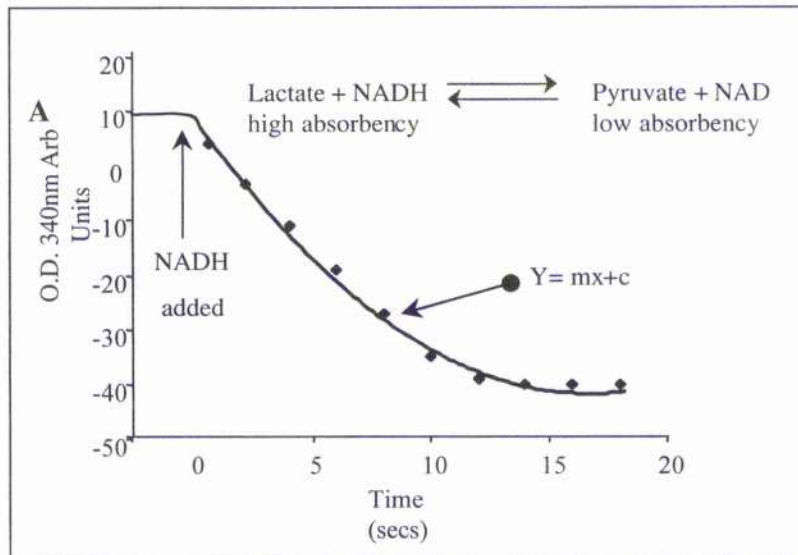
(O.D, Optical Density. Arb Units, Arbitrary Units).

Appendix 2 Lactate Dehydrogenase (LDH) analysis of cellular fractionation

Assessment of the subcellular distribution of PDE4B4 depended upon accurate fractionation of the transfected cells. To confirm the integrity of each compartment I measured the activity of LDH in each compartment. LDH is a cytosolic enzyme and should only appear to any extent in the S2 fraction. LDH catalyses the reaction:



The course of the reaction can be followed by measuring the decrease in absorption at 340nm, due to oxidation of NADH. Figure App 2.1A describes a typical plot from such an experiment. The rate of decrease in NADH absorption is proportional to the LDH activity and can be assessed by the gradient of the linear part of the curve. By comparing the activity of each fraction in the absence and presence of detergents that will lyse cells, allows assessment of the integrity of each fraction prepared in detergent free medium. Figure App 2.1B, presents three such experiments and demonstrates that most activity appears in the S2 fraction, and that little if any increase in LDH activity is seen when detergent is included (occluded). In the transfection, PDE4B4-2, significant activity is found in the P1 fraction suggesting contamination with S2 lysate. This lysate was duly excluded from further analysis.



B

	S2	P1	P2
Mock	-0.004	-0.001	-0.002
	-0.005	-0.002	-0.003
	-0.001	-0.001	-0.001
PDE4 B 4-1	-0.003	-0.001	-0.001
	-0.004	-0.001	-0.002
	-0.001	+0.00	-0.001
PDE4 B 4-2	-0.009	-0.004	-0.001
	-0.009	-0.012	-0.001
	-0.001	-	0.00

Fig App 2.1 Lactate dehydrogenase assay to confirm cellular fractionation

Cells were lysed in KHEM buffer by passage through a fine gauge needle. Lysates were subjected to low speed (15,000 rpm) and high speed (35,000rpm) centrifugation to fractionate into P1, low speed pellet; S2, high speed supernatant and P2 high speed pellet. To confirm the integrity of each pellet the activity of the enzyme lactate dehydrogenase (LDH) was assessed in each fraction. LDH is exclusively cytosolic in distribution and should only appear in the cytosolic (S2), fraction. LDH catalyses the reaction described in Fig App 2.1A. Activity of the enzyme can be assessed by the decrease in absorption of light at 340nm resulting from the oxidation of NADH. This activity is proportional to the gradient of the linear part of the NADH extinguish curve (fig App 2.1A). By comparing the activity of each fraction resuspended in KHEM (free) with the activity when each fraction is resuspended in detergent (occluded) the degree of contamination of each fraction can be assessed (fig App 2.1B). Thus in the S2 fraction if activity increases significantly in the occluded fraction. If there is significant activity in the pellet fractions it is likely that they are contaminated by S2 fraction. In the table above PDE4B4-2 lysis shows P1 contamination by S2 fraction or unlysed cells.

Appendix 3 Phosphodiesterase 4 activity in induced sputum from normal subjects

I wished to develop an assay for measuring the PDE activity from cells isolated from induced sputum to compare cell type against PDE4 activity. To investigate the ability of the standard assay protocol to measure sputum PDE4 activity I used two different subjects on three different days and isolated sputum using the induction method described. Sputum was processed to isolate cells and these were counted. PDE4 activity was measured in samples of lysed cells representing the same number of cells. I elected to use this method to reduce the effect of contaminating protein from non-cellular sources.

Fig App 4, demonstrates the variability that exists within samples isolated from the same subject on different days. This variability has a number of different possible explanations. Firstly environmental exposure to air-borne agents may influence the PDE4 activity in bronchial cells. Thus LPS may affect immune cells, and different quantities of LPS may be encountered on different days. Cellularity would not affect the data as this is controlled for, but the cell type may do so. It was the intention of my study to measure this aspect. PDE4 isoforms are very sensitive to the proteolytic effect of inflammatory proteases. Even in the presence of high doses of protease inhibitors it is likely that some degradation occurs. Finally the viability of the cells was measured during the counting process, however many cells may be going through stages of the apoptosis process while in the lung lumen and possibly during the subsequent processing. As has been described caspase 3, an essential apoptosis regulatory enzyme, cleaves and alters the activity of at least one PDE4 isoform

[232]. Thus many different factors may contribute to the intra-subject variability seen in induced sputum PDE4 activity.

As a result of the degree of variability and the requirement for involved and lengthy processing of material prior to performing the PDE4 assay, I elected not to use this method to analyse PDE4 further. Other methods that rely less on quantitative assay, such as rept. may prove to be a better tool to measure PDE4 isoform expression in cells isolated from induced sputum.

Summary

While PDE4 activity could be measured in reasonable quantity in induced sputum samples, the quality of the protein isolated was such that meaningful analysis was impossible at this stage. Other non-protein based methods may prove more useful in this tissue.

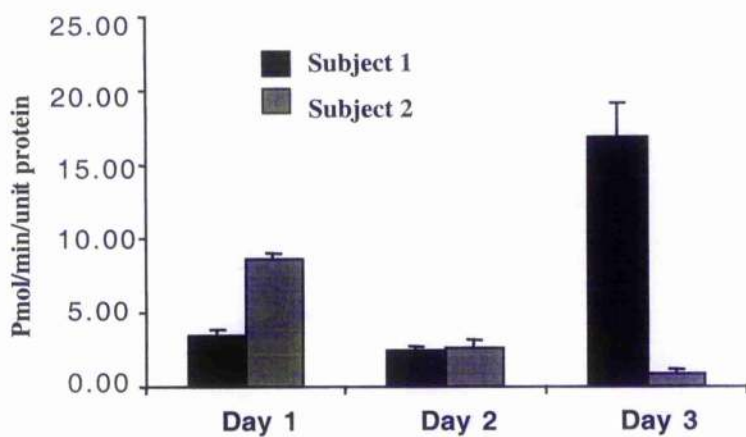


Fig App 3: Variability in PDE4 activity from induced sputum

Two normal subjects provided sputum samples as described. Samples from different days were processed, cell number counted and PDE4 activity was measured in lysed cells. PDE4 activity is presented, equalised for cell number to prevent non-cellular protein contamination. As can be seen considerable variability exists within the samples from different subjects.

References

1. Beavo, J.A. and L.L. Brunton, *Timeline: Cyclic nucleotide research; still expanding after half a century*. Nature Reviews Molecular Cell Biology, 2002. **3**(9): p. 710-8.
2. Strada, S. and W.J. Thompson, *Multiple forms of cyclic nucleotide phosphodiesterases: anomalies or biologic regulators?* Advances in Cyclic Nucleotide Research, 1978. **9**: p. 265-83.
3. Beavo, J.A., *Cyclic nucleotide phosphodiesterases: functional implications of multiple isoforms*. Physiological Reviews, 1995. **75**(4): p. 725-48.
4. Houslay, M. and G. Milligan, *Tailoring cAMP-signalling responses through isoform multiplicity*. Trends in Biochemical Sciences, 1997. **22**(6): p. 217-24.
5. Krupinski, J., et al., *Adenylyl cyclase amino acid sequence: possible channel- or transporter-like structure*. Science, 1989. **244**(4912): p. 1558-64.
6. Daniel, P., W. Walker, and J. Habener, *Cyclic AMP signalling and gene regulation*. Annual Review of Nutrition, 1998. **18**: p. 353-83.
7. Tang, W. and A. Gilman, *Construction of a soluble adenylyl cyclase activated by Gs alpha and forskolin*. Science, 1995. **268**(5218): p. 1769-72.
8. Hurley, JH, *Structure, mechanism and regulation of mammalian adenylyl cyclase*. The Journal of Biological Chemistry, 1999. **274**(12): p. 7599-7602.
9. Tang, W. and A. Gilman, *Type-specific regulation of adenylyl cyclase by G protein beta gamma subunits*. Science, 1991. **254**(5037): p. 1500-3.
10. Yan, S., et al., *Conversion of forskolin-insensitive to forskolin-sensitive (mouse-type IX) adenylyl cyclase*. Molecular Pharmacology, 1998. **53**(2): p. 182-7.

11. Yoshimura, M. and D. Cooper, *Cloning and expression of a Ca(2+)-inhibitable adenylyl cyclase from NCB-20 cells*. Proceedings of the National Academy of Sciences of the United States of America., 1992. **89**(15): p. 6716-20.
12. Dessauer, C., et al., *The interactions of adenylate cyclases with P-site inhibitors*. Trends in Pharmacological Sciences, 1999. **20**(5): p. 205-10.
13. Bol, G.F., A. Hulster, and T. Pfeuffer, *Adenylyl cyclase type II is stimulated by PKC via C-terminal phosphorylation*. Biochimica et Biophysica Acta, 1997. **1358**(3): p. 307-13.
14. Taussig, R., L. Quarmby, and A. Gilman, *Regulation of purified type I and type II adenylyl cyclases by G protein beta gamma subunits*. Journal of Biological Chemistry., 1993. **268**(1): p. 9-12.
15. Granneman, J., *Expression of adenylyl cyclase subtypes in brown adipose tissue: neural regulation of type III*. Endocrinology, 1995. **136**: p. 2007-12.
16. Gibson, R.M., Y. Ji-Buechler, and S.S. Taylor, *Interaction of the regulatory and catalytic subunits of cAMP-dependent protein kinase. Electrostatic sites on the type Ialpha regulatory subunit*. Journal of Biological Chemistry., 1997. **272**(26): p. 16343-50.
17. Francis, S. and J. Corbin, *Cyclic nucleotide-dependent protein kinases: intracellular receptors for cAMP and cGMP action*. Critical Reviews in Clinical Laboratory Sciences, 1999. **36**(4): p. 275-328.
18. Su, Y., et al., *Regulatory subunit of protein kinase A: structure of deletion mutant with cAMP binding domains*. Science, 1995. **269**(5225): p. 807-13.
19. Knighton, D., et al., *Crystal structure of the catalytic subunit of cyclic adenosine monophosphate-dependent protein kinase*. Science, 1991. **253**(5018): p. 407-14.
20. Roesler, W., Vandenberg GR, and Hanson. RW, *Cyclic AMP and the induction of eukaryotic gene transcription*. Journal of Biological Chemistry, 1988. **263**: p. 9063-66.

21. Kennelly, P.J. and Krebs, E.G., *Consensus sequences as substrate specificity determinants for protein kinase and protein phosphatases*. Journal of Biological Chemistry, 1991. **266**: p. 15555-58.
22. Richards, J., et al., *Analysis of the structural properties of cAMP-responsive element-binding protein (CREB) and phosphorylated CREB*. Journal of Biological Chemistry, 1996. **271**(23): p. 13716-23.
23. Anderson, A.E., et al., *Kv4.2 phosphorylation by cyclic AMP-dependent protein kinase*. Journal of Biological Chemistry, 2000. **275**(8): p. 5337-46.
24. Buchler, W., et al., *Regulation of gene expression by transfected subunits of cAMP-dependent protein kinase*. European Journal of Biochemistry, 1990. **188**(2): p. 253-9.
25. Montminy, M. and L. Bilezikjian, *Binding of a nuclear protein to the cyclic-AMP response element of the somatostatin gene*. Nature, 1987. **328**(6126): p. 175-8.
26. Parry, G.C. and N. Mackman, *Role of cyclic AMP response element-binding protein in cyclic AMP inhibition of NF-kappaB-mediated transcription*. Journal of Immunology, 1997. **159**(11): p. 5450-6.
27. Krebs, E. and J. Beavo, *Phosphorylation-dephosphorylation of enzymes*. Annual Review of Biochemistry, 1979. **48**: p. 923-59.
28. Hochstrasser, M., et al., *Paramecium has two regulatory subunits of cyclic AMP-dependent protein kinase, one unique to cilia*. Journal of Eukaryotic Microbiology, 1996. **43**(4): p. 356-62.
29. Brandon, E.P., et al., *Molecular structure of the C beta catalytic subunit of rat cAMP-dependent protein kinase and differential expression of C alpha and C beta isoforms in rat tissues and cultured cells*. Nature, 1996. **382**(6592): p. 622-6.
30. McKnight, G.S. and K.B. Foss, *Localization of the catalytic subunit C gamma of the cAMP-dependent protein kinase gene (PRKACG) to human chromosome region 9q13*. Neuron, 1989. **3**(1): p. 71-9.

31. Clegg, C., G. Cadd, and G.S. McKnight, *Genetic characterization of a brain-specific form of the type I regulatory subunit of cAMP-dependent protein kinase*. Proceedings of the National Academy of Sciences of the United States of America., 1988. **85**(11): p. 3703-7.
32. Ventra, C., et al., *The differential response of protein kinase A to cyclic AMP in discrete brain areas correlates with the abundance of regulatory subunit II*. Journal of Neurochemistry, 1996. **66**(4): p. 1752-61.
33. Macleod, J., et al., *Association of the regulatory subunit of a type II cAMP-dependent protein kinase and its binding proteins with the fibrous sheath of rat sperm flagellum*. European Journal of Biochemistry., 1994. **225**(1): p. 107-14.
34. Kondrashin, A.A., M.V. Nesterova, and Y.S. Cho-Chung, *Subcellular distribution of the R-subunits of cAMP-dependent protein kinase in LS-174T human colon carcinoma cells*. Biochemistry & Molecular Biology International., 1998. **45**(2): p. 237-44.
35. Sim, A.T. and J.D. Scott, *Targeting of PKA, PKC and protein phosphatases to cellular microdomains*. Cell Calcium, 1999. **26**(5): p. 209-17.
36. Dodge, K., et al., *mAkap assembles a protein kinase A/PDE4 phosphodiesterase cAMP signaling module*. EMBO Journal, 2001. **20**(8): p. 1921-30.
37. Kawasaki H, et al., *A family of cAMP-binding proteins that directly activate Rap 1*. Science, 1998. **282**: p. 2275-2279.
38. de Rooij, J., et al., *Epac is a Rap1 guanine-nucleotide-exchange factor directly activated by cyclic AMP*. Nature, 1998. **396**(6710): p. 474-7.
39. Asha, H., et al., *The Rap1 GTPase functions as a regulator of morphogenesis in vivo*. EMBO Journal, 1999. **18**(3): p. 605-15.
40. Hariharan, I., R. Carthew, and G. Rubin, *The Drosophila roughened mutation: activation of a rap homolog disrupts eye development and interferes with cell determination*. Cell, 1991. **67**(4): p. 717-22.

41. Grewal, S., et al., *Calcium and cAMP signals differentially regulate cAMP-responsive element-binding protein function via a Rap1-extracellular signal-regulated kinase pathway*. Journal of Biological Chemistry., 2000. **275**(44): p. 34433-41.
42. Franke, B., et al., *Sequential regulation of the small GTPase Rap1 in human platelets*. Molecular & Cellular Biology., 2000. **20**(3): p. 779-85.
43. Quilliam, L., et al., *Rap1A is a substrate for cyclic AMP-dependent protein kinase in human neutrophils*. Journal of Immunology, 1991. **147**(5): p. 1628-35.
44. Altschuler, D. and E.G. Lapetina, *Mutational analysis of the cAMP-dependent protein kinase-mediated phosphorylation site of Rap1b*. Journal of Biological Chemistry., 1993. **268**(10): p. 7527-31.
45. Kawasaki, H., et al., *A family of cAMP-binding proteins that directly activate Rap1*. Science., 1998. **282**(5397): p. 2275-9.
46. Hu, C., et al., *Effect of phosphorylation on activities of Rap1A to interact with Raf-1 and to suppress Ras-dependent Raf-1 activation*. Journal of Biological Chemistry., 1999. **274**(1): p. 48-51.
47. Beavo, J., J.G. Hardman, and E.W. Sutherland, *Hydrolysis of cyclic guanosine and adenosine 3',5'-monophosphates by rat and bovine tissues*. Journal of Biological Chemistry., 1970. **245**(21): p. 5649-55.
48. Patterson, W., J.G. Hardman, and E.W. Sutherland, *Apparent multiple forms of cyclic AMP phosphodiesterase from rat erythrocytes*. Molecular & Cellular Endocrinology, 1976. **5**(1-2): p. 51-66.
49. Thompson, W.J. and M.M. Appleman, *Multiple cyclic nucleotide phosphodiesterase activities from rat brain*. Biochemistry, 1971. **10**(2): p. 311-6.
50. Houslay, M., M. Sullivan, and G. Bolger, *The multienzyme PDE4 cyclic adenosine monophosphate-specific phosphodiesterase family: intracellular targeting, regulation, and selective inhibition by compounds exerting anti-inflammatory and antidepressant actions*. Advances in Pharmacology, 1998. **44**: p. 225-342.

51. Conti, M. and S. Jin, *The molecular biology of cyclic nucleotide phosphodiesterases*. Progress In Nucleic Acid Research, 2000. **63**: p. 1 - 37.
52. Omburo, G.A., et al., *Critical role of conserved histidine pairs HNXXH and HDXXH in recombinant human phosphodiesterase 4A*. Cell Signal, 1998. **10**(7): p. 491-7.
53. Watjen, W., et al., *Zn²⁺ and Cd²⁺ increase the cyclic GMP level in PC12 cells by inhibition of the cyclic nucleotide phosphodiesterase*. Toxicology, 2001. **157**(3): p. 167-75.
54. Richter, W., et al., *Identification of inhibitor binding sites of the cAMP-specific phosphodiesterase 4*. Cellular Signalling, 2001. **13**(4): p. 287-97.
55. Charbonneau, H., et al., *Evidence for domain organization within the 61-kDa calmodulin-dependent cyclic nucleotide phosphodiesterase from bovine brain*. Biochemistry, 1991. **30**(32): p. 7931-40.
56. Sonnenburg, W., et al., *Identification of inhibitory and calmodulin-binding domains of the PDE1A1 and PDE1A2 calmodulin-stimulated cyclic nucleotide phosphodiesterases*. Journal of Biological Chemistry., 1995. **270**(52): p. 30989-1000.
57. Rascon, A., et al., *Cloning and characterization of a cAMP-specific phosphodiesterase (TbPDE2B) from Trypanosoma brucei*. Proceedings of the National Academy of Sciences of the United States of America., 2002. **99**(7): p. 4714-9.
58. Fawcett, L., et al., *Molecular cloning and characterization of a distinct human phosphodiesterase gene family: PDE11A*. Proceedings of the National Academy of Sciences of the United States of America, 2000. **97**(7): p. 3702-7.
59. Qiu, Y. and R. Davis, *Genetic dissection of the learning/memory gene dunce of Drosophila melanogaster*. Genes & Development, 1993. **7**(7B): p. 1447-58.
60. Shakur, Y., et al., *Identification and characterization of the type-IVA cyclic AMP-specific phosphodiesterase RD1 as a membrane-bound protein expressed in cerebellum*. Biochemical Journal, 1995. **306**(Pt 3): p. 801-9.

61. Ye, Y., et al., *Development of rolipram-sensitive, cyclic AMP phosphodiesterase (PDE4) in rat primary neuronal cultures*. *Developmental Brain Research*, 2001. **130**(1): p. 115-21.
62. Sullivan, M., et al., *Identification and characterization of the human homologue of the short PDE4A cAMP-specific phosphodiesterase RD1 (PDE4A1) by analysis of the human HSPDE4A gene locus located at chromosome 19p13.2*. *Biochemical Journal*, 1998. **333**(Pt 3): p. 693-703.
63. Bolger, G., et al., *A family of human phosphodiesterases homologous to the dunce learning and memory gene product of Drosophila melanogaster are potential targets for antidepressant drugs*. *Molecular & Cellular Biology*, 1993. **13**(10): p. 6558-71.
64. Horton, Y., M. Sullivan, and M.D. Houslay, *Molecular cloning of a novel splice variant of human type IVA (PDE-IVA) cyclic AMP phosphodiesterase and localization of the gene to the p13.2-q12 region of human chromosome 19 [corrected]*. *Biochemical Journal*, 1995. **308**(Pt 2): p. 683-91.
65. MacKenzie, S., et al., *ERK2 mitogen-activated protein kinase binding, phosphorylation, and regulation of the PDE4D cAMP-specific phosphodiesterases. The involvement of COOH-terminal docking sites and NH2-terminal UCR regions*. *Journal of Biological Chemistry*, 2000. **275**(22): p. 16609-17.
66. Hoffmann, R., et al., *The MAP kinase ERK2 inhibits the cyclic AMP-specific phosphodiesterase HSPDE4D3 by phosphorylating it at Ser579*. *EMBO Journal*, 1999. **18**(4): p. 893-903.
67. Baillic, G., et al., *Sub-family selective actions in the ability of Erk2 MAP kinase to phosphorylate and regulate the activity of PDE4 cyclic AMP-specific phosphodiesterases*. *British Journal of Pharmacology*, 2000. **131**(4): p. 811-9.
68. Sette, C. and M. Conti, *Phosphorylation and activation of a cAMP-specific phosphodiesterase by the cAMP-dependent protein kinase. Involvement of serine 54 in the enzyme activation*. *Journal of Biological Chemistry*, 1996. **271**(28): p. 16526-34.

69. Beard, M., et al., *UCR1 and UCR2 domains unique to the cAMP-specific phosphodiesterase family form a discrete module via electrostatic interactions*. Journal of Biological Chemistry, 2000. **275**(14): p. 10349-58.
70. Houslay, M., et al., *Alternative splicing of the type-IVA cyclic AMP phosphodiesterase gene provides isoform variants with distinct N-terminal domains fused to a common, soluble catalytic unit: 'designer' changes in Vmax, stability and membrane association*. Biochemical Society Transactions, 1995. **23**(2): p. 393-8.
71. Shakur, Y., J.G. Pryde, and M.D. Houslay, *Engineered deletion of the unique N-terminal domain of the cyclic AMP-specific phosphodiesterase RD1 prevents plasma membrane association and the attainment of enhanced thermostability without altering its sensitivity to inhibition by rolipram*. Biochemical Journal, 1993. **292**(Pt 3): p. 677-86.
72. Scotland, G., et al., *Intracellular compartmentalization of PDE4 cyclic AMP-specific phosphodiesterases*. Methods (Duluth), 1998. **14**(1): p. 65-79.
73. Scotland, G. and M. Houslay, *Chimeric constructs show that the unique N-terminal domain of the cyclic AMP phosphodiesterase RD1 (RNPDE4A1A; rPDE-IVA1) can confer membrane association upon the normally cytosolic protein chloramphenicol acetyltransferase*. Biochemical Journal, 1995. **308**(Pt 2): p. 673-81.
74. Smith, K., et al., *Determination of the structure of the N-terminal splice region of the cyclic AMP-specific phosphodiesterase RD1 (RNPDE4A1) by 1H NMR and identification of the membrane association domain using chimeric constructs*. Journal of Biological Chemistry, 1996. **271**(28): p. 16703-11.
75. Baillie, G., et al., *TAPAS-1, a novel microdomain within the unique N-terminal region of the PDE4A1 cAMP-specific phosphodiesterase that allows rapid, Ca²⁺-triggered membrane association with selectivity for interaction with phosphatidic acid*. Journal of Biological Chemistry, 2002. **277**(31): p. 28298-309.
76. Huston, E., et al., *The human cyclic AMP-specific phosphodiesterase PDE-46 (HSPDE4A4B) expressed in transfected COS7 cells occurs as both particulate and cytosolic species that exhibit distinct kinetics of inhibition by the antidepressant rolipram*. Journal of Biological Chemistry, 1996. **271**(49): p. 31334-44.

77. Bolger, G., et al., *Characterization of five different proteins produced by alternatively spliced mRNAs from the human cAMP-specific phosphodiesterase PDE4D gene*. *Biochemical Journal*, 1997. **328**(Pt 2): p. 539-48.
78. Liu H and D. Maurice, *Phosphorylation-mediated activation and translocation of the cyclic AMP-specific phosphodiesterase PDE4D3 by cyclic AMP-dependent protein kinase and mitogen activated protein kinase*. *Journal of biological chemistry*, 1999. **274**(15): p. 10557-65.
79. Ramos-Morales, F., B.J. Druker, and S. Fischer, *Vav binds to several SH2/SH3 containing proteins in activated lymphocytes*. *Oncogene*, 1994. **9**(7): p. 1917-1923.
80. Vidal, M., V. Gigoux, and C. Garbay, *SH2 and SH3 domains as targets for anti-proliferative agents*. *Critical Reviews in Oncology Hematology*, 2001. **40**(2): p. 175-186.
81. O'Connell, J.C., et al., *The SH3 domain of Src tyrosyl protein kinase interacts with the N-terminal splice region of the PDE4A cAMP-specific phosphodiesterase RPDE-6 (RNPDE4A5)*. *Biochemical Journal*, 1996. **318**(Pt 1): p. 255-61.
82. McPhee, I., et al., *Association with the SRC family tyrosyl kinase LYN triggers a conformational change in the catalytic region of human cAMP-specific phosphodiesterase HSPDE4A4B. Consequences for rolipram inhibition*. *Journal of Biological Chemistry*, 1999. **274**(17): p. 11796-810.
83. Beard, M.B., et al., *The unique N-terminal domain of the cAMP phosphodiesterase PDE4D4 allows for interaction with specific SH3 domains*. *FEBS Letters*, 1999. **460**(1): p. 173-7.
84. Yarwood, S., et al., *The RACK1 signaling scaffold protein selectively interacts with the cAMP-specific phosphodiesterase PDE4D5 isoform*. *Journal of Biological Chemistry*, 1999. **274**(21): p. 14909-17.
85. Mochly-Rosen, D., et al., *Interaction of protein kinase C with RACK1, a receptor for activated C-kinase: a role in beta protein kinase C mediated signal transduction*. *Biochemical Society Transactions.*, 1995. **23**(3): p. 596-600.

86. Rodriguez, M., et al., *RACK1, a protein kinase C anchoring protein, coordinates the binding of activated protein kinase C and select pleckstrin homology domains in vitro*. *Biochemistry*, 1999. **38**(42): p. 13787-94.
87. Battaini, F., et al., *Protein kinase C anchoring deficit in postmortem brains of Alzheimer's disease patients*. *Experimental Neurology*, 1999. **159**(2): p. 559-64.
88. Liliental, J. and D.D. Chang, *Rack1, a receptor for activated protein kinase C, interacts with integrin beta subunit*. *Journal of Biological Chemistry*, 1998. **273**(4): p. 2379-83.
89. Geijsen, N., et al., *Association of RACK1 and PKCbeta with the common beta-chain of the IL-5/IL-3/GM-CSF receptor*. *Oncogene*, 1999. **18**(36): p. 5126-30.
90. Steele, M., et al., *Identification of a surface on the beta-propeller protein RACK1 that interacts with the cAMP-specific phosphodiesterase PDE4D5*. *Cellular Signalling*, 2001. **13**(7): p. 507-13.
91. Souness, J.E. and S. Rao, *Proposal for pharmacologically distinct conformers of PDE4 cyclic AMP phosphodiesterases*. *Cellular Signalling*, 1997. **9**(3-4): p. 227-36.
92. Souness, J.E., et al., *Evidence that cyclic AMP phosphodiesterase inhibitors suppress interleukin-2 release from murine splenocytes by interacting with a 'low-affinity' phosphodiesterase 4 conformer*. *British Journal of Pharmacology*, 1997. **121**(4): p. 743-50.
93. Martin, C., et al., *Airway relaxant and anti-inflammatory properties of a PDE4 inhibitor with low affinity for the high-affinity rolipram binding site*. *Naunyn Schmiedebergs Archives of Pharmacology*, 2002. **365**(4): p. 284-9.
94. Jacobitz, S., et al., *Role of conserved histidines in catalytic activity and inhibitor binding of human recombinant phosphodiesterase 4A*. *Molecular Pharmacology*, 1997. **51**(6): p. 999-1006.
95. Steiner, A., et al., *Compartmentalization of cyclic nucleotides and cyclic AMP-dependent protein kinases in rat liver: immunocytochemical demonstration*. *Advances in Cyclic Nucleotide Research*, 1978. **9**: p. 691-705.

96. Houslay, M., *Compartmentalization of cyclic AMP phosphodiesterases, signalling 'crosstalk', desensitization and the phosphorylation of Gi-2 add cell specific personalization to the control of the levels of the second messenger cyclic AMP.* *Advances in Enzyme Regulation*, 1995. **35**: p. 303-38.
97. Steinberg, S. and L. Brunton, *Compartmentation of G protein-coupled signalling pathways in cardiac myocytes.* *Annual Review Pharmacology and Toxicology*, 2001. **41**: p. 751 -73.
98. Chini, C.C., et al., *Compartmentalization of cAMP signaling in mesangial cells by phosphodiesterase isozymes PDE3 and PDE4. Regulation of superoxidation and mitogenesis.* *Journal of Biological Chemistry*, 1997. **272**(15): p. 9854-9.
99. Jurevicius, J. and R. Fischmeister, *Longitudinal distribution of Na⁺ and Ca²⁺ channels and beta-adrenoceptors on the sarcolemmal membrane of frog cardiomyocytes.* *Journal of Physiology.*, 1997. **503**(Pt 3): p. 471-7.
100. Barsony, J. and S. Marx, *Immunocytology on microwave-fixed cells reveals rapid and agonist-specific changes in subcellular accumulation patterns for cAMP or cGMP.* *Proceedings of the National Academy of Sciences of the United States of America*, 1990. **87**(3): p. 1188-1192.
101. Harootunian, A., et al., *Movement of the free catalytic subunit of cAMP-dependent protein kinase into and out of the nucleus can be explained by diffusion.* *Molecular Biology of the Cell*, 1992. **4**(10): p. 993-1002.
102. Ahmad, F., et al., *IL-3 and IL-4 activate cyclic nucleotide phosphodiesterases 3 (PDE3) and 4 (PDE4) by different mechanisms in FDCP2 myeloid cells.* *The Journal of Immunology*, 1999. **162**: p. 4864 - 4875.
103. Carr, D., et al., *Localization of the cAMP-dependent protein kinase to the postsynaptic densities by A-kinase anchoring proteins. Characterization of AKAP 79.* *Journal of Biological Chemistry.*, 1992. **267**(24): p. 16816-23.
104. Gray, P., et al., *Identification of a 15-kDa cAMP-dependent protein kinase-anchoring protein associated with skeletal muscle L-type calcium channels.* *Journal of Biological Chemistry.*, 1997. **272**(10): p. 6297-302.

105. Lin, R., S.B. Moss, and C.S. Rubin, *Characterization of S-AKAP84, a novel developmentally regulated A kinase anchor protein of male germ cells*. Journal of Biological Chemistry, 1995. **270**(46): p. 27804.
106. Juilfs, D., et al., *A subset of olfactory neurons that selectively express cGMP-stimulated phosphodiesterase (PDE2) and guanylyl cyclase-D define a unique olfactory signal transduction pathway*. Proceedings of the National Academy of Sciences of the United States of America, 1997. **94**(7): p. 3388-95.
107. Shakur, Y., et al., *Membrane localization of cyclic nucleotide phosphodiesterase 3 (PDE3). Two N-terminal domains are required for the efficient targeting to, and association of, PDE3 with endoplasmic reticulum*. Journal of Biological Chemistry, 2000. **275**(49): p. 38749-61.
108. Choi, Y., et al., *Identification of a novel isoform of the cyclic-nucleotide phosphodiesterase PDE3A expressed in vascular smooth-muscle myocytes*. Biochemical Journal, 2001. **353**(Pt 1): p. 41-50.
109. Lin, W. and B.C. Chen, *Distinct PKC isoforms mediate the activation of cPLA2 and adenylyl cyclase by phorbol ester in RAW264.7 macrophages*. British Journal of Pharmacology, 1998. **125**(7): p. 1601-9.
110. Dowd, D.R., et al., *Crosstalk during Ca²⁺-, cAMP-, and glucocorticoid-induced gene expression in lymphocytes*. Molecular & Cellular Endocrinology, 1997. **128**(1-2): p. 29-37.
111. Saxena, M., et al., *Crosstalk between cAMP-dependent kinase and MAP kinase through a protein tyrosine phosphatase*. Nature Cell Biology, 1999. **1**(5): p. 305-11.
112. MacKenzie, S., et al., *Stimulation of p70S6 kinase via a growth hormone-controlled phosphatidylinositol 3-kinase pathway leads to the activation of a PDE4A cyclic AMP-specific phosphodiesterase in 3T3-F442A preadipocytes*. Proceedings of the National Academy of Sciences of the United States of America, 1998. **95**(7): p. 3549-54.

113. Persson, C.G., *On the medical history of xanthines and other remedies for asthma: a tribute to HH Salter*. Thorax., 1985. **40**(12): p. 881-6.
114. Henney, C.S., H.R. Bourne, and L.M. Lichtenstein, *The role of cyclic 3',5' adenosine monophosphate in the specific cytolytic activity of lymphocytes*. Journal of Immunology, 1972. **108**(6): p. 1526-34.
115. Lichtenstein, L.M. and S. Margolis, *Histamine release in vitro: inhibition by catecholamines and methylxanthines*. Science, 1968. **161**(844): p. 902-3.
116. Essayan, D.M., *Cyclic nucleotide phosphodiesterase (PDE) inhibitors and immunomodulation*. Biochemical Pharmacology, 1999. **57**(9): p. 965-73.
117. Torphy, T.J., *Phosphodiesterase isozymes: molecular targets for novel antiasthma agents*. American Journal of Respiratory & Critical Care Medicine, 1998. **157**(2): p. 351-70.
118. Spina, D., L.J. Landells, and C.P. Page, *The role of phosphodiesterase enzymes in allergy and asthma*. Advances in Pharmacology (New York), 1998. **44**: p. 33-89.
119. Gantner, F., et al., *In vitro differentiation of human monocytes to macrophages: change of PDE profile and its relationship to suppression of tumour necrosis factor-alpha release by PDE inhibitors*. British Journal of Pharmacology, 1997. **121**(2): p. 221-31.
120. Peachell, P., et al., *Preliminary identification and role of phosphodiesterase isozymes in human basophils*. Journal of Immunology, 1992. **148**: p. 2503-10.
121. Weston, M.C. and P.T. Peachell, *Regulation of human mast cell and basophil function by cAMP*. General Pharmacology, 1998. **31**(5): p. 715-9.
122. Hatzelmann, A., H. Tenor, and C. Schudt, *Differential effects of non-selective phosphodiesterase inhibitors on human eosinophil functions*. British Journal Of Pharmacology, 1995. **114**: p. 821-31.
123. Dent, G., et al., *Inhibition of eosinophil cyclic nucleotide PDE activity and opsonised zymosan-stimulated respiratory burst by 'type IV'-selective PDE inhibitors*. British Journal of Pharmacology., 1991. **103**(2): p. 1339-46.

124. Souness, J., et al., *Suppression of eosinophil function by RP 73401, a potent and selective inhibitor of cyclic AMP-specific phosphodiesterase: comparison with rolipram*. British Journal of Pharmacology., 1995. **115**(1): p. 39-46.
125. Gantner, F., et al., *Phosphodiesterase profile of human B lymphocytes from normal and atopic donors and the effects of PDE inhibition on B cell proliferation*. British Journal of Pharmacology, 1998. **123**(6): p. 1031-8.
126. Gantner, F., et al., *Phosphodiesterase profiles of highly purified human peripheral blood leukocyte populations from normal and atopic individuals: a comparative study*. J Allergy Clin Immunol, 1997. **100**(4): p. 527-35.
127. Tenor, H., et al., *Cyclic nucleotide phosphodiesterase isoenzyme activities in human alveolar macrophages*. Clin Exp Allergy, 1995. **25**(7): p. 625-33.
128. Weston, M., N. Anderson, and P.T. Peachell, *Effects of phosphodiesterase inhibitors on human lung mast cell and basophil function*. British Journal of Pharmacology., 1997. **121**(2): p. 287-95.
129. Barnette, M., et al., *SB 207499 (Ariflo), a potent and selective second-generation phosphodiesterase 4 inhibitor: in vitro anti-inflammatory actions*. Journal of Pharmacology & Experimental Therapeutics., 1998. **284**(1): p. 420-6.
130. Souness, J., et al., *Characterization of guinea-pig eosinophil phosphodiesterase activity. Assessment of its involvement in regulating superoxide generation*. Biochemical Pharmacology., 1991. **42**(4): p. 937-45.
131. Underwood, D., et al., *Comparison of phosphodiesterase III, IV and dual III/IV inhibitors on bronchospasm and pulmonary eosinophil influx in guinea pigs*. Journal of Pharmacology & Experimental Therapeutics., 1994. **270**(1): p. 250-9.
132. Dent, G., et al., *Suppression of human eosinophil respiratory burst and cyclic AMP hydrolysis by inhibitors of type IV phosphodiesterase: interaction with the beta adrenoceptor agonist albuterol*. Journal of Pharmacology & Experimental Therapeutics, 1994. **271**(3): p. 1167-74.

133. Silva, P., et al., *Modulation of eotaxin formation and eosinophil migration by selective inhibitors of phosphodiesterase type 4 isoenzyme*. *British Journal of Pharmacology*, 2001. **134**(2): p. 283-94.
134. Trifilieff, A., et al., *Pharmacological profile of a novel phosphodiesterase 4 inhibitor, 4-(8-benzo[1,2,5]oxadiazol-5-yl-[1,7]naphthyridin-6-yl)-benzoic acid (NVP-ABE171), a 1,7-naphthyridine derivative, with anti-inflammatory activities*. *Journal of Pharmacology & Experimental Therapeutics*, 2002. **301**(1): p. 241-8.
135. Paul-Eugene, N., et al., *Role of cyclic nucleotides and nitric oxide in blood mononuclear cell IgE production stimulated by IL-4*. *Cytokine*, 1995. **7**(1): p. 64-9.
136. Kaminuma, O., et al., *Interleukin-5 production by peripheral blood mononuclear cells of asthmatic patients is suppressed by T-440: relation to phosphodiesterase inhibition*. *Journal of Pharmacology & Experimental Therapeutics*, 1996. **279**(1): p. 240-6.
137. Robicsek, S., et al., *Multiple high-affinity cAMP-phosphodiesterases in human T-lymphocytes*. *Biochemical Pharmacology*, 1991. **42**(4): p. 869-77.
138. Jimenez, J., et al., *Phosphodiesterase 4 inhibitors prevent cytokine secretion by T lymphocytes by inhibiting nuclear factor-kappaB and nuclear factor of activated T cells activation*. *Journal of Pharmacology & Experimental Therapeutics*, 2001. **299**(2): p. 753-9.
139. Banner, K.H. and C.P. Page, *Theophylline and selective phosphodiesterase inhibitors as anti-inflammatory drugs in the treatment of bronchial asthma*. *European Respiratory Journal*, 1995. **8**(6): p. 996-1000.
140. Li, L., C. Yee, and J.A. Beavo, *CD3- and CD28-dependent induction of PDE7 required for T cell activation*. *Science*, 1999. **283**(5403): p. 848-51.
141. Verghese, M.W., et al., *Differential regulation of human monocyte-derived TNF alpha and IL-1 beta by type IV cAMP-phosphodiesterase (cAMP-PDE) inhibitors*. *J Pharmacol Exp Ther*, 1995. **272**(3): p. 1313-20.
142. Seldon, P.M., et al., *Suppression of lipopolysaccharide-induced tumor necrosis factor-alpha generation from human peripheral blood monocytes by inhibitors of*

- phosphodiesterase 4: interaction with stimulants of adenylyl cyclase*. Mol Pharmacol, 1995. **48**(4): p. 747-57.
143. Griswold, D., et al., *Effect of selective phosphodiesterase type IV inhibitor, rolipram, on fluid and cellular phases of inflammatory response*. Inflammation., 1993. **17**(3): p. 333-44.
144. Grootendorst, D. and K. Rabe, *Selective phosphodiesterase inhibitors for the treatment of asthma and chronic obstructive pulmonary disease*. Current Opinion in Allergy and Clinical Immunology, 2002. **2**(1): p. 61-7.
145. Mazzeella, G., et al., *Role of monocyte/macrophage population in immune response*. Monaldi Archives for Chest Disease, 1998. **53**(1): p. 92-6.
146. Crapo, J., et al., *Morphometric characteristics of cells in the alveolar regions of mammalian lungs*. American review of Respiratory disease, 1983. **128**: p. 542-46.
147. Monick, M., et al., *Changes in PKC isoforms in human alveolar macrophages compared with blood monocytes*. American Journal of Physiology, 1998. **275**(2 Pt 1): p. L389-97.
148. Meerschaert, J. and M. Furie, *Monocytes use either CD11/CD18 or VLA-4 to migrate across human endothelium in vitro*. Journal of Immunology, 1994. **152**(4): p. 1915-26.
149. Rosseau, S., et al., *Monocyte migration through the alveolar epithelial barrier: adhesion molecule mechanisms and impact of chemokines*. Journal of Immunology, 2000. **164**(1): p. 427-35.
150. Schall, T.J., et al., *Selective attraction of monocytes and T lymphocytes of the memory phenotype by cytokine RANTES*. Nature., 1990. **347**(6294): p. 669-71.
151. Leonard, E. and T. Yoshimura, *Human monocyte chemoattractant protein-1 (MCP-1)*. Immunology Today, 1990. **11**(3): p. 97-101.
152. Sano, H., et al., *Human galectin-3 is a novel chemoattractant for monocytes and macrophages*. Journal of Immunology, 2000. **165**(4): p. 2156-64.

153. Huberman, E. and M.F. Callaham, *Induction of terminal differentiation in human promyelocytic leukemia cells by tumor-promoting agents*. Proceedings of the National Academy of Sciences of the United States of America, 1979. **76**(3): p. 1293-7.
154. Hass, R., et al., *TPA-induced differentiation and adhesion of U937 cells: changes in ultrastructure, cytoskeletal organization and expression of cell surface antigens*. European Journal of Cell Biology, 1989. **48**(2): p. 282-293.
155. Hass, R., et al., *Differentiation and retrodifferentiation of U937 cells: Reversible induction and suppression of intermediate filament protein synthesis*. European Journal of Cell Biology, 1990. **51**(2): p. 265-271.
156. Prudovsky, I., et al., *Antisense CD11b integrin inhibits the development of a differentiated monocyte/macrophage phenotype in human leukemia cells*. European Journal of Cell Biology, 2002. **81**(1): p. 36-42.
157. Kim, J.I., et al., *Induction of differentiation of the human histiocytic lymphoma cell line U-937 by hypericin*. Arch Pharm Res, 1998. **21**(1): p. 41-5.
158. Zeng, L. and M.D. Houslay, *Insulin and vasopressin elicit inhibition of cholera-toxin-stimulated adenylate cyclase activity in both hepatocytes and the P9 immortalized hepatocyte cell line through an action involving protein kinase C*. Biochemical Journal, 1995. **312**(Pt 3): p. 769-74.
159. Sands, W.A., et al., *Inhibition of nitric oxide synthesis by interleukin-4 may involve inhibiting the activation of protein kinase C epsilon*. European Journal of Immunology, 1994. **24**(10): p. 2345-50.
160. Valledor, A., et al., *Protein kinase C epsilon is required for the induction of mitogen-activated protein kinase phosphatase-1 in lipopolysaccharide-stimulated macrophages*. Journal of Immunology, 2000. **164**(1): p. 29-37.
161. Bingisser, R., et al., *Macrophage-Derived Nitric Oxide Regulates T Cell Activation via Reversible Disruption of the Jak3/STAT5 Signaling Pathway*. Journal of Immunology, 1998. **160**: p. 5729.

162. Olikowsky, T., et al., *Two distinct pathways of human macrophage differentiation are mediated by interferon-gamma and interleukin-10*. Immunology, 1997. **91**(1): p. 104-8.
163. Kambayashi, T., et al., *Cyclic nucleotide phosphodiesterase type IV participates in the regulation of IL-10 and in the subsequent inhibition of TNF-alpha and IL-6 release by endotoxin-stimulated macrophages*. Journal of Immunology, 1995. **155**(10): p. 4909-16.
164. Haslett, C., *Granulocyte apoptosis and its role in the resolution and control of lung inflammation*. American journal of critical care medicine, 1999. **160**: p. s5-s11.
165. Currie, A., G. Stewart, and A. McWilliam, *Alveolar macrophages bind and phagocytose allergen-containing pollen starch granules via C-type lectin and integrin receptors: implications for airway inflammatory disease*. Journal of Immunology, 2000. **164**: p. 3878-3886.
166. Pueringer, R., et al., *The relationship between alveolar macrophage TNF, IL-1, and PGE2 release, alveolitis, and disease severity in sarcoidosis*. Chest., 1993. **103**(3): p. 832-8.
167. Monick, M., J. Glazier, and G.W. Hunninghake, *Human alveolar macrophages suppress interleukin-1 (IL-1) activity via the secretion of prostaglandin E2*. American Review of Respiratory Disease, 1987. **135**(1): p. 72-7.
168. Catena, E., et al., *Phenotypic features and secretory pattern of alveolar macrophages in atopic asthmatic patients*. Monaldi Archives for Chest Disease, 1993. **48**(1): p. 6-15.
169. Marshall, B., et al., *Tumour necrosis factor alpha production in human alveolar macrophages: modulation by inhaled corticosteroid*. European respiratory journal, 2000. **15**: p. 764-770.
170. Hempel, S., M.M. Monick, and G.W. Hunninghake, *Effect of hypoxia on release of IL-1 and TNF by human alveolar macrophages*. American Journal of Respiratory Cell & Molecular Biology, 1996. **14**(2): p. 170-6.

171. Mitchell, R., et al., *Conservation of bronchiolar wall area during constriction and dilation of human airways*. Journal of Applied Physiology, 1997. **82**(3): p. 954-8.
172. Menard, G. and E.Y. Bissonnette, *Priming of alveolar macrophages by leukotriene D(4): potentiation of inflammation*. American Journal of Respiratory Cell & Molecular Biology., 2000. **23**(4): p. 572-7.
173. Furuie, H., et al., *Altered accessory cell function of alveolar macrophages: A possible mechanism for induction of Th2 secretory profile in idiopathic pulmonary fibrosis*. European Respiratory Journal, 1997. **10**(4): p. 787-794.
174. Viksman, M., et al., *Phenotypic analysis of alveolar macrophages and monocytes in allergic airway inflammation. I. Evidence for activation of alveolar macrophages, but not peripheral blood monocytes, in subjects with allergic rhinitis and asthma*. American Journal of Respiratory & Critical Care Medicine, 1997. **155**(3): p. 858-863.
175. Lensmar, C., et al., *Airway inflammation and altered alveolar macrophage phenotype pattern after repeated low-dose allergen exposure of atopic asthmatic subjects*. Clinical & Experimental Allergy, 1999. **29**(12): p. 1632-40.
176. Ouaz, F., et al., *Maturation of human myelomonocytic leukemia cells following ligation of the low affinity receptor for IgE (Fc epsilon RII/CD23)*. International Immunology, 1993. **5**(10): p. 1251-7.
177. Maus, U., et al., *Monocytes recruited into the alveolar air space of mice show a monocytic phenotype but upregulate CD14*. American Journal of Physiology - Lung Cellular & Molecular Physiology, 2001. **280**(1): p. I.58-68.
178. Strohmeier, G., et al., *Lipopolysaccharide binding protein potentiates airway reactivity in a murine model of allergic asthma*. Journal of Immunology, 2001. **166**(3): p. 2063-2070.
179. Barnes, P. and F. Liew, *Nitric oxide and asthmatic inflammation*. Immunology Today., 1995. **16**(3): p. 128-30.

180. Kline, J., et al., *Variable airway responsiveness to inhaled lipopolysaccharide*. American Journal of Respiratory & Critical Care Medicine., 1999. **160**(1): p. 297-303.
181. Held, H. and S. Uhlig, *Mechanisms of endotoxin-induced airway and pulmonary vascular hyperreactivity in mice*. American Journal of Respiratory & Critical Care Medicine, 2000. **162**(4 Pt 1): p. 1547-52.
182. Meerschaert, J., et al., *CD14(+) cells are necessary for increased survival of eosinophils in response to lipopolysaccharide*. American Journal of Respiratory Cell & Molecular Biology, 2000. **23**(6): p. 780-7.
183. Wollin, L., et al., *Granulocyte-macrophage colony-stimulating factor amplifies lipopolysaccharide-induced bronchoconstriction by a neutrophil- and cyclooxygenase 2-dependent mechanism*. American Journal of Respiratory & Critical Care Medicine, 2001. **163**(2): p. 443-50.
184. Martin, C., S. Uhlig, and V. Ullrich, *Cytokine-Induced Bronchoconstriction in Precision-Cut Lung Slices Is Dependent upon Cyclooxygenase-2 and Thromboxane Receptor Activation*. American Journal Respiratory Cellular & Molecular Biology., 2001. **24**((2)): p. 139-145.
185. Sousa, A., et al., *Enhanced expression of cyclo-oxygenase isoenzyme 2 (COX-2) in asthmatic airways and its cellular distribution in aspirin-sensitive asthma*. Thorax., 1997. **52**(11): p. 940-5.
186. Fuller, R.W., et al., *Human alveolar macrophage activation: inhibition by forskolin but not beta-adrenoceptor stimulation or phosphodiesterase inhibition*. Pulmonary Pharmacology., 1988. **1**(2): p. 101-6.
187. Hasko, G., et al., *Stimulation of beta-adrenoceptors inhibits endotoxin-induced IL-12 production in normal and IL-10 deficient mice*. Journal of Neuroimmunology, 1998. **88**(1-2): p. 57-61.
188. Sigola, L.B. and R.B. Zinyama, *Adrenaline inhibits macrophage nitric oxide production through beta1 and beta2 adrenergic receptors*. Immunology, 2000. **100**(3): p. 359-363.

189. Nakamura, A., et al., *Effect of beta2-adrenoceptor activation and angiotensin II on tumour necrosis factor and interleukin 6 gene transcription in the rat renal resident macrophage cells*. Cytokine, 1999. **11**(10): p. 759-765.
190. Panina-Bordignon, P., et al., *Beta2-agonists prevent Th1 development by selective inhibition of interleukin 12*. Journal of Clinical Investigation, 1997. **100**(6): p. 1513-9.
191. Siegmund, B., et al., *Adrenaline enhances LPS-induced IL-10 synthesis: evidence for protein kinase A-mediated pathway*. International Journal of Immunopharmacology, 1998. **20**(1-3): p. 57-69.
192. Hasko, G., et al., *Isoproterenol inhibits Il-10, TNF-alpha, and nitric oxide production in RAW 264.7 macrophages*. Brain Research Bulletin, 1998. **45**(2): p. 183-7.
193. Hubbard, N., et al., *Differential mRNA expression of prostaglandin receptor subtypes in macrophage activation*. Prostaglandins Leukotrienes & Essential Fatty Acids., 2001. **65**(5-6): p. 287-94.
194. Procopio, D.O., et al., *Differential inhibitory mechanism of cyclic AMP on TNF-alpha and IL-12 synthesis by macrophages exposed to microbial stimuli*. British Journal of Pharmacology, 1999. **127**(5): p. 1195-205.
195. Rossi, A.G., et al., *Regulation of macrophage phagocytosis of apoptotic cells by cAMP*. Journal of Immunology, 1998. **160**(7): p. 3562-8.
196. Coleman, D.L., J. Liu, and A.H. Bartiss, *Recombinant granulocyte-macrophage colony-stimulating factor increases adenylate cyclase activity in murine peritoneal macrophages*. Journal of Immunology, 1989. **143**(12): p. 4134-4140.
197. von Knethen, A., A. Lotero, and B. Brune, *Etoposide and cisplatin induced apoptosis in activated RAW 264.7 macrophages is attenuated by cAMP-induced gene expression*. Oncogene, 1998. **17**(3): p. 387-94.
198. Yasui, K., et al., *Theophylline accelerates human granulocyte apoptosis not via phosphodiesterase inhibition*. Journal of Clinical Investigation, 1997. **100**(7): p. 1677-84.

199. Chang, C., et al., *The involvement of tyrosine kinases, cyclic AMP/protein kinase A, and p38 mitogen-activated protein kinase in IL-13-mediated arginase I induction in macrophages: its implications in IL-13-inhibited nitric oxide production.* Journal of Immunology, 2000. **165**(4): p. 2134-41.
200. Delgado, M. and D. Ganea, *Vasoactive intestinal peptide and pituitary adenylate cyclase activating polypeptide inhibit the MEKK1/MEK4/JNK signaling pathway in LPS-stimulated macrophages.* Journal of Neuroimmunology, 2000. **110**(1-2): p. 97-105.
201. Kurokawa, K. and J. Kato, *Cyclic AMP delays G2 progression and prevents efficient accumulation of cyclin B1 proteins in mouse macrophage cells.* Cell Structure & Function, 1998. **23**(6): p. 357-65.
202. Banner, K., et al., *Possible Contribution of Prostaglandin E2 to the antiproliferative effect of phosphodiesterase 4 inhibitors in human mononuclear cells.* Biochemical Pharmacology, 1999. **58**(9): p. 1487-95.
203. Delgado, M., et al., *VIP and PACAP induce shift to a Th2 response by upregulating B7.2 expression.* Annals of the New York Academy of Sciences., 2000. **921**: p. 68-78.
204. Caron, E., A. Self, and A. Hall, *The GTPase Rap1 controls functional activation of macrophage integrin alphaMbeta2 by LPS and other inflammatory mediators.* Current Biology, 2000. **10**(16): p. 974-8.
205. Proffitt, J., et al., *An ATF/CREB-binding site is essential for cell-specific and inducible transcription of the murine MIP-1 beta cytokine gene.* Gene, 1995. **152**(2): p. 173-9.
206. Delgado, M., et al., *Vasoactive intestinal peptide and pituitary adenylate cyclase-activating polypeptide inhibit tumor necrosis factor alpha transcriptional activation by regulating nuclear factor-kB and cAMP response element-binding protein/c-Jun.* Journal of Biological Chemistry, 1998. **273**(47): p. 31427-36.

207. Vane, J., et al., *Inducible isoforms of cyclooxygenase and nitric-oxide synthase in inflammation*. Proceedings of the National Academy of Sciences of the United States of America, 1994. **91**(6): p. 2046-2050.
208. Savla, U., et al., *Prostaglandin E(2) regulates wound closure in airway epithelium*. American Journal of Physiology - Lung Cellular & Molecular Physiology, 2001. **280**(3): p. L421-31.
209. Fournier, T., V. Fadok, and P.M. Henson, *Tumor necrosis factor-alpha inversely regulates prostaglandin D2 and prostaglandin E2 production in murine macrophages. Synergistic action of cyclic AMP on cyclooxygenase-2 expression and prostaglandin E2 synthesis*. Journal of Biological Chemistry, 1997. **272**(49): p. 31065-72.
210. Fujimura, M., et al., *Effect of a thromboxane A2 receptor antagonist (AA-2414) on bronchial hyperresponsiveness to methacholine in subjects with asthma*. Journal of Allergy & Clinical Immunology., 1991. **87**(1 Pt 1): p. 23-7.
211. Pang, L., et al., *The COX-1/COX-2 balance in asthma*. Clinical & Experimental Allergy., 1998. **28**(9): p. 1050-8.
212. Wadleigh, D.J., et al., *Transcriptional activation of the cyclooxygenase-2 gene in endotoxin-treated RAW 264.7 macrophages*. Journal of Biological Chemistry, 2000. **275**(9): p. 6259-66.
213. Hinz, B., K. Brune, and A. Pahl, *Prostaglandin E2 upregulates cyclooxygenase-2 expression in lipopolysaccharide-stimulated RAW 264.7 macrophages*. Biochemical & Biophysical Research Communications, 2000. **272**(3): p. 744-748.
214. Lo, C.J., et al., *Cyclooxygenase 2 (COX-2) gene activation is regulated by cyclic adenosine monophosphate*. Shock, 2000. **13**(1): p. 41-5.
215. Hinz, B., K. Brune, and A. Pahl, *Cyclooxygenase-2 expression in lipopolysaccharide-stimulated human monocytes is modulated by cyclic AMP, prostaglandin E2, and nonsteroidal anti-inflammatory drugs*. Biochemical & Biophysical Research Communications, 2000. **278**(3): p. 790-796.

216. Caivano, M. and P. Cohen, *Role of mitogen-activated protein kinase cascades in mediating lipopolysaccharide-stimulated induction of cyclooxygenase-2 and IL-1 beta in RAW264 macrophages*. Journal of Immunology, 2000. **164**(6): p. 3018-25.
217. Miller, C., et al., *Transcriptional induction of cyclooxygenase-2 gene by okadaic acid inhibition of phosphatase activity in human chondrocytes: co-stimulation of AP-1 and CRE nuclear binding proteins*. Journal of Cellular Biochemistry, 1998. **69**(4): p. 392-413.
218. Gorgoni, B., et al., *The transcription factor C/EBPbeta is essential for inducible expression of the cox-2 gene in macrophages but not in fibroblasts*. Journal of Biological Chemistry., 2001. **276**(44): p. 40769-77.
219. Barnes, P., *Nitric oxide and airway disease*. Annals of Medicine, 1995. **27**(3): p. 389-93.
220. Nusing, R.M., et al., *Effect of cyclic AMP and prostaglandin E2 on the induction of nitric oxide- and prostanoid-forming pathways in cultured rat mesangial cells*. Biochemical Journal, 1996. **313**(Pt 2): p. 617-23.
221. Thompson, W., et al., *Cyclic adenosine 3':5'-monophosphate phosphodiesterase. Distinct forms in human lymphocytes and monocytes*. Journal of Biological Chemistry., 1976. **251**(16): p. 4922-9.
222. Manning, C., et al., *Prolonged beta adrenoceptor stimulation up-regulates cAMP phosphodiesterase activity in human monocytes by increasing mRNA and protein for phosphodiesterases 4A and 4B*. Journal of Pharmacology & Experimental Therapeutics., 1996. **276**(2): p. 810-8.
223. Souness, J.E., et al., *Evidence that cyclic AMP phosphodiesterase inhibitors suppress TNF alpha generation from human monocytes by interacting with a 'low-affinity' phosphodiesterase 4 conformer*. Br J Pharmacol, 1996. **118**(3): p. 649-58.
224. Verghese, M.W., et al., *Regulation of distinct cyclic AMP-specific phosphodiesterase (phosphodiesterase type 4) isozymes in human monocytic cells*. Mol Pharmacol, 1995. **47**(6): p. 1164-71.

225. Kelly, J.J., P.J. Barnes, and M.A. Giembycz, *Characterization of phosphodiesterase 4 in guinea-pig macrophages: multiple activities, association states and sensitivity to selective inhibitors*. British Journal of Pharmacology, 1998. **124**(1): p. 129-40.
226. Torphy, T.J., et al., *Salbutamol up-regulates PDE4 activity and induces a heterologous desensitization of U937 cells to prostaglandin E2. Implications for the therapeutic use of beta-adrenoceptor agonists*. J Biol Chem, 1995. **270**(40): p. 23598-604.
227. Chan, S.C., et al., *Immunochemical characterization of the distinct monocyte cyclic AMP-phosphodiesterase from patients with atopic dermatitis*. J Allergy Clin Immunol, 1993. **91**(6): p. 1179-88.
228. Tenor, H., et al., *Effects of theophylline and rolipram on leukotriene C4 (LTC4) synthesis and chemotaxis of human eosinophils from normal and atopic subjects*. Br J Pharmacol, 1996. **118**(7): p. 1727-35.
229. Landells, L., et al., *Identification and quantification of phosphodiesterase 4 subtypes in CD4 and CD8 lymphocytes from healthy and asthmatic subjects*. British Journal of Pharmacology, 2001. **133**(5): p. 722-9.
230. Corsini, F., et al., *A defective protein kinase C anchoring system underlying age-associated impairment in TNF-alpha production in rat macrophages*. Journal of Immunology., 1999. **163**(6): p. 3468-73.
231. Herrera-Velit, P. and N.E. Reiner, *Bacterial lipopolysaccharide induces the association and coordinate activation of p53/56lyn and phosphatidylinositol 3-kinase in human monocytes*. Journal of Immunology, 1996. **156**(3): p. 1157-65.
232. Huston, E., et al., *The cAMP-specific phosphodiesterase PDE4A5 is cleaved downstream of its SH3 interaction domain by caspase-3. Consequences for altered intracellular distribution*. Journal of Biological Chemistry, 2000. **275**(36): p. 28063-74.

233. Huston, E., et al., *Molecular cloning and transient expression in COS7 cells of a novel human PDE4B cAMP-specific phosphodiesterase, HSPDE4B3*. *Biochemical Journal*, 1997. **328**(Pt 2): p. 549-58.
234. Rena, G., et al., *Molecular cloning, genomic positioning, promoter identification, and characterization of the novel cyclic amp-specific phosphodiesterase PDE4A10*. *Molecular Pharmacology*, 2001. **59**(5): p. 996-1011.
235. McPhee, I., M.D. Houslay, and S.J. Yarwood, *Use of an activation-specific probe to show that Rap1A and Rap1B display different sensitivities to activation by forskolin in rat1 cells*. *FEBS Letters*, 2000. **477**(3): p. 213-8.
236. Szpirer, C., et al., *Chromosomal localization of the human and rat genes (PDE4D and PDE4B) encoding the cAMP-specific phosphodiesterases 3 and 4*. *Cytogenetics & Cell Genetics*, 1995. **69**(1-2): p. 11-4.
237. Milatovich, A., et al., *Chromosome localizations of genes for five cAMP-specific phosphodiesterases in man and mouse*. *Somatic Cell & Molecular Genetics*, 1994. **20**(2): p. 75-86.
238. Hoffmann, R., et al., *cAMP-specific phosphodiesterase HSPDE4D3 mutants which mimic activation and changes in rolipram inhibition triggered by protein kinase A phosphorylation of Ser-54: generation of a molecular model*. *Biochemical Journal*, 1998. **333**(Pt 1): p. 139-49.
239. MacKenzie, S., et al., *Long PDE4 cAMP specific phosphodiesterases are activated by protein kinase A-mediated phosphorylation of a single serine residue in Upstream Conserved Region 1 (UCR1)*. *British Journal of Pharmacology*, 2002. **136**(3): p. 421-33.
240. Pooley, L., et al., *Intracellular localization of the PDE4A cAMP-specific phosphodiesterase splice variant RD1 (RNPDE4A1A) in stably transfected human thyroid carcinoma FTC cell lines*. *Biochemical Journal*, 1997. **321**(Pt 1): p. 177-85.
241. O'Connell, J., et al., *The SH3 domain of Src tyrosyl protein kinase interacts with the N-terminal splice region of the PDE4A cAMP-specific phosphodiesterase RPDE-6 (RNPDE4A5)*. *Biochemical Journal*, 1996. **318**(Pt 1): p. 255-61.

242. von Knethen, A. and B. Brune, *Attenuation of macrophage apoptosis by the cAMP-signaling system*. Molecular & Cellular Biochemistry, 2000. **212**(1-2): p. 35-43.
243. Kamisato, S., et al., *Involvement of intracellular cyclic GMP and cyclic GMP-dependent protein kinase in alpha-elastin-induced macrophage chemotaxis*. Journal of Biochemistry, 1997. **121**(5): p. 862-7.
244. Katakami, Y., et al., *Regulation of tumour necrosis factor production by mouse peritoneal macrophages: the role of cellular cyclic AMP*. Immunology, 1988. **64**(4): p. 719-24.
245. Strassmann, G., et al., *Evidence for the involvement of interleukin 10 in the differential deactivation of murine peritoneal macrophages by prostaglandin E2*. Journal of Experimental Medicine, 1994. **180**(6): p. 2365-70.
246. Landells, L., et al., *A biochemical and functional assessment of monocyte phosphodiesterase activity in healthy and asthmatic subjects*. Pulmonary Pharmacology & Therapeutics., 2000. **13**(5): p. 231-9.
247. MacKenzie, S. and M.D. Houslay, *Action of rolipram on specific PDE4 cAMP phosphodiesterase isoforms and on the phosphorylation of cAMP-response-element-binding protein (CREB) and p38 mitogen-activated protein (MAP) kinase in U937 monocytic cells*. Biochemical Journal, 2000. **347**(Pt 2): p. 571-8.
248. DiSanto, M., K.B. Glaser, and R.J. Heaslip, *Phospholipid regulation of a cyclic AMP-specific phosphodiesterase (PDE4) from U937 cells*. Cellular Signalling., 1995. **7**(8): p. 827-35.
249. Lopez-Lluch, G., et al., *Redox regulation of cAMP levels by ascorbate in 1,25-dihydroxy- vitamin D3-induced differentiation of HL-60 cells*. Biochemical Journal, 1998. **331**(Pt 1): p. 21-7.
250. Allen, W., et al., *Rho, Rac and Cdc42 regulate actin organization and cell adhesion in macrophages*. Journal of Cell Science, 1997. **110**(Pt 6): p. 707-20.
251. Spertini, O., et al., *Monocyte attachment to activated human vascular endothelium in vitro is mediated by leukocyte adhesion molecule-1 (L-selectin) under nonstatic conditions*. Journal of Experimental Medicine, 1992. **175**(6): p. 1789-92.

252. Brown, G., M.M. Monick, and G.W. Hunninghake, *Human alveolar macrophage arachidonic acid metabolism*. American Journal of Physiology., 1988. **254**(6 Pt 1): p. C809-15.
253. Wang, P., et al., *Phosphodiesterase 4B2 is the predominant phosphodiesterase species and undergoes differential regulation of gene expression in human monocytes and neutrophils*. Molecular Pharmacology., 1999. **56**(1): p. 170-4.
254. Manning, C., et al., *Suppression of human inflammatory cell function by subtype-selective PDE4 inhibitors correlates with inhibition of PDE4A and PDE4B*. British Journal of Pharmacology., 1999. **128**(7): p. 1393-8.
255. Jin, S. and M. Conti, *Induction of the cyclic nucleotide phosphodiesterase PDE4B is essential for LPS-activated TNF-alpha responses*. Proceedings of the National Academy of Sciences of the United States of America., 2002. **99**(11): p. 7628-33.
256. Greten, T., et al., *The specific type IV phosphodiesterase inhibitor rolipram differentially regulates the proinflammatory mediators TNF-alpha and nitric oxide*. International Journal of Immunopharmacology, 1995. **17**(7): p. 605-10.
257. Liang, L., E. Beshay, and G.J. Prud'homme, *The phosphodiesterase inhibitors pentoxifylline and rolipram prevent diabetes in NOD mice*. Diabetes, 1998. **47**(4): p. 570-5.
258. Ezeamuzie, C., *Requirement of additional adenylate cyclase activation for the inhibition of human eosinophil degranulation by phosphodiesterase IV inhibitors*. European Journal of Pharmacology, 2001. **417**(1-2): p. 11-8.
259. Kotlyarov, A., et al., *MAPKAP kinase 2 is essential for LPS-induced TNF-alpha biosynthesis*. Nature Cell Biology, 1999. **1**(2): p. 94-7.
260. Meng, F. and C.A. Lowell, *Lipopolysaccharide (LPS)-induced macrophage activation and signal transduction in the absence of Src-family kinases Hck, Fgr, and Lyn*. Journal of Experimental Medicine., 1997. **185**(9): p. 1661-70.
261. Dhillon, A., et al., *Cyclic AMP-dependent kinase regulates Raf-1 kinase mainly by phosphorylation of serine 259*. Molecular & Cellular Biology., 2002. **22**(10): p. 3237-46.

262. Guthridge, C., et al., *Lipopolysaccharide and Raf-1 kinase regulate secretory interleukin-1 receptor antagonist gene expression by mutually antagonistic mechanisms*. *Molecular & Cellular Biology*, 1997. **17**(3): p. 1118-28.
263. Csar, X., et al., *cAMP suppresses p21ras and Raf-1 responses but not the Erk-1 response to granulocyte-colony-stimulating factor: possible Raf-1-independent activation of Erk-1*. *Biochemical Journal*, 1997. **322**(Pt 1): p. 79-87.
264. Vossler, M., et al., *cAMP activates MAP kinase and Elk-1 through a B-Raf- and Rap1-dependent pathway*. *Cell*, 1997. **89**(1): p. 73-82.
265. Mochizuki, N., et al., *Activation of the ERK/MAPK pathway by an isoform of rap1GAP associated with G alpha(i)*. *Nature*, 1999. **400**(6747): p. 891-4.
266. Marshall, C., *Signal transduction. Taking the Rap*. *Nature*, 1998. **392**(6676): p. 553-4.
267. Denfing, L., et al., *Nuclear translocation of NF-kappaB in lipopolysaccharide-treated macrophages fails to correspond to endotoxicity: evidence suggesting a requirement for a gamma interferon-like signal*. *Infection & Immunity*, 1998. **66**(4): p. 1638-47.
268. Fitzgerald, K., et al., *Mal (MyD88-adaptor-like) is required for Toll-like receptor-4 signal transduction*. *Nature*, 2001. **413**(6851): p. 78-83.
269. Mandriks, I., R. Muceniece, and J.F. Wikberg, *Effects of melanocortin peptides on lipopolysaccharide/interferon-gamma-induced NF-kappaB DNA binding and nitric oxide production in macrophage-like RAW 264.7 cells: evidence for dual mechanisms of action*. *Biochemical Pharmacology*, 2001. **61**(5): p. 613-21.
270. Corsini, E., et al., *Ontogenesis of protein kinase C betaII and its anchoring protein RACK1 in the maturation of alveolar macrophage functional responses*. *Immunology Letters*, 2001. **76**(2): p. 89-93.
271. Valledor, A., et al., *The differential time-course of extracellular-regulated kinase activity correlates with the macrophage response toward proliferation or activation*. *Journal of Biological Chemistry*, 2000. **275**(10): p. 7403-9.

272. Fiercn, M., et al., *Prostaglandin E2 inhibits the release of tumor necrosis factor-alpha, rather than interleukin 1 beta, from human macrophages*. Immunology Letters., 1992. **31**(1): p. 85-90.
273. Hruby, Z. and K. Beck, *Cytotoxic effect of autocrine and macrophage-derived nitric oxide on cultured rat mesangial cells*. Clinical & Experimental Immunology., 1997. **107**(1): p. 76-82.
274. Muhl, H., D. Kunz, and J. Pfeilschifter, *Expression of nitric oxide synthase in rat glomerular mesangial cells mediated by cyclic AMP*. British Journal of Pharmacology., 1994. **112**(1): p. 1-8.
275. Pang, L. and J. Hoult, *Repression of inducible nitric oxide synthase and cyclooxygenase-2 by prostaglandin E2 and other cyclic AMP stimulants in J774 macrophages*. Biochemical Pharmacology., 1997. **53**(4): p. 493-500.
276. de Rooij, J., et al., *Mechanism of regulation of the Epac family of cAMP-dependent RapGEFs*. Journal of Biological Chemistry., 2000. **275**(27): p. 20829-36.
277. Stork, P. and J.M. Schmitt, *Crosstalk between cAMP and MAP kinase signaling in the regulation of cell proliferation*. Trends in Cell Biology, 2002. **12**(6): p. 258-66.
278. Staples, K., et al., *Adenosine 3',5'-cyclic monophosphate (cAMP)-dependent inhibition of IL-5 from human T lymphocytes is not mediated by the cAMP-dependent protein kinase A*. Journal of Immunology., 2001. **167**(4): p. 2074-80.
279. Schwarze, S., et al., *In vivo protein transduction: delivery of a biologically active protein into the mouse*. Science., 1999. **285**(5433): p. 1569-72.
280. MarCarrio, M., Cubarsi, R, and A. and Villaverde, *Fine architecture of bacterial inclusion bodies*. FEBS Letts, 2000. **471**: p. 7-11.
281. Kozak, M., *Initiation of translation in prokaryotes and eukaryotes*. Gene, 1999. **234**: p. 187-208.
282. Frangioni, J. and B. Neel, *Solubilisation and purification of enzymatically active glutathione S-transferase (pGEX) fusion proteins*. Analytical Biochemistry, 1993. **210**: p. 179-187.

283. Lin, W. and J. Trough, *Renaturation of casein kinase II from recombinant subunits produced in escherichia coli: purification and characterisation of the reconstituted holoenzyme*. Protein Expression and Purification, 1993. 4: p. 256-264.
284. Wito Richter, T.H., Hauke Lilie, Ute Egerland, Rainer Rudolph, Thomas Kronbach and Dietrich dettmer, *Refolding, purification and characterisation of human recombinant PDE4A constructs expressed in escherichia coli*. Protein expression and purification, 2000. 19: p. 375-383.
285. Sweet, M. and D. Hume, *Endotoxin signal transduction in macrophages*. Journal of Leukocyte Biology., 1996. 60(1): p. 8-26.
286. Turner, N., et al., *The effect of cyclic AMP and cyclic GMP phosphodiesterase inhibitors on the superoxide burst of guinea-pig peritoneal macrophages*. British Journal of Pharmacology., 1993. 108(4): p. 876-83.
287. Baroja, M., et al., *Specific CD3 epsilon association of a phosphodiesterase 4B isoform determines its selective tyrosine phosphorylation after CD3 ligation*. Journal of Immunology., 1999. 162(4): p. 2016-23.
288. Beck, K., et al., *Inducible NO synthase: role in cellular signalling*. Journal of Experimental Biology., 1999. 202(Pt 6): p. 645-53.
289. Redington, A., et al., *Increased expression of inducible nitric oxide synthase and cyclo-oxygenase-2 in the airway epithelium of asthmatic subjects and regulation by corticosteroid treatment*. Thorax., 2001. 56(5): p. 351-7.
290. Liu, H., et al., *Expression of inducible nitric oxide synthase by macrophages in rat lung*. American Journal of Respiratory & Critical Care Medicine., 1997. 156(1): p. 223-8.
291. Germain, N., et al., *Selective phosphodiesterase inhibitors modulate the activity of alveolar macrophages from sensitized guinea-pigs*. European Respiratory Journal, 1998. 12(6): p. 1334-9.
292. Jeon, Y., et al., *Attenuation of inducible nitric oxide synthase gene expression by delta 9-tetrahydrocannabinol is mediated through the inhibition of nuclear factor-kappa B/Rel activation*. Molecular Pharmacology., 1996. 50(2): p. 334-41.

293. Rutherford, M. and L. Schook, *Macrophage function in response to PGE₂, L-arginine deprivation, and activation by colony-stimulating factors is dependent on hematopoietic stimulus*. *Journal of Leukocyte Biology*, 1992. **52**(2): p. 228-35.
294. Schwacha, M., et al., *Thermal injury alters macrophage responses to prostaglandin E₂: contribution to the enhancement of inducible nitric oxide synthase activity*. *Journal of Leukocyte Biology*, 1998. **64**(6): p. 740-6.
295. Lin, W.W., et al., *Modulation of inducible nitric oxide synthase induction by prostaglandin E₂ in macrophages: distinct susceptibility in murine J774 and RAW 264.7 macrophages*. *Prostaglandins & Other Lipid Mediators*, 1999. **58**(2-4): p. 87-101.
296. Delgado, M., et al., *Vasoactive intestinal peptide and pituitary adenylate cyclase-activating polypeptide prevent inducible nitric oxide synthase transcription in macrophages by inhibiting NF-kappa B and IFN regulatory factor 1 activation*. *Journal of Immunology*, 1999. **162**(8): p. 4685-96.
297. Morris, S., D. Kepka-Lenhart, and L.C. Chen, *Differential regulation of arginases and inducible nitric oxide synthase in murine macrophage cells*. *American Journal of Physiology*, 1998. **275**(5 Pt 1): p. E740-7.
298. Sowa, G. and R. Przewlocki, *cAMP analogues and cholera toxin stimulate the accumulation of nitrite in rat peritoneal macrophage cultures*. *European Journal of Pharmacology*, 1994. **266**(2): p. 125-9.
299. Mullett, D., et al., *An increase in intracellular cyclic AMP modulates nitric oxide production in IFN-gamma-treated macrophages*. *Journal of Immunology*, 1997. **158**(2): p. 897-904.
300. Kunz, D., et al., *Two distinct signaling pathways trigger the expression of inducible nitric oxide synthase in rat renal mesangial cells*. *Proceedings of the National Academy of Sciences of the United States of America*, 1994. **91**(12): p. 5387-91.
301. Eberhardt, W., D. Kunz, and J. Pfeilschifter, *Pyrrolidine dithiocarbamate differentially affects interleukin 1 beta- and cAMP-induced nitric oxide synthase*

- expression in rat renal mesangial cells*. Biochemical & Biophysical Research Communications., 1994. **200**(1): p. 163-70.
302. Okado-Matsumoto, A., et al., *Effect of cAMP on inducible nitric oxide synthase gene expression: its dual and cell-specific functions*. Antioxidants & Redox Signaling., 2000. **2**(4): p. 631-42.
303. Beshay, E., F. Croze, and G.J. Prud'homme, *The phosphodiesterase inhibitors pentoxifylline and rolipram suppress macrophage activation and nitric oxide production in vitro and in vivo*. Clinical Immunology., 2001. **98**(2): p. 272-9.
304. Caivano, M., et al., *The induction of cyclooxygenase-2 mRNA in macrophages is biphasic and requires both CCAAT enhancer-binding protein beta (C/EBP beta) and C/EBP delta transcription factors*. Journal of Biological Chemistry., 2001. **276**(52): p. 48693-701.
305. Juergens, U.R., et al., *New insights in the bronchodilatory and anti-inflammatory mechanisms of action of theophylline*. Arzneimittel-Forschung, 1999. **49**(8): p. 694-8.
306. Stanford, S.J., J.R. Pepper, and J.A. Mitchell, *Cyclooxygenase-2 regulates granulocyte-macrophage colony-stimulating factor, but not interleukin-8, production by human vascular cells: role of cAMP*. Arteriosclerosis, Thrombosis & Vascular Biology, 2000. **20**(3): p. 677-82.
307. Seldon, P.M., P.J. Barnes, and M.A. Giembycz, *Interleukin-10 does not mediate the inhibitory effect of PDE-4 inhibitors and other cAMP-elevating drugs on lipopolysaccharide-induced tumor necrosis factor-alpha generation from human peripheral blood monocytes*. Cell Biochemistry & Biophysics, 1998. **29**(1-2): p. 179-201.
308. Vial, D., et al., *Down-regulation by prostaglandins of type-II phospholipase A2 expression in guinea-pig alveolar macrophages: a possible involvement of cAMP*. Biochemical Journal, 1998. **330**(Pt 1): p. 89-94.
309. Hancock, W., M.E. Pleau, and L. Kobzik, *Recombinant granulocyte-macrophage colony-stimulating factor down-regulates expression of IL-2 receptor on human*

- mononuclear phagocytes by induction of prostaglandin E*. *Journal of Immunology*., 1988. **140**(9): p. 3021-5.
310. Miller, L.A., et al., *The engagement of beta1 integrins on promonocytic cells promotes phosphorylation of Syk and formation of a protein complex containing Lyn and beta1 integrin*. *European Journal of Immunology*, 1999. **29**(5): p. 1426-34.
311. Korchak, H. and L.E. Kilpatrick, *Roles for beta II-protein kinase C and RACK1 in positive and negative signaling for superoxide anion generation in differentiated HL60 cells*. *Journal of Biological Chemistry*., 2001. **276**(12): p. 8910-7.
312. Torphy, T., H.L. Zhou, and L.B. Cieslinski, *Stimulation of beta adrenoceptors in a human monocyte cell line (U937) up-regulates cyclic AMP-specific phosphodiesterase activity*. *Journal of Pharmacology & Experimental Therapeutics*., 1992. **263**(3): p. 1195-205.
313. DiSanto, M. and R. Heaslip, *Rolipram inhibition of phosphodiesterase-4 activation*. *European Journal of Pharmacology*., 1995. **290**(2): p. 169-72.
314. Alvarez, R., et al., *Activation and selective inhibition of a cyclic AMP-specific phosphodiesterase, PDE-4D3*. *Molecular Pharmacology*., 1995. **48**(4): p. 616-22.
315. Seybold, J., et al., *Induction of phosphodiesterases 3B, 4A4, 4D1, 4D2, and 4D3 in Jurkat T-cells and in human peripheral blood T-lymphocytes by 8-bromo-cAMP and Gs-coupled receptor agonists. Potential role in beta2-adrenoreceptor desensitization*. *Journal of Biological Chemistry*, 1998. **273**(32): p. 20575-88.
316. McPhee, I., S. Cochran, and M.D. Houslay, *The novel long PDE4A10 cyclic AMP phosphodiesterase shows a pattern of expression within brain that is distinct from the long PDE4A5 and short PDE4A1 isoforms*. *Cellular Signalling*., 2001. **13**(12): p. 911-8.
317. Ma, D., et al., *Phosphodiesterase 4B gene transcription is activated by lipopolysaccharide and inhibited by interleukin-10 in human monocytes*. *Molecular Pharmacology*., 1999. **55**(1): p. 50-7.

318. Geppert, T., et al., *Lipopolysaccharide signals activation of tumor necrosis factor biosynthesis through the ras/raf-1/MEK/MAPK pathway*. *Molecular Medicine*, 1994. **1**(1): p. 93-103.
319. Ahmad, F., et al., *IL-3 and IL-4 activate cyclic nucleotide phosphodiesterases 3 (PDE3) and 4 (PDE4) by different mechanisms in FDCP2 myeloid cells*. *Journal of Immunology*, 1999. **162**(8): p. 4864-75.
320. Diaz-Guerra, M., et al., *Negative regulation by phosphatidylinositol 3-kinase of inducible nitric oxide synthase expression in macrophages*. *Journal of Immunology*, 1999. **162**(10): p. 6184-90.
321. Vadiveloo, P., et al., *Differential regulation of cell cycle machinery by various antiproliferative agents is linked to macrophage arrest at distinct G1 checkpoints*. *Oncogene*, 1996. **13**(3): p. 599-608.
322. Kato, J., et al., *Cyclic AMP-induced G1 phase arrest mediated by an inhibitor (p27Kip1) of cyclin-dependent kinase 4 activation*. *Cell*, 1994. **79**(3): p. 487-96.
323. Okada, T., et al., *The strength of interaction at the Raf cysteine-rich domain is a critical determinant of response of Raf to Ras family small GTPases*. *Molecular & Cellular Biology*, 1999. **19**(9): p. 6057-64.
324. Dugan, L., et al., *Differential effects of cAMP in neurons and astrocytes. Role of B-raf*. *Journal of Biological Chemistry*, 1999. **274**(36): p. 25842-8.
325. Pazdrak, K., T. Adachi, and R. Alam, *Src homology 2 protein tyrosine phosphatase (SHPTP2)/Src homology 2 phosphatase 2 (SHP2) tyrosine phosphatase is a positive regulator of the interleukin 5 receptor signal transduction pathways leading to the prolongation of eosinophil survival*. *Journal of Experimental Medicine*, 1997. **186**(4): p. 561-8.
326. Miller, M., et al., *RalGDS functions in Ras- and cAMP-mediated growth stimulation*. *Journal of Biological Chemistry*, 1997. **272**(9): p. 5600-5.
327. Wolthuis, R., et al., *RalGDS-like factor (Rlf) is a novel Ras and Rap 1A-associating protein*. *Oncogene*, 1996. **13**(2): p. 353-62.

328. M'Rabet, L., et al., *Activation of the small GTPase rap1 in human neutrophils*. *Blood.*, 1998. **92**(6): p. 2133-40.
329. Schwarze, S., et al., *In vivo protein transduction: Delivery of a biologically active protein into the mouse*. *Science*, 1999. **285**(5433): p. 1569-1572.
330. MC. Shepherd, NC. Thomson, G. Bolger and MD. Houslay. The cloning and biochemical characterisation of a novel phosphodiesterase (PDE4B4). *Biochemical Journal* In press..

